

**The Role of Hydrogen Peroxide and Pneumolysin
in Pneumococcal Pathogenesis**

Inauguraldissertation

zur

Erlangung des akademischen Grades eines
Doktors der Naturwissenschaften (Dr. rer. nat.)
der
Mathematisch-Naturwissenschaftlichen Fakultät
der
Universität Greifswald

vorgelegt von

Surabhi Surabhi

geboren am 21. March 1993
in Kundapura, India

Greifswald, 18.08.2021

Dekan: Herr Prof. Dr. Gerald Kerth
1. Gutachter: Herr Prof. Dr. Nikolai Siemens
2. Gutachter: Herr Prof. Dr. Sven Hammerschmidt
3. Gutachter: Frau Prof. Dr. Simone Bergmann
Tag der Promotion: 18. 11.2021

न चोरहार्यं न च राज्यहार्यं न भ्रातृभाज्यं न च भारकारी ।
व्यये कृते वर्धत एव नित्यं विद्याधनं सर्वधनप्रधानम् ॥

Not stolen by thieves, not seized by kings, not divided amongst siblings, not heavy to carry;
the more you share with others, the more it grows, thus knowledge is the greatest wealth.

From Subhashita Ratnakar, Chapter 'Vidya Prasanshaa', shloka 4 [1]

Dedicated to my beloved Family

TABLE OF CONTENTS

LIST OF FIGURES	III
LIST OF TABLES	IV
LIST OF ABBREVIATIONS	V
1. ZUSAMMENFASSUNG	3
2. SUMMARY	7
3. INTRODUCTION.....	11
3.1 <i>Streptococcus pneumoniae</i>	11
3.1.1 Pneumolysin (Ply).....	12
3.1.2 Hydrogen peroxide (H ₂ O ₂).....	13
3.2 <i>Staphylococcus aureus</i>	13
3.3 Influenza A virus	14
3.4 Bacterial and viral co-infections.....	15
3.5 Innate host defence responses	16
3.5.1 Epithelial cell responses.....	16
3.5.2 Neutrophil responses.....	17
3.5.3 Cell death as innate immune response	19
3.5.3.1 Apoptosis.....	21
3.5.3.2 NLRP3 Inflammasome and pyroptosis.....	22
3.6 Aim of the thesis	25
4. EXPERIMENTAL APPROACH	29
4.1 Bacterial and viral strains	29
4.2 Experimental approaches	29
4.3 Enzyme-linked immunosorbent assay (ELISA).....	32
4.4 Microscopy.....	32
4.5 Statistical Analyses	33
4.6 Ethics Statement.....	33
5. RESULTS AND DISCUSSION.....	37
5.1 NLRP3 inflammasome plays a crucial role in pneumococcal infections	37
5.1.1 IL-1 β inhibiting drugs and their side effects	37
5.1.2 H ₂ O ₂ produced by pneumococci induces cell death.....	39
5.1.3 H ₂ O ₂ activates inflammasome signaling resulting in IL-1 β release.....	39
5.1.4 H ₂ O ₂ primes the NLRP3 inflammasome.....	41
5.1.5 IL-1 β release caused by H ₂ O ₂ is a result of inflammasome activation but not pyroptosis.....	42

TABLE OF CONTENTS

5.2	Host metabolome responses to respiratory infections.....	43
5.2.1	Pneumococcal infections result in intracellular citrate accumulation	44
5.2.2	Intracellular citrate accumulation is a consequence of the action of pneumococcal H ₂ O ₂	44
5.3	Influence of Ply-ATP interactions on neutrophil activation	46
5.3.1	Pneumolysin induces neutrophil activation.....	46
5.3.2	ATP neutralizes Ply-induced neutrophil lysis and activation.....	47
5.3.3	Ply and ATP directly interact with each other.....	48
5.4	Conclusion and future perspective.....	50
6.	REFERENCES	55
PAPER 1	65	
	The Role of NLRP3 Inflammasome in Pneumococcal Infections	65
PAPER 2	75	
	Hydrogen Peroxide is Crucial for NLRP3 Inflammasome Mediated IL-1 β Production and Cell Death in Pneumococcal Infections of Bronchial Epithelial Cells	75
PAPER 3	101	
	Bronchial Epithelial Cells Accumulate Citrate Intracellularly in Response to Pneumococcal Hydrogen Peroxide.....	101
PAPER 4	137	
	Adenosine Triphosphate Neutralizes Pneumolysin-Induced Neutrophil Activation.....	137
7.	APPENDIX	165
7.1	Eigenständigkeitserklärung.....	165
7.2	Curriculum vitae.....	166
7.3	Publications and conference contributions	167
7.3.1	Published peer-reviewed articles included in this thesis	167
7.3.2	Published peer-reviewed articles not included in this thesis	167
7.3.3	Submitted manuscripts included in this thesis.....	167
7.3.4	Submitted manuscripts not included in this thesis	167
7.3.5	Participation in Conferences and other Scientific Events	168
7.4	Acknowledgments	169

LIST OF FIGURES

Figure 3.1: Non-invasive and invasive diseases caused by pneumococci.	12
Figure 3.2: Apoptotic and pyroptotic cell death pathways.....	20
Figure 3.3: Priming and activation of canonical NLRP3 inflammasome.	23
Figure 4.1: Experimental approach used in paper II to study the impact of pneumococci derived H ₂ O ₂ on apoptotic and pyroptotic cell death pathways.	30
Figure 4.2: Experimental time scheme used in paper III to analyze the changes in the host metabolome post single bacterial (TIGR4 and LUG2012), viral and co-infections.	31
Figure 5.1: Pneumococcal H ₂ O ₂ primes and activates the NLRP3 inflammasome pathway resulting in pyroptosis-independent IL-1 β release.	43
Figure 5.2: Intracellular citrate accumulation is a consequence of pneumococcal H ₂ O ₂	46

LIST OF TABLES

Table 3.1: Families of pattern recognition receptors17

Table 4.1: List of bacterial and viral strains used in the study.....29

Table 5.1: Clinically approved IL-1 inhibiting drugs38

LIST OF ABBREVIATIONS

ACD	Accidental cell death
ADP	Adenosine di-phosphate
AIF	Apoptosis inducing factor
AIM2	Absent in melanoma 2
ALRs	AIM2-like receptor
Apaf-1	Apoptotic protease activating factor-1
ASC	Apoptosis-associated speck-like protein
ATP	Adenosine tri-phosphate
BAK	Bcl2 Antagonist Killer
BAX	Bcl2 Associated X-protein
BID	Bcl2 Interacting Protein
CAPS	Cryopyrin-Associated Periodic Syndromes
CDC	Cholesterol-dependent cytolysins
CIC	Mitochondrial citrate carrier
CLRs	C-type lectin receptors
DAMPs	Damage-associated molecular patterns
dATP	Deoxyadenosine triphosphate
DNA	Deoxy-ribonucleic acid
DRs	Death receptors
dsRNA/DNA	Double stranded RNA/DNA
ELISA	Enzyme-linked immunoassay
FCAS	Familial Cold Auto-inflammatory Syndrome
FDA	Food and Drug Administration
FESEM	Field emission scanning electron microscopy
GC-MS	Gas chromatography–mass spectrometry
GSDMD	Gasdermin-D
GSDMD-N	N-terminal GSDMD
GSDME	Gasdermin-E
H₂O₂	Hydrogen peroxide
HA	Hemagglutinin
IAV	Influenza A virus
IBD	Inflammatory bowel disease
IFNs	Interferons
IgG	Immunoglobulin G
IL	Interleukin
IL-1R	Interleukin-1 receptor
LPS	Lipopolysaccharide
mBMDMs	Mouse bone marrow-derived macrophages
MLKL	Mixed lineage kinase domain-like
MOMP	Mitochondrial outer membrane permeabilization
mRNA	Messenger ribonucleic acid

MRSA	Methicillin resistant <i>S. aureus</i>
mtDNA	Mitochondrial DNA
MWS	Muckle-Wells Syndrome
NA	Neuraminidase
NETs	Neutrophil extracellular traps
NF-κB	nuclear factor kappa-light-chain-enhancer of activated B cells
NLRP3	Nod-like receptor protein 3
NLRs	NOD-like receptors
NOD	Nucleotide-binding and oligomerization domain
P2X₇R	P2X purinoceptor 7
PAK2	p21-activated kinase 2
PAMPs	Pathogen-associated molecular patterns
PARP	Poly (ADP-ribose) polymerase
PCA	Principal component analysis
Ply	Pneumolysin
PRRs	Pattern recognition receptors
PVL	Panton Valentine Leukocidin
qRT-PCR	Quantitative real time polymerase chain reaction
RCD	Regulated cell death
RIG	Retinoic acid-inducible gene
RIP	Receptor-interacting protein
RLRs	RIG-I-like receptors
ROS	Reactive oxygen species
SCV	Small-colony variant
TCA	Tricarboxylic acid
TLR	Toll-like receptor
TNF	Tumor Necrosis Factor
TRAIL	TNF-related apoptosis-inducing ligand
WHO	World Health Organization

Chapter **1**

ZUSAMMENFASSUNG

1. Zusammenfassung

Die angeborene Immunantwort des Menschen spielt eine zentrale Rolle bei der Erkennung von „Pathogen-“, und/oder „Damage-Associated Molecular Patterns“ (PAMPs und DAMPs) und trägt zu der damit verbundenen wichtigen Entzündungsreaktion bei. PAMPs oder DAMPs werden vom Immunsystem des Wirtes über „Pattern Recognition Rezeptoren“ (PRRs) erkannt. Das „NLR Family Pyrin Domain-containing 3“ (NLRP3) Inflammasom ist ein solcher PRR. NLRP3 ist ein zytoplasmatischer Immunsensor, der durch die Aktivierung die Produktion von proinflammatorischen Zytokinen, wie z.B. IL-1 β und IL-18, anregt. Diese Zytokine induzieren eine Vielzahl von für den Wirt schützenden Signalwegen, die darauf abzielen, den Erreger zu eliminieren. Eine übermäßige oder chronische Inflammasom-Aktivierung wird jedoch mit der Entstehung verschiedener Autoimmun- und autoinflammatorischer Erkrankungen in Verbindung gebracht. Als Konsequenz, werden pharmakologische Inhibitoren von IL-1 häufig zur Bekämpfung dieser Erkrankungen therapeutisch eingesetzt. In **Publikation I** wurden die derzeit verfügbaren IL-1 β -hemmenden Therapien in Form eines Übersichtsartikels zusammengefasst. Patienten, die sich diesen Behandlungen unterziehen, haben ein unverhältnismäßig hohes Risiko invasive bakterielle Infektionen zu entwickeln. Weiterhin wurde auch der begrenzte Wissensstand über die Rolle des NLRP3-Inflammasoms in der Pathogenese von Pneumokokken zusammen.

Wasserstoffperoxid (H₂O₂) ist ein physiologisches Produkt und eine wichtige Virulenzdeterminante, das von Pneumokokken produziert wird. H₂O₂ wirkt stark zytotoxisch auf Wirtszellen, jedoch ist nicht viel über dessen Auswirkung auf den programmierten Zelltod wie z.B. NLRP3-Inflammasom vermittelte Pyroptose bekannt. In **Publikation II** wurde die Wirkung von Pneumokokken-produzierten H₂O₂ auf die Epithelzellen untersucht. Der Fokus der Untersuchungen lag auf dem Zusammenspiel zweier wichtiger Zelltodsignalwege, der Apoptose und Pyroptose. Die Untersuchungen haben gezeigt, dass H₂O₂ das NLRP3-Inflammasom sowohl primen als auch aktivieren kann. Darüber hinaus wurde festgestellt, dass das von Pneumokokken gebildete H₂O₂ den Zelltod sowohl über die Aktivierung apoptotischer als auch pyroptotischer Wege einleitet. Diese werden durch die Aktivierung von Caspase-3/7 bzw. Caspase-1 vermittelt. Die H₂O₂-vermittelte Inflammasom-Aktivierung führt zu einer Caspase-1-abhängigen IL-1 β -Produktion. Jedoch ist die endgültige IL-1 β -Freisetzung unabhängig von Gasdermin-D (GSDMD) und wird hauptsächlich von der apoptotischen Zelllyse vermittelt.

In **Publikation III** wurden die metabolischen Reaktionen des Wirtes auf Infektionen mit Erregern, die Atemwegserkrankungen verursachen, untersucht. Es wurde ein Metabolom-Profil von bakteriell und viral einzel- und ko-infizierten Bronchialepithelzellen erstellt. Folgende Erreger wurden für Infektionen genutzt: Influenza A Virus (IAV), *Streptococcus pneumoniae* und *Staphylococcus aureus*. Die Untersuchungen zeigten, dass IAV und *S. aureus* die Ressourcen des Wirtes zum Überleben und zur Vermehrung nutzen und nur minimale Auswirkungen auf das Metabolom des Wirtes haben. Im Gegensatz dazu beeinflussten Pneumokokken verschiedene Stoffwechselwege des Wirtes erheblich. Die größten Veränderungen wurden in der Glykolyse, dem Tricarbonsäurezyklus (TCA) und Aminosäurestoffwechsel festgestellt. Ein wichtiges Kennzeichen von Pneumokokken-Infektionen ist die intrazelluläre Akkumulierung von Citrat, die direkt auf die Wirkung von Pneumokokken-produzierten H₂O₂ zurückgeführt werden konnte.

Der Tod von Wirtszellen während einer Infektion führt zur Freisetzung von entzündungsfördernden Zytokinen und Gefahrensignalen wie z.B. das ATP. Freigesetztes ATP kann die Chemotaxis der Neutrophilen auslösen, die durch purinerge Signalübertragung vermittelt wird. Neutrophile sind in der Regel die ersten Leukozyten, die am Ort der Infektion rekrutiert werden und spielen eine Schlüsselrolle bei der Eliminierung von Bakterien. Eine übermäßige Aktivierung der Neutrophilen ist jedoch mit weiteren Gewebeschäden verbunden. In **Publikation IV** wurde die Rolle von ATP in Pneumokokkeninfektionen untersucht. Der Fokus dabei lag insbesondere auf den Neutrophilen. Die Untersuchungen ergaben, dass Pneumolysin (Ply), ein hochwirksames porenbildendes Toxin, welches von Pneumokokken produziert wird, ein starker Aktivator der Neutrophilen ist. Bindungsstudien ergaben, dass Ply und ATP miteinander interagieren. Die ATP-Bindung neutralisierte Ply-vermittelte Neutrophilen-Degranulierung, was darauf hindeutet, dass Ply-ATP-Interaktionen im Verlauf der Infektion möglicherweise von Vorteil sein könnten. Die ATP-vermittelte Ply-Inhibierung könnte u.a. die Lungenschädigung infolge einer übermäßigen Ply-vermittelten Neutrophilenaktivierung begrenzen.

Chapter 2

SUMMARY

2. Summary

The human innate response plays a pivotal role in detection of pathogen- or damage-associated molecular patterns (PAMPs and DAMPs) and contributes to a crucial inflammatory response. PAMPs or DAMPs are recognized by the host immune system via pattern recognition receptors (PRRs). NLR family pyrin domain-containing 3 (NLRP3) inflammasome is one of these PRRs. NLRP3 is a cytoplasmic immune sensor that upon activation produce pro-inflammatory cytokines such as IL-1 β and IL-18. These cytokines induce a diverse range of protective host pathways aiming to eradicate the pathogen. However, excessive or chronic inflammasome activation are implicated in the pathogenesis of several autoimmune and auto-inflammatory disorders. Pharmacologic inhibitors of IL-1 are commonly used to combat these disorders. In **paper I**, we explore the currently available IL-1 β inhibiting therapies and how patients undergoing these treatments are at a disproportionate risk to experience invasive bacterial infections. We also summarize the limited knowledge on the role of NLRP3 inflammasome in pneumococcal pathogenesis.

Hydrogen peroxide (H₂O₂) is a physiological metabolite and an important virulence determinant produced by pneumococci. It is highly cytotoxic to host cells. However, not much is known about its impact on host cell death pathways such as NLRP3 inflammasome mediated pyroptosis. In **Paper II**, we examined the effect of pneumococci-derived H₂O₂ on epithelial cells by analyzing the interplay between two key cell death pathways, namely apoptosis and pyroptosis. We show that H₂O₂ can prime as well as activate the NLRP3 inflammasome. Furthermore, we demonstrate that pneumococcal H₂O₂ initiates cell death via the activation of both apoptotic as well as pyroptotic pathways, mediated by the activation of caspase-3/7 and caspase-1, respectively. H₂O₂ mediated inflammasome activation results in caspase-1 dependent IL-1 β production. However, we show that the final IL-1 β release is independent of gasdermin-D (GSDMD) and mainly dependent on the apoptotic cell lysis.

In **paper III**, we focused on understanding the host metabolic responses to infections with pathogens which cause respiratory diseases. We performed metabolome profiling of *in vitro* single bacterial and viral as well as co-infections of bronchial epithelial cells with Influenza A virus (IAV), *Streptococcus pneumoniae*, and *Staphylococcus aureus*. We show that IAV and *S. aureus* use the host resources for survival and multiplication and have minimal effects on the host metabolome. In contrast, pneumococci significantly alter various host metabolome

pathways, including glycolysis, tricarboxylic acid (TCA) cycle and amino-acid metabolism. A hallmark of pneumococcal infections was the intracellular citrate accumulation, which was directly attributed to the action of pneumococci-derived H₂O₂.

Host cell death during an infection results in the release of pro-inflammatory cytokines and danger signals such as ATP. Released ATP can induce neutrophil chemotaxis mediated via purinergic signaling. Neutrophils are typically the first leukocytes to be recruited to the site of infection and are key players in bacterial clearance. However, excessive neutrophil activation is associated with further tissue injury. In **paper IV**, we investigated the role of ATP in neutrophil response to pneumococcal infections. We show that pneumolysin (Ply), a highly effective pore-forming toxin produced by pneumococci, is a potent activator of neutrophils. Microscale Thermophoresis analysis revealed that Ply and ATP bind to each other. Subsequently, ATP binding neutralizes Ply-mediated neutrophil degranulation, suggesting that Ply-ATP interactions are potentially beneficial during the course of the infection as this could limit the lung injury resulting from excessive Ply-mediated neutrophil activation.

Chapter 3

INTRODUCTION

3. Introduction

The world we live in is heavily populated by both pathogenic and non-pathogenic microbes that threaten cellular homeostasis. The nasopharynx is an ecological niche for many commensal bacteria as well as potential respiratory pathogens. *Streptococcus pneumoniae* and *Staphylococcus aureus* are two of the most common colonizers of the upper respiratory tract [2]. Every individual is asymptotically colonized with both bacteria at least once in their lifetime [3-8]. However, under certain stressful conditions, for example following viral infections, or in individuals with a weakened immune system including young children, elderly and immunocompromised persons, they can cause a wide range of life-threatening diseases, such as pneumonia, meningitis or sepsis [9, 10].

3.1 *Streptococcus pneumoniae*

Streptococcus pneumoniae (the pneumococcus) is an encapsulated Gram-positive diplococcus that thrives in both aerobic and anaerobic environments. It is phenotypically characterized by α -hemolysis, catalase negativity, bile solubility, and optochin susceptibility [11]. Pneumococcus is a highly successful pathogen partly due to its high level of capsule diversity resulting in over 100 serotypes, which vary markedly in their ability to cause invasive infections [12-15]. It is an quiescent opportunistic pathobiont that asymptotically colonizes mucosal surfaces of the human upper respiratory tract in healthy individuals [16]. Epidemiological studies suggest that up to 27–65% of children and about 10% of adults are pneumococcal carriers [8, 17-19]. Nevertheless, the pneumococcus can cause various diseases ranging from non-invasive pneumococcal diseases such as sinusitis, otitis media and pneumonia without bacteremia to life-threatening invasive pneumococcal diseases (IPDs) such as pneumonia with bacteremia, meningitis or sepsis (Fig. 3.1) [20]. However, the majority of IPDs occur in children under the age of five, as well as in elderly and immunocompromised people due to their undeveloped or weakened immune system, respectively [20]. Furthermore, synergy of pneumococci with seasonal viruses, e.g., Influenza A virus (IAV), can lead to bacterial dissemination to the lower respiratory tract causing IPDs [21-23]. The World Health Organization (WHO) estimates that 1.6 million people die from pneumococcal disease every year, including 0.7 million to 1 million children younger than 5 years of age [24].

Non-invasive and invasive pneumococcal diseases

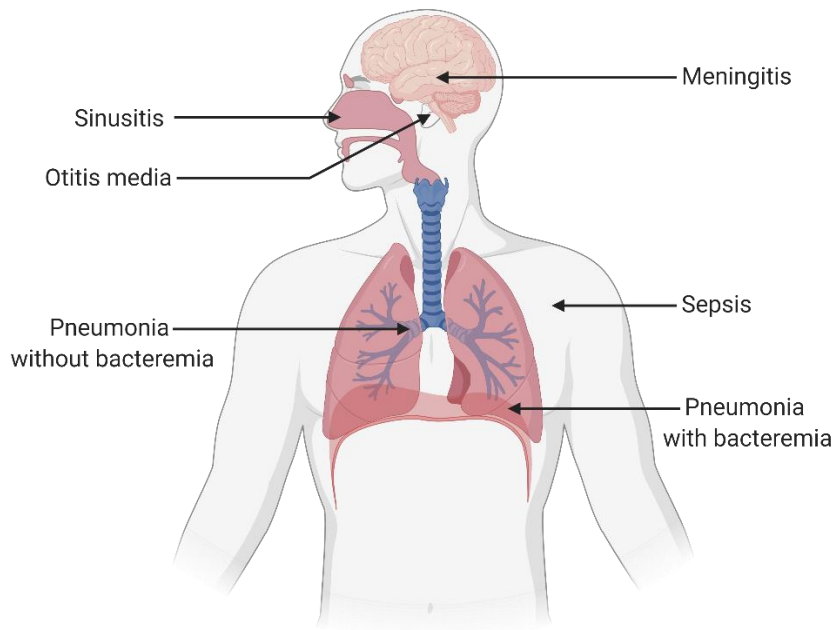


Figure 3.1: Non-invasive and invasive diseases caused by pneumococci.

Pneumococci can cause non-invasive diseases such as sinusitis, otitis media and pneumonia without bacteremia and life-threatening invasive diseases such as pneumonia with bacteremia, meningitis or sepsis. Figure created with BioRender.

S. pneumoniae produces a myriad of virulence factors that are indispensable for disease progression and pathogenesis. These virulence factors aid pneumococci to establish direct contact with host tissue surface receptors, and escape bacterial clearance mediated by host immune cells [25-27]. Two crucial virulence determinants that are cytotoxic to host cells are pneumolysin (Ply) and hydrogen peroxide (H_2O_2).

3.1.1 Pneumolysin (Ply)

Ply is a 53-kDa pore-forming toxin produced by all clinical isolates of the *S. pneumoniae* and belongs to a family of thiol-activated, cholesterol-dependent cytolysins (CDCs) [28]. In contrast to all other known members of the CDC family, Ply does not get actively secreted due to a lack of an N-terminal secretion signal [29]. The mechanism by which Ply is released remains debatable. Some studies suggest that Ply is released following cell wall hydrolysis instigated by the pneumococcal autolysin LytA [28, 30], while others claim that the Ply release occurs in an autolysis-independent manner [31, 32]. Released Ply binds to the cholesterol containing host cell membranes and forms large pores (up to 26 nm in diameter) by the oligomerization of up to 42 toxin monomers [33-35]. Intracellular calcium influx via Ply pores

can trigger host cell DNA and mitochondrial damage, culminating in host cell death via apoptosis [36-39]. TLR4 was also implicated in the host cell apoptotic response to Ply [40]. As a pore-forming toxin, Ply is involved in the activation of the inflammasome and the pyroptotic cell death pathway [41-44]. In addition to cell lysis, Ply hampers ciliary beating of respiratory epithelial cells resulting in impaired mucociliary clearance of pneumococci [45]. Furthermore, Ply can activate the complement system and modulate chemokine and cytokine production, resulting in a highly pro-inflammatory environment which facilitates bacterial shedding and host-to-host transmission [46, 47]. As one of the most important virulence factor of pneumococci, Ply remains to be one of the promising candidates included in protein-based vaccines that have progressed through the initial stages of clinical trials [48].

3.1.2 Hydrogen peroxide (H₂O₂)

Apart from Ply, pneumococci also produce prodigious amounts of H₂O₂. It is produced as a product of the pneumococcal carbohydrate-metabolizing enzyme pyruvate oxidase SpxB [49]. Secreted H₂O₂ diffuses through the host cell membrane and induces toxic DNA double-strand breaks and oxidative damage, which finally culminates in apoptotic cell death [50, 51]. Pneumococcal mutants deficient in H₂O₂ production are characterized by a reduced virulence *in vivo* [49]. H₂O₂ is also a vasodilator and contributes to the cerebral hyperemia during early stages of meningitis and therapies with antioxidants alleviate the pathophysiological responses [52, 53]. It attenuates ciliary function by slowing the ciliary beat frequency and impairing the structural integrity of human ciliated epithelium [54, 55]. Furthermore, several studies showed that cell injury induced by pneumococcal mutants lacking Ply activity was comparable to that of the parental strain, implicating H₂O₂ as a major factor responsible for the cell cytotoxicity [56, 57]. The pneumococcus not only utilizes H₂O₂ as a virulence determinant. Released H₂O₂ eliminates microbial competitors in the nasopharynx such as *Haemophilus influenzae*, *Staphylococcus aureus*, *Neisseria meningitidis* and *Moraxella catarrhalis*, and thereby promotes pneumococcal colonization [58, 59].

3.2 *Staphylococcus aureus*

Staphylococcus aureus (*S. aureus*) is a Gram-positive opportunistic pathogen that predominantly colonizes the human anterior nares, the axillae and the skin in one-third of the human population [60, 61]. In general, *S. aureus* infections can range from superficial infections

such as stye and sinusitis, to more invasive and lethal infections such as pneumonia, toxic shock syndrome, and necrotizing soft tissue infections [62, 63]. The ability of *S. aureus* to cause such a magnitude of infections is directly associated to the production of a wide array of virulence factors including highly active pore-forming toxins. Pore-forming toxins of *S. aureus* can be broadly classified into 2 sub-groups based on their mode of action:

(i) Receptor-dependent

Binding of α -toxin and bi-component leukocidins to specific receptors on host cell membrane leads to the formation of a pore. Receptors have been identified for α -toxin, Pantone Valentine Leukocidin (PVL), LukAB, and LukDE. Gamma-toxin probably also binds to a specific receptor [64, 65].

(ii) Membrane interference without receptor interaction

Similar to Ply, phenol-soluble modulins (PSMs) are believed to bind to the cytoplasmic membrane in a non-specific manner and cause membrane rupture [65].

An important feature of staphylococcal infection is the long-term persistence [66]. Besides professional phagocytes, *S. aureus* can internalize into other cell-types like epithelial cells, endothelial cells, fibroblasts, keratinocytes and osteoblasts [67]. The bacteria can survive within host cells by switching to small-colony variant (SCV) phenotype. SCVs are normally associated with persistent infections, which may be both chronic and recurrent [66, 68]. Additionally, *S. aureus* can adapt their regulatory network to the intracellular environment, enabling prolonged intracellular survival [69, 70].

3.3 Influenza A virus

Influenza A virus (IAV) is a member of the family *Orthomyxoviridae*. IAV is characterized by segmented, negative-sense, single-stranded RNA genomes [71, 72]. Its genome consists of eight segments that encode for at least 17 viral proteins [73]. IAV is an enveloped virus and is covered with the projections of three proteins: hemagglutinin (HA), neuraminidase (NA) and matrix 2 [74]. HA regulates the attachment of virus to the host receptors [75, 76]. While NA regulates the release of progeny virus from the host cell [75, 77]. Based on the antigenicity of their HA and NA, IAV are classified into 18 classical HA and 11 classical NA subtypes [78, 79]. IAV are evolutionarily dynamic viruses with highly variable genomes. They possess an error-prone RNA polymerase that lacks the ability of proof-reading, which results in a very high mutation rate (ranging from 10^{-3} to 10^{-4} substitutions per site per year) [80, 81]. This mechanism of changing genetic make-up is termed antigenic drift. However, having a

segmented genome also allows for another way to change its composition, via reassortment or antigenic shift. This occurs when one cell is simultaneously infected by two different influenza A viruses [71]. Antigenic shift is both common and essential for IAV host switching and evolution [82]. Unlike antigenic drift, antigenic shift leads to drastic changes in the antigenicity of the HA; and is associated with IAV pandemics [83]. The WHO estimates that seasonal epidemics of influenza account for ~1 billion infections, 3–5 million severe cases and 290,000–650,000 deaths annually [84]. Influenza disease is normally characterized by a rapid onset of fever, muscle aches, and fatigue. Influenza can progress to pneumonia, which can be a result of either primary viral infection or a secondary bacterial infection [22, 85, 86]. Hospitalization and death occur mainly among high risk groups including pregnant women, children under the age of 5, elderly, and immuno-compromised individuals [84, 87]. Vaccines are manufactured on a yearly cycle to account for the viral antigenic drift and shift [88, 89].

3.4 Bacterial and viral co-infections

Since 1510, IAV has been responsible for approximately 14 pandemics [90]. In 1918, the most devastating influenza pandemic was recorded, infecting 50% of the world's population and resulting in more than 40 million deaths worldwide [91]. However, secondary bacterial pneumonia is estimated to have occurred in up to 95% of the fatalities during this pandemic [92]. The majority of those deaths were due to secondary pneumococcal infections [92-94]. *S. pneumoniae* continues to be associated with secondary infections during influenza pandemics followed mainly by *S. aureus* [85, 95] and *H. influenzae* [85, 92, 94]. To this day, co-infections with these pathogens remain to be the cause of high mortality, especially among high-risk groups such as elderly (age >65), pregnant women, children under the age of one, people with chronic medical conditions, and immunocompromised [96].

Several mechanisms by which viral respiratory infections may predispose patients to subsequent bacterial infections have been described. Some of which are listed below.

- IAV disrupts lung physiology: Epithelial damage, decreased ciliary beat frequency, and surfactant disruption caused by an IAV infection provide access and a nutrient source, supporting bacterial growth [97-99]
- Increased receptor availability: Viral NA contributes to bacterial adherence to airway epithelium by cleaving sialic acid and exposing receptors for attachment [21].

Damaged epithelia, whether damaged directly by the virus or by the inflammatory response, provide additional bacterial adhesion sites [92, 100].

- Alterations of innate immune responses: IAV modifies the immune response either by diminishing the ability of the host to clear bacteria or by amplification of the inflammatory cascade causing lung injury. Both of these events likely aid a subsequent bacterial infection [22, 85, 101]. Insufficient immune response to fight bacterial infection is primarily attributed to the production of interferons (IFNs) which results in an antiviral state [102]. Concurrent with their antiviral effect, IFN production can inhibit various important antibacterial immune responses. For example, type I IFNs selectively inhibit the production of neutrophil chemoattractants KC and MIP-2 [102] and macrophage chemoattractant CCL2 [103]. The inhibition of these chemoattractants results in impaired recruitment of immune cells leading to inefficient bacterial clearance. Additionally, a general anti-inflammatory state is orchestrated dedicated to the restoration of lung immune homeostasis post IAV clearance. IL-10 production during this wound healing phase [104] broadly suppresses several mechanisms that are involved in bacterial recognition and clearance [105].

3.5 Innate host defence responses

The innate immune system accounts for all defence mechanisms that come into play when the host is challenged with a certain pathogen for the first time. In majority of the cases, the quick nature of the innate response is sufficient to restrict as well as resolve the infection. The adaptive immune response is only required when the pathogen manages to evade or overwhelm the innate host defences [106].

3.5.1 Epithelial cell responses

The respiratory epithelia are constantly exposed to toxins and pathogens during respiration. Despite exposure, the frequency of severe respiratory infections is relatively low in healthy individuals [107]. The ability of the respiratory epithelium to serve as an efficient barrier against pathogens can be attributed to its well-established defense system [108, 109].

Epithelial cells are held together by tight junctions, which effectively protect the internal tissue environment [110]. They secrete mucus rich in mucin glycoproteins, that traps microbes and other particulate matter [111]. The entrapped particles or microbes are further expelled via

mucociliary clearance driven by the beating of epithelial cilia [112]. Apart from being a physical barrier, epithelial cells are also immunologically active. They produce anti-microbial peptides such as β -defensins and LL-37, that aid in elimination of the invading microbe [113, 114]. Additionally, airway epithelial cells are equipped with receptors called pattern recognition receptors (PRRs). PRRs are specialized in the recognition of both extracellular and intracellular pathogen- or damage-associated molecular patterns (PAMPs and DAMPs) [115]. PRRs are classified into five families, namely Toll-like receptors (TLRs), Nucleotide-binding and oligomerization domain (NOD)-like receptors (NLRs), Retinoic acid-inducible gene (RIG)-I-like receptors (RLRs), C-type lectin receptors (CLRs), and Absent in melanoma 2 (AIM2)-like receptor (ALRs) (Table 3.1) [115].

Table 3.1: Families of pattern recognition receptors

PRRs	Localization	Sub-types	PAMPs/DAMPs	References
TLRs	Cell and endosomal membrane	10 (humans) and 13 (mice)	extracellular or endosomal PAMPs	[116, 117]
NLRs	Cytoplasm	4 subfamilies, with a total of 22 types	endogenous or microbial molecules	[118]
RLRs	Cytoplasm	3	dsRNA	[119]
CLRs	Cell membrane	17 sub-groups	Carbohydrate structures	[120]
ALRs	Cytoplasm	2	dsDNA	[121-123]

Detection of PAMPs/DAMPs triggers sophisticated intracellular signaling pathways resulting in the production of multiple effector molecules, including cytokines and chemokines as well as antimicrobial proteins [115]. Other immune cells, including neutrophils, macrophages, and lymphocytes are recruited to the sites of infection as major bio effectors. These cells are involved in the eradication and disposal of pathogens, or, if needed, partake in the adaptive immune response.

3.5.2 Neutrophil responses

Neutrophils or polymorphonuclear leukocytes (PMNs) are short lived cells that belong to the myeloid lineage of immune cells [124]. They are characterized by a segmented nucleus and contain high amounts of cytoplasmic granules. In addition, PMNs are the most abundant leukocytes in the circulation and are regarded as first line of defence in the innate immune system.

Neutrophils are produced every day in large numbers ($\sim 10^{11}$ cell per day) in the bone marrow [125]. They enter the blood and patrol for signs of microbial infections. At the end of their lifespan, they enter the tissue and are cleared by tissue resident macrophages via phagocytosis [126]. However, when neutrophils detect microbial pathogens, they deploy different mechanism to capture and destroy the invading pathogen, such as:

- (i) **Phagocytosis:** Recognition of the microbes by the phagocytic receptors such as Fc γ receptors, leads to the ingestion of the microbe into a plasma membrane derived vacuole called the phagosome [127]. The phagosome upon maturation is called the phagolysosome [128]. Phagolysosomes have highly acidic environment and contain many degrading enzymes, including various cathepsins, proteases, lysozymes, and lipases. They also contain NADPH oxidase that generates reactive oxygen species (ROS). The highly oxidative and degradative milieu leads to the destruction of the ingested pathogen [129].
- (ii) **Neutrophil extracellular trap (NET) formation:** NETs are filamentous extracellular structures composed of decondensed chromatin and mitochondrial DNA loaded with granule-derived proteins. They are released by neutrophils to immobilize and kill pathogens [130]. Mechanism of NET formation is also associated with a form of pathogen-induced cell death, named as NETotic cell death [131, 132].
- (iii) **Degranulation:** Neutrophils contain four different types of granules: (1) primary or azurophilic granules; (2) secondary or specific granules; (3) tertiary or gelatinase granules; and (4) secretory vesicles [133]. The primary granules mainly contain toxic mediators, such as elastase, myeloperoxidase, lysozyme, azurocidin, cathepsins, resistin and defensins. The secondary and tertiary granules have overlapping contents, however they mainly contain lactoferrin and gelatinase, respectively, among other substances. The secretory vesicles mainly contain plasma proteins such as human serum albumin [133-135].

Degranulation occurs in response to elevating concentrations of Ca²⁺ [136]. Increase in the intracellular Ca²⁺ initiates granules translocation to the phagosomal or plasma membrane, where it fuses with the membrane to release its contents [136, 137]. The granules are released in a hierarchical manner. Secretory vesicles are released first followed by tertiary and secondary granules and finally the primary granules [138, 139]. Therefore, primary granules serve as markers for neutrophil degranulation.

Neutrophil response is crucial for pathogen clearance, however, is also associated with collateral tissue injury. Excessive neutrophil degranulation has been implicated in many inflammatory disorders such as acute lung injury, rheumatoid arthritis, and septic shock [140, 141].

3.5.3 Cell death as innate immune response

Cell death has been dismissed as a mere consequence of cellular life cycle. However, over the past few decades, studies have revealed the crucial role of cell death in host immune response to harmful stimuli [142]. Pertaining to infections, cell death not only assists in elimination of intracellular niches of the pathogens [143], but also simultaneously facilitates the recruitment of phagocytic immune cells that promote resolution of the infection. However, pathogens also induce host cell death as a strategy to efficiently exit the host cell, spread to neighboring cells, and/or gain nutrients [144]. As per the Nomenclature Committee on Cell Death (NCCD), cell death can be classified as either regulated (RCD) or accidental (ACD). ACD is an unregulated and instantaneous form of cell death resulting from the exposure to physical, chemical or mechanical injury, while RCD is a controlled cell death mechanism regulated by tightly structured signalling cascades [132]. RCD can either be non-lytic and immunologically silent (i.e., apoptosis and autophagy) or highly inflammatory in nature (i.e., necroptosis and pyroptosis). Recent studies have revealed cross-talks among the various RCD pathways; for example, despite having a primary role in inducing apoptosis, caspase-3 can also induce pyroptosis [145, 146] and conversely, caspase-1 involved in pyroptosis can trigger apoptosis [147].

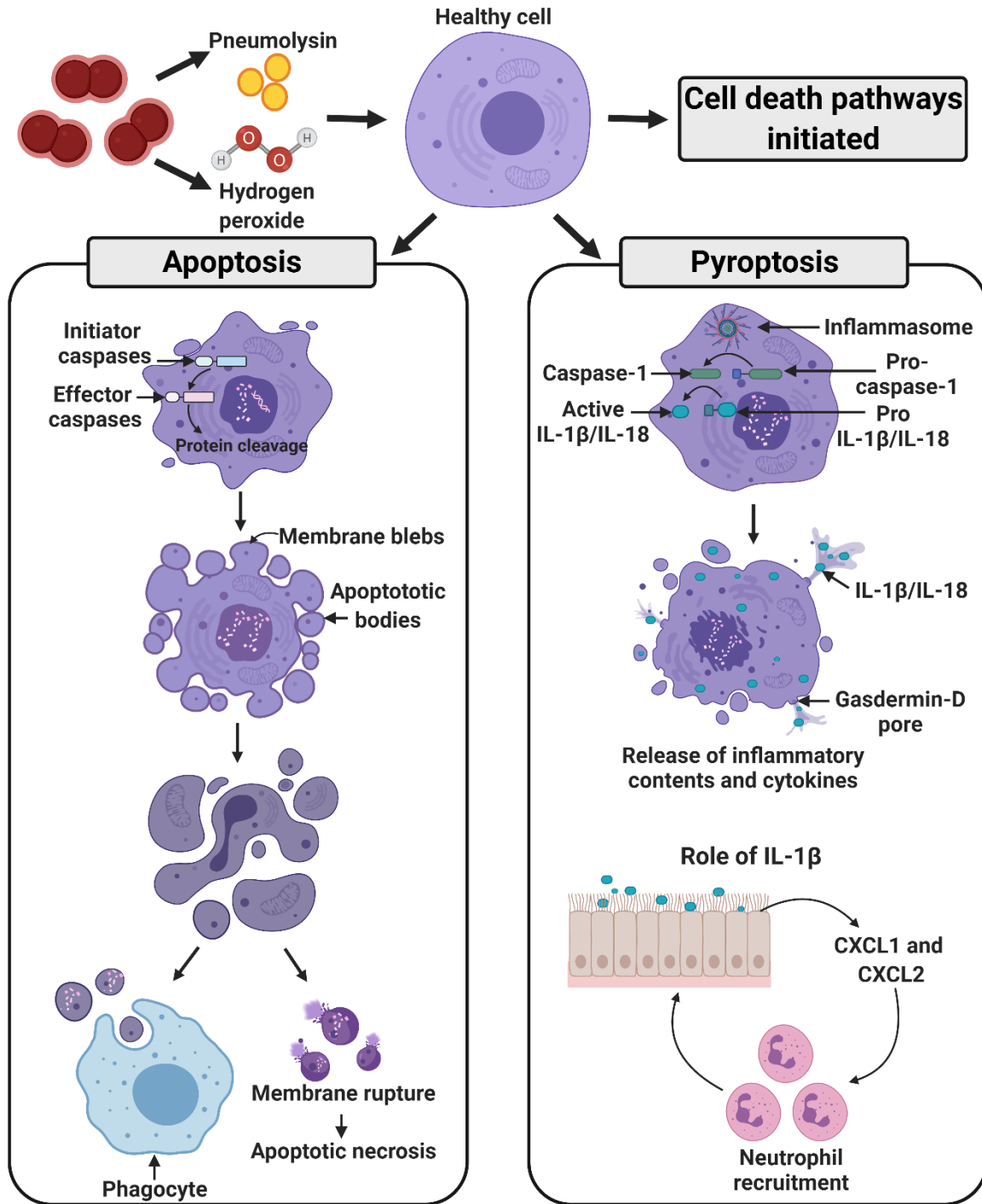


Figure 3.2: Apoptotic and pyroptotic cell death pathways.

Healthy cells respond to death-inducing stimuli by initiating cell death pathways. Apoptosis involves activation of initiator caspases that activate effector caspases to cleave various cellular substrates. Morphological features of apoptotic cells are cytoplasmic and nuclear condensation, formation of apoptotic bodies, maintenance of an intact plasma membrane, and exposure of surface molecules to initiate phagocytosis by professional phagocytes. However, lack of phagocytosis leads to lysis of the apoptotic bodies resulting in apoptotic necrosis. Apoptosis is generally a silent cell death, while pyroptosis is inherently pro-inflammatory. Pyroptosis is mediated by the activation of caspase-1, that leads to activation and release of inflammatory cytokines such as IL-1 β , and IL-18. These cytokines act as chemo-attractants for other immune cells such as neutrophils. Pyroptosis culminates in cell lysis via GSDMD pore formation. Figure created with BioRender.

3.5.3.1 Apoptosis

The phenomena of apoptosis was first described by the German Scientist Carl Vogt in 1842 [148]. However, the term was coined by Kerr and colleagues in 1972 to define a specific morphological pattern of cell death observed during embryonic development and normal cell turnover in healthy adult tissue [149]. Today, apoptosis is classified as a non-inflammatory form of RCD characterized by cytoplasmic shrinking, cell rounding, chromatin condensation, DNA fragmentation and membrane blebbing (Figure 3.2) [150, 151]. It is mediated by apoptotic caspases and can be initiated via 2 distinct pathways.

(i) **Intrinsic pathway**

This pathway is activated by cell intrinsic stresses such as DNA damage, which leads to mitochondrial outer membrane permeabilization (MOMP) [152]. The MOMP pore appears to be formed by the action of Bcl-2 family members, Bcl2 Associated X-protein (BAX) and Bcl2 Antagonist Killer (BAK) [153]. MOMP results in the release of mitochondrial contents including cytochrome c into the cytoplasm. Oligomerization of cytochrome c, apoptotic protease activating factor-1 (Apaf-1) and pro-caspase-9 form an apoptosome, which serves as a platform for initiator caspase-9 activation [154]. Activated caspase 9 in turn cleaves and activates the effector caspases 3 and 7 [155].

(ii) **Extrinsic pathway**

This pathway is activated by cell extrinsic stress signals, which bind to death receptors (DRs) such as Fas and tumor necrosis factor (TNF) receptors. Typical death stimuli include Fas ligand, TNF and TNF-related apoptosis-inducing ligand (TRAIL) [156]. Triggering of DRs by specific death ligands results in the formation of a death-inducing signalling complex (DISC). DISC initiates proximity induced cleavage of pro-caspase-8/10 to active caspase-8/10 [154, 157, 158]. Activated caspase-8/10 further cleaves pro-caspase-3 to active caspase-3. Caspase-8 can also cleave Bcl2 Interacting Protein (BID) into tBID, initiating MOMP and subsequently resulting in the activation of the intrinsic pathway [159]. Thus, caspase-8 activation connects both extrinsic and intrinsic apoptosis.

Both intrinsic and extrinsic pathways, culminate in the activation of the effector caspases. Once activated, they cleave various intracellular substrates such as α -fodrin, gelsolin, p21-activated kinase 2 (PAK2) and many more [160]. Effector caspases cause chromatin

condensation, formation of cytoplasmic blebs and apoptotic bodies which expose surface molecules (Figure 3.2) [161]. Professional phagocytes such as macrophages recognize the apoptotic bodies and ingest them making this form of cell death less inflammatory in nature [162]. If not cleared, the apoptotic bodies rupture, releasing cytosolic DAMPs into the extracellular space, subsequently resulting in apoptotic necrosis (Figure 3.2) [163].

3.5.3.2 NLRP3 Inflammasome and pyroptosis

Pyroptosis was first described in 1992 in *Shigella flexneri* infected macrophages [164], and shortly thereafter a similar cell death phenotype was observed in *S. typhimurium* infected cells [165-167]. The observed phenotype was termed apoptosis based on morphologic characteristics of cell surface blebbing, DNA fragmentation, and chromatin condensation [164-168]. Pyroptosis was subsequently shown to be distinct from apoptosis, due its dependence on caspase-1 [169-171] and the name was coined in 2001 [172]. The definition of pyroptosis now also included cell death executed by other inflammatory caspases, such as human caspase-4, human caspase-5, and mouse caspase-11 [173].

Pyroptosis is driven by activation of multi-protein complexes called the inflammasomes. They are one of the most recently discovered classes of NLRs [174]. Of the 22 NLRs, NLR and pyrin domain containing receptor 3 (NLRP3) inflammasome is by far the best characterized [175]. Caspase-1 is activated in canonical inflammasomes (Figure 3.2 and 3.3), while related caspase-4/5 (human) and caspase-11 (mice) are activated in the non-canonical pathway [176, 177]. Additionally, the non-canonical inflammasome activation only comes in to play in Gram-negative bacterial infections [178].

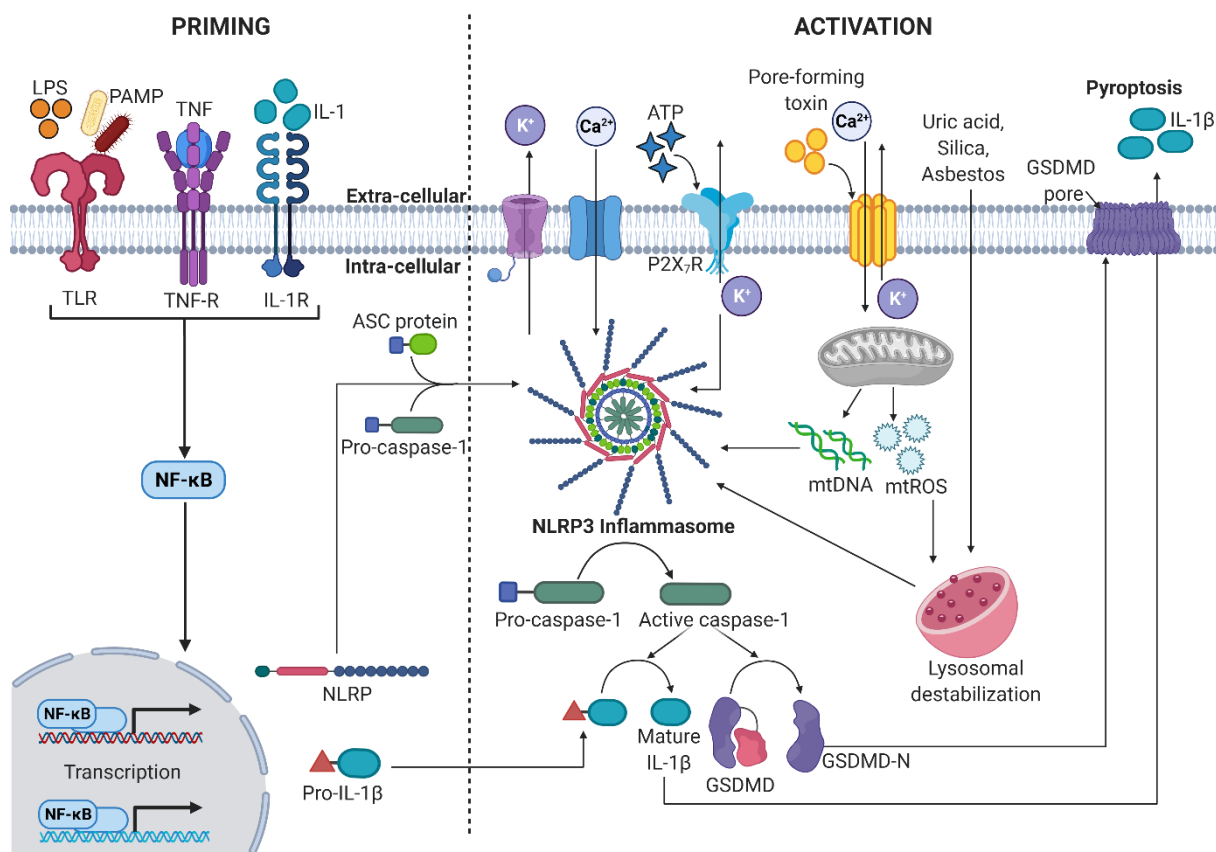


Figure 3.3: Priming and activation of canonical NLRP3 inflammasome.

Microbial molecules such as LPS or endogenous cytokines such as TNF and IL-1 α/β can act as priming molecules. Priming result in the upregulation of *NLRP3* and *pro-IL-1 β* through the activation of the transcription factor NF- κ B. The activation signal is provided by various stimuli, such as pore-forming toxins, ATP and particulate matter. Ca²⁺/K⁺ signaling induced mitochondrial dysfunction results in the release of mitochondrial reactive oxygen species (mtROS) and oxidized mtDNA which activate the inflammasome. Particulate matter can cause lysosomal destabilization which results in inflammasome activation. Activation involves the assembly of NLRP3, ASC-protein and pro-caspase-1 to form the NLRP3 inflammasome, followed by activation of caspase-1. Active caspase-1 cleaves pro-IL-1 β and GSDMD to mature IL-1 β and GSDMD-N, respectively. GSDMD-N pores facilitate the release of IL-1 β to the extracellular environment. Figure created with BioRender.

In most cells, the inflammasome activation occurs in a two-step process, namely, priming and activation (Figure 3.3) [179, 180]. In the priming step, inflammatory triggers such as TLR4 agonists, TNF or IL-1 family proteins, induce the NF- κ B-mediated expression of NLRP3 and pro-IL-1 β [181]. Exposure to an activating signal leads to the assembly and activation of the NLRP3 inflammasome. Common activators of the NLRP3 inflammasome are pathogens [182], pathogen associated RNA, proteins and toxins [183-185], heme [186], endogenous factors (amyloid- β , cholesterol crystals, uric acid crystals) [187-189], and environmental factors (silica and aluminum salts) [189, 190]. ATP released into the extracellular environment by stressed or dying cells can also activate the inflammasome via the purinergic P2X₇ receptor (P2X₇R) [191-195]. However, interaction of any of these activators directly with NLRP3 is

unlikely. It is expected that a common cellular event induced by the activators is sensed by the inflammasome. Currently, cellular events such as changes in cell volume [196], ionic fluxes [197], lysosomal damage [198], ROS production, and/or mitochondrial dysfunction [199] have been implicated in inflammasome activation (Figure 3.3). Upon sensing the activation signal, NLRP3 inflammasome assembly occurs via the oligomerization of the sensor NLRP3 protein, an adaptor apoptosis-associated speck-like protein (ASC), and the zymogen procaspase-1 [200]. Recruited procaspase-1 is converted to bioactive caspase-1 [201], which further cleaves pro-IL-1 β and pro-IL-18 into their respective mature forms. Simultaneously, caspase-1 cleaves gasdermin-D (GSDMD). The N-terminal GSDMD (GSDMD-N) fragment integrates into the cell membrane and forms pores through which IL-1 β , IL-18, other pro-inflammatory cytokines, ATP, eicosanoids, and alarmins are secreted into the extracellular environment. GSDMD-N pores also cause cell lysis and thereby pyroptotic cell death (Figure 3.3) [168, 202, 203]. Released pro-inflammatory compounds accentuate the inflammatory state by recruiting additional inflammatory immune cells of different lineages (Figure 3.2) [204-209]. For example, ATP released through the cell lysis mediates purinergic chemotaxis resulting in neutrophil recruitment and activation at the site of inflammation [191, 210].

3.6 Aim of the thesis

This project focusses on two important virulence factors of pneumococci, namely, H₂O₂ and Ply. These factors have been previously implicated in all phases of pneumococcal disease, including transmission, colonization, and infection. The aim of the thesis was to determine their impact on various innate host defense mechanism.

Specific aims are:

- To summarize the current limited knowledge of inflammasome activation in pneumococcal infections of the respiratory tract and understand why immunocompromised individuals are disproportionately susceptible to bacterial infections.
- To delineate the impact of pneumococcal H₂O₂ on two crucial cell death pathways, namely apoptosis and pyroptosis.
- To understand host metabolic responses in bronchial epithelial cells to pathogens such as Influenza A virus, *Streptococcus pneumoniae*, and *Staphylococcus aureus*.
- To investigate the role of ATP in neutrophil response to pneumococcal infections.

Chapter **4**

METHODOLOGY

4. Experimental approach

This section provides a summary of the main experimental techniques used in this thesis. A detailed description of the experimental procedures is available in the respective articles and manuscripts.

4.1 Bacterial and viral strains

All bacterial and viral strains used in this study are listed in Table 4.1. Detailed description of culture media and growth conditions are mentioned in the respective articles and manuscripts.

Table 4.1: List of bacterial and viral strains used in the study.

Project	Strain and Genotype*	Source or reference	
Paper II	<i>S. pneumoniae</i>	SP408- 19F	[211]
		SP261- TIGR4 (serotype 4)	[212]
		SP257- D39 (serotype 2)	NCTC 7466
		PN111- D39 Δ <i>cps</i> (serotype 2)	[213]
		PN419- D39 Δ <i>cps</i> Δ <i>ply</i>	In this study
		PN777- D39 Δ <i>cps</i> Δ <i>spxB</i>	In this study
		PN778- D39 Δ <i>cps</i> Δ <i>ply</i> Δ <i>spxB</i>	In this study
		<i>S. aureus</i>	LUG2012 (USA300 lineage)
	<i>S. pyogenes</i>	Strain 5448	[215]
Paper III	<i>S. pneumoniae</i>	SP261- TIGR4 (serotype 4)	[212]
		PN779- TIGR4 Δ <i>spxB</i>	In this study
	<i>S. aureus</i>	LUG2012 (USA300 lineage)	[214]
	IAV	A/Bavaria/74/2009 (rH1N1)	In this study
Paper IV	<i>S. pneumoniae</i>	SP261- TIGR4 (serotype 4)	[212]
		PN699- TIGR4 Δ <i>ply</i>	In this study

*Numbering for the pneumococcal strains is from the internal lists of the Department of Molecular Genetics and Infection Biology, Interfaculty Institute of Genetics and Functional Genomics, Center for Functional Genomics of Microbes, University of Greifswald

4.2 Experimental approaches

Epithelial cells span the entire length of the respiratory tract and act as a functional barrier providing critical defense against respiratory pathogens [216]. Bronchial epithelial 16HBE14o-cells (16HBE) [217] were used in **papers II** and **III**, to study the host responses to bacterial and viral infections.

The experimental workflow shown in Fig. 4.1 was used in **paper II** to analyze the impact of pneumococci-derived H_2O_2 on cell death pathways. 16HBE cells were either infected with pneumococci or stimulated with different concentrations of H_2O_2 . For inflammasome related studies, it is crucial to choose the suitable priming agent. LPS is a well-studied TLR agonist and is commonly used as a priming agent [179, 218, 219]. However, during a pneumococcal infection in the lung, pneumococcal lipoproteins can mediate a TLR2 response [220] and could also play a role in priming [221, 222]. Additionally, cytokines such as TNF can prime the cells for inflammasome activation [200, 219]. In **paper II**, cells were stimulated with either LPS or TNF prior to an infection or H_2O_2 stimulation. To inactivate H_2O_2 -mediated actions, catalase was added to the experiments. Samples were collected at different time points for various assays such as qRT-PCR, ELISA and immunoblots.

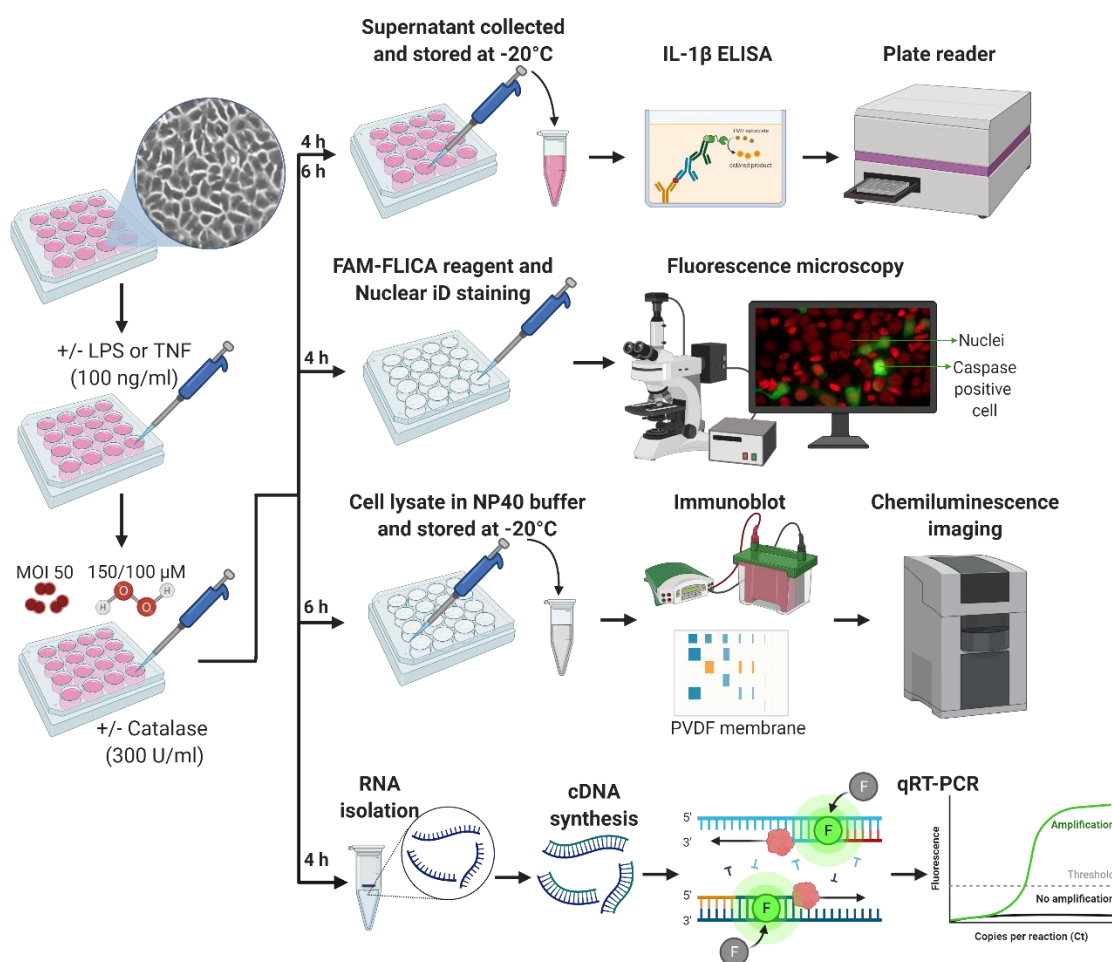


Figure 4.1: Experimental approach used in paper II to study the impact of pneumococci derived H_2O_2 on apoptotic and pyroptotic cell death pathways.

16HBE cells were either infected with pneumococci or stimulated with different concentrations of H_2O_2 for 4 or 6 h in the presence or absence of priming agents. Infected cells were stained with FAM-FLICA reagents to quantify caspase activation. Infection supernatants were used for LDH and $IL-1\beta$ quantification. Cell lysates were used for GSDMN detection via immunoblots. RNA isolation was conducted to determine the relative gene expression of *NLRP3* and *pro-IL-1\beta*. Figure created with BioRender.

Paper III aimed to elucidate the impact of various respiratory pathogens on the host cell metabolome. 16HBE cells were infected with pneumococci, *S. aureus* or H1N1. Viral infections were performed for 24 h, while bacterial infections were conducted for 2 h following the viral infection. Media containing antibiotics were added for additional 2 h and 24 h for pneumococcal and *S. aureus* infections, respectively. Samples for metabolome analysis were collected as shown in the experimental time scheme (Fig. 4.2). The time between harvesting the sample and freezing can be critical. Delay in freezing can result in inconsistent metabolite concentrations [223]. Therefore, samples were immediately snap frozen in liquid nitrogen to minimize enzymatic reactions that can potentially alter the metabolic profile.

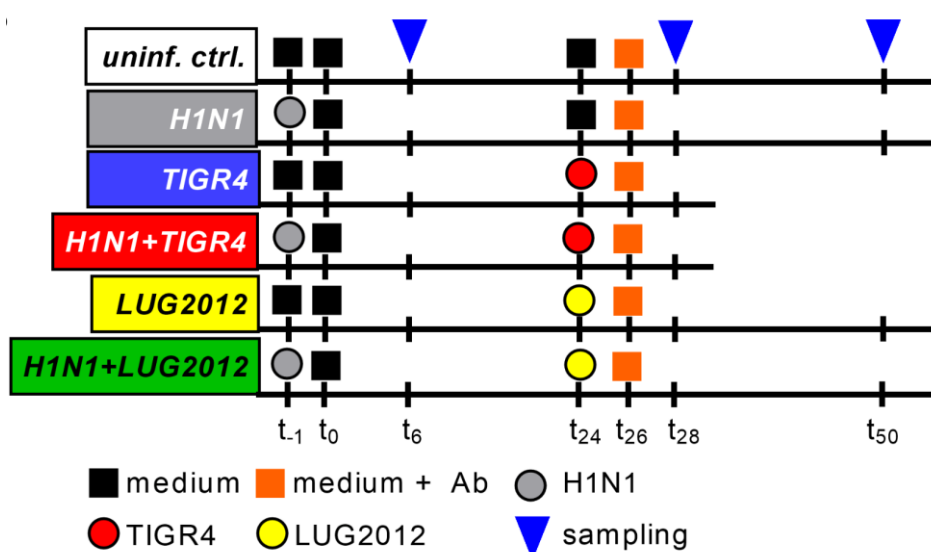


Figure 4.2: Experimental time scheme used in paper III to analyze the changes in the host metabolome post single bacterial (TIGR4 and LUG2012), viral and co-infections.

16HBE cells were infected with the IAV for 24 h, followed by bacterial infections for 2 h. Media containing antibiotics were added for additional 2 h and 24 h for pneumococcal and *S. aureus* infections, respectively. Sampling for metabolome analysis was conducted at t_6 , t_{28} and t_{50} .

Neutrophils are amongst the first immune cells that are recruited to the site of infection and play a major role in clearing the infection via various mechanisms such as phagocytosis, degranulation and NETosis [127, 130, 224]. In **paper IV**, we aimed to determine the interaction between human neutrophils and pneumococcal pore-forming toxin Ply. Primary human neutrophils were isolated from healthy donors using polymorphoprep density gradient centrifugation. Given the relatively brief lifespan of neutrophils in culture, it was important to start the experiments immediately following their isolation from blood. Neutrophils are exquisitely sensitive and undergo rapid activation, thus the isolation technique and handling can have a great influence of the quality and quantity of the isolated neutrophils. Unless stated otherwise, the cells were always maintained at physiologic pH and in the absence of divalent

cations to help reduce activation. All media components that came in contact with blood or cells were pyrogen-free. Pyrogen-free polypropylene tubes were used to limit adherence-induced activation.

Freshly isolated neutrophils were either infected with pneumococci or stimulated with different concentrations of recombinant Ply, ATP, or bacterial lysates. Neutrophil supernatants were used to analyze the secretome, cell cytotoxicity and resistin release. Microscale thermophoresis, FACS analysis and Field Emission Scanning Electron Microscopy (FESEM) techniques were used to elucidate the interaction between Ply, ATP and neutrophils. Donor variations are always a challenge when working with primary cells. Thus, the number of biological replicates were increased up to 10 for some of the experiments to reduce standard deviation.

4.3 Enzyme-linked immunosorbent assay (ELISA)

ELISA is a widely used method to quantitatively detect soluble antigens such as peptides, proteins and hormones, using antibodies conjugated with reporter enzyme. Upon addition of the substrate, the reporter enzyme catalyzes the production of a colorimetric molecule that can be quantified using a plate reader. ELISA can be used to detect a wide range of targets from diverse sample types such as cell lysate, culture supernatants, blood samples and many more. [225]. In **paper II**, ELISA was used to quantify IL-1 β release from cells infected or stimulated with pneumococci or H₂O₂, respectively. In **paper III**, resistin concentrations in supernatants of neutrophils were measured as an indicator of neutrophil degranulation post stimulation with Ply. Freeze thaw cycles can highly impact cytokine and protein concentrations in the sample [226]. Thus, freeze-thaw cycles were avoided to obtain accurate results.

4.4 Microscopy

Microscopy based methods have been very useful during the course of the project. Fluorescence microscopy was used in **paper II** to characterize and quantify caspase activation in the intracellular environment as a result of pneumococcal infection or H₂O₂ stimulation. Cell permeable fluorescent probes FAM-YVAD-FMK FLICA or FAM-DEVD-FMK FLICA were used to label active caspase-1 and caspase-3/7, respectively. The staining was visualized using an Axio Observer Z1 microscope (Zeiss). Quantification of active caspases was conducted by enumerating the caspase-1 or caspase-3/7 active cells in relation to the total cell number. Multiple technical and biological replicates were maintained to overcome human bias.

Field emission scanning electron microscopy (FESEM) was used in **paper IV** to visualize the impact of Ply vs Ply-ATP interaction on neutrophil morphology and activation. FESEM was performed with multiple biological replicates to account for donor variations.

4.5 Statistical Analyses

Statistics were performed using GraphPad Prism software, version 7. If not otherwise indicated, statistical significance of difference was determined using Kruskal Wallis test with Dunn post-test. A *P* value less than 0.05 was considered significant (*, $p < 0.05$; **, $p < 0.01$; ***, $p < 0.001$).

4.6 Ethics Statement

Paper III mainly involved working with blood samples from healthy volunteer. Donors were well acquainted with the research conducted and written informed consent was obtained to perform the study. The ethical research committee at the University Medicine Greifswald approved the study (BB 006/18). All experiments were carried out in accordance with the approved guidelines.

Chapter **5**

RESULTS AND DISCUSSION

5. Results and Discussion

5.1 NLRP3 inflammasome plays a crucial role in pneumococcal infections

The innate immune response is the first line of defence against invading pathogens. It limits the spread of the pathogen and initiates specific adaptive immune responses. The intracellular Nod-like receptor NLRP3 is by far the best characterized innate immune receptor [175]. NLRP3 is expressed in many cell types including immune cells and epithelial cells, and is known to play a crucial role in the regulation of the host innate immune response [227]. Of all the 22 NLRs, NLRP3 is the most diverse innate immune receptor because of its broad specificity in mediating immune response to a wide range of stimuli [200]. Several studies have now uncovered the pivotal role of the NLRP3 inflammasome in microbial infections. NLRP3 inflammasome induces state of inflammation following detection of PAMPs/DAMPs in the cellular cytoplasm, thereby resulting in pathogen clearance [228].

In **paper I**, we discuss the structure, assembly and activation of the NLRP3 inflammasome. We explore various IL-1 β inhibiting drugs and summarize the current limited knowledge of inflammasome activation in pneumococcal respiratory tract infections.

5.1.1 IL-1 β inhibiting drugs and their side effects

The unregulated activation of the NLRP3 inflammasome has been implicated in the onset of various diseases, including gout [189], inflammatory bowel disease (IBD) [229], Alzheimer's disease [230, 231], atherosclerosis [188], type II diabetes [232, 233], and Cryopyrin-associated periodic syndrome (CAPS) [234]. Its role in various types of cancer such as colon cancer, breast cancer, melanoma, and gastrointestinal cancers has also been reported [235]. Although these diseases are very diverse in nature, they are all characterized by IL-1 β mediated inflammation. Therefore, NLRP3 inflammasome signaling cascade and IL-1 β are considered promising targets for the treatment of these auto-inflammatory and autoimmune diseases [236]. Although several inhibitors of the NLRP3 inflammasome have been developed (**paper I**, Table 1), only three drugs have been clinically approved by the FDA, namely Anakinra, Riloncept and Canakinumab (Table 5.1) [237].

Table 5.1: Clinically approved IL-1 inhibiting drugs

Drug	Target	Inhibition mechanism	Side effects	Reference
Anakinra	IL-1 receptor	IL-1 receptor antagonist	Increased risk to infections such as cellulitis, pneumonia, and bone and joint infections	[238]
Rilonacept	IL-1 α and IL-1 β	IL-1 blocker	Patients are prone to skin reactions and upper respiratory tract infections	[239, 240]
Canakinumab	IL-1 β	Monoclonal IgG1 antibody	Respiratory tract infections are a major side effect	[239, 241, 242]

Anakinra is a reversible IL-1 receptor (IL-1R) antagonist and can competitively inhibit both IL-1 α and IL-1 β . It is commonly used for the treatment of RA, acute gouty arthritis, and CAPS [237, 243, 244]. Unlike anakinra that interacts with the IL-1 receptor, rilonacept binds directly to IL-1 α and IL-1 β . It is a dimeric fusion protein that consists of the ligand-binding domains of the extracellular portions of the human IL-1R component and IL-1R accessory protein linked in-line to the Fc portion of human IgG1 [239, 240]. It is used to treat CAPS, including Familial Cold Auto-inflammatory Syndrome (FCAS) and Muckle-Wells Syndrome (MWS) [240]. While anakinra and rilonacept block the activity of both IL-1 isoforms, Canakinumab is a monoclonal IgG1 designed to specifically target the activity of IL-1 β . It is commonly used for treatment of Periodic Fever Syndromes, MWS, and acute gouty arthritis [239, 241, 242].

Although all above-mentioned therapies are well tolerated in the majority of patients, they also have side effects (table 5.1). Anakinra was approved in 2001 by FDA and has been used for a longer period as compared to rilonacept or canakinumab. Therefore, more adverse reactions post treatment with anakinra are documented [238-241]. From the clinical trial data as well as increasing clinical usage, it is evident that patients undergoing IL-1 inhibiting therapies are disproportionately susceptible to bacterial infections such as pneumonia and sepsis [237, 245]. Therefore, it is of high importance to understand the role of NLRP3 inflammasome in bacterial pathogenesis. The current literature on the impact of NLRP3 inflammasome on pneumococcal infections is limited. While inflammasome activation is deemed to be protective in pneumococcal pneumonia [41, 42], it is considered detrimental in pneumococcal meningitis [246]. This indicates that well-orchestrated inflammasome activation results in bacterial clearance, while a hyper-reactive response is injurious to the host. For instance, IL-1 β produced upon NLRP3 activation is a chemoattractant for neutrophils and macrophages, both of which are responsible for clearing the infection [207, 208]. However, uncontrolled inflammasome

activation and inflammation can result in pyroptosis and tissue injury [247-249]. This tissue damage can aid in bacterial dissemination to the deeper tissue layers [9, 249].

5.1.2 H₂O₂ produced by pneumococci induces cell death

Pneumococci are equipped with a repertoire of virulence factors allowing them to circumvent the host immune response. Apart from Ply, pneumococci release high amounts of H₂O₂ as a product of the pneumococcal carbohydrate-metabolizing enzyme pyruvate oxidase SpxB [49]. Although previous literature indicates the importance of pneumococcal H₂O₂ in causing cell damage, not much is known about its impact on the activation of cell death pathways such as apoptosis and pyroptosis [250, 251].

In **paper II**, we aimed to determine the role of H₂O₂ in NLRP3 inflammasome activation and cell death. Isogenic single *ply* and *spxB* as well as double mutants were generated in the D39Δ*cps* background. *Ply*-deficient mutants were included in this study to exclude Ply-mediated cytotoxic effects. Mutants were verified by using both nucleic acid techniques as well as immunoblots targeting Ply and SpxB proteins (**paper II**, Supplementary Fig. S3). In addition, H₂O₂ production by all four strains was verified (**paper II**, Fig. 2b).

To elucidate the role of an active SpxB in pneumococcal infections of human bronchial epithelial cells, 16HBE cells were infected with D39Δ*cps* or its isogenic mutants. Analyses of the cell viability revealed that infections with pneumococci harboring an active *spxB* gene were characterized by a time-dependent increase in cell cytotoxicity (**paper II**, Fig. 2f). In contrast, pneumococcal mutants lacking *spxB* were not cytotoxic (**paper II**, Fig. 2f). Addition of catalase to D39Δ*cps* infections significantly diminished the cytotoxicity (**paper II**, Fig. 1a). Therefore, these results clearly implicate pneumococcal H₂O₂ as a primary cause of epithelial cell death in the early stages of infection.

5.1.3 H₂O₂ activates inflammasome signaling resulting in IL-1β release

Cell death is the most common outcome during infections. An infected cell can undergo different modes of cell death depending on the nature of the infection [252]. However, in **paper II**, we focused on the impact of pneumococcal H₂O₂ on two main caspase dependent cell death pathways, namely apoptosis and pyroptosis. Since NLRP3 inflammasome activation involves a priming step for NF-κB activation and subsequent transcription of pro-*IL-1β* and *NLRP3* [253], cells were stimulated with LPS and TNF prior to infections/stimulations.

To assess caspase activation prior to the excessive cell lysis, unprimed and primed 16HBE cells were infected with pneumococcal strains for 4 h. Caspase-1 and caspase-3/7 activation was determined via fluorescent probing with FAM-YVAD-FMK FLICA and FAM-DEVD-FMK FLICA, respectively. D39 *spxB*-positive strains were slightly cytotoxic and activated caspase-1 and caspase-3/7 were detected in 10-20% of the infected cells (**paper II**, Fig. 3 and S4a). In contrast, *spxB* mutants did not cause cell lysis and cells remained negative for active caspases (**paper II**, Fig. 3 and S4a). To confirm that caspase activation and the consequential cell death are caused by H₂O₂, 16HBE cells were stimulated directly with H₂O₂. H₂O₂ stimulations were associated with a dose-dependent increase in cytotoxicity towards the cells and the addition of catalase reverted this cytolytic effect (**paper II**, Fig. S5). Microscopic analysis of caspase activation revealed caspase-1 and caspase-3/7 activation in H₂O₂ stimulated cells (**paper II**, Fig. 4 and S4b). Caspase activation in these cells was accompanied by minor cytotoxic activity. Addition of catalase significantly reduced the H₂O₂-mediated cytotoxic effects as well as caspase activation (**paper II**, Fig. 4 and S4b). The observed infection and stimulation phenotypes were independent of priming.

Active caspase-1 readily cleaves pro-IL-1 β into mature form [200, 247]. The mature IL-1 β is mostly released from the cells via GSDMD pores [168, 202, 203, 247, 254]. IL-1 β concentrations in 4 h and 6 h infection/stimulation supernatants were quantified using IL-1 β ELISA. Consistent with the cytotoxicity data (**paper II**, Fig. 2f), IL-1 β was exclusively detected after 6 h of infections with *SpxB*-positive strains (**paper II**, Fig. 5a). Additionally, the highest amounts of IL-1 β were detected 6 h post H₂O₂ stimulations (**paper II**, Fig. 5b). Addition of catalase neutralized H₂O₂-mediated IL-1 β release in both D39 Δ *cps* infections and H₂O₂ stimulations (**paper II**, Fig. 1b and 5a). Both assessed parameters i.e., caspase activation and IL-1 β release confirm that pneumococcal H₂O₂ triggers both apoptotic as well as pyroptotic pathways (Fig. 5.1). These results are also consistent with the literature that indicates that H₂O₂ is a potent activator of apoptosis [38, 251]. In contrast, only one study analyzed H₂O₂-mediated effects on the NLRP3 inflammasome in pneumococcal infections. Ertmann and Gekara have shown that pneumococcal H₂O₂ suppresses ATP-mediated inflammasome activation in mouse bone marrow-derived macrophages (mBMDMs). The authors suggested that pneumococci use H₂O₂ to suppress the immune system and establish colonization [218]. However, this study considered the impact of pneumococcal H₂O₂ at very early stages (30 min) of pneumococcal infection. In contrast, we observed that pneumococcal infections were highly damaging in nature. This result is consistent with other studies which show that H₂O₂ is highly cytotoxic

[250, 255]. Pneumococci-derived H₂O₂ can cause oxidative damage to nuclear and mitochondrial DNA (mtDNA) [250, 251] resulting in activation of both apoptosis [256, 257] and NLRP3 inflammasome [258-260].

Similar to H₂O₂, Ply has also been implicated in many cytotoxic processes [42, 261, 262]. Previous studies have shown that Ply activates the NLRP3 inflammasome [41]. However, it is noteworthy to mention that Ply is only released at the late stage of growth [31]. Additionally, in **paper IV**, we also show that Ply-deficient mutants are as cytotoxic as their parental strain in the early phase of infection (**paper IV**, Fig. 2a) [57]. Therefore, it is plausible that H₂O₂ mediated effects on inflammasome mediated cell death are observed earlier during the infection, while Ply mediated effects occur at the later stages of infection.

5.1.4 H₂O₂ primes the NLRP3 inflammasome

In cells such as macrophages and epithelial cells, priming is indispensable for the activation of the NLRP3 inflammasome [179, 180]. NF-κB is activated upon detection of a priming signal, which further upregulates the gene expression of *NLRP3* and *pro-IL-1β*. The exposure to an activating signal leads to the assembly and activation of the NLRP3 inflammasome and cleavage of the pro-IL-1β to its mature form [263]. However, in this study, all assessed parameters, namely cytotoxicity, caspase activation as well as IL-1β release, were independent of a priming step. This indicated the plausible role of H₂O₂ as a priming agent. To confirm this hypothesis, *NLRP3* and *pro-IL-1β* mRNA expression in the infected and H₂O₂ stimulated cells was quantified using qRT-PCR. Cells stimulated with LPS and ATP served as a positive control. *NLRP3* and *pro-IL-1β* expression were upregulated in cells infected with *spxB* positive strains compared to the *spxB* mutants (**paper II**, Fig. 5c-d). Upregulation in the expression of both genes was also detected in cells stimulated with H₂O₂ and addition of catalase reversed this effect (**paper II**, Fig. 5c-d). These results confirmed that H₂O₂ can prime as well as activate the inflammasome in epithelial cells (Fig. 5.1). This finding is further supported by previous studies which show that H₂O₂ can directly activate NF-κB through the NF-κB-inducing kinase (NIK) [264-266].

5.1.5 IL-1 β release caused by H₂O₂ is a result of inflammasome activation but not pyroptosis

To confirm the involvement of apoptotic and pyroptotic pathways on cell death, pathway inhibition studies were performed. D39 Δ *cps* infections as well as H₂O₂ stimulations of host cells for 6 h resulted in cell death and subsequent IL-1 β release. However, blocking either one or both host cell death pathways resulted in significantly reduced cell death (**paper II**, Fig. 6a and 6c). Interestingly, significantly reduced IL-1 β release was observed when infected/stimulated cells were pretreated with only apoptotic pathway inhibitor (**paper II**, Fig. 6b and 6d). Release of mature IL-1 β occurs in pyroptotic cells via GSDMD pores [168, 202, 203, 247, 254]. However, our results indicated that although H₂O₂ instigates IL-1 β production, the final IL-1 β release is also dependent on the apoptotic cell death pathway. To validate these findings, infected/stimulated cell lysates were analyzed for GSDMD cleavage products. Western blot analysis revealed that GSDMD either remained intact or was cleaved by caspase-3 to an inactive 43 kDa fragment [267] in cells stimulated with H₂O₂ (**paper II**, Fig. 6f and Fig. S8). Results from the inhibition studies and lack of the active 30 kDa fragment (active fragment cleaved by caspase-1) suggest that the IL-1 β release in pneumococcal infections is independent of GSDMD and relies on apoptotic cell lysis. These results are in line with previous studies suggesting that prolonged stimulation of the inflammasome can potentially result in GSDMD-independent cell death and IL-1 β release [268].

A linear model of pyroptosis has been followed for years, wherein activated caspase-1 cleaves pro-IL-1 β and GSDMD to IL-1 β and GSDMD-N, respectively. The GSDMD-N forms membrane pores through which IL-1 β is released [168, 202, 203]. However, in complex cellular environment this is not always true. Cross-talks between various cell death pathways determine the final fate of the cell. Studies have shown that caspase-1 can redundantly activate apoptotic executioner caspase-3 and caspase-7 [269]. Additionally, caspase-3 can induce secondary necrotic/pyroptotic cell death via GSDME/DFNA5 mediated pore formation [247, 270]. H₂O₂ can also induce necroptosis through the RIP1/RIP3-PARP-AIF pathway [271]. Studies have shown that mixed lineage kinase domain-like (MLKL), a marker for necroptosis, activates the inflammasome and the consequential IL-1 β release is a result of MLKL mediated cell rupture [272]. Complex interplay between effector molecules of various cell death pathways can also result in the formation of PANoptosome (Pyroptosis, Apoptosis, Necroptosis). Activation of the PANoptosome results in a highly interconnected cell death called PANoptosis.

Therefore, further studies into other cell death pathways such as necroptosis and PANoptosis are required to delineate the true nature of cell death induced by pneumococcal- H_2O_2 .

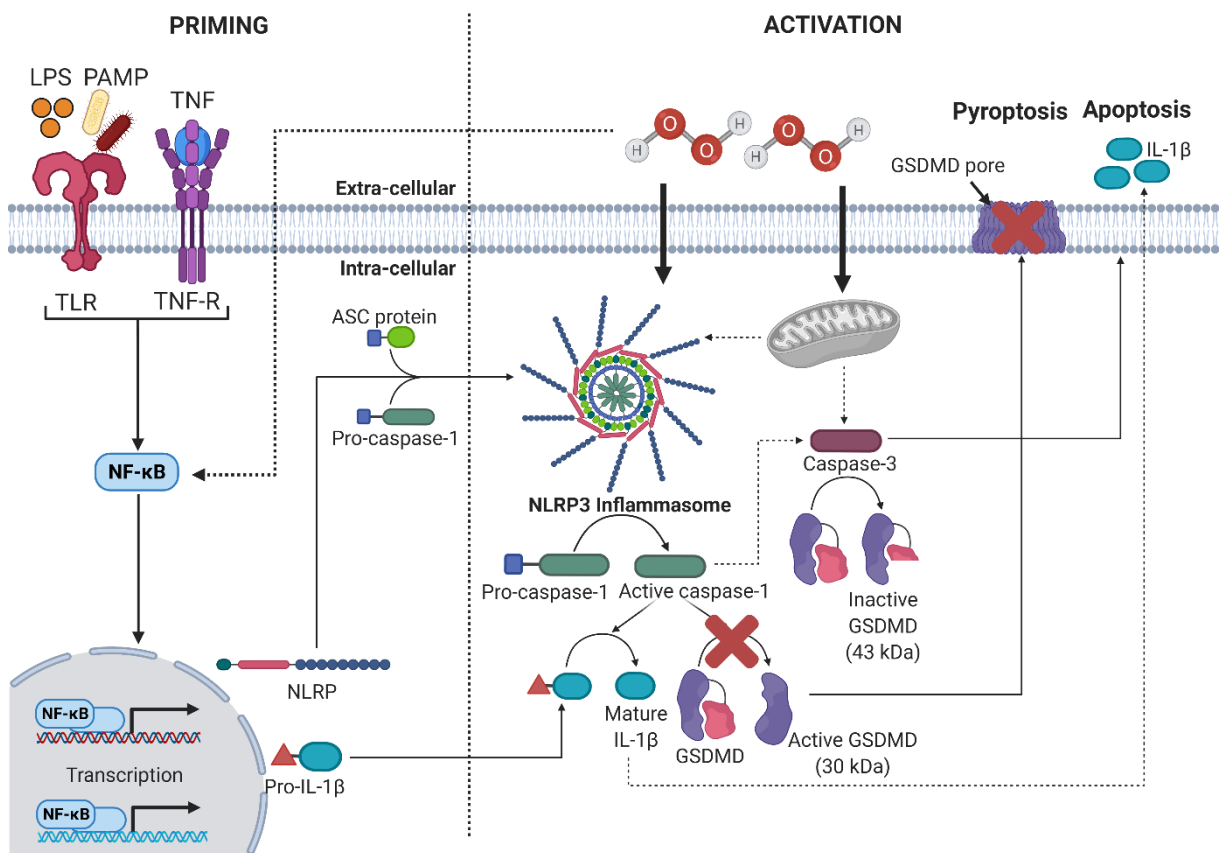


Figure 5.1: Pneumococcal H_2O_2 primes and activates the NLRP3 inflammasome pathway resulting in pyroptosis-independent $IL-1\beta$ release.

H_2O_2 primes 16HBE cells resulting in NF- κ B activation, which initiates the transcription of *NLRP* and *pro-IL-1\beta*. H_2O_2 also activates caspase-3 and initiates the assembly of the NLRP3 inflammasome. Pro-caspase-1 is activated to active caspase-1 by the inflammasome. Caspase-1 cleaves pro- $IL-1\beta$ to active $IL-1\beta$. Meanwhile, GSDMD is cleaved to an inactive form by caspase-3. Therefore, the final $IL-1\beta$ release is mediated by caspase-3 dependent apoptotic cell lysis. Figure created with BioRender.

5.2 Host metabolome responses to respiratory infections

To unravel the dynamic nature of host pathogen interactions, it is crucial to understand host cellular metabolome as it directly influences the infection phenotype [273]. Active cellular metabolome helps maintain cellular health as well as indirectly facilitates mucociliary pathogen clearance [274]. Energy derived from active metabolic pathways are utilized by lung epithelial cells for specialized functions such as surfactant production and ciliary beating [275]. Recent studies have linked the metabolic dysfunction of lung epithelial cells to the pathobiology of respiratory diseases [275]. In **paper III**, we performed a comparative host metabolome

profiling of *in vitro* single bacterial and viral as well as co-infections of bronchial epithelial cells with IAV, *Streptococcus pneumoniae*, and *Staphylococcus aureus*.

5.2.1 Pneumococcal infections result in intracellular citrate accumulation

To understand the impact of bacterial and viral mono- and bacterial-viral co-infections on the host metabolome, a cell culture-based system of 16HBE cells was used (**paper III**, Fig. 1a). Intracellular metabolites of glycolysis, TCA cycle, and amino acids metabolism were quantified by GC-MS analysis. *S. pneumoniae* significantly altered several host metabolic pathways (**paper III**, Fig. 2-3). Intracellular citrate accumulation was the most prominent signature of pneumococcal infections (Fig. 5.2, **paper III**, Fig. 3a). However, concentrations of other TCA cycle metabolites decreased in response to pneumococcal infections (Fig. 5.2, Fig. 3c-g). Unlike pneumococci, IAV and *S. aureus* survive silently within the cells with almost negligible effects on the host metabolome and no specific co-infection signatures were observed (**paper III**, Fig. 2-3). Staphylococci can thrive intracellularly for prolonged periods of time by adapting their regulatory network to the intracellular environment [69, 70]. Previous studies have shown that infection of A549 cells with a high inoculum of *S. aureus* leads to significant changes in the host metabolome, especially after 6 hours of infection [276]. In contrast, we observed only minor changes in the host metabolome, most likely due to the cell-specific responses to low inoculum infections. Similar to *S. aureus*, viral infections also had minimal effects on the host metabolome. Viral replication and protein production are accompanied by a “host shutoff”, that leads to downregulation of host gene expression [277, 278]. However, studies have also shown that increased glucose uptake and upregulation of glycolysis support viral replication [279, 280]. The mild infectivity of the 2009 pandemic H1N1 IAV strain used in this study may explain the incongruence of our results with these studies.

5.2.2 Intracellular citrate accumulation is a consequence of the action of pneumococcal H₂O₂

Citrate is a key substrate in cellular energy metabolism. Once produced in the mitochondria, it most likely undergoes different fates: (i) by the action of aconitase, citrate is isomerized to isocitrate, and proceeds into the TCA cycle, or (ii) it is exported to the cytoplasm via the mitochondrial citrate carrier (CIC) [281].

Inhibition of either aconitase or CIC during pneumococcal infection could explain the accumulation of citrate. Consequently, citrate accumulation potentially blocks the entire TCA cycle. No major changes were detected in transcription of *SLC25A* (encodes CIC) [281], *ACO1* and *ACO2* (encode aconitase) compared to the uninfected control (**paper III**, Table S1), indicating a plausible inhibition potentially at the protein level. The *Bacillus subtilis* protein CcpC has been shown to inhibit aconitase transcription and CcpC orthologs have also been found in pneumococci [282, 283]. Whether pneumococcal orthologs are able to inhibit host aconitase remains to be determined. Additionally, studies show that iron-sulfur cluster-containing enzymes such as aconitase are irreversibly inactivated by reactive oxygen species, including H₂O₂ [284-286]. Therefore, to determine the impact of pneumococcal H₂O₂ on intracellular citrate accumulation, we generated a TIGR4 Δ *spxB* mutant. The SpxB-deficient mutant produced significantly lower amounts of H₂O₂ as compared to the wild-type strain (**paper III**, Fig. 4b). 16HBE cells were infected with TIGR4 or the *spxB*-deficient mutant, following the protocol outlined in **paper III**, Fig. 1a. Direct stimulations with H₂O₂ were also performed. In addition, catalase was added to wild-type infection and H₂O₂ stimulation to neutralize the effects of H₂O₂. Consequently, intracellular citrate accumulation was only observed in TIGR4 wild-type infection and H₂O₂ stimulation (**paper III**, Fig. 4d). Intracellular citrate concentrations significantly decreased in infections/stimulations supplemented with catalase and remained at the level of uninfected control in infections with TIGR4 Δ *spxB*. These results clearly demonstrated that pneumococcal H₂O₂ contributes to intracellular citrate accumulation in 16HBE cells (Fig. 5.2). Mitochondrial ROS formation induced by excessive citrate accumulation has been shown to activate the NLRP3 inflammasome in *Salmonella typhimurium* infections [287]. We have shown in **paper II** that pneumococci-derived H₂O₂ activates the NLRP3 inflammasome and induces apoptosis in 16HBE cells. However, the role of excessive intracellular citrate in H₂O₂-mediated inflammasome activation and cell death remains to be elucidated.

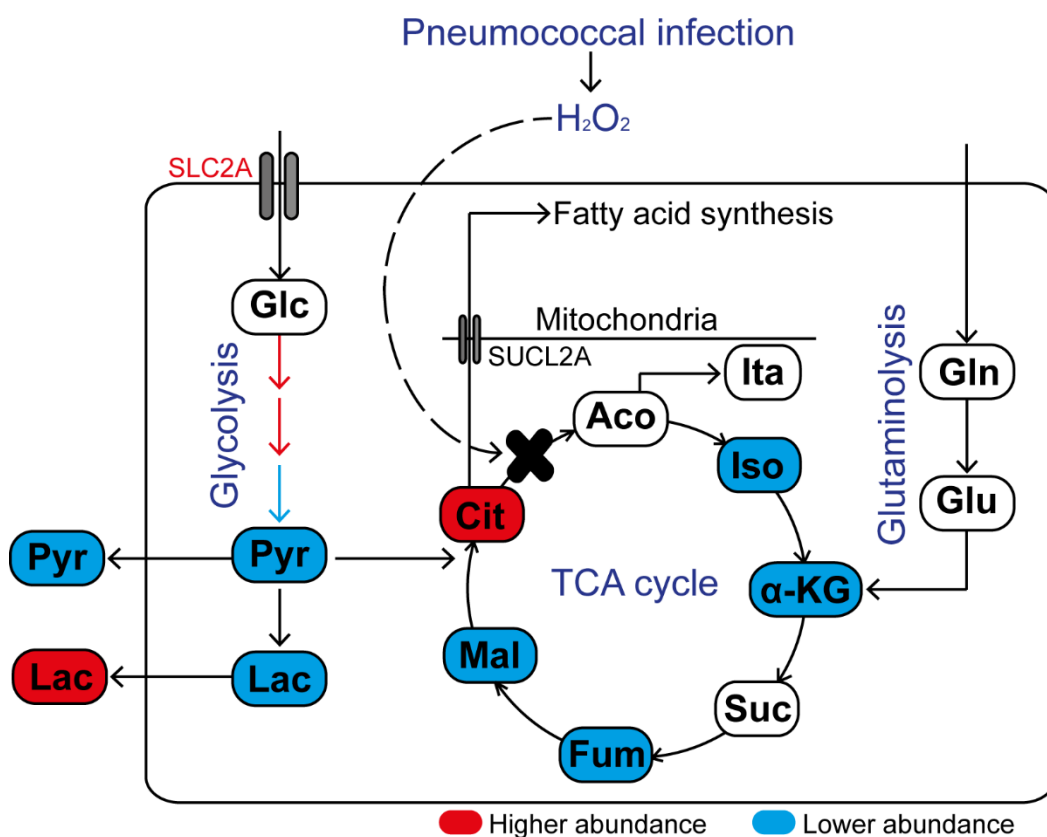


Figure 5.2: Intracellular citrate accumulation is a consequence of pneumococcal H_2O_2 .

Pneumococci significantly alter various host metabolome pathways such as glycolysis, TCA cycle and amino acid metabolism. Intracellular citrate accumulation is a hallmark of pneumococcal infection and is directly attributed to the action of pneumococci-derived H_2O_2 .

5.3 Influence of Ply-ATP interactions on neutrophil activation

Pathogen-induced host cell death is accompanied by the release of pro-inflammatory cytokines and DAMPs such as ATP. Once in the extracellular milieu, ATP can initiate purinergic signaling and neutrophil chemotaxis [191, 288, 289]. Neutrophils are the most abundant leukocytes in humans and are the first recruited responders at the site of infection. They eliminate pathogens through various mechanisms such as phagocytosis, degranulation, and the formation of NETs [127, 130, 290]. However, excessive neutrophil activation is associated with hyper inflammation and tissue damage [291]. In **paper IV**, we aimed to investigate the role of ATP in neutrophil response to pneumococcal toxin Ply.

5.3.1 Pneumolysin induces neutrophil activation

To determine the effect of Ply on neutrophil activation, purified neutrophils were stimulated with the cytoplasmic fraction of TIGR4 wild-type (wt) and Δply lysates. Resistin was used as a

marker to determine neutrophil activation. Stimulation of neutrophils with the cytoplasmic fraction of TIGR4 wt had minor cytolytic effects but resulted in high resistin release (**paper IV**, Fig. 2c-d). In contrast, Δply lysates did not induce cytotoxicity or neutrophil activation (**paper IV**, Fig. 2c-d). This result suggests that Ply is one of the major pneumococcal cytoplasmic components responsible for neutrophil activation. TIGR4 wt and Δply infections of whole blood and purified neutrophils were also performed. Both strains showed minor cytotoxic effects and induced neutrophil activation to the same extent (**paper IV**, Fig. 1d and 2a-b), indicating Ply-independent neutrophil activation. This effect may be caused by pneumococcal- H_2O_2 , because it can induce disruption of neutrophil barrier properties and cell death [292]. However, possible neutrophil activation by other pneumococcal virulence factors cannot be excluded.

Furthermore, neutrophils were also stimulated with different concentrations of purified Ply. Stimulations were performed with and without supplementation of autologous plasma. A concentration-dependent lysis of neutrophils was observed (**paper IV**, Fig. 3a). Based on cytotoxicity assays with plasma supplementation, 0.3125 μg and 2.5 μg Ply were defined as sublytic and lytic amounts of Ply, respectively. Both sublytic and lytic concentrations of Ply were able to induce neutrophil degranulation (**paper IV**, Fig. 3b). Immunofluorescence imaging of Ply-stimulated neutrophils confirmed the presence of Ply on neutrophil surface even at sublytic concentrations (**paper IV**, Fig. 3c).

5.3.2 ATP neutralizes Ply-induced neutrophil lysis and activation

Studies suggest that Ply induces neutrophil activation through specific interactions with the purinergic receptor P2X₇R [293]. The P2X₇R also serves as a pattern recognition receptor for extracellular ATP-mediated apoptotic cell death and inflammasome activation [193, 210]. Under physiological conditions, ATP is present in low concentrations in the extracellular milieu and is mainly released from dying cells [194, 195, 294]. Nevertheless, as a result of tissue infections, extracellular ATP levels can reach up to mM ranges [191, 295]. Once outside, it functions as a danger signal and is involved in neutrophil chemotaxis mediated by purinergic signaling [191, 288, 289]. To investigate the direct effect of Ply and ATP on neutrophil activation, we stimulated purified neutrophils with sublytic and lytic concentrations of Ply in the presence and/or absence of P2X₇R agonist ATP and/or pharmacological P2X₇R inhibitor AZ10606120 (**paper IV**, Fig. 4 and Supplementary Fig. 3). Ply-mediated neutrophil lysis (**paper IV**, Supplementary Fig. 3) and degranulation (**paper IV**, Fig. 4a), diminished with

increasing concentration of ATP. AZ10606120 did not affect Ply-neutrophil interactions. This result contradicts studies by Domon et. al., suggesting that Ply interacts with P2X₇R to induce neutrophil cytotoxicity [293]. However, it cannot be excluded that Ply interacts with other neutrophil receptors to initiate activation.

To further validate these results, we analyzed the secretome composition of neutrophils stimulated with Ply and ATP. Samples stimulated with both Ply and ATP had significantly fewer peptides/proteins than those stimulated with Ply alone (**paper IV**, Fig. 4b and Supplementary Table 1). Principal component analysis (PCA) showed that samples exposed to both sublytic and lytic concentrations of Ply clustered together, suggesting that a sublytic amount of Ply potentially activates neutrophils (**paper IV**, Fig. 4c). The released granule content of stimulations with sublytic Ply concentration was equivalent to that of lytic stimulations (**paper IV**, Fig. 4b and Supplementary Tables 5 and 6). The secretome of Ply-ATP stimulated neutrophils had significantly lower protein abundance compared to neutrophils stimulated with Ply alone. Additionally, using g:Profiler pathway analyzes, we confirmed that use of ATP inhibited various neutrophil defense mechanisms such as activation, degranulation, and immune responses (**paper IV**, Fig. 5).

5.3.3 Ply and ATP directly interact with each other

Ply mediated neutrophil degranulation was independent of P2X₇R. However, addition of ATP significantly diminished Ply mediated neutrophil degranulation. Therefore, we hypothesized that ATP and Ply interact with each other in the extracellular space. Microscale thermophoresis revealed that both ATP and ADP interact with Ply, albeit weakly (**paper IV**, Fig. 6a and 6c). On the contrary, dATP showed no such interaction (**paper IV**, Fig. 6b). Flow cytometry analysis further confirmed this finding. Addition of ATP to Ply stimulations almost completely abolished Ply binding to the neutrophils (**paper IV**, Figure 6d). These results confirmed that ATP directly binds to Ply thereby dampening Ply mediated neutrophil degranulation. Our results are further supported by the studies which show that vital pneumococci can suppress ATP-mediated responses of alveolar epithelial cells [296].

The biological relevance of Ply-ATP interactions remains debatable. On the one hand, Ply-ATP interactions can potentially be beneficial for the host. Firstly, tissue damage caused by excessive activation of neutrophils is diminished as a result of Ply-ATP binding. Secondly, both Ply and ATP can initiate inflammasome activation, resulting in pyroptotic cell death [179, 192, 193,

263]. Further increments to host tissue damage induced by uncontrolled inflammasome activation could be possibly limited by Ply-ATP interactions. On the other hand, surfactant secretion in a healthy lung is regulated by ATP mediated purinergic signaling [297]. Lack of surfactant production promotes alveolar instability and collapse, thereby making the host vulnerable to developing severe infection [298, 299]. The observed Ply-ATP interaction instigates a discussion on whether surfactant disruption during pneumococcal infection is due to inhibition of purinergic signaling caused by Ply-ATP interactions.

5.4 Conclusion and future perspective

Streptococcus pneumoniae is a common colonizer of the human upper respiratory tract. However, under certain conditions, for example, in individuals with a weakened immune system, or following viral infections, it can cause a wide range of life-threatening diseases. This project was designed to understand the effect of pneumococcal derived H₂O₂ and Ply on the host innate immune defenses.

Paper I and II

In **paper I** we discussed about the structure, assembly and activation of the NLRP3 inflammasome. We explored various IL-1 β inhibiting drugs and summarized the current limited knowledge of inflammasome activation in pneumococcal pathogenesis. Although previous studies have revealed the importance of pneumococcal H₂O₂ in causing cell damage, not much is known about its impact on the activation of cell death pathways. Therefore, in **paper II**, we determined the impact of pneumococcal H₂O₂ on two crucial cell death pathways, namely apoptosis and pyroptosis. We show that:

- pneumococci-derived H₂O₂ has a detrimental effect on human bronchial epithelial cells.
- H₂O₂ mediates priming and activation of the NLRP3 inflammasome, resulting in caspase-1 dependent IL-1 β production.
- IL-1 β release is independent of GSDMD and mainly dependent on the apoptotic cell lysis.

In a multifaceted cellular environment, it is plausible to expect cross-talks between the various cell death pathways. Therefore, to delineate the complex nature of cell death induced by H₂O₂, further studies pertaining to cross-talks with other cellular pathways such as necroptosis and PANoptosis are warranted.

Paper III

To understand the disease pathology, it is important to understand host metabolic responses to an infection. In **paper III**, we performed metabolome profiling of *in vitro* single bacterial and viral as well as co-infections of bronchial epithelial cells with Influenza A virus, *Streptococcus pneumoniae*, and *Staphylococcus aureus*. We show that each respiratory pathogen has its unique way of interaction with host metabolome. On the one hand, pathogens such as IAV and *S. aureus* use the host resources for survival and multiplication. On the other hand, pneumococci significantly alter various host metabolic pathways. Additionally,

pneumococcal infections were characterized by TCA cycle inhibition and intracellular citrate accumulation. Intracellular citrate accumulation was directly attributed to the action of pneumococci-derived H₂O₂. However, further *in vivo* experiments should be performed to understand the relevance of citrate accumulation in pneumococcal infections. Another unexplored question is to determine whether intracellular citrate accumulation plays a role in activation of the cell death pathways.

Paper IV

Neutrophils are typically the first leukocytes to be recruited to the site of infection and are capable of eliminating pathogens by various mechanisms. However, excessive activation of neutrophils is associated with tissue injury, which results in the release of intracellular ATP. In **paper IV**, we aimed to investigate the role of ATP in neutrophil response to pneumococcal infections. We show that:

- Ply is one of the major pneumococcal neutrophil activators.
- ATP significantly neutralizes Ply-mediated neutrophil degranulation.
- The reduction in neutrophil activation is attributed to the binding of ATP to Ply.

Our data suggests that Ply-ATP interactions are potentially beneficial during the course of the infection as they limit the excessive Ply-mediated neutrophil activation. Further studies to determine the impact of these interactions on inflammasome activation and surfactant production would shed more light on the biological significance of this interaction. Additionally, whether such ATP interactions apply to other cholesterol-dependent cytolysins, including streptolysin O, listeriolysin O, or sUILysin would warrant further studies.

Chapter 6

REFERENCES

6. References

1. Bhatavadekar, K.S., Subhashita Ratnakara; a collection of witty and epigrammatic sayings in Sanskrit. 1888, Bombay: Narayan. 362, 43 p.
2. Bogaert, D., B. Keijsers, S. Huse, J. Rossen, R. Veenhoven, E. van Gils, et al., Variability and diversity of nasopharyngeal microbiota in children: a metagenomic analysis. *PLoS one*, 2011. **6**(2): p. e17035-e17035.
3. Huang, Y.C. and C.J. Chen, Nasal carriage of methicillin-resistant *Staphylococcus aureus* during the first 2 years of life in children in northern Taiwan. *Pediatr Infect Dis J*, 2015. **34**(2): p. 131-5.
4. Shiri, T., M.C. Nunes, P.V. Adrian, N. Van Niekerk, K.P. Klugman, and S.A. Madhi, Interrelationship of *Streptococcus pneumoniae*, *Haemophilus influenzae* and *Staphylococcus aureus* colonization within and between pneumococcal-vaccine naïve mother-child dyads. *BMC Infect Dis*, 2013. **13**: p. 483.
5. Bogaert, D., A. van Belkum, M. Sluijter, A. Luijendijk, R. de Groot, H.C. Rümke, et al., Colonisation by *Streptococcus pneumoniae* and *Staphylococcus aureus* in healthy children. *Lancet*, 2004. **363**(9424): p. 1871-2.
6. De Lencastre, H., K.G. Kristinsson, A. Brito-Avô, I.S. Sanches, R. Sá-Leão, J. Saldanha, et al., Carriage of respiratory tract pathogens and molecular epidemiology of *Streptococcus pneumoniae* colonization in healthy children attending day care centers in Lisbon, Portugal. *Microb Drug Resist*, 1999. **5**(1): p. 19-29.
7. Vives, M., M.E. Garcia, P. Saenz, M.A. Mora, L. Mata, H. Sabharwal, et al., Nasopharyngeal colonization in Costa Rican children during the first year of life. *Pediatr Infect Dis J*, 1997. **16**(9): p. 852-8.
8. Yahiaoui, R.Y., C. den Heijer, E.M. van Bijnen, W.J. Paget, M. Pringle, H. Goossens, et al., Prevalence and antibiotic resistance of commensal *Streptococcus pneumoniae* in nine European countries. *Future Microbiol*, 2016. **11**: p. 737-44.
9. Siemens, N., S. Oehmcke-Hecht, T.C. Mettenleiter, B. Kreikemeyer, P. Valentin-Weigand, and S. Hammerschmidt, Port d'Entrée for Respiratory Infections - Does the Influenza A Virus Pave the Way for Bacteria? *Front Microbiol*, 2017. **8**: p. 2602.
10. Malosh, R.E., E.T. Martin, J.R. Ortiz, and A.S. Monto, The risk of lower respiratory tract infection following influenza virus infection: A systematic and narrative review. *Vaccine*, 2018. **36**(1): p. 141-147.
11. Peter, G. and J.O. Klein, Chapter 123 - *Streptococcus pneumoniae*, in *Principles and Practice of Pediatric Infectious Disease* (Third Edition), S.S. Long, Editor. 2008, W.B. Saunders: Edinburgh. p. 725-733.
12. Ganaie, F., J.S. Saad, L. McGee, A.J. van Tonder, S.D. Bentley, S.W. Lo, et al., A New Pneumococcal Capsule Type, 10D, is the 100th Serotype and Has a Large cps Fragment from an Oral *Streptococcus*. *mBio*, 2020. **11**(3): p. e00937-20.
13. Ganaie, F., K. Maruhn, C. Li, R.J. Porambo, P.L. Elverdal, C. Abeygunwardana, et al., Structural, genetic, and serological elucidation of *Streptococcus pneumoniae* serogroup 24 serotypes: Discovery of a new serotype, 24C, with a variable capsule structure. *J Clin Microbiol*, 2021.
14. Pimenta, F., B. Moiane, R.E. Gertz, Jr., S. Chochua, P.M. Snippes Vagnone, R. Lynfield, et al., New Pneumococcal Serotype 15D. *J Clin Microbiol*, 2021. **59**(5).
15. Geno, K.A., G.L. Gilbert, J.Y. Song, I.C. Skovsted, K.P. Klugman, C. Jones, et al., Pneumococcal Capsules and Their Types: Past, Present, and Future. *Clin Microbiol Rev*, 2015. **28**(3): p. 871-99.
16. Weiser, J.N., D.M. Ferreira, and J.C. Paton, *Streptococcus pneumoniae*: transmission, colonization and invasion. *Nat Rev Microbiol*, 2018. **16**(6): p. 355-367.
17. Abdullahi, O., A. Karani, C.C. Tigoi, D. Mugo, S. Kungu, E. Wanjiru, et al., The Prevalence and Risk Factors for Pneumococcal Colonization of the Nasopharynx among Children in Kilifi District, Kenya. *PLOS ONE*, 2012. **7**(2): p. e30787.
18. Joloba, M.L., S. Bajaksouzian, E. Palavecino, C. Whalen, and M.R. Jacobs, High prevalence of carriage of antibiotic-resistant *Streptococcus pneumoniae* in children in Kampala Uganda. *International Journal of Antimicrobial Agents*, 2001. **17**(5): p. 395-400.
19. Mills, R.O., M.R. Abdullah, S.A. Akwetey, D.C. Sappor, I. Cole, M. Baffuor-Asare, et al., Post-Vaccination *Streptococcus pneumoniae* Carriage and Virulence Gene Distribution among Children Less Than Five Years of Age, Cape Coast, Ghana. *Microorganisms*, 2020. **8**(12).
20. Bogaert, D., R. de Groot, and P.W.M. Hermans, *Streptococcus pneumoniae* colonisation: the key to pneumococcal disease. *The Lancet Infectious Diseases*, 2004. **4**(3): p. 144-154.
21. McCullers, J.A. and K.C. Bartmess, Role of Neuraminidase in Lethal Synergism between Influenza Virus and *Streptococcus pneumoniae*. *The Journal of Infectious Diseases*, 2003. **187**(6): p. 1000-1009.
22. McCullers, J.A., Insights into the interaction between influenza virus and pneumococcus. *Clin Microbiol Rev*, 2006. **19**(3): p. 571-82.
23. Siemens, N., S. Oehmcke-Hecht, T.C. Mettenleiter, B. Kreikemeyer, P. Valentin-Weigand, and S. Hammerschmidt, Port d'Entrée for Respiratory Infections - Does the Influenza A Virus Pave the Way for Bacteria? *Front Microbiol*, 2017. **8**: p. 2602.
24. Pneumococcal conjugate vaccine for childhood immunization—WHO position paper. *Wkly Epidemiol Rec*, 2007. **82**(12): p. 93-104.
25. Brooks, L.R.K. and G.I. Mias, *Streptococcus pneumoniae*'s Virulence and Host Immunity: Aging, Diagnostics, and Prevention. *Front Immunol*, 2018. **9**: p. 1366.
26. Jedrzejewski, M.J., Pneumococcal virulence factors: structure and function. *Microbiology and molecular biology reviews* : MMBR, 2001. **65**(2): p. 187-207.

27. Bergmann, S. and S. Hammerschmidt, Versatility of pneumococcal surface proteins. *Microbiology (Reading)*, 2006. **152**(Pt 2): p. 295-303.
28. Ogunniyi, A.D. and J.C. Paton, Chapter 4 - Vaccine Potential of Pneumococcal Proteins, in *Streptococcus Pneumoniae*, J. Brown, S. Hammerschmidt, and C. Orihuela, Editors. 2015, Academic Press: Amsterdam. p. 59-78.
29. Walker, J.A., R.L. Allen, P. Falmagne, M.K. Johnson, and G.J. Boulnois, Molecular cloning, characterization, and complete nucleotide sequence of the gene for pneumolysin, the sulfhydryl-activated toxin of *Streptococcus pneumoniae*. *Infection and Immunity*, 1987. **55**(5): p. 1184-1189.
30. Mellroth, P., R. Daniels, A. Eberhardt, D. Rönnlund, H. Blom, J. Widengren, et al., LytA, major autolysin of *Streptococcus pneumoniae*, requires access to nascent peptidoglycan. *The Journal of biological chemistry*, 2012. **287**(14): p. 11018-11029.
31. Benton, K.A., J.C. Paton, and D.E. Briles, Differences in virulence for mice among *Streptococcus pneumoniae* strains of capsular types 2, 3, 4, 5, and 6 are not attributable to differences in pneumolysin production. *Infection and Immunity*, 1997. **65**(4): p. 1237-1244.
32. Balachandran, P., S.K. Hollingshead, J.C. Paton, and D.E. Briles, The autolytic enzyme LytA of *Streptococcus pneumoniae* is not responsible for releasing pneumolysin. *J Bacteriol*, 2001. **183**(10): p. 3108-16.
33. Tilley, S.J., E.V. Orlova, R.J. Gilbert, P.W. Andrew, and H.R. Saibil, Structural basis of pore formation by the bacterial toxin pneumolysin. *Cell*, 2005. **121**(2): p. 247-56.
34. Marshall, J.E., B.H.A. Faraj, A.R. Gingras, R. Lonnen, M.A. Sheikh, M. El-Mezgueldi, et al., The Crystal Structure of Pneumolysin at 2.0 Å Resolution Reveals the Molecular Packing of the Pre-pore Complex. *Scientific Reports*, 2015. **5**(1): p. 13293.
35. van Pee, K., A. Neuhaus, E. D'Imprima, D.J. Mills, W. Kühlbrandt, and Ö. Yildiz, CryoEM structures of membrane pore and prepore complex reveal cytolytic mechanism of Pneumolysin. *eLife*, 2017. **6**: p. e23644.
36. Rai, P., F. He, J. Kwang, B.P. Engelward, and V.T.K. Chow, Pneumococcal Pneumolysin Induces DNA Damage and Cell Cycle Arrest. *Scientific reports*, 2016. **6**: p. 22972-22972.
37. Braun, J.S., O. Hoffmann, M. Schickhaus, D. Freyer, E. Dagand, D. Bermpohl, et al., Pneumolysin causes neuronal cell death through mitochondrial damage. *Infect Immun*, 2007. **75**(9): p. 4245-54.
38. Braun, J.S., J.E. Sublett, D. Freyer, T.J. Mitchell, J.L. Cleveland, E.I. Tuomanen, et al., Pneumococcal pneumolysin and H(2)O(2) mediate brain cell apoptosis during meningitis. *J Clin Invest*, 2002. **109**(1): p. 19-27.
39. Nerlich, A., M. Mieth, E. Letsiou, D. Fatykhova, K. Zscheppang, A. Imai-Matsushima, et al., Pneumolysin induced mitochondrial dysfunction leads to release of mitochondrial DNA. *Scientific Reports*, 2018. **8**(1): p. 182.
40. Srivastava, A., P. Henneke, A. Visintin, S.C. Morse, V. Martin, C. Watkins, et al., The apoptotic response to pneumolysin is Toll-like receptor 4 dependent and protects against pneumococcal disease. *Infection and immunity*, 2005. **73**(10): p. 6479-6487.
41. McNeela, E.A., A. Burke, D.R. Neill, C. Baxter, V.E. Fernandes, D. Ferreira, et al., Pneumolysin activates the NLRP3 inflammasome and promotes proinflammatory cytokines independently of TLR4. *PLoS Pathog*, 2010. **6**(11): p. e1001191.
42. Witzenthath, M., F. Pache, D. Lorenz, U. Koppe, B. Gutbier, C. Tabeling, et al., The NLRP3 inflammasome is differentially activated by pneumolysin variants and contributes to host defense in pneumococcal pneumonia. *J Immunol*, 2011. **187**(1): p. 434-40.
43. Rabes, A., N. Sutorp, and B. Opitz, Inflammasomes in Pneumococcal Infection: Innate Immune Sensing and Bacterial Evasion Strategies. *Curr Top Microbiol Immunol*, 2016. **397**: p. 215-27.
44. Shoma, S., K. Tsuchiya, I. Kawamura, T. Nomura, H. Hara, R. Uchiyama, et al., Critical Involvement of Pneumolysin in Production of Interleukin-1 β and Caspase-1-Dependent Cytokines in Infection with *Streptococcus pneumoniae* In Vitro: a Novel Function of Pneumolysin in Caspase-1 Activation. *Infection and Immunity*, 2008. **76**(4): p. 1547-1557.
45. Marriott, H.M., T.J. Mitchell, and D.H. Dockrell, Pneumolysin: a double-edged sword during the host-pathogen interaction. *Curr Mol Med*, 2008. **8**(6): p. 497-509.
46. Steel, H.C., R. Cockeran, R. Anderson, and C. Feldman, Overview of community-acquired pneumonia and the role of inflammatory mechanisms in the immunopathogenesis of severe pneumococcal disease. *Mediators of inflammation*, 2013. **2013**: p. 490346-490346.
47. Zafar, M.A., Y. Wang, S. Hamaguchi, and J.N. Weiser, Host-to-Host Transmission of *Streptococcus pneumoniae* Is Driven by Its Inflammatory Toxin, Pneumolysin. *Cell host & microbe*, 2017. **21**(1): p. 73-83.
48. Pichichero, M.E., Pneumococcal whole-cell and protein-based vaccines: changing the paradigm. *Expert review of vaccines*, 2017. **16**(12): p. 1181-1190.
49. Spellerberg, B., D.R. Cundell, J. Sandros, B.J. Pearce, I. Idanpaan-Heikkila, C. Rosenow, et al., Pyruvate oxidase, as a determinant of virulence in *Streptococcus pneumoniae*. *Mol Microbiol*, 1996. **19**(4): p. 803-13.
50. Bienert, G.P., J.K. Schjoerring, and T.P. Jahn, Membrane transport of hydrogen peroxide. *Biochimica et Biophysica Acta (BBA) - Biomembranes*, 2006. **1758**(8): p. 994-1003.
51. Rai, P., M. Parrish, I.J. Tay, N. Li, S. Ackerman, F. He, et al., *Streptococcus pneumoniae* secretes hydrogen peroxide leading to DNA damage and apoptosis in lung cells. *Proc Natl Acad Sci U S A*, 2015. **112**(26): p. E3421-30.
52. Hoffmann, O.M., D. Becker, and J.R. Weber, Bacterial hydrogen peroxide contributes to cerebral hyperemia during early stages of experimental pneumococcal meningitis. *J Cereb Blood Flow Metab*, 2007. **27**(11): p. 1792-7.
53. Pfister, H.W., U. Koedel, S. Lorenzl, and A. Tomasz, Antioxidants attenuate microvascular changes in the early phase of experimental pneumococcal meningitis in rats. *Stroke*, 1992. **23**(12): p. 1798-804.
54. Feldman, C., R. Anderson, R. Cockeran, T. Mitchell, P. Cole, and R. Wilson, The effects of pneumolysin and hydrogen peroxide, alone and in combination, on human ciliated epithelium in vitro. *Respir Med*, 2002. **96**(8): p. 580-5.

55. Hirst, R.A., K.S. Sikand, A. Rutman, T.J. Mitchell, P.W. Andrew, and C. O'Callaghan, Relative roles of pneumolysin and hydrogen peroxide from *Streptococcus pneumoniae* in inhibition of ependymal ciliary beat frequency. *Infect Immun*, 2000. **68**(3): p. 1557-62.
56. Duane, P.G., J.B. Rubins, H.R. Weisel, and E.N. Janoff, Identification of hydrogen peroxide as a *Streptococcus pneumoniae* toxin for rat alveolar epithelial cells. *Infect Immun*, 1993. **61**(10): p. 4392-7.
57. Cuypers, F., B. Klabunde, M. Gesell Salazar, S. Surabhi, S.B. Skorcka, G. Burchhardt, et al., Adenosine Triphosphate Neutralizes Pneumolysin-Induced Neutrophil Activation. *J Infect Dis*, 2020. **222**(10): p. 1702-1712.
58. Regev-Yochay, G., K. Trzcinski, C.M. Thompson, R. Malley, and M. Lipsitch, Interference between *Streptococcus pneumoniae* and *Staphylococcus aureus*: In vitro hydrogen peroxide-mediated killing by *Streptococcus pneumoniae*. *J Bacteriol*, 2006. **188**(13): p. 4996-5001.
59. Pericone, C.D., K. Overweg, P.W. Hermans, and J.N. Weiser, Inhibitory and bactericidal effects of hydrogen peroxide production by *Streptococcus pneumoniae* on other inhabitants of the upper respiratory tract. *Infect Immun*, 2000. **68**(7): p. 3990-7.
60. Mehraj, J., W. Witte, M.K. Akmatov, F. Layer, G. Werner, and G. Krause, Epidemiology of *Staphylococcus aureus* Nasal Carriage Patterns in the Community, in *How to Overcome the Antibiotic Crisis : Facts, Challenges, Technologies and Future Perspectives*, M. Stadler and P. Dersch, Editors. 2016, Springer International Publishing: Cham. p. 55-87.
61. Sakr, A., F. Brégeon, J.L. Mège, J.M. Rolain, and O. Blin, *Staphylococcus aureus* Nasal Colonization: An Update on Mechanisms, Epidemiology, Risk Factors, and Subsequent Infections. *Front Microbiol*, 2018. **9**: p. 2419.
62. Wertheim, H.F., D.C. Melles, M.C. Vos, W. van Leeuwen, A. van Belkum, H.A. Verbrugh, et al., The role of nasal carriage in *Staphylococcus aureus* infections. *Lancet Infect Dis*, 2005. **5**(12): p. 751-62.
63. Ondusko, D.S. and D. Nolt, *Staphylococcus aureus*. *Pediatr Rev*, 2018. **39**(6): p. 287-298.
64. Spaan, A.N., J.A.G. van Strijp, and V.J. Torres, Leukocidins: staphylococcal bi-component pore-forming toxins find their receptors. *Nature reviews. Microbiology*, 2017. **15**(7): p. 435-447.
65. Shumba, P., S. Mairpady Shambat, and N. Siemens, The Role of Streptococcal and Staphylococcal Exotoxins and Proteases in Human Necrotizing Soft Tissue Infections. *Toxins (Basel)*, 2019. **11**(6).
66. Tuchscher, L., B. Löffler, and R.A. Proctor, Persistence of *Staphylococcus aureus*: Multiple Metabolic Pathways Impact the Expression of Virulence Factors in Small-Colony Variants (SCVs). *Frontiers in Microbiology*, 2020. **11**(1028).
67. Josse, J., F. Laurent, and A. Diot, Staphylococcal Adhesion and Host Cell Invasion: Fibronectin-Binding and Other Mechanisms. *Frontiers in microbiology*, 2017. **8**: p. 2433-2433.
68. Proctor, R.A., C. von Eiff, B.C. Kahl, K. Becker, P. McNamara, M. Herrmann, et al., Small colony variants: a pathogenic form of bacteria that facilitates persistent and recurrent infections. *Nature Reviews Microbiology*, 2006. **4**(4): p. 295-305.
69. Fraunholz, M. and B. Sinha, Intracellular *Staphylococcus aureus*: live-in and let die. *Front Cell Infect Microbiol*, 2012. **2**: p. 43.
70. Surmann, K., S. Michalik, P. Hildebrandt, P. Gierok, M. Depke, L. Brinkmann, et al., Comparative proteome analysis reveals conserved and specific adaptation patterns of *Staphylococcus aureus* after internalization by different types of human non-professional phagocytic host cells. *Front Microbiol*, 2014. **5**: p. 392.
71. Shao, W., X. Li, M.U. Goraya, S. Wang, and J.L. Chen, Evolution of Influenza A Virus by Mutation and Re-Assortment. *Int J Mol Sci*, 2017. **18**(8).
72. Paules, C. and K. Subbarao, Influenza. *Lancet*, 2017. **390**(10095): p. 697-708.
73. Li, X., M. Gu, Q. Zheng, R. Gao, and X. Liu, Packaging signal of influenza A virus. *Virology Journal*, 2021. **18**(1): p. 36.
74. Bouvier, N.M. and P. Palese, The biology of influenza viruses. *Vaccine*, 2008. **26 Suppl 4**(Suppl 4): p. D49-53.
75. Byrd-Leotis, L., R.D. Cummings, and D.A. Steinhauer, The Interplay between the Host Receptor and Influenza Virus Hemagglutinin and Neuraminidase. *Int J Mol Sci*, 2017. **18**(7).
76. Böttcher-Friebertshäuser, E., W. Garten, M. Matrosovich, and H.D. Klenk, The hemagglutinin: a determinant of pathogenicity. *Curr Top Microbiol Immunol*. 2014. **385**: p. 3-34.
77. Rossman, J.S. and R.A. Lamb, Influenza virus assembly and budding. *Virology*, 2011. **411**(2): p. 229-36.
78. Tong, S., X. Zhu, Y. Li, M. Shi, J. Zhang, M. Bourgeois, et al., New world bats harbor diverse influenza A viruses. *PLoS Pathog*, 2013. **9**(10): p. e1003657.
79. Jang, J. and S.E. Bae, Comparative Co-Evolution Analysis Between the HA and NA Genes of Influenza A Virus. *Virology (Auckl)*, 2018. **9**: p. 1178122x18788328.
80. Chen, R. and E.C. Holmes, Avian influenza virus exhibits rapid evolutionary dynamics. *Mol Biol Evol*, 2006. **23**(12): p. 2336-41.
81. Ahlquist, P., RNA-dependent RNA polymerases, viruses, and RNA silencing. *Science*, 2002. **296**(5571): p. 1270-3.
82. Garten, R.J., C.T. Davis, C.A. Russell, B. Shu, S. Lindstrom, A. Balish, et al., Antigenic and genetic characteristics of swine-origin 2009 A(H1N1) influenza viruses circulating in humans. *Science*, 2009. **325**(5937): p. 197-201.
83. Krammer, F., G.J.D. Smith, R.A.M. Fouchier, M. Peiris, K. Kedzierska, P.C. Doherty, et al., Influenza. *Nature Reviews Disease Primers*, 2018. **4**(1): p. 3.
84. WHO. Influenza (Seasonal). 2018; Available from: [https://www.who.int/news-room/fact-sheets/detail/influenza-\(seasonal\)](https://www.who.int/news-room/fact-sheets/detail/influenza-(seasonal)).
85. Morris, D.E., D.W. Cleary, and S.C. Clarke, Secondary Bacterial Infections Associated with Influenza Pandemics. *Front Microbiol*, 2017. **8**: p. 1041.
86. Kalil, A.C. and P.G. Thomas, Influenza virus-related critical illness: pathophysiology and epidemiology. *Critical Care*, 2019. **23**(1): p. 258.

REFERENCES

87. Mertz, D., T.H. Kim, J. Johnstone, P.-P. Lam, M. Science, S.P. Kuster, et al., Populations at risk for severe or complicated influenza illness: systematic review and meta-analysis. *BMJ : British Medical Journal*, 2013. **347**: p. f5061.
88. Vemula, S.V., E.E. Sayedahmed, S. Sambhara, and S.K. Mittal, Vaccine approaches conferring cross-protection against influenza viruses. *Expert Rev Vaccines*, 2017. **16**(11): p. 1141-1154.
89. Boni, M.F., Vaccination and antigenic drift in influenza. *Vaccine*, 2008. **26 Suppl 3**(Suppl 3): p. C8-14.
90. Taubenberger, J.K. and D.M. Morens, Pandemic influenza--including a risk assessment of H5N1. *Rev Sci Tech*, 2009. **28**(1): p. 187-202.
91. Johnson, N.P. and J. Mueller, Updating the accounts: global mortality of the 1918-1920 "Spanish" influenza pandemic. *Bull Hist Med*, 2002. **76**(1): p. 105-15.
92. Morens, D.M., J.K. Taubenberger, and A.S. Fauci, Predominant role of bacterial pneumonia as a cause of death in pandemic influenza: implications for pandemic influenza preparedness. *J Infect Dis*, 2008. **198**(7): p. 962-70.
93. Bogdanow, B., X. Wang, K. Eichelbaum, A. Sadewasser, I. Husic, K. Paki, et al., The dynamic proteome of influenza A virus infection identifies M segment splicing as a host range determinant. *Nature Communications*, 2019. **10**(1): p. 5518.
94. Brundage, J.F. and G.D. Shanks, Deaths from bacterial pneumonia during 1918-19 influenza pandemic. *Emerg Infect Dis*, 2008. **14**(8): p. 1193-9.
95. Mulcahy, M.E. and R.M. McLoughlin, Staphylococcus aureus and Influenza A Virus: Partners in Coinfection. *mBio*, 2016. **7**(6): p. e02068-16.
96. Joseph, C., Y. Togawa, and N. Shindo, Bacterial and viral infections associated with influenza. *Influenza Other Respir Viruses*, 2013. **7 Suppl 2**(Suppl 2): p. 105-13.
97. Loosli, C.G., S.F. Stinson, D.P. Ryan, M.S. Hertweck, J.D. Hardy, and R. Serebrin, The destruction of type 2 pneumocytes by airborne influenza PR8-A virus; its effect on surfactant and lecithin content of the pneumonic lesions of mice. *Chest*, 1975. **67**(2 Suppl): p. 7s-14s.
98. Levandowski, R.A., T.R. Gerrity, and C.S. Garrard, Modifications of lung clearance mechanisms by acute influenza A infection. *J Lab Clin Med*, 1985. **106**(4): p. 428-32.
99. Siegel, S.J., A.M. Roche, and J.N. Weiser, Influenza promotes pneumococcal growth during coinfection by providing host sialylated substrates as a nutrient source. *Cell Host Microbe*, 2014. **16**(1): p. 55-67.
100. Plotkowski, M.C., O. Bajolet-Laudinat, and E. Puchelle, Cellular and molecular mechanisms of bacterial adhesion to respiratory mucosa. *Eur Respir J*, 1993. **6**(6): p. 903-16.
101. Beadling, C. and M.K. Slifka, How do viral infections predispose patients to bacterial infections? *Curr Opin Infect Dis*, 2004. **17**(3): p. 185-91.
102. Shahangian, A., E.K. Chow, X. Tian, J.R. Kang, A. Ghaffari, S.Y. Liu, et al., Type I IFNs mediate development of postinfluenza bacterial pneumonia in mice. *J Clin Invest*, 2009. **119**(7): p. 1910-20.
103. Nakamura, S., K.M. Davis, and J.N. Weiser, Synergistic stimulation of type I interferons during influenza virus coinfection promotes Streptococcus pneumoniae colonization in mice. *J Clin Invest*, 2011. **121**(9): p. 3657-65.
104. van der Sluijs, K.F., L.J. van Elden, M. Nijhuis, R. Schuurman, J.M. Pater, S. Florquin, et al., IL-10 is an important mediator of the enhanced susceptibility to pneumococcal pneumonia after influenza infection. *J Immunol*, 2004. **172**(12): p. 7603-9.
105. Metzger, D.W. and K. Sun, Immune dysfunction and bacterial coinfections following influenza. *J Immunol*, 2013. **191**(5): p. 2047-52.
106. Janeway CA Jr, T.P., Walport M, et al., Immunobiology: The Immune System in Health and Disease., in Janeway CA Jr, Travers P, Walport M, et al., N.Y.G. Science, Editor. 2001.
107. Meyer, K.C., Aging. *Proceedings of the American Thoracic Society*, 2005. **2**(5): p. 433-439.
108. Schleimer, R.P., A. Kato, R. Kern, D. Kuperman, and P.C. Avila, Epithelium: at the interface of innate and adaptive immune responses. *J Allergy Clin Immunol*, 2007. **120**(6): p. 1279-84.
109. Hewitt, R.J. and C.M. Lloyd, Regulation of immune responses by the airway epithelial cell landscape. *Nature Reviews Immunology*, 2021. **21**(6): p. 347-362.
110. Garcia, M.A., W.J. Nelson, and N. Chavez, Cell-Cell Junctions Organize Structural and Signaling Networks. *Cold Spring Harb Perspect Biol*, 2018. **10**(4).
111. Linden, S.K., P. Sutton, N.G. Karlsson, V. Korolik, and M.A. McGuckin, Mucins in the mucosal barrier to infection. *Mucosal Immunology*, 2008. **1**(3): p. 183-197.
112. Bustamante-Marin, X.M. and L.E. Ostrowski, Cilia and Mucociliary Clearance. *Cold Spring Harb Perspect Biol*, 2017. **9**(4).
113. Geitani, R., C.A. Moubareck, Z. Xu, D. Karam Sarkis, and L. Touqui, Expression and Roles of Antimicrobial Peptides in Innate Defense of Airway Mucosa: Potential Implication in Cystic Fibrosis. *Frontiers in Immunology*, 2020. **11**(1198).
114. Bals, R., Epithelial antimicrobial peptides in host defense against infection. *Respir Res*, 2000. **1**(3): p. 141-50.
115. Takeuchi, O. and S. Akira, Pattern recognition receptors and inflammation. *Cell*, 2010. **140**(6): p. 805-20.
116. Kawai, T. and S. Akira, TLR signaling. *Cell Death & Differentiation*, 2006. **13**(5): p. 816-825.
117. Zheng, C., The emerging roles of NOD-like receptors in antiviral innate immune signaling pathways. *International Journal of Biological Macromolecules*, 2021. **169**: p. 407-413.
118. Kim, Y.K., J.S. Shin, and M.H. Nahm, NOD-Like Receptors in Infection, Immunity, and Diseases. *Yonsei Med J*, 2016. **57**(1): p. 5-14.
119. Rehwinkel, J. and M.U. Gack, RIG-I-like receptors: their regulation and roles in RNA sensing. *Nature Reviews Immunology*, 2020. **20**(9): p. 537-551.
120. Zelensky, A.N. and J.E. Gready, The C-type lectin-like domain superfamily. *Febs j*, 2005. **272**(24): p. 6179-217.

121. Wang, L., L. Sun, K.M. Byrd, C.-C. Ko, Z. Zhao, and J. Fang, AIM2 Inflammasome's First Decade of Discovery: Focus on Oral Diseases. *Frontiers in Immunology*, 2020. **11**(1487).
122. Sharma, B.R., R. Karki, and T.D. Kanneganti, Role of AIM2 inflammasome in inflammatory diseases, cancer and infection. *Eur J Immunol*, 2019. **49**(11): p. 1998-2011.
123. Caneparo, V., S. Landolfo, M. Gariglio, and M. De Andrea, The Absent in Melanoma 2-Like Receptor IFN-Inducible Protein 16 as an Inflammasome Regulator in Systemic Lupus Erythematosus: The Dark Side of Sensing Microbes. *Front Immunol*, 2018. **9**: p. 1180.
124. Pillay, J., I. den Braber, N. Vrisekoop, L.M. Kwast, R.J. de Boer, J.A.M. Borghans, et al., In vivo labeling with ²H₂O reveals a human neutrophil lifespan of 5.4 days. *Blood*, 2010. **116**(4): p. 625-627.
125. Borregaard, N., Neutrophils, from Marrow to Microbes. *Immunity*, 2010. **33**(5): p. 657-670.
126. Bratton, D.L. and P.M. Henson, Neutrophil clearance: when the party is over, clean-up begins. *Trends Immunol*, 2011. **32**(8): p. 350-7.
127. Lee, W.L., R.E. Harrison, and S. Grinstein, Phagocytosis by neutrophils. *Microbes Infect*, 2003. **5**(14): p. 1299-306.
128. Fairn, G.D. and S. Grinstein, How nascent phagosomes mature to become phagolysosomes. *Trends in Immunology*, 2012. **33**(8): p. 397-405.
129. Uribe-Querol, E. and C. Rosales, Control of Phagocytosis by Microbial Pathogens. *Frontiers in Immunology*, 2017. **8**(1368).
130. Brinkmann, V., U. Reichard, C. Goosmann, B. Fauler, Y. Uhlemann, D.S. Weiss, et al., Neutrophil extracellular traps kill bacteria. *Science*, 2004. **303**(5663): p. 1532-5.
131. Pérez-Figueroa, E., P. Álvarez-Carrasco, E. Ortega, and C. Maldonado-Bernal, Neutrophils: Many Ways to Die. *Frontiers in Immunology*, 2021. **12**(509).
132. Galluzzi, L., I. Vitale, S.A. Aaronson, J.M. Abrams, D. Adam, P. Agostinis, et al., Molecular mechanisms of cell death: recommendations of the Nomenclature Committee on Cell Death 2018. *Cell Death & Differentiation*, 2018. **25**(3): p. 486-541.
133. Borregaard, N., O.E. Sørensen, and K. Theilgaard-Mönch, Neutrophil granules: a library of innate immunity proteins. *Trends Immunol*, 2007. **28**(8): p. 340-5.
134. Borregaard, N. and J.B. Cowland, Granules of the human neutrophilic polymorphonuclear leukocyte. *Blood*, 1997. **89**(10): p. 3503-21.
135. Kjeldsen, L., H. Sengeløv, K. Løllike, M.H. Nielsen, and N. Borregaard, Isolation and characterization of gelatinase granules from human neutrophils. *Blood*, 1994. **83**(6): p. 1640-9.
136. Sengeløv, H., L. Kjeldsen, and N. Borregaard, Control of exocytosis in early neutrophil activation. *J Immunol*, 1993. **150**(4): p. 1535-43.
137. Lacy, P., Mechanisms of Degranulation in Neutrophils. *Allergy, Asthma & Clinical Immunology*, 2006. **2**(3): p. 98.
138. Ramadass, M. and S.D. Catz, Molecular mechanisms regulating secretory organelles and endosomes in neutrophils and their implications for inflammation. *Immunol Rev*, 2016. **273**(1): p. 249-65.
139. Bentwood, B.J. and P.M. Henson, The sequential release of granule constituents from human neutrophils. *J Immunol*, 1980. **124**(2): p. 855-62.
140. Shen, X., K. Cao, Y. Zhao, and J. Du, Targeting Neutrophils in Sepsis: From Mechanism to Translation. *Frontiers in Pharmacology*, 2021. **12**(353).
141. Fresneda Alarcon, M., Z. McLaren, and H.L. Wright, Neutrophils in the Pathogenesis of Rheumatoid Arthritis and Systemic Lupus Erythematosus: Same Foe Different M.O. *Frontiers in Immunology*, 2021. **12**(570).
142. Rock, K.L., J.J. Lai, and H. Kono, Innate and adaptive immune responses to cell death. *Immunol Rev*, 2011. **243**(1): p. 191-205.
143. Shubina, M., B. Tummers, D.F. Boyd, T. Zhang, C. Yin, A. Gautam, et al., Necroptosis restricts influenza A virus as a stand-alone cell death mechanism. *J Exp Med*, 2020. **217**(11).
144. Kim, M., H. Ashida, M. Ogawa, Y. Yoshikawa, H. Mimuro, and C. Sasakawa, Bacterial interactions with the host epithelium. *Cell Host Microbe*, 2010. **8**(1): p. 20-35.
145. Jiang, M., L. Qi, L. Li, and Y. Li, The caspase-3/GSDME signal pathway as a switch between apoptosis and pyroptosis in cancer. *Cell Death Discovery*, 2020. **6**(1): p. 112.
146. Yu, J., S. Li, J. Qi, Z. Chen, Y. Wu, J. Guo, et al., Cleavage of GSDME by caspase-3 determines lobaplatin-induced pyroptosis in colon cancer cells. *Cell Death & Disease*, 2019. **10**(3): p. 193.
147. Tsuchiya, K., S. Nakajima, S. Hosojima, D. Thi Nguyen, T. Hattori, T. Manh Le, et al., Caspase-1 initiates apoptosis in the absence of gasdermin D. *Nature Communications*, 2019. **10**(1): p. 2091.
148. Clarke, P.G. and S. Clarke, Nineteenth century research on naturally occurring cell death and related phenomena. *Anat Embryol (Berl)*, 1996. **193**(2): p. 81-99.
149. Kerr, J.F., A.H. Wyllie, and A.R. Currie, Apoptosis: a basic biological phenomenon with wide-ranging implications in tissue kinetics. *Br J Cancer*, 1972. **26**(4): p. 239-57.
150. Häcker, G., The morphology of apoptosis. *Cell Tissue Res*, 2000. **301**(1): p. 5-17.
151. Elmore, S., Apoptosis: a review of programmed cell death. *Toxicol Pathol*, 2007. **35**(4): p. 495-516.
152. Chipuk, J.E., L. Bouchier-Hayes, and D.R. Green, Mitochondrial outer membrane permeabilization during apoptosis: the innocent bystander scenario. *Cell Death & Differentiation*, 2006. **13**(8): p. 1396-1402.
153. Dewson, G. and R.M. Kluck, Mechanisms by which Bak and Bax permeabilise mitochondria during apoptosis. *J Cell Sci*, 2009. **122**(Pt 16): p. 2801-8.
154. Boatright, K.M., M. Renatus, F.L. Scott, S. Sperandio, H. Shin, I.M. Pedersen, et al., A Unified Model for Apical Caspase Activation. *Molecular Cell*, 2003. **11**(2): p. 529-541.
155. Slee, E.A., C. Adrain, and S.J. Martin, Serial killers: ordering caspase activation events in apoptosis. *Cell Death Differ*, 1999. **6**(11): p. 1067-74.

REFERENCES

156. Guicciardi, M.E. and G.J. Gores, Life and death by death receptors. *Faseb j*, 2009. **23**(6): p. 1625-37.
157. Salvesen, G.S. and V.M. Dixit, Caspase activation: the induced-proximity model. *Proc Natl Acad Sci U S A*, 1999. **96**(20): p. 10964-7.
158. Boatright, K.M., C. Deis, J.B. Denault, D.P. Sutherlin, and G.S. Salvesen, Activation of caspases-8 and -10 by FLIP(L). *Biochem J*, 2004. **382**(Pt 2): p. 651-7.
159. Li, H., H. Zhu, C.J. Xu, and J. Yuan, Cleavage of BID by caspase 8 mediates the mitochondrial damage in the Fas pathway of apoptosis. *Cell*, 1998. **94**(4): p. 491-501.
160. Porter, A.G. and R.U. Jänicke, Emerging roles of caspase-3 in apoptosis. *Cell Death Differ*, 1999. **6**(2): p. 99-104.
161. Kitazumi, I. and M. Tsukahara, Regulation of DNA fragmentation: the role of caspases and phosphorylation. *Febs j*, 2011. **278**(3): p. 427-41.
162. Fink, S.L. and B.T. Cookson, Apoptosis, pyroptosis, and necrosis: mechanistic description of dead and dying eukaryotic cells. *Infect Immun*, 2005. **73**(4): p. 1907-16.
163. Poon, I.K., C.D. Lucas, A.G. Rossi, and K.S. Ravichandran, Apoptotic cell clearance: basic biology and therapeutic potential. *Nat Rev Immunol*, 2014. **14**(3): p. 166-80.
164. Zychlinsky, A., M.C. Prevost, and P.J. Sansonetti, *Shigella flexneri* induces apoptosis in infected macrophages. *Nature*, 1992. **358**(6382): p. 167-9.
165. Chen, L.M., K. Kaniga, and J.E. Galán, *Salmonella* spp. are cytotoxic for cultured macrophages. *Mol Microbiol*, 1996. **21**(5): p. 1101-15.
166. Monack, D.M., B. Raupach, A.E. Hromockyj, and S. Falkow, *Salmonella typhimurium* invasion induces apoptosis in infected macrophages. *Proc Natl Acad Sci U S A*, 1996. **93**(18): p. 9833-8.
167. Hersh, D., D.M. Monack, M.R. Smith, N. Ghori, S. Falkow, and A. Zychlinsky, The *Salmonella* invasive SipB induces macrophage apoptosis by binding to caspase-1. *Proceedings of the National Academy of Sciences*, 1999. **96**(5): p. 2396-2401.
168. He, W.T., H. Wan, L. Hu, P. Chen, X. Wang, Z. Huang, et al., Gasdermin D is an executor of pyroptosis and required for interleukin-1beta secretion. *Cell Res*, 2015. **25**(12): p. 1285-98.
169. Brennan, M.A. and B.T. Cookson, *Salmonella* induces macrophage death by caspase-1-dependent necrosis. *Mol Microbiol*, 2000. **38**(1): p. 31-40.
170. Watson, P.R., A.V. Gautier, S.M. Paulin, A.P. Bland, P.W. Jones, and T.S. Wallis, *Salmonella enterica* serovars Typhimurium and Dublin can lyse macrophages by a mechanism distinct from apoptosis. *Infect Immun*, 2000. **68**(6): p. 3744-7.
171. Boise, L.H. and C.M. Collins, *Salmonella*-induced cell death: apoptosis, necrosis or programmed cell death? *Trends Microbiol*, 2001. **9**(2): p. 64-7.
172. Cookson, B.T. and M.A. Brennan, Pro-inflammatory programmed cell death. *Trends in Microbiology*, 2001. **9**(3): p. 113-114.
173. Man, S.M. and T.D. Kanneganti, Converging roles of caspases in inflammasome activation, cell death and innate immunity. *Nat Rev Immunol*, 2016. **16**(1): p. 7-21.
174. Martinon, F., K. Burns, and J. Tschopp, The inflammasome: a molecular platform triggering activation of inflammatory caspases and processing of proIL-beta. *Mol Cell*, 2002. **10**(2): p. 417-26.
175. Saxena, M. and G. Yeretssian, NOD-Like Receptors: Master Regulators of Inflammation and Cancer. *Frontiers in Immunology*, 2014. **5**: p. 327.
176. Yang, Y., H. Wang, M. Kouadir, H. Song, and F. Shi, Recent advances in the mechanisms of NLRP3 inflammasome activation and its inhibitors. *Cell Death & Disease*, 2019. **10**(2): p. 128.
177. Baker, P.J., D. Boucher, D. Bierschenk, C. Tebartz, P.G. Whitney, D.B. D'Silva, et al., NLRP3 inflammasome activation downstream of cytoplasmic LPS recognition by both caspase-4 and caspase-5. *Eur J Immunol*, 2015. **45**(10): p. 2918-26.
178. Elizagaray, M.L., M.T.R. Gomes, E.S. Guimaraes, M. Rumbo, D.F. Hozbor, S.C. Oliveira, et al., Canonical and Non-canonical Inflammasome Activation by Outer Membrane Vesicles Derived From *Bordetella pertussis*. *Frontiers in Immunology*, 2020. **11**: p. 1879.
179. Netea, M.G., C.A. Nold-Petry, M.F. Nold, L.A. Joosten, B. Opitz, J.H. van der Meer, et al., Differential requirement for the activation of the inflammasome for processing and release of IL-1beta in monocytes and macrophages. *Blood*, 2009. **113**(10): p. 2324-35.
180. Gritsenko, A., S. Yu, F. Martin-Sanchez, I.D. del Olmo, E.-M. Nichols, D.M. Davis, et al., Priming is dispensable for NLRP3 inflammasome activation in human monocytes. *bioRxiv*, 2020: p. 2020.01.30.925248.
181. Bauernfeind, F.G., G. Horvath, A. Stutz, E.S. Alnemri, K. MacDonald, D. Speert, et al., Cutting edge: NF-kappaB activating pattern recognition and cytokine receptors license NLRP3 inflammasome activation by regulating NLRP3 expression. *J Immunol*, 2009. **183**(2): p. 787-91.
182. Lamkanfi, M. and V.M. Dixit, Modulation of inflammasome pathways by bacterial and viral pathogens. *J Immunol*, 2011. **187**(2): p. 597-602.
183. Greaney, A.J., S.H. Leppla, and M. Moayeri, Bacterial Exotoxins and the Inflammasome. *Frontiers in Immunology*, 2015. **6**(570).
184. Eigenbrod, T. and A.H. Dalpke, Bacterial RNA: An Underestimated Stimulus for Innate Immune Responses. *J Immunol*, 2015. **195**(2): p. 411-8.
185. Wang, W., G. Li, W. De, Z. Luo, P. Pan, M. Tian, et al., Zika virus infection induces host inflammatory responses by facilitating NLRP3 inflammasome assembly and interleukin-1 β secretion. *Nat Commun*, 2018. **9**(1): p. 106.
186. Erdei, J., A. Tóth, E. Balogh, B.B. Nyakundi, E. Bányai, B. Ryffel, et al., Induction of NLRP3 Inflammasome Activation by Heme in Human Endothelial Cells. *Oxid Med Cell Longev*, 2018. **2018**: p. 4310816.

187. Nakanishi, A., N. Kaneko, H. Takeda, T. Sawasaki, S. Morikawa, W. Zhou, et al., Amyloid β directly interacts with NLRP3 to initiate inflammasome activation: identification of an intrinsic NLRP3 ligand in a cell-free system. *Inflamm Regen*, 2018. **38**: p. 27.
188. Duewell, P., H. Kono, K.J. Rayner, C.M. Sirois, G. Vladimer, F.G. Bauernfeind, et al., NLRP3 inflammasomes are required for atherogenesis and activated by cholesterol crystals. *Nature*, 2010. **464**(7293): p. 1357-1361.
189. Martinon, F., V. Pétrilli, A. Mayor, A. Tardivel, and J. Tschopp, Gout-associated uric acid crystals activate the NALP3 inflammasome. *Nature*, 2006. **440**(7081): p. 237-41.
190. Hornung, V., F. Bauernfeind, A. Halle, E.O. Samstad, H. Kono, K.L. Rock, et al., Silica crystals and aluminum salts activate the NALP3 inflammasome through phagosomal destabilization. *Nat Immunol*, 2008. **9**(8): p. 847-56.
191. Trautmann, A., Extracellular ATP in the immune system: more than just a "danger signal". *Sci Signal*, 2009. **2**(56): p. pe6.
192. Amores-Iniesta, J., M. Barberà-Cremades, C.M. Martínez, J.A. Pons, B. Revilla-Nuin, L. Martínez-Alarcón, et al., Extracellular ATP Activates the NLRP3 Inflammasome and Is an Early Danger Signal of Skin Allograft Rejection. *Cell Rep*, 2017. **21**(12): p. 3414-3426.
193. Karmakar, M., M.A. Katsnelson, G.R. Dubyak, and E. Pearlman, Neutrophil P2X7 receptors mediate NLRP3 inflammasome-dependent IL-1 β secretion in response to ATP. *Nature Communications*, 2016. **7**(1): p. 10555.
194. Cuillin, I., A. Gombault, and L. Baron, ATP release and purinergic signaling in NLRP3 inflammasome activation. *Frontiers in Immunology*, 2013. **3**(414).
195. Ayna, G., D.V. Krysko, A. Kaczmarek, G. Petrovski, P. Vandenabeele, and L. Fésüs, ATP release from dying autophagic cells and their phagocytosis are crucial for inflammasome activation in macrophages. *PloS one*, 2012. **7**(6): p. e40069-e40069.
196. Compan, V., A. Baroja-Mazo, G. López-Castejón, A.I. Gomez, C.M. Martínez, D. Angosto, et al., Cell volume regulation modulates NLRP3 inflammasome activation. *Immunity*, 2012. **37**(3): p. 487-500.
197. Gong, T., Y. Yang, T. Jin, W. Jiang, and R. Zhou, Orchestration of NLRP3 Inflammasome Activation by Ion Fluxes. *Trends Immunol*, 2018. **39**(5): p. 393-406.
198. Kinnunen, K., N. Piippo, S. Loukovaara, M. Hytti, K. Kaarniranta, and A. Kauppinen, Lysosomal destabilization activates the NLRP3 inflammasome in human umbilical vein endothelial cells (HUVECs). *J Cell Commun Signal*, 2017. **11**(3): p. 275-279.
199. Heid, M.E., P.A. Keyel, C. Kamga, S. Shiva, S.C. Watkins, and R.D. Salter, Mitochondrial reactive oxygen species induces NLRP3-dependent lysosomal damage and inflammasome activation. *J Immunol*, 2013. **191**(10): p. 5230-8.
200. Swanson, K.V., M. Deng, and J.P.Y. Ting, The NLRP3 inflammasome: molecular activation and regulation to therapeutics. *Nature Reviews Immunology*, 2019. **19**(8): p. 477-489.
201. Elliott, J.M., L. Rouge, C. Wiesmann, and J.M. Scheer, Crystal structure of procaspase-1 zymogen domain reveals insight into inflammatory caspase autoactivation. *J Biol Chem*, 2009. **284**(10): p. 6546-53.
202. Shi, J., Y. Zhao, K. Wang, X. Shi, Y. Wang, H. Huang, et al., Cleavage of GSDMD by inflammatory caspases determines pyroptotic cell death. *Nature*, 2015. **526**(7575): p. 660-5.
203. Liu, X., Z. Zhang, J. Ruan, Y. Pan, V.G. Magupalli, H. Wu, et al., Inflammasome-activated gasdermin D causes pyroptosis by forming membrane pores. *Nature*, 2016. **535**(7610): p. 153-8.
204. Lamkanfi, M., A. Sarkar, L. Vande Walle, A.C. Vitari, A.O. Amer, M.D. Wewers, et al., Inflammasome-dependent release of the alarmin HMGB1 in endotoxemia. *J Immunol*, 2010. **185**(7): p. 4385-92.
205. Schiraldi, M., A. Ruccia, L.M. Muñoz, E. Livoti, B. Celona, E. Venereau, et al., HMGB1 promotes recruitment of inflammatory cells to damaged tissues by forming a complex with CXCL12 and signaling via CXCR4. *J Exp Med*, 2012. **209**(3): p. 551-63.
206. von Moltke, J., N.J. Trinidad, M. Moayeri, A.F. Kintzer, S.B. Wang, N. van Rooijen, et al., Rapid induction of inflammatory lipid mediators by the inflammasome in vivo. *Nature*, 2012. **490**(7418): p. 107-11.
207. Biondo, C., G. Mancuso, A. Midiri, G. Signorino, M. Domina, V. Lanza Cariccio, et al., The Interleukin-1 β /CXCL1/2/Neutrophil Axis Mediates Host Protection against Group B Streptococcal Infection. *Infection and Immunity*, 2014. **82**(11): p. 4508-4517.
208. Lemon, J.K., M.R. Miller, and J.N. Weiser, Sensing of interleukin-1 cytokines during *Streptococcus pneumoniae* colonization contributes to macrophage recruitment and bacterial clearance. *Infect Immun*, 2015. **83**(8): p. 3204-12.
209. Jorgensen, I., J.P. Lopez, S.A. Laufer, and E.A. Miao, IL-1 β , IL-18, and eicosanoids promote neutrophil recruitment to pore-induced intracellular traps following pyroptosis. *Eur J Immunol*, 2016. **46**(12): p. 2761-2766.
210. Savio, L.E.B., P. de Andrade Mello, C.G. da Silva, and R. Coutinho-Silva, The P2X7 Receptor in Inflammatory Diseases: Angel or Demon? *Frontiers in Pharmacology*, 2018. **9**(52).
211. Junges, R., M. Maienschein-Cline, D.A. Morrison, F.C. Petersen, and J.C.D. Hotopp, Complete Genome Sequence of *Streptococcus pneumoniae* Serotype 19F Strain EF3030. *Microbiology Resource Announcements*, 2019. **8**(19): p. e00198-19.
212. Tettelin, H., K.E. Nelson, I.T. Paulsen, J.A. Eisen, T.D. Read, S. Peterson, et al., Complete genome sequence of a virulent isolate of *Streptococcus pneumoniae*. *Science*, 2001. **293**(5529): p. 498-506.
213. Rennemeier, C., S. Hammerschmidt, S. Niemann, S. Inamura, U. Zähringer, and B.E. Kehrel, Thrombospondin-1 promotes cellular adherence of gram-positive pathogens via recognition of peptidoglycan. *Faseb j*, 2007. **21**(12): p. 3118-32.
214. Shambat Srikanth Mairpady, H.A., Vandenesch Francois, Lina Gerard, van Wamel Willem J. B., Arakere Gayathri, Svensson Mattias, Norrby-Teglund Anna Levels of Alpha-Toxin Correlate with Distinct Phenotypic Response Profiles of Blood Mononuclear Cells and with agr Background of Community-Associated *Staphylococcus aureus* Isolates. *PLoS One*, 2014. **9**(8).

215. Siemens, N., B. Chakrakodi, S.M. Shambat, M. Morgan, H. Bergsten, O. Hyldegaard, et al., Biofilm in group A streptococcal necrotizing soft tissue infections. *JCI Insight*, 2016. **1**(10): p. e87882.
216. LeMessurier, K.S., M. Tiwary, N.P. Morin, and A.E. Samarasinghe, Respiratory Barrier as a Safeguard and Regulator of Defense Against Influenza A Virus and *Streptococcus pneumoniae*. *Frontiers in Immunology*, 2020. **11**: p. 3-3.
217. Mairpady Shambat, S., P. Chen, A.T. Nguyen Hoang, H. Bergsten, F. Vandenesch, N. Siemens, et al., Modelling staphylococcal pneumonia in a human 3D lung tissue model system delineates toxin-mediated pathology. *Dis Model Mech*, 2015. **8**(11): p. 1413-25.
218. Erttmann, S.F. and N.O. Gekara, Hydrogen peroxide release by bacteria suppresses inflammasome-dependent innate immunity. *Nat Commun*, 2019. **10**(1): p. 3493.
219. Kelley, N., D. Jeltema, Y. Duan, and Y. He, The NLRP3 Inflammasome: An Overview of Mechanisms of Activation and Regulation. *Int J Mol Sci*, 2019. **20**(13).
220. Tomlinson, G., S. Chimalapati, T. Pollard, T. Lapp, J. Cohen, E. Camberlein, et al., TLR-mediated inflammatory responses to *Streptococcus pneumoniae* are highly dependent on surface expression of bacterial lipoproteins. *J Immunol*, 2014. **193**(7): p. 3736-45.
221. Jang, H.M., J.Y. Park, Y.J. Lee, M.J. Kang, S.G. Jo, Y.J. Jeong, et al., TLR2 and the NLRP3 inflammasome mediate IL-1 β production in *Prevotella nigrescens*-infected dendritic cells. *Int J Med Sci*, 2021. **18**(2): p. 432-440.
222. Jones, C.L. and D.S. Weiss, TLR2 signaling contributes to rapid inflammasome activation during *F. novicida* infection. *PLoS One*, 2011. **6**(6): p. e20609.
223. Haukaas, T.H., S.A. Moestue, R. Vettukattil, B. Sitter, S. Lamichhane, R. Segura, et al., Impact of Freezing Delay Time on Tissue Samples for Metabolomic Studies. *Front Oncol*, 2016. **6**: p. 17.
224. Selders, G.S., A.E. Fetz, M.Z. Radic, and G.L. Bowlin, An overview of the role of neutrophils in innate immunity, inflammation and host-biomaterial integration. *Regen Biomater*, 2017. **4**(1): p. 55-68.
225. Alhaji, M. and A. Farhana, Enzyme Linked Immunosorbent Assay, in *StatPearls*. 2021, StatPearls Publishing Copyright © 2021, StatPearls Publishing LLC.: Treasure Island (FL).
226. de Jager, W., K. Bourcier, G.T. Rijkers, B.J. Prakken, and V. Seyfert-Margolis, Prerequisites for cytokine measurements in clinical trials with multiplex immunoassays. *BMC Immunol*, 2009. **10**: p. 52.
227. Palazon-Riquelme, P. and G. Lopez-Castejon, The inflammasomes, immune guardians at defence barriers. *Immunology*, 2018. **155**(3): p. 320-330.
228. Storek, K.M. and D.M. Monack, Bacterial recognition pathways that lead to inflammasome activation. *Immunol Rev*, 2015. **265**(1): p. 112-29.
229. Zhen, Y. and H. Zhang, NLRP3 Inflammasome and Inflammatory Bowel Disease. *Front Immunol*, 2019. **10**: p. 276.
230. Heneka, M.T., M.P. Kummer, A. Stutz, A. Delekate, S. Schwartz, A. Vieira-Saecker, et al., NLRP3 is activated in Alzheimer's disease and contributes to pathology in APP/PS1 mice. *Nature*, 2013. **493**(7434): p. 674-8.
231. Halle, A., V. Hornung, G.C. Petzold, C.R. Stewart, B.G. Monks, T. Reinheckel, et al., The NALP3 inflammasome is involved in the innate immune response to amyloid-beta. *Nat Immunol*, 2008. **9**(8): p. 857-65.
232. Masters, S.L., A. Dunne, S.L. Subramanian, R.L. Hull, G.M. Tannahill, F.A. Sharp, et al., Activation of the NLRP3 inflammasome by islet amyloid polypeptide provides a mechanism for enhanced IL-1 β in type 2 diabetes. *Nat Immunol*, 2010. **11**(10): p. 897-904.
233. Lee, H.M., J.J. Kim, H.J. Kim, M. Shong, B.J. Ku, and E.K. Jo, Upregulated NLRP3 inflammasome activation in patients with type 2 diabetes. *Diabetes*, 2013. **62**(1): p. 194-204.
234. Booshehri, L.M. and H.M. Hoffman, CAPS and NLRP3. *J Clin Immunol*, 2019. **39**(3): p. 277-286.
235. Lee, C., H.T.T. Do, J. Her, Y. Kim, D. Seo, and I. Rhee, Inflammasome as a promising therapeutic target for cancer. *Life Sci*, 2019. **231**: p. 116593.
236. Seok, J.K., H.C. Kang, Y.-Y. Cho, H.S. Lee, and J.Y. Lee, Therapeutic regulation of the NLRP3 inflammasome in chronic inflammatory diseases. *Archives of Pharmacal Research*, 2021. **44**(1): p. 16-35.
237. Pile, K.D., G.G. Graham, and S.M. Mahler, Interleukin 1 Inhibitors, in *Encyclopedia of Inflammatory Diseases*, M. Parnham, Editor. 2015, Springer Basel: Basel. p. 1-5.
238. US Food and Drug Administration (FDA). Kineret (anakinra) Initial U.S. Approval. 2001 December 2012; Available from: https://www.accessdata.fda.gov/drugsatfda_docs/label/2012/103950s51361bl.pdf.
239. Dubois, E.A., R. Rissmann, and A.F. Cohen, Riloncept and canakinumab. *Br J Clin Pharmacol*, 2011. **71**(5): p. 639-41.
240. US Food and Drug Administration (FDA). Arcalyst (Riloncept) Initial U.S. Approval 2008; Available from: https://www.accessdata.fda.gov/drugsatfda_docs/label/2020/125249s0451bl.pdf.
241. US Food and Drug Administration (FDA). Ilaris (Canakinumab) Initial U.S. Approval. 2009; Available from: https://www.accessdata.fda.gov/drugsatfda_docs/label/2020/125319s1001bl.pdf.
242. Lachmann, H.J., I. Kone-Paut, J.B. Kummerle-Deschner, K.S. Leslie, E. Hachulla, P. Quartier, et al., Use of canakinumab in the cryopyrin-associated periodic syndrome. *N Engl J Med*, 2009. **360**(23): p. 2416-25.
243. Ottaviani, S., A. Moltó, H.-K. Ea, S. Neveu, G. Gill, L. Brunier, et al., Efficacy of anakinra in gouty arthritis: a retrospective study of 40 cases. *Arthritis Research & Therapy*, 2013. **15**(5): p. R123.
244. Mertens, M. and J.A. Singh, Anakinra for rheumatoid arthritis: a systematic review. *J Rheumatol*, 2009. **36**(6): p. 1118-25.
245. LaRock, C.N., J. Todd, D.L. LaRock, J. Olson, A.J. O'Donoghue, A.A.B. Robertson, et al., IL-1 β is an innate immune sensor of microbial proteolysis. *Science Immunology*, 2016. **1**(2): p. 3539-3539.
246. Hoegen, T., N. Tremel, M. Klein, B. Angele, H. Wagner, C. Kirschning, et al., The NLRP3 inflammasome contributes to brain injury in pneumococcal meningitis and is activated through ATP-dependent lysosomal cathepsin B release. *J Immunol*, 2011. **187**(10): p. 5440-51.

247. de Vasconcelos, N.M. and M. Lamkanfi, Recent Insights on Inflammasomes, Gasdermin Pores, and Pyroptosis. *Cold Spring Harb Perspect Biol*, 2020. **12**(5).
248. Malik, A. and T.D. Kanneganti, Inflammasome activation and assembly at a glance. *J Cell Sci*, 2017. **130**(23): p. 3955-3963.
249. Balamayooran, G., S. Batra, M.B. Fessler, K.I. Happel, and S. Jeyaseelan, Mechanisms of neutrophil accumulation in the lungs against bacteria. *Am J Respir Cell Mol Biol*, 2010. **43**(1): p. 5-16.
250. Gao, Y., W. Xu, X. Dou, H. Wang, X. Zhang, S. Yang, et al., Mitochondrial DNA Leakage Caused by *Streptococcus pneumoniae* Hydrogen Peroxide Promotes Type I IFN Expression in Lung Cells. *Front Microbiol*, 2019. **10**: p. 630.
251. Rai, P., M. Parrish, I.J.J. Tay, N. Li, S. Ackerman, F. He, et al., *Streptococcus pneumoniae* secretes hydrogen peroxide leading to DNA damage and apoptosis in lung cells. *Proceedings of the National Academy of Sciences*, 2015. **112**(26): p. E3421-E3430.
252. Labbé, K. and M. Saleh, Cell death in the host response to infection. *Cell Death & Differentiation*, 2008. **15**(9): p. 1339-1349.
253. Zheng, D., T. Liwinski, and E. Elinav, Inflammasome activation and regulation: toward a better understanding of complex mechanisms. *Cell Discovery*, 2020. **6**(1): p. 36.
254. He, W.-t., H. Wan, L. Hu, P. Chen, X. Wang, Z. Huang, et al., Gasdermin D is an executor of pyroptosis and required for interleukin-1 β secretion. *Cell Research*, 2015. **25**(12): p. 1285-1298.
255. Brissac, T., A.T. Shenoy, L.A. Patterson, and C.J. Orihuela, Cell Invasion and Pyruvate Oxidase-Derived H₂O₂ Are Critical for *Streptococcus pneumoniae*-Mediated Cardiomyocyte Killing. *Infect Immun*, 2018. **86**(1).
256. Ricci, C., V. Pastukh, J. Leonard, J. Turrens, G. Wilson, D. Schaffer, et al., Mitochondrial DNA damage triggers mitochondrial-superoxide generation and apoptosis. *American Journal of Physiology-Cell Physiology*, 2008. **294**(2): p. C413-C422.
257. Norbury, C.J. and B. Zhivotovsky, DNA damage-induced apoptosis. *Oncogene*, 2004. **23**(16): p. 2797-2808.
258. Bedi, B., N.M. Maurice, Z. Yuan, Z. Prasla, and R.T. Sadikot, Mitochondrial DNA damage associated activation of NLRP3 inflammasome impairs host defense during *P. aeruginosa* infection. *The FASEB Journal*, 2019. **33**(S1): p. 549.3-549.3.
259. Shimada, K., T.R. Crother, J. Karlin, J. Dagvadorj, N. Chiba, S. Chen, et al., Oxidized mitochondrial DNA activates the NLRP3 inflammasome during apoptosis. *Immunity*, 2012. **36**(3): p. 401-14.
260. Hasegawa, T., M. Nakashima, and Y. Suzuki, Nuclear DNA damage-triggered NLRP3 inflammasome activation promotes UVB-induced inflammatory responses in human keratinocytes. *Biochem Biophys Res Commun*, 2016. **477**(3): p. 329-35.
261. Fatykhova, D., A. Rabes, C. Machnik, K. Guruprasad, F. Pache, J. Berg, et al., Serotype 1 and 8 Pneumococci Evade Sensing by Inflammasomes in Human Lung Tissue. *PLoS One*, 2015. **10**(8): p. e0137108.
262. Jahn, K., S. Handtke, R. Palankar, S. Weissmuller, G. Nouailles, T.P. Kohler, et al., Pneumolysin induces platelet destruction, not platelet activation, which can be prevented by immunoglobulin preparations in vitro. *Blood Adv*, 2020. **4**(24): p. 6315-6326.
263. Surabhi, S., F. Cuypers, S. Hammerschmidt, and N. Siemens, The Role of NLRP3 Inflammasome in Pneumococcal Infections. *Frontiers in Immunology*, 2020. **11**(3277).
264. Li, Q., S. Sanlioglu, S. Li, T. Ritchie, L. Oberley, and J.F. Engelhardt, GPx-1 gene delivery modulates NFkappaB activation following diverse environmental injuries through a specific subunit of the IKK complex. *Antioxid Redox Signal*, 2001. **3**(3): p. 415-32.
265. Schreck, R., P. Rieber, and P.A. Baeuerle, Reactive oxygen intermediates as apparently widely used messengers in the activation of the NF-kappa B transcription factor and HIV-1. *Embo j*, 1991. **10**(8): p. 2247-58.
266. Zhang, J., G. Johnston, B. Stebler, and E.T. Keller, Hydrogen peroxide activates NFkappaB and the interleukin-6 promoter through NFkappaB-inducing kinase. *Antioxid Redox Signal*, 2001. **3**(3): p. 493-504.
267. Taabazuing, C.Y., M.C. Okondo, and D.A. Bachovchin, Pyroptosis and Apoptosis Pathways Engage in Bidirectional Crosstalk in Monocytes and Macrophages. *Cell Chem Biol*, 2017. **24**(4): p. 507-514.e4.
268. Monteleone, M., A.C. Stanley, K.W. Chen, D.L. Brown, J.S. Bezradica, J.B. von Pein, et al., Interleukin-1 β Maturation Triggers Its Relocation to the Plasma Membrane for Gasdermin-D-Dependent and -Independent Secretion. *Cell Rep*, 2018. **24**(6): p. 1425-1433.
269. de Vasconcelos, N.M., N. Van Opendenbosch, H. Van Gorp, R. Martín-Pérez, A. Zecchin, P. Vandenabeele, et al., An Apoptotic Caspase Network Safeguards Cell Death Induction in Pyroptotic Macrophages. *Cell Rep*, 2020. **32**(4): p. 107959.
270. Rogers, C., T. Fernandes-Alnemri, L. Mayes, D. Alnemri, G. Cingolani, and E.S. Alnemri, Cleavage of DFNA5 by caspase-3 during apoptosis mediates progression to secondary necrotic/pyroptotic cell death. *Nat Commun*, 2017. **8**: p. 14128.
271. Zhao, L., H. Lin, S. Chen, S. Chen, M. Cui, D. Shi, et al., Hydrogen peroxide induces programmed necrosis in rat nucleus pulposus cells through the RIP1/RIP3-PARP-AIF pathway. *J Orthop Res*, 2018. **36**(4): p. 1269-1282.
272. Gutierrez, K.D., M.A. Davis, B.P. Daniels, T.M. Olsen, P. Ralli-Jain, S.W. Tait, et al., MLKL Activation Triggers NLRP3-Mediated Processing and Release of IL-1 β Independently of Gasdermin-D. *J Immunol*, 2017. **198**(5): p. 2156-2164.
273. Tan, K.C., S.V. Ipcho, R.D. Trengove, R.P. Oliver, and P.S. Solomon, Assessing the impact of transcriptomics, proteomics and metabolomics on fungal phytopathology. *Mol Plant Pathol*, 2009. **10**(5): p. 703-15.
274. Liu, G. and R. Summer, Cellular Metabolism in Lung Health and Disease. *Annu Rev Physiol*, 2019. **81**: p. 403-428.
275. Hiemstra, P.S. and A.M. van der Does, Reprogramming of cellular metabolism: driver for airway remodelling in COPD? *European Respiratory Journal*, 2017. **50**(5): p. 1702197.

REFERENCES

276. Gierok, P., M. Harms, K. Methling, F. Hochgräfe, and M. Lalk, Staphylococcus aureus Infection Reduces Nutrition Uptake and Nucleotide Biosynthesis in a Human Airway Epithelial Cell Line. *Metabolites*, 2016. **6**(4).
277. Rivas, H.G., S.K. Schmalting, and M.M. Gaglia, Shutoff of Host Gene Expression in Influenza A Virus and Herpesviruses: Similar Mechanisms and Common Themes. *Viruses*, 2016. **8**(4): p. 102.
278. Bercovich-Kinori, A., J. Tai, I.A. Gelbart, A. Shitrit, S. Ben-Moshe, Y. Drori, et al., A systematic view on influenza induced host shutoff. *Elife*, 2016. **5**.
279. Ritter, J.B., A.S. Wahl, S. Freund, Y. Genzel, and U. Reichl, Metabolic effects of influenza virus infection in cultured animal cells: Intra- and extracellular metabolite profiling. *BMC Syst Biol*, 2010. **4**: p. 61.
280. Petiot, E., D. Jacob, S. Lanthier, V. Lohr, S. Ansorge, and A.A. Kamen, Metabolic and kinetic analyses of influenza production in perfusion HEK293 cell culture. *BMC Biotechnol*, 2011. **11**: p. 84.
281. Palmieri, F., The mitochondrial transporter family SLC25: Identification, properties and physiopathology. *Molecular Aspects of Medicine*, 2013. **34**(2): p. 465-484.
282. Iyer, R., N.S. Baliga, and A. Camilli, Catabolite Control Protein A (CcpA) Contributes to Virulence and Regulation of Sugar Metabolism in *Streptococcus pneumoniae*. *Journal of Bacteriology*, 2005. **187**(24): p. 8340-8349.
283. Jourlin-Castelli, C., N. Mani, M.M. Nakano, and A.L. Sonenshein, CcpC, a novel regulator of the LysR family required for glucose repression of the citB gene in *Bacillus subtilis*. *J Mol Biol*, 2000. **295**(4): p. 865-78.
284. Cantu, D., J. Schaack, and M. Patel, Oxidative inactivation of mitochondrial aconitase results in iron and H₂O₂-mediated neurotoxicity in rat primary mesencephalic cultures. *PLoS one*, 2009. **4**(9): p. e7095-e7095.
285. Flint, D.H., J.F. Tuminello, and M.H. Emptage, The inactivation of Fe-S cluster containing hydro-lyases by superoxide. *J Biol Chem*, 1993. **268**(30): p. 22369-76.
286. Nulton-Persson, A.C. and L.I. Szveda, Modulation of Mitochondrial Function by Hydrogen Peroxide *. *Journal of Biological Chemistry*, 2001. **276**(26): p. 23357-23361.
287. Wynosky-Dolfi, M.A., A.G. Snyder, N.H. Philip, P.J. Doonan, M.C. Poffenberger, D. Avizonis, et al., Oxidative metabolism enables Salmonella evasion of the NLRP3 inflammasome. *J Exp Med*, 2014. **211**(4): p. 653-68.
288. Wang, X. and D. Chen, Purinergic Regulation of Neutrophil Function. *Front Immunol*, 2018. **9**: p. 399.
289. Chen, Y., R. Corriden, Y. Inoue, L. Yip, N. Hashiguchi, A. Zinkernagel, et al., ATP release guides neutrophil chemotaxis via P2Y₂ and A₃ receptors. *Science*, 2006. **314**(5806): p. 1792-5.
290. Kolaczowska, E. and P. Kubes, Neutrophil recruitment and function in health and inflammation. *Nat Rev Immunol*, 2013. **13**(3): p. 159-75.
291. Mortaz, E., S.D. Alipoor, I.M. Adcock, S. Mumby, and L. Koenderman, Update on Neutrophil Function in Severe Inflammation. *Frontiers in Immunology*, 2018. **9**(2171).
292. Kavalenka, A.I., G.N. Semenкова, and S.N. Cherenkevich, Effects of hydrogen peroxide on neutrophil ability to generate reactive oxygen and chlorine species and to secrete myeloperoxidase in vitro. *Cell and Tissue Biology*, 2007. **1**(6): p. 551-559.
293. Domon, H., M. Oda, T. Maekawa, K. Nagai, W. Takeda, and Y. Terao, *Streptococcus pneumoniae* disrupts pulmonary immune defence via elastase release following pneumolysin-dependent neutrophil lysis. *Scientific Reports*, 2016. **6**(1): p. 38013.
294. Zamaraeva, M.V., R.Z. Sabirov, E. Maeno, Y. Ando-Akatsuka, S.V. Bessonova, and Y. Okada, Cells die with increased cytosolic ATP during apoptosis: a bioluminescence study with intracellular luciferase. *Cell Death & Differentiation*, 2005. **12**(11): p. 1390-1397.
295. Falzoni, S., G. Donvito, and F. Di Virgilio, Detecting adenosine triphosphate in the pericellular space. *Interface Focus*, 2013. **3**(3): p. 20120101.
296. Olotu, C., F. Lehmsiek, B. Koch, M. Kiefmann, A.-K. Riegel, S. Hammerschmidt, et al., *Streptococcus pneumoniae* inhibits purinergic signaling and promotes purinergic receptor P2Y₂ internalization in alveolar epithelial cells. *The Journal of biological chemistry*, 2019. **294**(34): p. 12795-12806.
297. Wirsching, E., M. Fauler, G. Fois, and M. Frick, P₂ Purinergic Signaling in the Distal Lung in Health and Disease. *International journal of molecular sciences*, 2020. **21**(14): p. 4973.
298. Jobe, A.H., Pulmonary surfactant therapy. *N Engl J Med*, 1993. **328**(12): p. 861-8.
299. Günther, A., C. Ruppert, R. Schmidt, P. Markart, F. Grimminger, D. Walrmath, et al., Surfactant alteration and replacement in acute respiratory distress syndrome. *Respiratory Research*, 2001. **2**(6): p. 353.

PAPER 1

The Role of NLRP3 Inflammasome in Pneumococcal Infections

Surabhi Surabhi, Fabian Cuypers, Sven Hammerschmidt and Nikolai Siemens

Published in Frontiers in Immunology, 2020 Dec, 14,
DOI: 10.3389/fimmu.2020.614801

Author contributions:

As first author in this publication, **SS** actively participated in the design and construction of this scientific review. Furthermore, **SS** collected and analyzed all the relevant references needed in the preparation of the main manuscript. **SS** wrote the main manuscript draft and had a significant contribution in the scientific revision and editing of the final version of this manuscript.

Conception and design: **SS** and NS

Collection and analysis of information: **SS**, FC and NS

Manuscript draft preparation: **SS**, FC and NS

Critical revision and editing: **SS**, FC, NS, and SH

Surabhi Surabhi

Prof. Dr. Nikolai Siemens



The Role of NLRP3 Inflammasome in Pneumococcal Infections

Surabhi Surabhi, Fabian Cuypers, Sven Hammerschmidt and Nikolai Siemens*

Department of Molecular Genetics and Infection Biology, University of Greifswald, Greifswald, Germany

OPEN ACCESS

Edited by:

Oleg Chernikov,
G.B. Elyakov Pacific Institute of
Bioorganic Chemistry, (RAS), Russia

Reviewed by:

Bastian Opitz,
Charité – Universitätsmedizin Berlin,
Germany

Aixin Li,
Swedish National Heritage Board,
Sweden

*Correspondence:

Nikolai Siemens
nikolai.siemens@uni-greifswald.de

Specialty section:

This article was submitted to
Inflammation,
a section of the journal
Frontiers in Immunology

Received: 07 October 2020

Accepted: 16 November 2020

Published: 14 December 2020

Citation:

Surabhi S, Cuypers F,
Hammerschmidt S and Siemens N
(2020) The Role of
NLRP3 Inflammasome in
Pneumococcal Infections.
Front. Immunol. 11:614801.
doi: 10.3389/fimmu.2020.614801

Inflammasomes are innate immune sensors that regulate caspase-1 mediated inflammation in response to environmental, host- and pathogen-derived factors. The NLRP3 inflammasome is highly versatile as it is activated by a diverse range of stimuli. However, excessive or chronic inflammasome activation and subsequent interleukin-1 β (IL-1 β) release are implicated in the pathogenesis of various autoimmune diseases such as rheumatoid arthritis, inflammatory bowel disease, and diabetes. Accordingly, inflammasome inhibitor therapy has a therapeutic benefit in these diseases. In contrast, NLRP3 inflammasome is an important defense mechanism against microbial infections. IL-1 β antagonizes bacterial invasion and dissemination. Unfortunately, patients receiving IL-1 β or inflammasome inhibitors are reported to be at a disproportionate risk to experience invasive bacterial infections including pneumococcal infections. Pneumococci are typical colonizers of immunocompromised individuals and a leading cause of community-acquired pneumonia worldwide. Here, we summarize the current limited knowledge of inflammasome activation in pneumococcal infections of the respiratory tract and how inflammasome inhibition may benefit these infections in immunocompromised patients.

Keywords: nucleotide-binding and oligomerization domain-like receptors and pyrin domain containing receptor 3, inflammasome, pneumococcus (*Streptococcus pneumoniae*), respiratory infection, immune response

INTRODUCTION

The human innate immunity axis plays a pivotal role in detection of pathogen- or damage-associated molecular patterns (PAMPs and DAMPs) and contributes to a crucial inflammatory response. To sense PAMPs and DAMPs, innate immune cells express pattern recognition receptors (PRRs). PRRs are classified into five families: Toll-like receptors (TLRs), Nucleotide-binding and oligomerization domain (NOD)-like receptors (NLRs), Retinoic acid-inducible gene (RIG)-I-like receptors, C-type lectin receptors, and Absent in melanoma 2 (AIM2)-like receptor (ALR) (1). Furthermore, other molecules such as cyclic GMP-AMP synthase can sense pathogen-derived DNA (2). Inflammasomes are one of the most recently discovered classes of NLRs (3).

To date, 22 human NLRs are described. Among them, NLR and pyrin domain containing receptor 3 (NLRP3) is by far the best characterized (4). A wide range of stimuli including bacterial pore forming toxins can activate the NLRP3 inflammasome (5). The subsequent release of interleukins (IL) IL-1 β and IL-18 induces a diverse range of protective host pathways aiming to eradicate the pathogen (6). However, uncontrolled and excessive hyper-inflammation can be a driver of several inflammatory and autoimmune diseases (7, 8). Implication of the NLRP3

inflammasome in inflammatory diseases has provided new avenues for designing drugs which target the inflammasome and its signaling cascade. However, it is observed that patients who receive NLRP3 or IL-1 β inhibitors are disproportionately susceptible to bacterial infections (9). Therefore, it is of high importance to understand the role of NLRP3 inflammasome in bacterial pathogenesis.

CANONICAL NLRP3 INFLAMMASOME ACTIVATION

NLRP3 inflammasome is a multi-protein complex comprising of a sensor NLRP3 protein, an adaptor apoptosis-associated speck-like protein (ASC), and the zymogen procaspase-1 (10). The cytosolic NLRP3 protein contains an N-terminal Pyrin domain (PYD), a central NACHT domain, and a C-terminal leucine-rich repeat (LRR) domain. The NACHT domain possesses adenosine triphosphatase (ATPase) activity and comprises of nucleotide-binding domain (NBD), helical domain 1 (HD1), winged helix domain (WHD) and helical domain 2 (HD2) (11). The ASC domain is a bipartite molecule that contains an N-terminal PYD domain and a C-terminal caspase activation and recruitment domain (CARD). Procaspase-1 consists of an N-terminal CARD, a central large catalytic p20 subunit, and a C-terminal small catalytic p10 subunit (12).

In resting macrophages, the NLRP3 and pro-IL-1 β concentrations are insufficient to initiate activation of the inflammasome (13). Therefore, the NLRP3 inflammasome is activated in a two-step process. The first, so called priming step, is initiated *via* the inflammatory stimuli which are detected by TLRs, tumor necrosis factor receptors (TNFR) or IL-1R. These actions activate downstream the transcription factor NF- κ B. NF- κ B, in turn, upregulates the expression of NLRP3 and pro-IL-1 β . In contrast, the priming step does not affect the expression of ASC, procaspase-1 or IL-18 (14–16). Following priming, a second activation step is essential for the assembly of the inflammasome. NLRP3 is highly diverse in nature and a wide range of stimuli can activate it. Common activators of the NLRP3 inflammasome are pathogens (17), extracellular ATP (18), pathogen associated RNA, proteins and toxins (5, 19, 20), heme (21), endogenous factors (amyloid- β , cholesterol crystals, uric acid crystals) (22–24), and environmental factors (silica and aluminum salts) (24, 25). These activators do not directly interact with the inflammasome but rather cause various changes at the cellular level. These include changes in cell volume (26), ionic fluxes (27), lysosomal damage (28), ROS production, and mitochondrial dysfunction (29). The second activation step is essential for cells such as macrophages and epithelial cells. In contrast, human monocytes can release mature IL-1 β already after priming (30, 31). Upon activation, oligomerization of the NLRP3 complex occurs *via* homotypic PYD-PYD interaction of the sensor and adaptor protein, and CARD-CARD interaction of the adaptor and procaspase-1 (Figure 1). Following assembly, recruited procaspase-1 is converted to bioactive caspase-1 through proximity induced

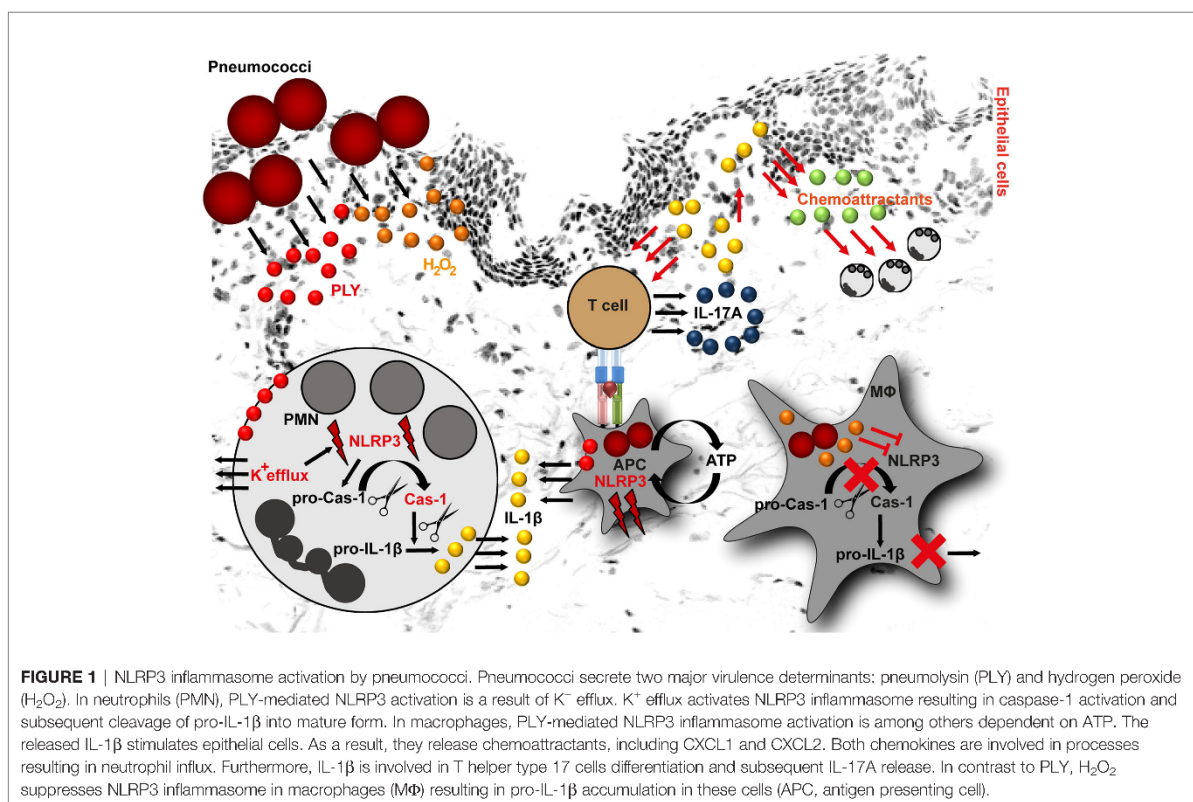
auto-proteolytic cleavage (32). Subsequently, caspase-1 cleaves the cytokine precursors pro-IL-1 β and pro-IL-18 into mature forms. Simultaneously, caspase-1 cleaves gasdermin-D (GSDMD). After proteolytic cleavage, the C-terminal GSDMD (GSDMD-C) remains in the cytosol, while GSDMD-N anchors the cell membrane lipid. The lipid binding allows GSDMD-N to enter the lipid bilayer. Subsequent GSDMD-N oligomerization within the membrane results in pore formation leading to cell swelling and lysis. The pores serve thereby as protein secretion channels for IL-1 β and IL-18. This form of a programmed inflammatory cell death is called pyroptosis (33–35). However, lytic GSDMD-N dependent secretion of IL-1 β does not apply universally to all cell types. Studies on neutrophils have shown that GSDMD-N does not localize at the plasma membrane. Instead, it co-localizes with membranes of azurophilic granules and LC3⁺ autophagosomes resulting in a non-lytic pathway dependent IL-1 β secretion which depends on autophagy machinery (36). Alongside with IL-1 β , other pro-inflammatory cytokines, eicosanoids, and alarmins are released into the extracellular space. These actions accentuate the inflammatory state by recruiting additional inflammatory immune cells of different lineages (37–39).

Apart from the canonical, non-canonical NLRP3 inflammasome activation is described (40). Non-canonical inflammasome activation is triggered by caspases-4/5 in humans (41). However, the noncanonical form can sense only Gram-negative bacteria. Therefore, it potentially does not play a role in Gram-positive bacterial infections (40).

APPROVED IL-1 β INHIBITING DRUGS AND THEIR SIDE-EFFECTS IN PATIENTS

NLRP3 inflammasome signaling is implicated in the onset of a number of diseases, including gout (24), atherosclerosis (23), type II diabetes (42, 43), Cryopyrin-associated periodic syndrome (CAPS) (44), various types of cancer (45), and inflammatory bowel disease (IBD) (46). In the following, we give just two examples of the role of NLRP3 in auto-inflammatory and auto-immune diseases.

CAPS summarizes three auto-inflammatory diseases caused by mutations in the *NLRP3* gene. These include familial cold auto-inflammatory syndrome (FCAS), Muckle-Wells syndrome (MWS), and neonatal onset multisystem inflammatory disease (NOMID). In most cases, CAPS manifests during the childhood and is characterized by spontaneous NLRP3 activation and excessive IL-1 β production resulting in frequent episodes of fever, skin rashes, joint and eye inflammation. In severe cases, children can suffer from periorbital edema, amyloidosis, polyarthralgia, growth retardation, and death (47, 48). *In vivo* studies with transgenic mice expressing the human disease-associated R258W (MWS) or A350V and L351P (FCAS) mutations in the *NLRP3* gene demonstrated the detrimental role of IL-1 β in these diseases (49, 50). Genetic deletion of the IL-1R efficiently rescued *NLRP3*^{A350V} and partially *NLRP3*^{L351P} mice from neonatal lethality (49).



Rheumatoid arthritis (RA) is a chronic autoimmune disease characterized by persistent synovial inflammation and hyperplasia of the diarthrodial joints and progressive destruction of cartilage and bone (51). In particular, chondrocytes- and monocytes-derived TNF and IL-1 β are associated with hyper-inflammatory processes in affected joints (52). At the local level, even low concentrations of IL-1 β induce production and secretion of matrix metalloproteinases, which are mainly involved in destructive processes (53). Furthermore, IL-1 β assists in T helper type 17 (Th17) cells differentiation and subsequent IL-17A production. Both processes further contribute to the hyper-inflammatory state of RA (54). These data implicate NLRP3 inflammasome as one of the contributing factors to RA progression. In line with this, several studies have shown that *NLRP3* and other inflammasome-related genes are highly upregulated in monocytes, macrophages, and dendritic cells of RA patients. Furthermore, *NLRP3* gene polymorphisms (e.g., rs35829419, rs10754558, rs4612666) were associated with RA manifestation and pathogenesis [reviewed in (55)].

Although the above mentioned diseases affect different organs and are diverse in nature, they are also characterized by a common feature, namely elevated levels of IL-1 β . It is of significance to mention that IL-1 β release is not limited to NLRP3 inflammasome activation. A variety of mechanisms, including AIM2 inflammasome activation, which also plays a crucial role in bacterial detection, can result in production and release of IL-1 β [reviewed in (56)]. Therefore, treatments target

various components of the signaling cascade and particularly IL-1. Several strategies that combat IL-1 action have undergone substantial clinical trials. Some of them are summarized in **Table 1**. Anakinra, Riloncept, and Canakinumab are clinically approved IL-1 inhibiting drugs and the best studied agents (73). Anakinra is an IL-1 receptor antagonist and is used among others for the treatment of RA, acute gouty arthritis, and CAPS. It blocks the action of both IL-1 α and IL-1 β (74–76). Clinical trials with Anakinra reported elevated numbers of infectious episodes in Anakinra-treated patients as compared to the placebo-treated group during the first 6 months of treatment. Furthermore, the incidence of serious infections was increased. These infections comprised mainly of cellulitis, pneumonia, and bone and joint infections as well (57). Riloncept is a dimeric fusion protein that contains two IL-1 receptors attached to the Fc portion of human IgG1. Similar to Anakinra, it blocks the activity of IL-1 isoforms but does not interact with the IL-1 receptor. Riloncept is used to treat CAPS and the most reported side-effects include skin reactions and upper respiratory tract infections (58). Canakinumab is a monoclonal IgG1 that specifically targets IL-1 β and is commonly used for treatment of Periodic Fever Syndromes, MWS, and acute gouty arthritis (59, 60). Among the various side effects, respiratory tract infections were the most reported side effect in clinical trials (60).

All IL-1 inhibiting strategies are well tolerated in the majority of patients. The most common adverse effect is a dose-dependent

TABLE 1 | NLRP3 inflammasome inhibitors used in clinics.

Drug	Target	Inhibition mechanism	Treatment	Reference
Anakinra	IL-1 receptor	IL-1 receptor antagonist	Rheumatoid arthritis, Cryopyrin-associated periodic syndrome	(57)
Rilonacept	IL-1 α and IL-1 β	IL-1 blocker	Cryopyrin-associated periodic syndrome	(58, 59)
Canakinumab	IL-1 β	Monoclonal IgG1 antibody	CAPS and other Periodic Fever Syndromes, active Still's disease	(59–61)
Tranilast*	NACHT domain	Inhibits the NLRP3 oligomerization	Bronchial asthma, atypical dermatitis, allergic conjunctivitis, keloids, and hypertrophic scar	(62)
Gevokizumab [#]	IL-1 β	Monoclonal anti-IL-1 β antibody	Diabetes, autoimmune disease	(63, 64)
LY2189102 [#]	IL-1 β	Humanized monoclonal anti-IL-1 β antibody	Rheumatoid arthritis, Type 2 diabetes	(65)
Glyburide [#]	ATP-sensitive K ⁺ channels	Indirect inhibition of the NLRP3 inflammasome	Type 2 diabetes, gestational diabetes	(66–68)
VX-740 [#] (Pralnacasan)	Caspase-1	Non-peptide caspase-1 inhibitor	Osteoarthritis and rheumatoid arthritis	(69)
VX-765 [#] (Behnacasan)	Caspase-1 Caspase-4	Peptidomimetic metabolite/Caspase-1/4 inhibitor	Rheumatoid arthritis	(70)
OLT1177 [#]	NLRP3 ATPase	Blocks NLRP3 ATPase activity, restricts inflammasome activation	Osteoarthritis	(71)
AMG108	IL-1R1	Human monoclonal IL-1R1-antibody	Osteoarthritis	(72)

*approved drug but not for NLRP3; [#]ongoing clinical trials.

skin irritation at the injection site. However, a substantially increased incidence of bacterial infections of the respiratory tract caused by Gram-positive bacteria, including pneumococci, *Staphylococcus aureus* (SA), and/or group A streptococci (GAS) are reported (77). Furthermore, IL-1 inhibiting therapies were associated with a higher incidence of fatal infections as compared to the placebo treated group. Therefore, treatment with IL-1 inhibiting drugs is not recommended for patients with an ongoing infection or with a history of severe infections (59, 77, 78).

ROLE OF NLRP3 INFLAMMASOME IN PNEUMOCOCCAL INFECTIONS

Pneumococci, SA, and GAS are frequent colonizers of the upper respiratory tract (79). Colonization is usually asymptomatic in healthy individuals. However, imbalances in the immune system can lead to severe, invasive and even life-threatening diseases such as pneumonia and sepsis. The occurrence of the more severe forms of infection is commonly found in children younger than 5 years of age, elderly, and immuno-compromised population (80). Due to the immunosuppressive nature of IL-1 inhibiting agents, patients undergoing treatment seem to be at higher risk to develop infections caused by these bacteria (77, 81). In general, inflammation plays a crucial role in infectious diseases. Impaired or insufficient inflammatory response can result in prolonged and/or recurrent infections. In contrast, excessive hyper-inflammation is associated with fatal outcome (82, 83).

Pneumococci colonize the nasopharyngeal cavity of 20%–50% of children and 8%–30% of adults. They have been implicated as the most common etiologic agent of community-acquired pneumonia (80, 84). However, only limited number of studies investigated the role of inflammasome in pneumococcal infections and contrary results are reported. For example, one murine model study reported that *NLRP3*^{-/-} mice are more

susceptible to pneumococcal pneumonia (85). In contrast, a study on pneumococcal meningitis showed that mice with an active NLRP3 signaling have higher clinical scores, suggesting that NLRP3 activation contributes to brain injury (86). Since the incidence of respiratory tract infections is elevated in patient receiving IL-1 inhibiting agent, we will solely focus on the role of NLRP3 in respiratory pneumococcal infections.

Two of the most important secreted pneumococcal virulence determinants are hydrogen peroxide (H₂O₂) and the cholesterol-dependent cytolysin, pneumolysin (PLY) (87). Both factors are implicated in inflammasome activating and suppressive processes. Based on the pneumococcal serotypes used for the infection, the NLRP3-dependent IL-1 β secretion by human cells varies. Macrophages infected with serotypes that are associated with invasive diseases and express low/non-hemolytic PLY (serotypes 1, 7F and 8), release lower amounts of IL-1 β as compared to macrophages infected with serotypes expressing a fully active PLY (serotypes 2, 3, 6B, 9N) (88, 89). Being poor activators of the inflammasome, the invasive serotypes are potentially less efficiently recognized by the innate immune system and therefore, are less susceptible to immuno-mediated clearance. However, the exact mechanism of NLRP3 activation by PLY is unknown. This process is most likely of indirect nature (Figure 1). Studies on human neutrophils have shown that PLY-mediated NLRP3 activation is a result of potassium ion (K⁺) efflux. Experimental inhibition of K⁺ efflux in neutrophils resulted in impaired caspase-1 activation and subsequently in diminished IL-1 β processing (Figure 1). Furthermore, it was shown that lysosomal destabilization did not play a role in PLY-mediated IL-1 β processing in neutrophils (90). In general, IL-1 β induces the production of chemoattractants, such as CXCL1 and CXCL2 by lung epithelial cells, which enhance neutrophil influx (91) and subsequent bacterial clearance at the site of infection (92, 93). Studies on pneumococcal infections of mouse peritoneal neutrophils indicate that NLRP3 inflammasome is mainly responsible for IL-1 β secretion, while the AIM2 and NLRC4 inflammasomes are dispensable in these type of immune

cells (94). Furthermore, neutrophil-derived IL-1 β is involved in activation of Th17 cells. Th17-derived IL-17A acts as an additional chemoattractant-stimulating agent (95, 96) and indirectly mediates neutrophilia in the infected organs (**Figure 1**) (97). Nonetheless, neutrophil influx alone is not sufficient to clear pneumococci and macrophage influx is essential to ensure bacterial elimination (93, 98). A study by Hoegen and colleagues demonstrated that PLY was a key inducer of NLRP3 inflammasome and IL-1 β expression in human differentiated THP-1 cells (86). In contrast to neutrophils, NLRP3 inflammasome activity was dependent on lysosomal destabilization, release of ATP, and cathepsin B activation (86). Furthermore, NLRP3 inflammasome activating synergistic effects of PLY and TLR agonists in dendritic cells and macrophages are reported (85, 88). However, this is rather a general inflammasome activating/priming effect. Apart from NLRP3, PLY can also activate AIM2 inflammasomes (99).

In contrast to PLY, only one study investigated the pneumococci-derived H₂O₂ and inflammasome interplay. By utilizing mouse bone marrow-derived macrophages (mBMDMs), Ertmann and Gekara have shown that mBMDMs infected with pneumococci accumulate large amounts of pro-IL-1 β and procaspase-1 (100). Detection of the processed forms of IL-1 β and caspase-1 was highly delayed and remained undetectable until 12 h post infection. However, the ratio of processed IL-1 β and caspase-1 to their precursors was still very low (100). In contrast, *spxB*-mutant strain, which lacked H₂O₂ production, showed an intrinsically increased capacity to activate the inflammasome. The authors suggested that pneumococci employ H₂O₂-mediated inflammasome inhibition as a colonization strategy (100). Although the study provides highly relevant new insights into pneumococci-host interplay, verification of these results in human host system is warranted. However, host factors upstream or downstream of NLRP3 inflammasome also play a crucial role in colonization and infection processes. Studies in aged mice have suggested that an increase in endoplasmic reticulum stress and enhanced unfolded protein responses contribute to diminished assembly and activation of the NLRP3 resulting in failed clearance of pneumococci (101). In support of this, Krone and colleagues demonstrated that aged mice shows a delayed clearance of pneumococci in the nasopharynx as compared to young mice (102). The authors attributed the observed phenotype to the impaired innate mucosal immune responses in aged mice, including NLRP3 and IL-1 β suppression. Furthermore, Lemon and colleagues demonstrated a prolonged colonization of *IL1R*^{-/-} adult mice as compared to wild-type mice (93). The prolonged colonization was linked to reduced numbers of neutrophils at early stages of infection and reduced macrophage influx at later time points of carriage in *IL1R*^{-/-} mice (93).

Apart from the bacterial pore-forming toxins, microbial RNA has also been implicated as a direct NLRP3 inflammasome activator (19). Studies showed that even small fragments of staphylococcal or group B streptococcal (GBS) RNA are sufficient for inflammasome activation in human THP-1-derived

and mouse macrophages (103, 104). Based on detailed analyses of GBS and mouse macrophages interplay, Gupta and colleagues proposed that bacteria-mediated activation of NLRP3 inflammasomes requires bacterial uptake, phagolysosomal acidification, and toxin-mediated leakage. Subsequently, the free accessible bacterial RNA interacts with NLRP3 and activates the inflammasome cascade (104). Whether such mechanism applies to pneumococcal infections, remains to be elucidated.

In general, tightly controlled inflammasome activation in pneumococcal pneumonia is one of many important host defense mechanisms contributing to bacterial clearance (56). However, excessive NLRP3 activation can also lead to uncontrolled pyroptosis. The disproportionate gasdermin-D mediated cell membrane rupture in a variety of lung cells may result in a release of plethora of alarmins, including processed antigens, ATP, HMGB1, reactive oxygen species, cytokines, and chemokines (105). These prompt an immediate reaction from resident and recruited immune cells leading to a pyroptotic chain reaction with subsequent excessive tissue pathology (106). Furthermore, pathogen-associated antigens might disseminate to other organs resulting in a severe systemic hyper-inflammatory response (105). Whether such actions apply to pneumococcal pneumonia remains to be shown.

CONCLUSION

Besides the crucial role of NLRP3 inflammasome activation in inflammation, many studies implicate NLRP3 inflammasome in the pathology of several autoimmune and auto-inflammatory disorders. Currently, the most common therapy for such diseases involves the use of immuno-suppressive, cytokine inhibiting therapies, such as IL-1 inhibitors. The immuno-suppression of patients by these agents results in side effects that often include respiratory tract infections caused by pneumococci. However, only a limited number of studies investigated the role of the NLRP3 inflammasome in pneumococcal respiratory infections. Future studies, especially those considering the complex interplay of human genetics, immuno-suppressive status, and age with pneumococcal colonization are needed to better understand the role of NLRP3 inflammasome in such infections.

AUTHOR CONTRIBUTIONS

SS and NS conceived the concept for this review article. SS, FC, and NS wrote the manuscript. All authors contributed to the article and approved the submitted version.

FUNDING

This research is supported by the Federal Excellence Initiative of Mecklenburg Western Pomerania and European Social Fund (ESF) Grant KoInfekt (ESF_14-BM-A55-0001_16).

REFERENCES

- Takeuchi O, Akira S. Pattern recognition receptors and inflammation. *Cell* (2010) 140:805–20. doi: 10.1016/j.cell.2010.01.022
- Ruiz-Moreno JS, Hamann L, Jin L, Sander LE, Puzianowska-Kuznicka M, Cambier J, et al. The cGAS/STING Pathway Detects Streptococcus pneumoniae but Appears Dispensable for Antipneumococcal Defense in Mice and Humans. *Infect Immun* (2018) 86. doi: 10.1128/IAI.00849-17
- Martinon F, Burns K, Tschopp J. The inflammasome: a molecular platform triggering activation of inflammatory caspases and processing of proIL- β . *Mol Cell* (2002) 10:417–26. doi: 10.1016/S1097-2765(02)00599-3
- Saxena M, Yeretssian G. NOD-Like Receptors: Master Regulators of Inflammation and Cancer. *Front Immunol* (2014) 5. doi: 10.3389/fimmu.2014.00327
- Greaney AJ, Leppla SH, Moayeri M. Bacterial Exotoxins and the Inflammasome. *Front Immunol* (2015) 6. doi: 10.3389/fimmu.2015.00570
- Storek KM, Monack DM. Bacterial recognition pathways that lead to inflammasome activation. *Immunol Rev* (2015) 265:112–29. doi: 10.1111/imr.12289
- Mangan MSJ, Olhava EJ, Roush WR, Seidel HM, Glick GD, Latz E. Targeting the NLRP3 inflammasome in inflammatory diseases. *Nat Rev Drug Discov* (2018) 17:588–606. doi: 10.1038/nrd.2018.97
- Wang Z, Zhang S, Xiao Y, Zhang W, Wu S, Qin T, et al. NLRP3 Inflammasome and Inflammatory Diseases. *Oxid Med Cell Longevity* (2020) 2020:4063562. doi: 10.1155/2020/4063562
- LaRock CN, Todd J, LaRock DL, Olson J, O'Donoghue AJ, Robertson AAB, et al. IL-1 β is an innate immune sensor of microbial proteolysis. *Sci Immunol* (2016) 1:caah3539–caah. doi: 10.1126/sciimmunol.aah3539
- Swanson KV, Deng M, Ting JPY. The NLRP3 inflammasome: molecular activation and regulation to therapeutics. *Nat Rev Immunol* (2019) 19:477–89. doi: 10.1038/s41577-019-0165-0
- Sharif H, Wang L, Wang WL, Magupalli VG, Andreeva L, Qiao Q, et al. Structural mechanism for NEK7-licensed activation of NLRP3 inflammasome. *Nature* (2019) 570:338–43. doi: 10.1038/s41586-019-1295-z
- Lavrik IN, Golks A, Krammer PH. Caspases: pharmacological manipulation of cell death. *J Clin Invest* (2005) 115:2665–72. doi: 10.1172/JCI26252
- Kelley N, Jeltema D, Duan Y, He Y. The NLRP3 Inflammasome: An Overview of Mechanisms of Activation and Regulation. *Int J Mol Sci* (2019) 20. doi: 10.3390/ijms20133328
- Knop J, Spilgies LM, Ruffli S, Reinhart R, Vasilikos L, Yabal M, et al. TNFR2 induced priming of the inflammasome leads to a RIPK1-dependent cell death in the absence of XIAP. *Cell Death Dis* (2019) 10:700. doi: 10.1038/s41419-019-1938-x
- Xing Y, Yao X, Li H, Xue G, Guo Q, Yang G, et al. Cutting Edge: TRAF6 Mediates TLR/IL-1R Signaling-Induced Nontranscriptional Priming of the NLRP3 Inflammasome. *J Immunol (Baltimore Md 1950)* (2017) 199:1561–6. doi: 10.4049/jimmunol.1700175
- Bauernfeind FG, Horvath G, Stutz A, Alnemri ES, MacDonald K, Speert D, et al. Cutting edge: NF- κ B activating pattern recognition and cytokine receptors license NLRP3 inflammasome activation by regulating NLRP3 expression. *J Immunol (Baltimore Md 1950)* (2009) 183:787–91. doi: 10.4049/jimmunol.0901363
- Lamkanfi M, Dixit VM. Modulation of inflammasome pathways by bacterial and viral pathogens. *J Immunol (Baltimore Md 1950)* (2011) 187:597–602. doi: 10.4049/jimmunol.1100229
- Amores-Iniesta J, Barberà-Cremades M, Martínez CM, Pons JA, Revilla-Nuñ B, Martínez-Alarcón L, et al. Extracellular ATP Activates the NLRP3 Inflammasome and Is an Early Danger Signal of Skin Allograft Rejection. *Cell Rep* (2017) 21:3414–26. doi: 10.1016/j.celrep.2017.11.079
- Eigenbrod T, Dalpke AH. Bacterial RNA: An Underestimated Stimulus for Innate Immune Responses. *J Immunol (Baltimore Md 1950)* (2015) 195:411–8. doi: 10.4049/jimmunol.1500530
- Wang W, Li G, De W, Luo Z, Pan P, Tian M, et al. Zika virus infection induces host inflammatory responses by facilitating NLRP3 inflammasome assembly and interleukin-1 β secretion. *Nat Commun* (2018) 9:106. doi: 10.1038/s41467-017-02645-3
- Erdei J, Tóth A, Balogh E, Nyakundi BB, Bányai E, Ryffel B, et al. Induction of NLRP3 Inflammasome Activation by Heme in Human Endothelial Cells. *Oxid Med Cell Longevity* (2018) 2018:4310816. doi: 10.1155/2018/4310816
- Nakanishi A, Kaneko N, Takeda H, Sawasaki T, Morikawa S, Zhou W, et al. Amyloid β directly interacts with NLRP3 to initiate inflammasome activation: identification of an intrinsic NLRP3 ligand in a cell-free system. *Inflammation Regeneration* (2018) 38:27. doi: 10.1186/s41232-018-0085-6
- Duewell P, Kono H, Rayner KJ, Sirois CM, Vladimer G, Bauernfeind FG, et al. NLRP3 inflammasomes are required for atherogenesis and activated by cholesterol crystals. *Nature* (2010) 464:1357–61. doi: 10.1038/nature08938
- Martinon F, Pétrilli V, Mayor A, Tardivel A, Tschopp J. Gout-associated uric acid crystals activate the NALP3 inflammasome. *Nature* (2006) 440:237–41. doi: 10.1038/nature04516
- Hornung V, Bauernfeind F, Halle A, Samstad EO, Kono H, Rock KL, et al. Silica crystals and aluminum salts activate the NALP3 inflammasome through phagosomal destabilization. *Nat Immunol* (2008) 9:847–56. doi: 10.1038/ni.1631
- Compan V, Baroja-Mazo A, López-Castejón G, Gomez AI, Martínez CM, Angosto D, et al. Cell volume regulation modulates NLRP3 inflammasome activation. *Immunity* (2012) 37:487–500. doi: 10.1016/j.immuni.2012.06.013
- Gong T, Yang Y, Jin T, Jiang W, Zhou R. Orchestration of NLRP3 Inflammasome Activation by Ion Fluxes. *Trends Immunol* (2018) 39:393–406. doi: 10.1016/j.it.2018.01.009
- Kinnunen K, Piippo N, Loukovaara S, Hytti M, Kaarniranta K, Kauppinen A. Lysosomal destabilization activates the NLRP3 inflammasome in human umbilical vein endothelial cells (HUVECs). *J Cell Commun Signaling* (2017) 11:275–9. doi: 10.1007/s12079-017-0396-4
- Heid ME, Keyel PA, Kamga C, Shiva S, Watkins SC, Salter RD. Mitochondrial reactive oxygen species induces NLRP3-dependent lysosomal damage and inflammasome activation. *J Immunol (Baltimore Md 1950)* (2013) 191:5230–8. doi: 10.4049/jimmunol.1301490
- Gritsenko A, Yu S, Martin-Sanchez F, del Olmo ID, Nichols E-M, Davis DM, et al. Priming is dispensable for NLRP3 inflammasome activation in human monocytes. *bioRxiv* (2020) 2020.01.30.925248. doi: 10.3389/fimmu.2020.565924
- Netea MG, Nold-Petry CA, Nold MF, Joosten LA, Opitz B, van der Meer JH, et al. Differential requirement for the activation of the inflammasome for processing and release of IL-1 β in monocytes and macrophages. *Blood* (2009) 113:2324–35. doi: 10.1182/blood-2008-03-146720
- Elliott JM, Rouge L, Wiesmann C, Scher JM. Crystal structure of procaspase-1 zymogen domain reveals insight into inflammatory caspase autoactivation. *J Biol Chem* (2009) 284:6546–53. doi: 10.1074/jbc.M806121200
- Shi J, Zhao Y, Wang K, Shi X, Wang Y, Huang H, et al. Cleavage of GSDMD by inflammatory caspases determines pyroptotic cell death. *Nature* (2015) 526:660–5. doi: 10.1038/nature15514
- Liu X, Zhang Z, Ruan J, Pan Y, Magupalli VG, Wu H, et al. Inflammasome-activated gasdermin D causes pyroptosis by forming membrane pores. *Nature* (2016) 535:153–8. doi: 10.1038/nature18629
- He WT, Wan H, Hu L, Chen P, Wang X, Huang Z, et al. Gasdermin D is an executor of pyroptosis and required for interleukin-1 β secretion. *Cell Res* (2015) 25:1285–98. doi: 10.1038/cr.2015.139
- Karmakar M, Minns M, Greenberg EN, Diaz-Aponte J, Pestonjams P, Johnson JL, et al. N-GSDMD trafficking to neutrophil organelles facilitates IL-1 β release independently of plasma membrane pores and pyroptosis. *Nat Commun* (2020) 11:2212. doi: 10.1038/s41467-020-16043-9
- Lamkanfi M, Sarkar A, Vande Walle L, Vitari AC, Amer AO, Wewers MD, et al. Inflammasome-dependent release of the alarmin HMGB1 in endotoxemia. *J Immunol (Baltimore Md 1950)* (2010) 185:4385–92. doi: 10.4049/jimmunol.1000803
- Schiraldi M, Raucchi A, Muñoz LM, Livoti E, Celona B, Venereau E, et al. HMGB1 promotes recruitment of inflammatory cells to damaged tissues by forming a complex with CXCL12 and signaling via CXCR4. *J Exp Med* (2012) 209:551–63. doi: 10.1084/jem.20111739
- von Mollke J, Trinidad NJ, Moayeri M, Kintzer AF, Wang SB, van Rooijen N, et al. Rapid induction of inflammatory lipid mediators by the inflammasome in vivo. *Nature* (2012) 490:107–11. doi: 10.1038/nature11351
- Yang Y, Wang H, Kouadir M, Song H, Shi F. Recent advances in the mechanisms of NLRP3 inflammasome activation and its inhibitors. *Cell Death Dis* (2019) 10:128. doi: 10.1038/s41419-019-1413-8

41. Baker PJ, Boucher D, Bierschenk D, Tebartz C, Whitney PG, D'Silva DB, et al. NLRP3 inflammasome activation downstream of cytoplasmic LPS recognition by both caspase-4 and caspase-5. *Eur J Immunol* (2015) 45:2918–26. doi: 10.1002/eji.201545655
42. Masters SL, Dunne A, Subramanian SL, Hull RL, Tannahill GM, Sharp FA, et al. Activation of the NLRP3 inflammasome by islet amyloid polypeptide provides a mechanism for enhanced IL-1 β in type 2 diabetes. *Nat Immunol* (2010) 11:897–904. doi: 10.1038/ni.1935
43. Lee HM, Kim JJ, Kim HJ, Shong M, Ku BJ, Jo EK. Upregulated NLRP3 inflammasome activation in patients with type 2 diabetes. *Diabetes* (2013) 62:194–204. doi: 10.2337/db12-0420
44. Booshehri LM, Hoffman HM. CAPS and NLRP3. *J Clin Immunol* (2019) 39:277–86. doi: 10.1007/s10875-019-00638-z
45. Lee C, Do HTT, Her J, Kim Y, Seo D, Rhee I. Inflammasome as a promising therapeutic target for cancer. *Life Sci* (2019) 231:116593. doi: 10.1016/j.lfs.2019.116593
46. Zhen Y, Zhang H. NLRP3 Inflammasome and Inflammatory Bowel Disease. *Front Immunol* (2019) 10:276. doi: 10.3389/fimmu.2019.00276
47. Hoffman HM, Mueller JL, Broide DH, Wanderer AA, Kolodner RD. Mutation of a new gene encoding a putative pyrin-like protein causes familial cold autoinflammatory syndrome and Muckle-Wells syndrome. *Nat Genet* (2001) 29:301–5. doi: 10.1038/ng756
48. Hoffman HM, Wanderer AA, Broide DH. Familial cold autoinflammatory syndrome: phenotype and genotype of an autosomal dominant periodic fever. *J Allergy Clin Immunol* (2001) 108:615–20. doi: 10.1067/mai.2001.118790
49. Brydges SD, Mueller JL, McGeough MD, Pena CA, Misaghi A, Gandhi C, et al. Inflammasome-mediated disease animal models reveal roles for innate but not adaptive immunity. *Immunity* (2009) 30:875–87. doi: 10.1016/j.immuni.2009.05.005
50. Meng G, Zhang F, Fuss I, Kitani A, Strober W. A mutation in the Nlrp3 gene causing inflammasome hyperactivation potentiates Th17 cell-dominant immune responses. *Immunity* (2009) 30:860–74. doi: 10.1016/j.immuni.2009.04.012
51. McInnes IB, Schett G. The pathogenesis of rheumatoid arthritis. *New Engl J Med* (2011) 365:2205–19. doi: 10.1056/NEJMra1004965
52. Brennan FM, McInnes IB. Evidence that cytokines play a role in rheumatoid arthritis. *J Clin Invest* (2008) 118:3537–45. doi: 10.1172/JCI36389
53. Dayer JM. The pivotal role of interleukin-1 in the clinical manifestations of rheumatoid arthritis. *Rheumatol (Oxford)* (2003) 42 Suppl 2:ii3–10. doi: 10.1093/rheumatology/keg326
54. Zhang H, Huang Y, Wang S, Fu R, Guo C, Wang H, et al. Myeloid-derived suppressor cells contribute to bone erosion in collagen-induced arthritis by differentiating to osteoclasts. *J Autoimmun* (2015) 65:82–9. doi: 10.1016/j.jaut.2015.08.010
55. Li Z, Guo J, Bi L. Role of the NLRP3 inflammasome in autoimmune diseases. *BioMed Pharmacother* (2020) 130:110542. doi: 10.1016/j.biopha.2020.110542
56. Rabes A, Suttorp N, Opitz B. Inflammasomes in Pneumococcal Infection: Innate Immune Sensing and Bacterial Evasion Strategies. *Curr Top Microbiol Immunol* (2016) 397:215–27. doi: 10.1007/978-3-319-41171-2_11
57. US Food and Drug Administration (FDA). *Kineret (anakinra) Initial U.S. Approval*. Available at: https://www.accessdata.fda.gov/drugsatfda_docs/label/2012/103950s136lbl.pdf.
58. US Food and Drug Administration (FDA). *Arcalyst (Riloncept) Initial U.S. Approval*. Available at: https://www.accessdata.fda.gov/drugsatfda_docs/label/2020/125249s045lbl.pdf.
59. Dubois EA, Rissmann R, Cohen AF. Riloncept and canakinumab. *Br J Clin Pharmacol* (2011) 71:639–41. doi: 10.1111/j.1365-2125.2011.03958.x
60. US Food and Drug Administration (FDA). *Ilaris (Canakinumab) Initial U.S. Approval*. Available at: https://www.accessdata.fda.gov/drugsatfda_docs/label/2020/125319s100lbl.pdf.
61. Lachmann HJ, Kone-Paut I, Kuemmerle-Deschner JB, Leslie KS, Hachulla E, Quartier P, et al. Use of canakinumab in the cryopyrin-associated periodic syndrome. *N Engl J Med* (2009) 360:2416–25. doi: 10.1056/NEJMoa0810787
62. Jiang H, He H, Chen Y, Huang W, Cheng J, Ye J, et al. Identification of a selective and direct NLRP3 inhibitor to treat inflammatory disorders. *J Exp Med* (2017) 214:3219–38. doi: 10.1084/jem.20171419
63. Cavelti-Weder C, Babians-Brunner A, Keller C, Stahel MA, Kurz-Levin M, Zayed H, et al. Effects of gevokizumab on glycemia and inflammatory markers in type 2 diabetes. *Diabetes Care* (2012) 35:1654–62. doi: 10.2337/dc11-2219
64. Krickelbein JE, Tucker WR, Bhatt N, Armbrust K, Valent D, Obiyor D, et al. Gevokizumab in the Treatment of Autoimmune Non-necrotizing Anterior Scleritis: Results of a Phase I/II Clinical Trial. *Am J Ophthalmol* (2016) 172:104–10. doi: 10.1016/j.ajo.2016.09.017
65. Bihorel S, Fiedler-Kelly J, Ludwig E, Sloan-Lancaster J, Raddad E. Population pharmacokinetic modeling of LY2189102 after multiple intravenous and subcutaneous administrations. *AAPS J* (2014) 16:1009–17. doi: 10.1208/s12248-014-9623-6
66. Lamkanfi M, Mueller JL, Vitari AC, Misaghi S, Fedorova A, Deshayes K, et al. Glyburide inhibits the Cryopyrin/Nalp3 inflammasome. *J Cell Biol* (2009) 187:61–70. doi: 10.1083/jcb.200903124
67. Kahn SE, Hafner SM, Heise MA, Herman WH, Holman RR, Jones NP, et al. Glycemic durability of rosiglitazone, metformin, or glyburide monotherapy. *N Engl J Med* (2006) 355:2427–43. doi: 10.1056/NEJMoa066224
68. Langer O, Conway DL, Berkus MD, Xenakis EM, Gonzales O. A comparison of glyburide and insulin in women with gestational diabetes mellitus. *N Engl J Med* (2000) 343:1134–8. doi: 10.1056/NEJM200010193431601
69. Rudolph K, Gerwin N, Verzijl N, van der Kraan P, van den Berg W, Pralncasan, an inhibitor of interleukin-1 β converting enzyme, reduces joint damage in two murine models of osteoarthritis. *Osteoarthritis Cartilage* (2003) 11:738–46. doi: 10.1016/S1063-4584(03)00153-5
70. Wannamaker W, Davies R, Namchuk M, Pollard J, Ford P, Ku G, et al. (S)-1-((S)-2-{{1-(4-amino-3-chloro-phenyl)-methanoyl}-amino}-3,3-dimethylbutanoyl)-pyrrolidine-2-carboxylic acid ((2R,3S)-2-ethoxy-5-oxo-tetrahydro-furan-3-yl)-amide (VX-765), an orally available selective interleukin (IL)-converting enzyme/caspase-1 inhibitor, exhibits potent anti-inflammatory activities by inhibiting the release of IL-1 β and IL-18. *J Pharmacol Exp Ther* (2007) 321:509–16. doi: 10.1124/jpet.106.111344
71. Marchetti C, Swartzwelder B, Gamboni F, Neff CP, Richter K, Azam T, et al. OLT1177, a β -sulfonyl nitrile compound, safe in humans, inhibits the NLRP3 inflammasome and reverses the metabolic cost of inflammation. *Proc Natl Acad Sci* (2018) 115:E1530–9. doi: 10.1073/pnas.1716095115
72. Cohen SB, Proudman S, Kivitz AJ, Burch FX, Donohue JP, Burstein D, et al. A randomized, double-blind study of AMG 108 (a fully human monoclonal antibody to IL-1R1) in patients with osteoarthritis of the knee. *Arthritis Res Ther* (2011) 13:R125. doi: 10.1186/ar3430
73. Pile KD, Graham GG, Mahler SM. "Interleukin 1 Inhibitors". In: M Parnham, editor. *Encyclopedia of Inflammatory Diseases*. Basel: Springer Basel (2015). p. 1–5.
74. Ottaviani S, Moltó A, Ea H-K, Neveu S, Gill G, Brunier L, et al. Efficacy of anakinra in gouty arthritis: a retrospective study of 40 cases. *Arthritis Res Ther* (2013) 15:R123. doi: 10.1186/ar4303
75. Mertens M, Singh JA. Anakinra for rheumatoid arthritis: a systematic review. *J Rheumatol* (2009) 36:1118–25. doi: 10.3899/jrheum.090074
76. Larsen CM, Faulenbach M, Vaag A, Volund A, Ehlers JA, Seifert B, et al. Interleukin-1 receptor antagonist in type 2 diabetes mellitus. *N Engl J Med* (2007) 356:1517–26. doi: 10.1056/NEJMoa065213
77. Fleischmann RM, Schechtman J, Bennett R, Handel ML, Burmester GR, Tesser J, et al. Anakinra, a recombinant human interleukin-1 receptor antagonist (r-metHuIL-1ra), in patients with rheumatoid arthritis: A large, international, multicenter, placebo-controlled trial. *Arthritis Rheumatism* (2003) 48:927–34. doi: 10.1002/art.10870
78. Bettiol A, Lopalco G, Emmi G, Cantarini L, Urban ML, Vitale A, et al. Unveiling the Efficacy, Safety, and Tolerability of Anti-Interleukin-1 Treatment in Monogenic and Multifactorial Autoinflammatory Diseases. *Int J Mol Sci* (2019) 20. doi: 10.3390/ijms20081898
79. Siemens N, Oehmcke-Hecht S, Mettenleiter TC, Kreikemeyer B, Valentin-Weigand P, Hammerschmidt S. Port d'Entree for Respiratory Infections - Does the Influenza A Virus Pave the Way for Bacteria? *Front Microbiol* (2017) 8:2602. doi: 10.3389/fmicb.2017.02602
80. McCullers JA. Insights into the interaction between influenza virus and pneumococcus. *Clin Microbiol Rev* (2006) 19:571–82. doi: 10.1128/CMR.00058-05

81. Ozen G, Pedro S, England BR, Mehta B, Wolfe F, Michaud K. Risk of Serious Infection in Patients With Rheumatoid Arthritis Treated With Biologic Versus Nonbiologic Disease-Modifying Antirheumatic Drugs. *ACR Open Rheumatol* (2019) 1:424–32. doi: 10.1002/acr2.11064
82. Yau B, Hunt NH, Mitchell AJ, Too LK. Blood–Brain Barrier Pathology and CNS Outcomes in Streptococcus pneumoniae Meningitis. *Int J Mol Sci* (2018) 19. doi: 10.3390/ijms19113555
83. Geldhoff M, Mook-Kanamori BB, Brouwer MC, Troost D, Leemans JC, Flavell RA, et al. Inflammasome activation mediates inflammation and outcome in humans and mice with pneumococcal meningitis. *BMC Infect Dis* (2013) 13:358. doi: 10.1186/1471-2334-13-358
84. Weiser JN, Ferreira DM, Paton JC. Streptococcus pneumoniae: transmission, colonization and invasion. *Nat Rev Microbiol* (2018) 16:355–67. doi: 10.1038/s41579-018-0001-8
85. McNeela EA, Burke A, Neill DR, Baxter C, Fernandes VF, Ferreira D, et al. Pneumolysin activates the NLRP3 inflammasome and promotes proinflammatory cytokines independently of TLR4. *PLoS Pathog* (2010) 6: e1001191. doi: 10.1371/journal.ppat.1001191
86. Hoegen T, Tremel N, Klein M, Angele B, Wagner H, Kirschning C, et al. The NLRP3 inflammasome contributes to brain injury in pneumococcal meningitis and is activated through ATP-dependent lysosomal cathepsin B release. *J Immunol (Baltimore Md 1950)* (2011) 187:5440–51. doi: 10.4049/jimmunol.1100790
87. Kadioglu A, Weiser JN, Paton JC, Andrew PW. The role of Streptococcus pneumoniae virulence factors in host respiratory colonization and disease. *Nat Rev Microbiol* (2008) 6:288–301. doi: 10.1038/nrmicro1871
88. Witznath M, Pache F, Lorenz D, Koppe U, Gutbier B, Tabeling C, et al. The NLRP3 inflammasome is differentially activated by pneumolysin variants and contributes to host defense in pneumococcal pneumonia. *J Immunol (Baltimore Md 1950)* (2011) 187:434–40. doi: 10.4049/jimmunol.1003143
89. Fatykhova D, Rabes A, Machnik C, Guruprasad K, Pache F, Berg J, et al. Serotype 1 and 8 Pneumococci Evade Sensing by Inflammasomes in Human Lung Tissue. *PLoS One* (2015) 10:e0137108. doi: 10.1371/journal.pone.0137108
90. Karmakar M, Katsnelson M, Malak HA, Greene NG, Howell SJ, Hise AG, et al. Neutrophil IL-1 β processing induced by pneumolysin is mediated by the NLRP3/ASC inflammasome and caspase-1 activation and is dependent on K⁺ efflux. *J Immunol (Baltimore Md 1950)* (2015) 194:1763–75. doi: 10.4049/jimmunol.1401624
91. Biondo C, Mancuso G, Midiri A, Signorino G, Domina M, Lanza Cariccio V, et al. The Interleukin-1 β /CXCL1/2/Neutrophil Axis Mediates Host Protection against Group B Streptococcal Infection. *Infect Immun* (2014) 82:4508–17. doi: 10.1128/IAI.02104-14
92. Matsumura T, Takahashi Y. The role of myeloid cells in prevention and control of group A streptococcal infections. *Biosafety Health* (2020) 2:130–4. doi: 10.1016/j.bsheal.2020.05.006
93. Lemon JK, Miller MR, Weiser JN. Sensing of interleukin-1 cytokines during Streptococcus pneumoniae colonization contributes to macrophage recruitment and bacterial clearance. *Infect Immun* (2015) 83:3204–12. doi: 10.1128/IAI.00224-15
94. Zhang T, Du H, Feng S, Wu R, Chen T, Jiang J, et al. NLRP3/ASC/Caspase-1 axis and serine protease activity are involved in neutrophil IL-1 β processing during Streptococcus pneumoniae infection. *Biochem Biophys Res Commun* (2019) 513:675–80. doi: 10.1016/j.bbrc.2019.04.004
95. Gaffen SL, Jain R, Garg AV, Cua DJ. The IL-23–IL-17 immune axis: from mechanisms to therapeutic testing. *Nat Rev Immunol* (2014) 14:585–600. doi: 10.1038/nri3707
96. Onishi RM, Gaffen SL. Interleukin-17 and its target genes: mechanisms of interleukin-17 function in disease. *Immunology* (2010) 129:311–21. doi: 10.1111/j.1365-2567.2009.03240.x
97. Hassane M, Demon D, Souillard D, Fontaine J, Keller LE, Patin EC, et al. Neutrophilic NLRP3 inflammasome-dependent IL-1 β secretion regulates the gammadeltaT17 cell response in respiratory bacterial infections. *Mucosal Immunol* (2017) 10:1056–68. doi: 10.1038/mi.2016.113
98. Zhang Z, Clarke TB, Weiser JN. Cellular effectors mediating Th17-dependent clearance of pneumococcal colonization in mice. *J Clin Invest* (2009) 119:1899–909. doi: 10.1172/JCI36731
99. Fang R, Tsuchiya K, Kawamura I, Shen Y, Hara H, Sakai S, et al. Critical roles of ASC inflammasomes in caspase-1 activation and host innate resistance to Streptococcus pneumoniae infection. *J Immunol (Baltimore Md 1950)* (2011) 187:4890–9. doi: 10.4049/jimmunol.1100381
100. Erttmann SF, Gekara NO. Hydrogen peroxide release by bacteria suppresses inflammasome-dependent innate immunity. *Nat Commun* (2019) 10:3493. doi: 10.1038/s41467-019-11169-x
101. Cho SJ, Rooney K, Choi AMK, Stout-Delgado HW. NLRP3 inflammasome activation in aged macrophages is diminished during Streptococcus pneumoniae infection. *Am J Physiol Lung Cell Mol Physiol* (2018) 314: L372–187. doi: 10.1152/ajplung.00393.2017
102. Krone CL, Trzcinski K, Zborowski T, Sanders EA, Bogaert D. Impaired innate mucosal immunity in aged mice permits prolonged Streptococcus pneumoniae colonization. *Infect Immun* (2013) 81:4615–25. doi: 10.1128/IAI.00618-13
103. Sha W, Mitoma H, Hanabuchi S, Bao M, Weng I, Sugimoto N, et al. Human NLRP3 inflammasome senses multiple types of bacterial RNAs. *Proc Natl Acad Sci U S A* (2014) 111:16059–64. doi: 10.1073/pnas.1412487111
104. Gupta R, Ghosh S, Monks B, DeOliveira RB, Tzeng TC, Kalantari P, et al. RNA and β -hemolysin of group B Streptococcus induce interleukin-1 β (IL-1 β) by activating NLRP3 inflammasomes in mouse macrophages. *J Biol Chem* (2014) 289:13701–5. doi: 10.1074/jbc.C114.548982
105. Yap JKY, Moriyama M, Iwasaki A. Inflammasomes and Pyroptosis as Therapeutic Targets for COVID-19. *J Immunol (Baltimore Md 1950)* (2020) 205:307–12. doi: 10.4049/jimmunol.2000513
106. Snall J, Linner A, Uhlmann J, Siemens N, Ibold H, Janos M, et al. Differential neutrophil responses to bacterial stimuli: Streptococcal strains are potent inducers of heparin-binding protein and resistin-release. *Sci Rep* (2016) 6:21288. doi: 10.1038/srep21288

Conflict of Interest: The authors declare that the research was conducted in the absence of any commercial or financial relationships that could be construed as a potential conflict of interest.

Copyright © 2020 Surabhi, Cuypers, Hammerschmidt and Siemens. This is an open-access article distributed under the terms of the Creative Commons Attribution License (CC BY). The use, distribution or reproduction in other forums is permitted, provided the original author(s) and the copyright owner(s) are credited and that the original publication in this journal is cited, in accordance with accepted academic practice. No use, distribution or reproduction is permitted which does not comply with these terms.

PAPER 2

Hydrogen Peroxide is Crucial for NLRP3 Inflammasome Mediated IL-1 β Production and Cell Death in Pneumococcal Infections of Bronchial Epithelial Cells

Surabhi Surabhi, Lana H. Jachmann, Patience Shumba, Gerhard Burchhardt, Sven Hammerschmidt, and Nikolai Siemens

Published in Journal of Innate immunity, 2021 June, 14,
[DOI: 10.1159/000517855](https://doi.org/10.1159/000517855)

Author contributions:

As first author in this publication, **SS** significantly contributed with the conception, execution and analysis of all the experiments performed in this study. Additionally, **SS** prepared the manuscript draft, participated in the construction of the figures and was involved in the scientific revision and editing of the final version of this manuscript.

Conception and design: **SS**, **SH** and **NS**

Experimental work: **SS**, **LJ**, **PS**, and **GB**

Collection and analysis of the data: **SS**, **LJ**, and **NS**

Manuscript draft preparation: **SS** and **NS**

Critical revision and editing of the manuscript: **SS**, **LJ**, **PS**, **GB**, **SH**, and **NS**

Surabhi Surabhi

Prof. Dr. Nikolai Siemens

Hydrogen Peroxide Is Crucial for NLRP3 Inflammasome-Mediated IL-1 β Production and Cell Death in Pneumococcal Infections of Bronchial Epithelial Cells

Surabhi Surabhi Lana H. Jachmann Patience Shumba Gerhard Burchhardt
Sven Hammerschmidt Nikolai Siemens

Department of Molecular Genetics and Infection Biology, Interfaculty Institute for Genetics and Functional Genomics, Center for Functional Genomics of Microbes, University of Greifswald, Greifswald, Germany

Keywords

Streptococcus pneumoniae · NLRP3 inflammasome · Cell death · Caspase-1 · Caspase-3/7 · IL-1 β · Pyroptosis · Apoptosis

Abstract

Epithelial cells play a crucial role in detection of the pathogens as well as in initiation of the host immune response. *Streptococcus pneumoniae* (pneumococcus) is a typical colonizer of the human nasopharynx, which can disseminate to the lower respiratory tract and subsequently cause severe invasive diseases such as pneumonia, sepsis, and meningitis. Hydrogen peroxide (H₂O₂) is produced by pneumococci as a product of the pyruvate oxidase SpxB. However, its role as a virulence determinant in pneumococcal infections of the lower respiratory tract is not well understood. In this study, we investigated the role of pneumococcal-derived H₂O₂ in initiating epithelial cell death by analyzing the interplay between 2 key cell death pathways, namely, apoptosis and pyroptosis. We demonstrate that H₂O₂ primes as well as activates the NLRP3 inflammasome and thereby mediates IL-1 β production and release. Furthermore, we show that pneumococcal H₂O₂ causes cell death via the activation of both

apoptotic as well as pyroptotic pathways which are mediated by the activation of caspase-3/7 and caspase-1, respectively. However, H₂O₂-mediated IL-1 β release itself occurs mainly via apoptosis.

© 2021 The Author(s)
Published by S. Karger AG, Basel

Introduction

Streptococcus pneumoniae (pneumococcus), a Gram-positive bacterium and a typical asymptomatic colonizer of the human upper respiratory tract, remains the most commonly identified cause of community-acquired pneumonia [1]. Pneumococci are equipped with a variety of virulence factors allowing them to circumvent the host immune response. In many cases, initial mild manifestations may result in severe invasive diseases such as pneumonia, meningitis, and sepsis [2, 3]. One of the most important and well-studied secreted virulence factors of pneumococci is the pore-forming cytolysin pneumolysin (Ply) [4]. Moreover, pneumococci secrete high amounts of hydrogen peroxide (H₂O₂) as a product of the pneumococcal carbohydrate-metabolizing enzyme pyruvate oxidase SpxB [5]. It is believed that secreted H₂O₂ dif-

karger@karger.com
www.karger.com/jin

Karger
OPEN ACCESS

© 2021 The Author(s)
Published by S. Karger AG, Basel

This is an Open Access article licensed under the Creative Commons Attribution-NonCommercial 4.0 International License (CC BY-NC) (<http://www.karger.com/Services/OpenAccessLicense>), applicable to the online version of the article only. Usage and distribution for commercial purposes requires written permission.

Correspondence to:
Nikolai Siemens, nikolai.siemens@uni-greifswald.de

fuses through the host cell membrane and causes oxidative damage [6]. Consequently, Spellerberg and colleagues have shown that *S. pneumoniae* mutants deficient in H₂O₂ production are characterized by a reduced virulence in vivo [5]. Furthermore, it was demonstrated that pneumococci-derived H₂O₂ is a major vasodilator and contributes to the cerebral hyperemia during early stages of meningitis and therapies with antioxidants attenuate the pathophysiological responses [7, 8]. *In vitro* studies with cells of the respiratory tract showed that both H₂O₂ and Ply attenuate ciliary function by (i) slowing down the ciliary beat frequency and (ii) impairing the structural integrity of human ciliated epithelium [9, 10]. Furthermore, studies on rat alveolar epithelial cells have demonstrated that cell injury induced by *S. pneumoniae* mutants that lacked Ply activity was comparable to that of the parental strain. H₂O₂ was identified as a major factor responsible for the cell cytotoxicity [11].

Epithelial cells span the entire length of the respiratory tract and were initially presumed to solely serve as a physical barrier for inhaled particles or microorganisms [12]. However, many studies have shown their significance as important immune sentinels [13, 14]. They possess a diverse repertoire of pattern-recognition receptors that assist in detection of various pathogen and danger-associated molecular patterns [15]. Once the healthy host cells encounter a death-inducing stimulus, they can initiate a variety of molecular cell death pathways. Apoptosis is a controlled form of cell death, which features the activation of initiator caspases like caspases-2, 8, 9, and 10. Subsequently, these caspases activate effector caspases such as caspases-3, 6, and 7 [16]. Once activated, the effector caspases cleave various intracellular substrates, including α -fodrin, gelsolin, p21-activated kinase 2, and inhibitor of caspase-activated DNase/DNA fragmentation factor-45 [17]. The final stage of apoptotic cell death includes the formation of apoptotic bodies which expose surface molecules. Professional phagocytes including macrophages recognize the apoptotic bodies and ingest them, making this form of cell death less inflammatory in nature [16].

Pyroptosis is another form of programmed cell death, and in contrast to apoptosis, it is more of a pro-inflammatory nature. Pyroptosis is driven by the activation of a diverse range of inflammasomes. Inflammasomes are multiprotein complexes that assemble based on the detection of danger signals [18]. Of the various inflammasomes, NLRP3 inflammasome is the most unique as it is activated by a wide range of stimuli, such as whole pathogens [19], extracellular ATP [20], and pathogen-associated RNA and toxins [21, 22]. The NLRP3 inflammasome

is activated in a two-step process, namely priming and activation [23, 24]. The priming step is essential to increase the intracellular concentrations of NLRP3 and pro-interleukin (IL)-1 β . The transcription factor NF- κ B is activated upon detection of a priming signal via toll-like receptors, tumor necrosis factor receptors, or interleukin-1 receptors. NF- κ B further upregulates the gene expression of NLRP3 and pro-IL-1 β . However, the priming step itself does not result in IL-1 β secretion. Next, the exposure to an activating signal leads to the assembly and activation of the NLRP3 inflammasome [18]. Active NLRP3 inflammasome converts recruited procaspase-1 to bioactive caspase-1, which further cleaves inactive pro-IL-1 β and pro-IL-18 into mature IL-1 β and IL-18, respectively. Furthermore, caspase-1 cleaves 50-kDa gasdermin-D (GSDMD) into an active 30-kDa GSDMD-N (N-terminal domain of GSDMD) fragment. GSDMD-N integrates into the cell membrane and forms pores through which IL-1 β and IL-18 are secreted into the extracellular space. This form of controlled cell lysis is termed pyroptotic cell death [25–27].

It must be noted that although previous studies indicate the importance of pneumococcal H₂O₂ in causing cell damage, not much is known about its impact on the activation of cell death pathways. A study by Erttmann and Gekara [28] suggested that H₂O₂ blocks ATP-mediated NLRP3 inflammasome activation in mouse macrophages. However, this study analyzed exclusively very early events (30 min) of pneumococcal infections and was limited to inflammasome activation and not cell death. In contrast, studies on human macrophages suggest that NLRP3 is activated in reactive oxygen species-sensitive manner including H₂O₂ [29, 30]. Furthermore, it was shown that the addition of H₂O₂ alone to human THP-1 macrophages is sufficient to trigger NLRP3-caspase 1-mediated IL-1 β release [30].

Here, we aimed to analyze the impact of pneumococci-derived H₂O₂ on cell death pathways. We show that H₂O₂ damages bronchial epithelial cells and induces caspase-1 activation, resulting in IL-1 β release. However, GSDMD-N, a cleavage product of caspase-1, was not detected and therefore, IL-1 β is mainly released through the apoptotic pathway.

Materials and Methods

Bacterial Strains

Encapsulated *S. pneumoniae* wild-type strains TIGR4, 19F, and D39 and nonencapsulated *S. pneumoniae* D39 Δ *cps* and its isogenic mutants Δ *cps* Δ *ply*, Δ *cps* Δ *spxB*, and Δ *cps* Δ *ply* Δ *spxB* were cul-

tured on Columbia blood agar plates (Oxoid) and in Todd-Hewitt broth supplemented with 0.5% (w/v) yeast extract (THY; Roth). *Streptococcus pyogenes* strain 5448 was cultured overnight in THY [31]. *Staphylococcus aureus* strain LUG2012 (USA300 lineage) was cultured overnight at 37°C in casein hydrolysate and yeast extract medium with agitation [32]. All static bacterial cultures were maintained at 37°C and 5% CO₂. For growth analysis, pneumococcal strains were cultured in THY, and the growth behavior was monitored by measuring the optical density (OD_{600 nm}).

S. pneumoniae Mutant Generation

Genomic DNA of the D39Δ*cps* strain served as a template for the knock-out of the *ply* gene (SPD1726). Briefly, SPD1725 was amplified using the following primers: 5'-CGGGATCCG-CAAATAAAGCAGTAAATGAC-3' and 5'-GACTCTAGAG-GATCCCCGGGTCAACAGACACTCATCCACATTC-3'. The resulting PCR product was digested with *Sac*II, ligated into the pGEM-T Easy vector, and transformed into *E. coli* DH5α. To delete the *ply* gene, the recombinant plasmid was used as a template for an inverse PCR with the following primers: 5'-CTATT-TGGGGATCGATTCTCTATCCTCAGG-3' and 5'-CCGGAA-GCTTAACAGCGTCTACGCTGACTGTATA-3'. The chloramphenicol (*Cm*) resistance gene cassette was amplified using the following primers: 5'-CGCGAAGCTTCGAAAATTTGTTGAT-TTTTAATGG-3' and 5'-GATAATCGATCGGGTTCGGAGG-TTCAACGTC-3'. Both PCR products were digested with *Cl*af and *H*indIII, ligated, and transformed into *E. coli* DH5α. The resulting recombinant plasmid pGEM-TΔ*ply*::*Cm* was transformed into *S. pneumoniae* D39Δ*cps* as described previously [33, 34]. Recombinant *S. pneumoniae* clones were selected on blood agar containing chloramphenicol (5 μg/mL). Replacement of the *ply* gene was analyzed via PCR using the following primers: 5'-CGGGATC-CGCAAATAAAGCAGTAAATGAC-3' and 5'-GCGGTACCCT-AGTCATTTCTACCTGAG-3'.

Genomic DNA of the D39Δ*spxB* mutant, which was kindly provided by K. Mühlemann (University of Bern, Bern, Switzerland) [35], served as a template for *spxB* gene knock-out. Briefly, the mutated *spxB* gene region containing the erythromycin (*ermB*) resistance gene cassette was amplified using the following primers: 5'-GGAGAACGTTTCCAATTCTATG-3' and 5'-GACCGGATT-GCTCCGATCTT-3'. The resulting 3.1-kb fragment was digested with *X*cmI, ligated into the pGXT plasmid (Promega), and transformed into *E. coli* DH5α. The purified pGXT-*spxB*::*erm* plasmid was used for transformation of D39Δ*cps* and Δ*cps*Δ*ply* as described previously [33, 34]. Bacteria were grown for 2 h at 37°C and plated on blood agar plates containing 5 μg/mL erythromycin. The resulting *S. pneumoniae* D39 *spxB*-deficient mutants were screened by colony PCR using the following primers: 5'-GCGCGCTAGCACT-CAAGGGAAAATTACTGC-3' and 5'-GCGCGAGCTCTATT-TAATTGCGCGTGATTG-3'. Gene organization in D39Δ*cps* and respective mutant strains are depicted in online suppl. Figure 1; see www.karger.com/doi/10.1159/000517855 for all online suppl. material.

In addition, the lack of SpxB and Ply was confirmed via Western blot analyses. Briefly, D39Δ*cps* mutants were cultivated in THY medium until the late exponential growth phase was reached, bacteria were lysed, and protein extracts were separated via SDS-PAGE and transferred onto a nitrocellulose membrane. For detection of SpxB and Ply [36], mouse polyclonal antibodies (in-house production by the laboratory of S.H.) were used.

Measurement of H₂O₂ Production by Pneumococci

S. pneumoniae strains were cultured in a chemically defined medium (RPMI1640 containing 2 mM L-glutamine medium [Hy-Cone] supplemented with 30.5 mM glucose, 0.65 mM uracil, 0.27 mM adenine, 1.1 mM glycine, 0.24 mM choline chloride, 1.7 mM NaH₂PO₄·H₂O, 3.8 mM Na₂HPO₄·2H₂O, and 27 mM NaHCO₃) at 37°C and 5% CO₂ without agitation (OD_{600 nm} of 0.80–1.0) [37]. Bacteria were pelleted at 10,000 × *g* for 2 min and the culture supernatants were collected. Five hundred microliters of the culture supernatant was mixed with 500 μL Titanium-(IV)-oxide-sulfate-sulfuric acid solution (Sigma-Aldrich). The samples were incubated at room temperature in the dark for 5 min and the OD of the resulting solution was determined at 407 nm. A standard curve containing defined concentrations of H₂O₂ was used to determine H₂O₂ concentrations in bacterial culture supernatants.

Infections, Stimulations, and Cell Culture Conditions

Bronchial epithelial 16HBE14o-cells (16HBE) were used in all infection and stimulation experiments. Cells were cultured in a minimum essential medium (Gibco) supplemented with 10% (v/v) fetal bovine serum (Life Technologies), 2 mM L-glutamine (Invitrogen), 10 mM HEPES, and 1% (v/v) minimal essential amino acids (both GE Healthcare) in fibronectin-coated flasks (Corning) at 37°C and 5% CO₂ atmosphere.

For pneumococcal infections or H₂O₂ stimulations, 3 × 10⁵ cells/well were seeded in 24-well tissue culture plates (Greiner) and maintained at 37°C and 5% CO₂ atmosphere. All experiments were performed in minimum essential media. The cells were either infected with bacteria (MOI 50) or stimulated with different concentrations of H₂O₂ for 2, 4, or 6 h. To activate NLRP3 inflammasome, additional experiments included 4 h of 100 ng/mL LPS or 100 ng/mL TNFα cell stimulations prior to an infection or H₂O₂ stimulation. To inactivate H₂O₂-mediated actions, 300 U/mL of catalase was added to the experiments.

To assess bacterial infectivity, 16HBE cells were infected with pneumococci for 2, 4, or 6 h. At indicated time points, the cells were washed, detached, lysed, and the viable counts of pneumococci (colony-forming units) released from lysed cells were determined by plating serial dilutions on blood agar.

Caspase-1 and Caspase-3/7 Activities

All infection and stimulation experiments were performed as described above. Four hours post infections/stimulation, active caspase-1 and caspase-3/7 were labeled with cell-permeable fluorescent probes FAM-YVAD-FMK FLICA or FAM-DEVD-FMK FLICA (both Bio-Rad) according to the manufacturer's instructions. The cell nuclei were stained with Nuclear-ID Red DNA stain (Enzo Life Sciences). The staining was visualized using an Axio Observer Z1 microscope (Zeiss). To quantify the amount of caspase-positive cells, random images were taken and caspase-activated cells are presented as a percentage of caspase-1- or caspase-3/7-active cells in relation to the total cell number.

Cytotoxicity Analysis and IL-1β ELISA

To determine the cytotoxic responses, supernatants of bacterial infections or H₂O₂ cell stimulations were collected and LDH release from cells was quantified using CytoTox 96 Non-Radioactive Cytotoxicity Assay (Promega) according to the manufacturer's instructions. The IL-1β release was quantified using Human IL-1β ELISA (R&D Systems) according to the manufacturer's instructions.

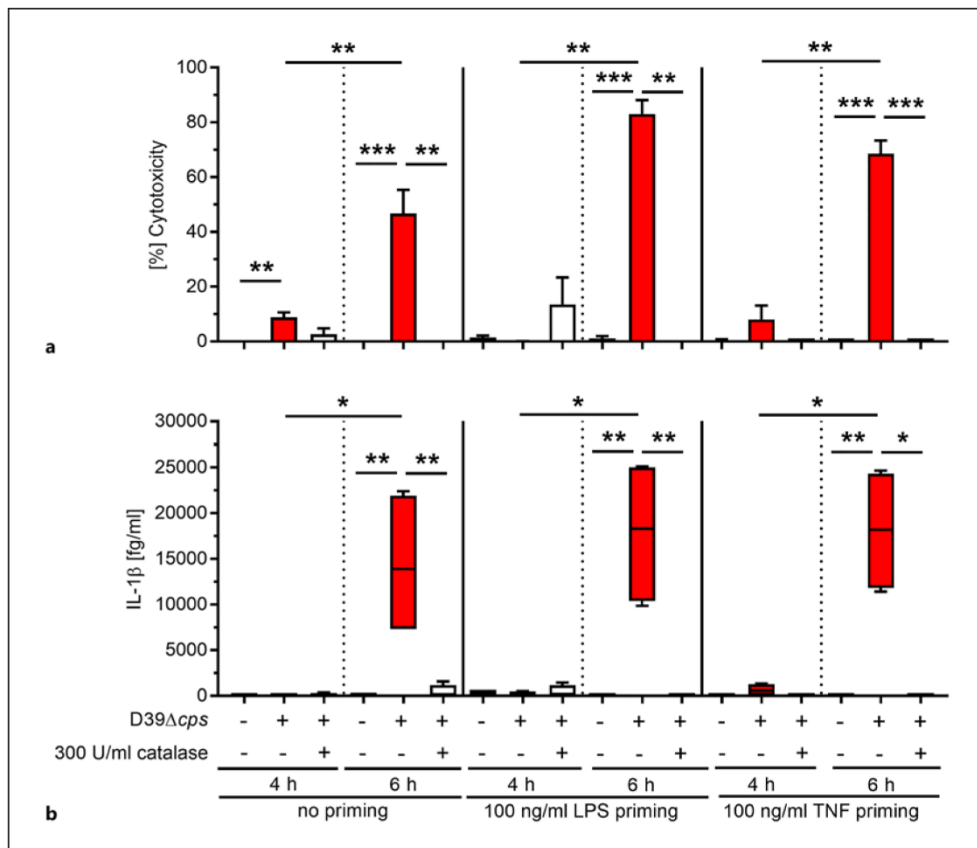


Fig. 1. H₂O₂-mediated cytotoxicity and IL-1β release by human bronchial epithelial cells. Unprimed, LPS-, or TNF-primed human bronchial epithelial cells were infected with D39Δcps at MOI 50 in the presence or absence of catalase for 4 and 6 h. Cytotoxicity (**a**) and IL-1β release (**b**) were evaluated at the indicated time points. Bars (**a**) denote mean values ± standard deviation (SD). The data in (**b**) are displayed as box plots. The level of significance was determined using Kruskal-Wallis test with Dunn's post-test ($n \geq 4$; * $p < 0.05$; ** $p < 0.01$; *** $p < 0.001$).

Inhibition Studies

The irreversible caspase-1 inhibitor Ac-YVAD-cmk (InvivoGen), caspase-3/7 inhibitor Ac-DEVD-CHO (Enzo Life Sciences), and NLRP3 inhibitor MCC950 (InvivoGen) were used in this study. All inhibitors were dissolved in DMSO and were added to the 16HBE cells 1 h prior to the other stimuli. The following concentrations were used: 50 μM (Ac-YVAD-cmk and Ac-DEVD-CHO) and 200 nM (MCC950). Cell treated with 1% DMSO served as a vehicle control.

SDS-PAGE and Immuno-Detection of Gasdermin D

16HBE cells (1×10^6 /well) were seeded in 6-well tissue culture plate and stimulated with 150 μM H₂O₂, 150 μM H₂O₂, and 300 U/mL catalase or left untreated. After 6 h of incubation, cells were washed and lysed using NP-40 lysis buffer (150 mM NaCl, 1% [v/v] NP40, 50 mM Tris-HCl, pH 8.0-containing protease inhibi-

tor mixture [Cell Signaling Technology]). Samples were normalized to equal amounts of protein (20 μg) and boiled in sample buffer (100 mM Tris [pH 6.8], 2% [w/v] SDS, 10% [v/v] β-mercaptoethanol, 20% [v/v] glycerol, and 0.05% [w/v] bromophenol blue). As molecular mass marker, prestained protein standards (Bio-Rad) were used. The samples were separated by 12% SDS-PAGE and transferred to a PVDF membrane. The membranes were blocked with 3% (v/v) skim milk prior to primary antibody incubations. Antibody incubations were performed according to manufacturer's guidelines. The following antibodies were used: Gasdermin D (E8G3F) Rabbit mAb, Cleaved Gasdermin D (E7H9G) Rabbit mAb, β-Actin (D6A8) Rabbit mAb (all from Cell Signaling Technology), and secondary anti-rabbit IgG horseradish peroxidase linked Fab fragment (GE Healthcare). Quantification of the Western blots was performed using ImageJ software.

Quantitative Reverse Transcription PCR Analysis

Total RNA was isolated from cells using RiboPure RNA Purification Kit (Ambion) according to manufacturer's instructions. cDNA synthesis was performed using Superscript first-strand synthesis system for RT-PCR (Invitrogen). Quantitative reverse transcription PCR was performed using the SYBR GreenER Kit (Bio-Rad). All samples were normalized to levels of β -actin transcription. The following primers were used: NLRP3-for, 5'-GCAAA-AAGAGATGAGCCGAAGT-3'; NLRP3-rev, 5'-GCTGTCTTCC-TGGCATATCACA-3'; IL-1 β -for, 5'-CACGATGCACCTGTA-CGATCA-3'; IL-1 β -rev, 5'-GTTGCTCCATATCCTGTCCCT-3'; h-betaAct-for, 5'-CTCTTCCAGCCTTCCCTTCT-3'; h-betaAct-rev, 5'-AGCACTGTGTTGGCGTACAG-3'.

Statistical Analyses

Statistics were performed using GraphPad Prism version 7.0 (GraphPad). Statistical significance of differences was determined using Kruskal-Wallis test with Dunn's post-test. A *p* value <0.05 was considered significant.

Results

H₂O₂ Produced by Pneumococci Induces Cell Death and IL-1 β Release

Infections of rat alveolar epithelial cells have demonstrated that Ply-deficient *S. pneumoniae* mutants are as cytotoxic as their parental strains [11]. To assess whether H_2O_2 production by pneumococci can be directly linked to the cell-damaging events and potentially to inflammatory activation, human bronchial epithelial cells were infected with *S. pneumoniae* D39 Δ *cps* in the presence or absence of catalase. Potential catalase-mediated bactericidal effects were excluded (online suppl. Fig. 1). Since NLRP3 inflammasome activation involves a priming step for NF- κ B activation and subsequent transcription of pro-IL-1 β and NLRP3 [38], cells were also stimulated with LPS or TNF α prior to infections. Four and six hours postinfection, cytotoxicity as well as IL-1 β release was determined (Fig. 1). While 4 h of pneumococcal infection remained almost nontoxic to the cells, a significant increase in cytotoxicity was observed at 6 h postinfection (Fig. 1a). The cytotoxicity was significantly diminished in infections which were supplemented with catalase (Fig. 1a). IL-1 β was only detected in cell culture supernatants at 6-h postinfection and only in congruence with the high cell cytotoxicity (Fig. 1b). Both assessed parameters, cytotoxicity and IL-1 β release, did not require a priming step.

Active SpxB and Resulting H₂O₂ Production Are Responsible for the Cell Cytotoxicity

Pneumococci exploit pyruvate oxidase enzyme SpxB to produce H_2O_2 [5]. To study the impact of H_2O_2 on cell

death, isogenic *spxB*-deficient mutants were constructed. To exclude Ply-mediated cytotoxic effects, *ply*-deficient mutants were also included in this study. Single *ply* and *spxB* as well as double mutants were generated in D39 Δ *cps* background. In addition to the nucleic acid techniques (Methods section), the knock-outs were also verified via immunoblots targeting Ply and SpxB proteins (online suppl. Fig. 3). Next, functional assays were performed. Growth analyses confirmed that single as well as double knock-outs of *spxB* or/and *ply* in *S. pneumoniae* D39 Δ *cps* did not affect bacterial growth behavior in complex THY media (Fig. 2a). Furthermore, H_2O_2 production by all 4 strains was verified. To exclude potential capsule-mediated effects on H_2O_2 release, encapsulated wild-type strains were also included in the analysis. SpxB-deficient mutants (Δ *cps* Δ *spxB* and Δ *cps* Δ *ply* Δ *spxB*) produced significantly lower amounts of H_2O_2 as compared to D39 Δ *cps* or D39 Δ *cps* Δ *ply* mutants (Fig. 2b). The presence or absence of capsule did not play a role in pneumococcal H_2O_2 production and release (Fig. 2b).

To determine the role of an active SpxB in pneumococcal infections of bronchial epithelial cells, 16HBE cells were infected with pneumococcal wild-type strains as well as D39 Δ *cps* and its isogenic mutants lacking *spxB*, *ply*, or both genes for 2, 4, or 6 h. Total bacterial infectivity (Fig. 2c, e) as well as cytotoxicity toward the cells (Fig. 2d, f) was assessed. After an initial increase of bacterial counts from 2 to 4 h of infection, a significant drop in infection rates for unencapsulated *spxB*-positive strains was observed (Fig. 2c). In contrast, the bacterial counts of *spxB* mutants remained at a constant level between 4 and 6 h of infection (Fig. 2c). Analyses of the cell viability revealed that 16HBE infections with pneumococci harboring an active *spxB* gene were characterized by a time-dependent cell cytotoxicity (Fig. 2d). In contrast, mutant strains lacking *spxB* were not cytotoxic (Fig. 2d). To assess if direct contact is required for H_2O_2 -mediated damage of the cells, infections with encapsulated wild-type strains, which are known to adhere to a lesser extent as compared to the nonencapsulated strains, were also performed. After 4 h of infection, total infectivity of D39 and TIGR4 was approximately 10-fold lower compared to the D39 Δ *cps* strain (Fig. 2c, e). 19F strain adhered to the cells even at much lower rates (Fig. 2e). However, the encapsulated wild-type strains were as cytotoxic as the nonencapsulated mutants (Fig. 2d, f). Taken together, these results indicate that cell cytotoxicity at the early stages of infection can be primarily attributed to the influence of H_2O_2 produced by pneumococci.

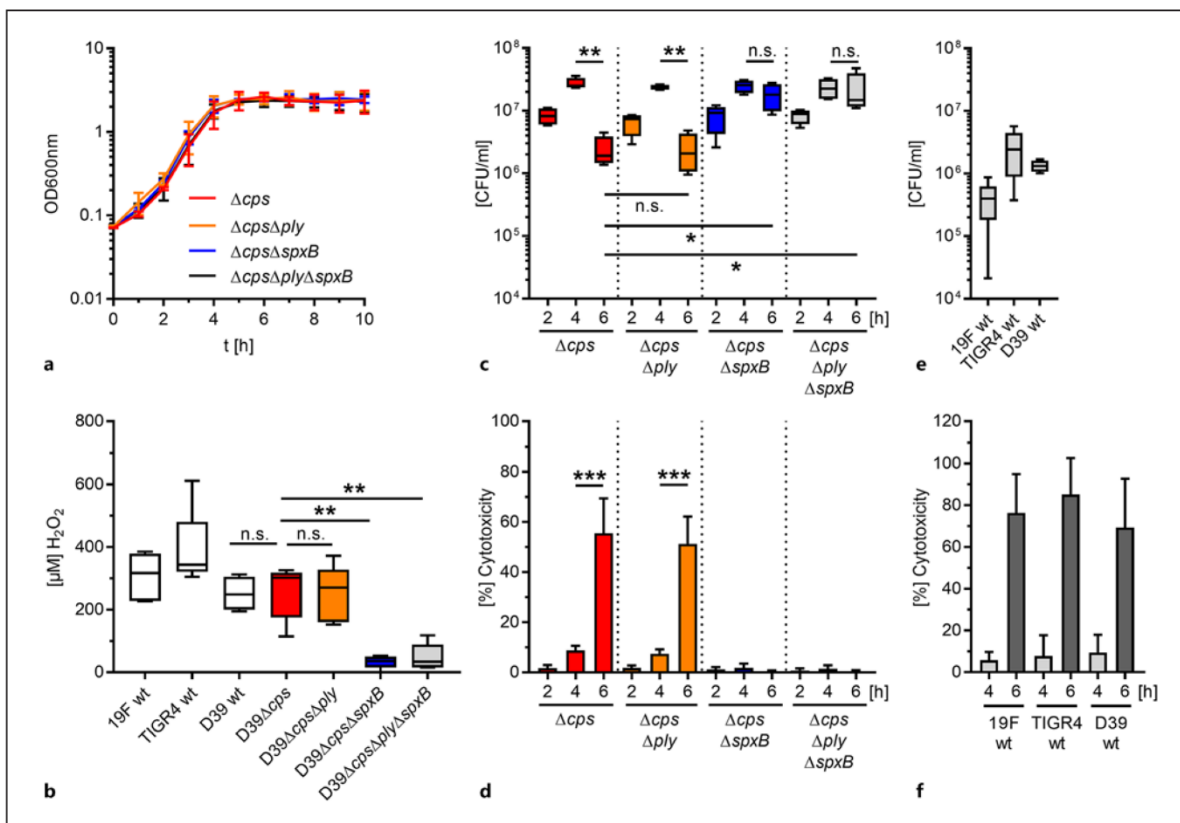


Fig. 2. Pneumococcal H_2O_2 is responsible for bronchial epithelial cell lysis. **a** Monitoring of growth behavior of *S. pneumoniae* D39 Δcps , $\Delta cps\Delta ply$, $\Delta cps\Delta spxB$, and $\Delta cps\Delta ply\Delta spxB$ mutant strains in THY medium ($n = 3$). **b** H_2O_2 production by pneumococci was determined by colorimetric analysis of bacterial culture supernatants ($n = 4$). 16HBE cells were infected with pneumococcal strains, and bacterial infectivity (**c, e**) and cytotoxicity toward

the cells (**d, f**) were assessed at indicated time points ($n \geq 4$). The data in (**b, c, e**) are displayed as box plots. Bars in (**d, f**) denote mean values \pm SD. The level of significance was determined using Kruskal-Wallis test with Dunn's post-test ($n \geq 4$; n.s., not significant; * $p < 0.05$; ** $p < 0.01$; *** $p < 0.001$). CFU, colony-forming unit; SD, standard deviation; THY, Todd-Hewitt broth supplemented with 0.5% (w/v) yeast extract.

H_2O_2 Activates Caspase-1 and Caspase-3/7 in 16HBE Cells

Both H_2O_2 -mediated cytotoxicity toward 16HBE cells and subsequent IL-1 β release suggest the involvement of NLRP3 inflammasome in pneumococcal infections. To assess the NLRP3 axis prior to the excessive cell lysis, unprimed 16HBE cells were infected with pneumococcal strains for 4 h and caspase-1 activation was determined via fluorescent probing with FAM-YVAD-FMK FLICA. In addition, caspase-3/7 activation as a marker for apoptosis was analyzed. Although initial data indicated that LPS or TNF priming is dispensable, LPS was kept through the entire series of experiments as a generally accepted

inflammasome model control. Only minor cytotoxic events were observed in infections with D39 SpxB-expressing strains (Fig. 3a). Activated caspase-1 was detected in 10–20% of the infected cells (Fig. 3b, d). In contrast, *spxB* mutants did not cause cell lysis (Fig. 3a) and 16HBE cells remained negative for active caspase-1 (Fig. 3b, d). Analyses of active caspase-3/7 revealed a similar pattern. While infections with SpxB-expressing D39 strains activated caspase-3/7, infections with *spxB* mutants did not (Fig. 3c, d). The observed infection phenotype was independent of priming (Fig. 3 and online suppl. Fig. 4a).

To confirm that the activation of caspases and thereby an increase in cytotoxicity were associated with H_2O_2 ,

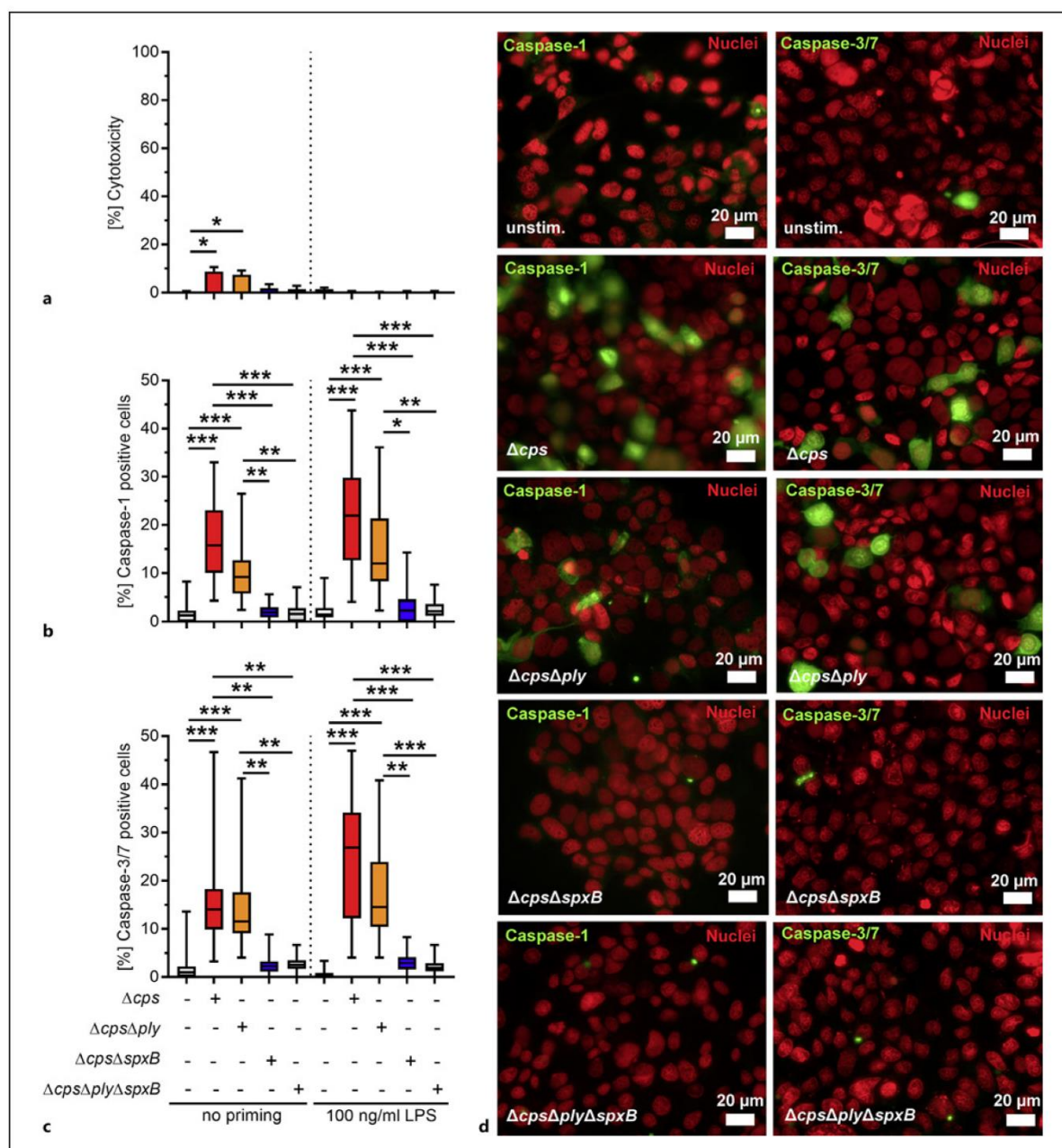


Fig. 3. *S. pneumoniae* strains with functional SpxB activate caspase-1 and caspase-3/7. Unprimed or primed 16HBE cells were infected with indicated pneumococcal strains for 4 h and cytotoxicity (**a**) as well as caspase-1 and caspase-3/7 (**b–d**) activation was assessed. The infected cells were stained using fluorescent inhibitor probe FAM-YVAD-FMK (**b, d** left panel) and FAM-DEVD-FMK (**c, d** right panel) to microscopically visualize active caspase-1 and

caspase-3/7, respectively. Nuclear-ID stain was used to visualize cell nuclei. Caspase-1- and caspase-3/7-positive cells were counted and are presented as a percentage of positive cells in relation to the total number of cells (**b, c**). Bars (**a**) denote mean values \pm SD. The data in (**b, c**) are displayed as box plots. The level of significance was determined using Kruskal-Wallis test with Dunn's post-test ($n = 4$; * $p < 0.05$; ** $p < 0.01$; *** $p < 0.001$). SD, standard deviation.

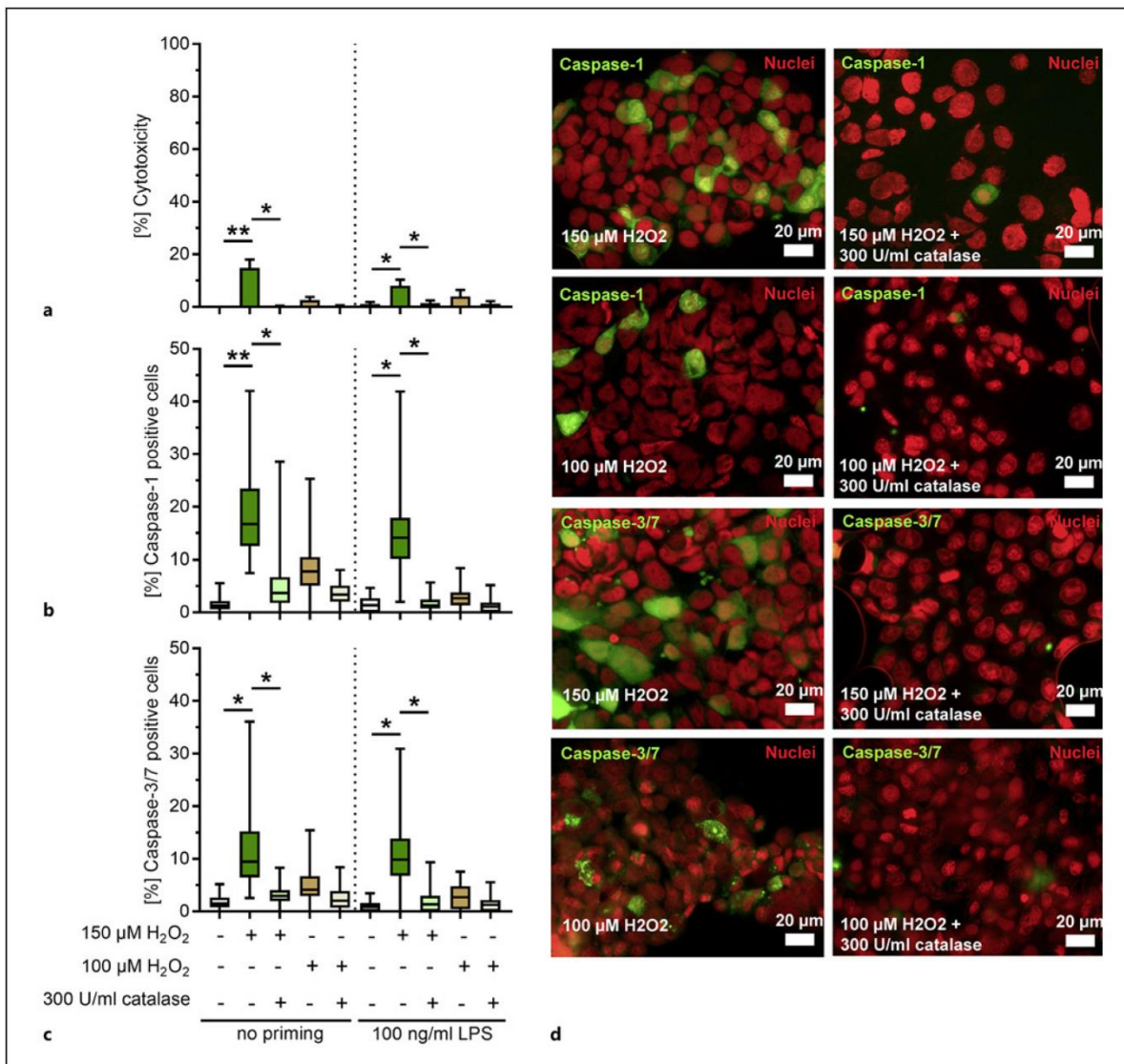


Fig. 4. H_2O_2 activates caspase-1 and caspase-3/7 in bronchial epithelial cells. Unprimed or primed 16HBE cells were stimulated with 150 and 100 μM H_2O_2 in the presence or absence of catalase for 4 h and cytotoxicity (a) as well as caspase-1 and caspase-3/7 (b-d) activation was assessed. The stimulated cells were stained using fluorescent inhibitor probe FAM-YVAD-FMK (b, d) and FAM-DEVD-FMK (c, d) to microscopically visualize active caspase-1 and caspase-3/7, respectively. Nuclear-ID stain was used to

visualize cell nuclei. Caspase-1- and caspase-3/7-positive cells were counted and are presented as a percentage of positive cells in relation to the total number of cells (b, c). Bars (a) denote mean values \pm SD. The data in (b, c) are displayed as box plots. The level of significance was determined using Kruskal Wallis test with Dunn's post-test ($n = 4$; * $p < 0.05$; ** $p < 0.01$; *** $p < 0.001$). SD, standard deviation.

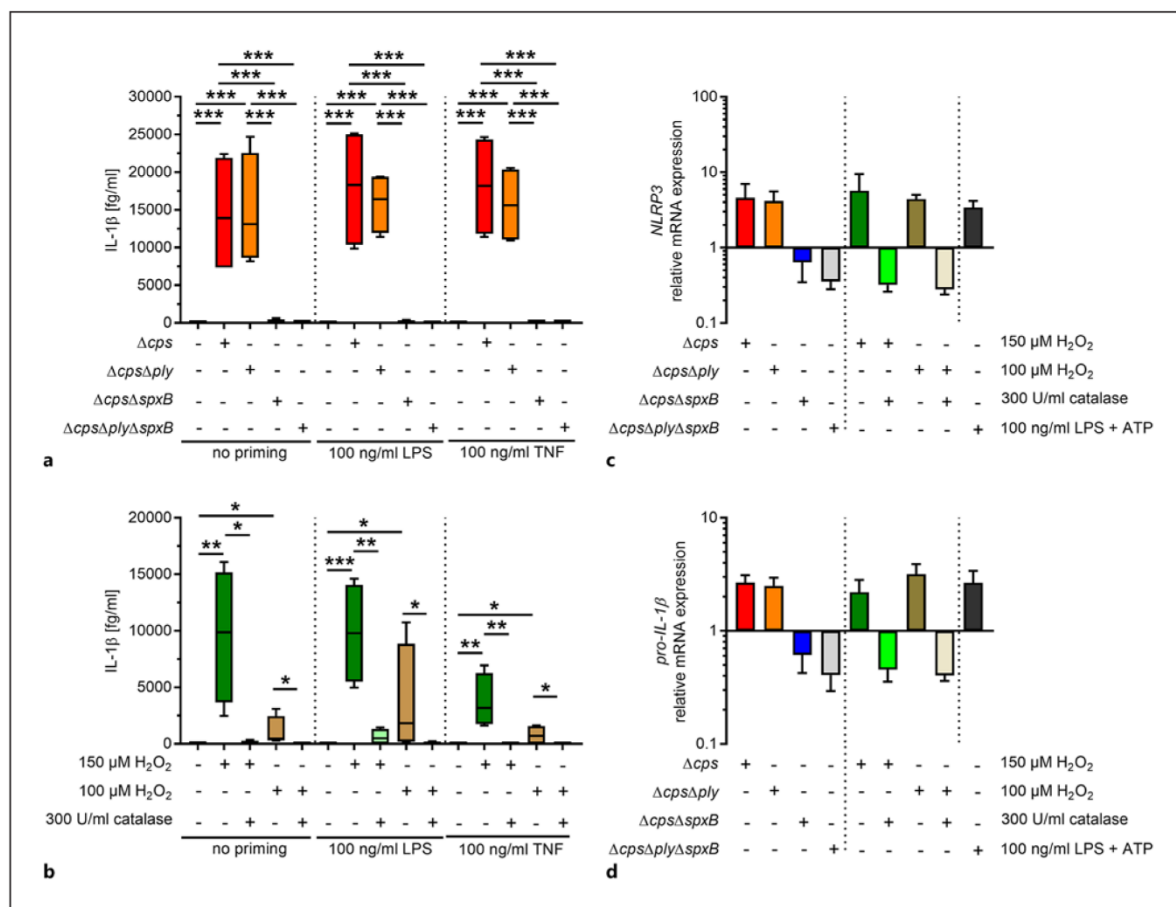
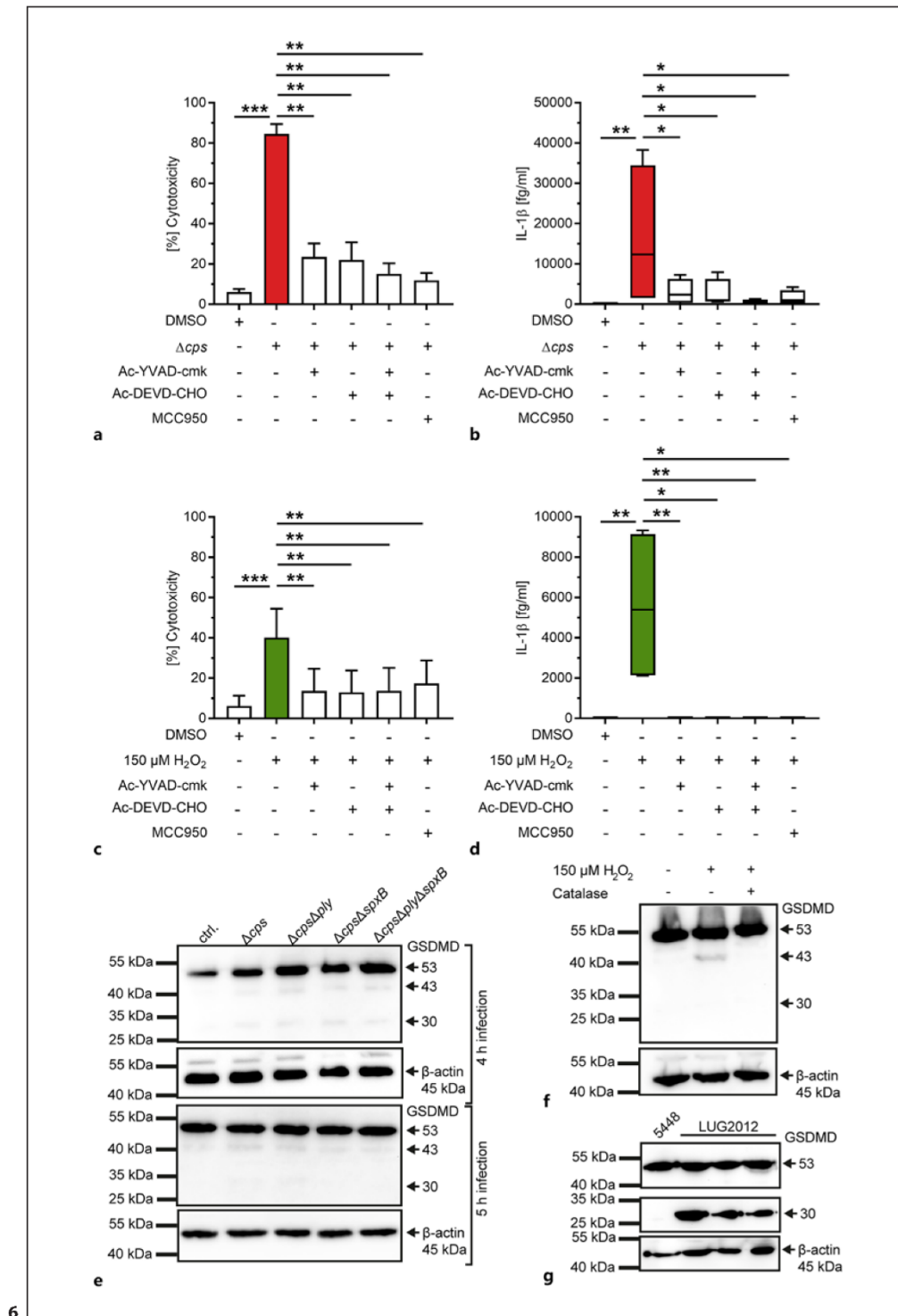


Fig. 5. SpxB-mediated H_2O_2 production induces IL-1 β release after 6 h of stimulation. Unprimed, LPS-, or TNF-primed human bronchial epithelial cells were infected with D39 Δcps and the isogenic mutants at MOI 50 (**a, c, d**), or stimulated with 150 and 100 μM H_2O_2 in the presence or absence of catalase (**b-d**). IL-1 β release was evaluated at 6 h post infection (**a**) or stimulation (**b**). Relative

mRNA expression of *NLRP3* (**c**) and *pro-IL-1 β* (**d**) was quantified in infected and stimulated cells. The data in (**a, b**) are displayed as box plots. Bars in (**c, d**) denote mean values \pm SD. The level of significance was determined using Kruskal-Wallis test with Dunn's post-test ($n \geq 4$; * $p < 0.05$; ** $p < 0.01$; *** $p < 0.001$). SD, standard deviation.

16HBE cells were stimulated with pure H_2O_2 for 4 or 6 h. A dose-dependent increase in cytotoxicity toward the cells was observed (online suppl. Fig. 5). Addition of catalase to the stimulations reverted the cytolytic events (online suppl. Fig. 5). H_2O_2 concentrations of 100 and 150 μM , which were approximately of equivalent cytotoxicity as compared to the D39 Δcps strain infections, were used to study the activation of caspases in primed and unprimed cells. Minor cytotoxicity was only observed in stimulations with 150 μM H_2O_2 (Fig. 4a). Cells with active caspase-1 were mostly detected in these stim-

ulations (Fig. 4b, d). Furthermore, caspase-3/7 activation followed exactly the same pattern (Fig. 4c, d; online suppl. Fig. 4b). Addition of catalase to the stimulations reduced the H_2O_2 -mediated cytotoxicity and activation of caspase-1 and caspase-3/7 (Fig. 4 and online suppl. Fig. 5). These results confirm that H_2O_2 induces cell death and caspase-1 as well as caspase-3/7 activation in 16HBE cells.



(For legend see next page.)

H₂O₂ Activates Inflammasome Signaling Resulting in IL-1 β Release

Since active caspase-1 cleaves pro-IL-1 β into mature form, which is mostly released via pyroptosis, IL-1 β release post bacterial infections or H₂O₂ stimulations was determined in culture supernatants. To confirm that the priming step is dispensable, TNF and LPS stimulation were performed prior to infections. In line with the cytotoxicity data (Fig. 2d), IL-1 β was exclusively detected after 6 h of infections with SpxB-positive strains (Fig. 5a; online suppl. Fig. 6a). H₂O₂ stimulations of 16HBE cells confirmed this phenotype. The highest amounts of IL-1 β were detected 6 h post stimulations (Fig. 5b; online suppl. Fig. 6b). Addition of catalase neutralized H₂O₂-mediated IL-1 β release.

Our data clearly indicate that H₂O₂-mediated cytotoxicity and IL-1 β release do not require a priming step. To further delineate the role of H₂O₂ in NLRP3 inflammasome activation, NLRP3 and *pro-IL-1 β* mRNA expression in the infected and H₂O₂-stimulated cells was analyzed (Fig. 5c, d). Cells stimulated with LPS and ATP served as a positive control. Upregulation in the expression of both genes, NLRP3 and *pro-IL-1 β* , was detected in cells infected with D39 Δ *cps* and D39 Δ *cps* Δ *ply* as compared to the *spxB* mutant infections (Fig. 5c, d). Furthermore, both genes were upregulated in response to H₂O₂ stimulations (Fig. 5c, d). Addition of catalase reversed this effect. These results confirm that H₂O₂ alone is sufficient for priming and activating the NLRP3 inflammasome in 16HBE cells.

IL-1 β Release Caused by H₂O₂ Is a Result of NLRP3 Inflammasome Activation but Not Pyroptosis

Caspase-1 activation, cell death, and subsequent IL-1 β release are the hallmarks of inflammasome signaling. To

confirm that these H₂O₂-induced responses were indeed mediated via the inflammasome pathway, cells were pre-treated with caspase-1 inhibitor Ac-YVAD-cmk or an inhibitor of NLRP3 conformational change and oligomerization MCC950. Since caspase-3/7 activation was also observed, Ac-DEVD-CHO was used to block apoptosis. As previously shown, both D39 Δ *cps* infections and H₂O₂ stimulations of cells for 6 h resulted in cell death and subsequent IL-1 β release (Fig. 6a–d). Blocking of NLRP3, caspase-1, caspase-3/7, or both caspases resulted in significantly diminished cell death and IL-1 β amounts in cell culture supernatants (Fig. 6a–d). These results indicate that H₂O₂ leads to NLRP3 inflammasome activation and IL-1 β production; however, the final IL-1 β release is also dependent on the apoptotic cell death pathway. To verify these results, it was essential to determine the GSDMD cleavage products, including full-length GSDMD (50 kDa) and fragments of GSDMD cleaved by caspase-1 (30 kDa) or caspase-3/7 (43 kDa) (Fig. 6e, f), in infected and H₂O₂-stimulated cells. While the 43-kDa GSDMD is inactive, the 30-kDa GSDMD-N is mainly responsible for the cell membrane perforation and pyroptosis. Western blot analyses revealed that full length and small amounts of the inactivated 43-kDa fragment of GSDMD are present in both infected and H₂O₂-stimulated cells (Fig. 6e, f; online suppl. Fig. 7). No or traces of the 30-kDa product were detected in 5 or 4 h infections, respectively (Fig. 6e; online suppl. Fig. 7). However, 30-kDa GSDMD-N was not detected in any of the pneumococcal infections if a specific antibody was used (online suppl. Fig. 7). To show that GSDMD can be cleaved to GSDMD-N (30 kDa) in 16HBE cells, infections with *S. pyogenes* 5448 and *S. aureus* LUG2012 were also performed (Fig. 6g). While GSDMD-N was not detected in 5448 infections, it was readily detectable in LUG2012 infections (Fig. 6g). Lack of the active 30-kDa fragment in pneumococcal infections and inhibition studies suggest that the IL-1 β release is independent of GSDMD.

Discussion/Conclusion

Epithelial cells of the respiratory tract are the first responders to an infection or pathogenic stimuli. They respond by secreting various effector molecules such as cytokines and antimicrobial peptides that facilitate an influx of professional phagocytes to engulf the pathogens or infected and dying cells [39]. Here, we report that pneumococci-derived H₂O₂ induces epithelial cell cytotoxicity by priming the cells as well as activating the NLRP3 in-

Fig. 6. H₂O₂-mediated IL-1 β release is a result of NLRP3 inflammasome activation. Unprimed human bronchial epithelial cells were infected with D39 Δ *cps* at MOI 50 (a, b), or stimulated with 150 μ M H₂O₂ (c, d). Cells were treated with Ac-YVAD-cmk, Ac-DEVD-CHO, and MCC950, 1 h prior to the other stimuli. Cytotoxicity (a, c) and IL-1 β release (b, d) were evaluated at the 6-h time point. The data are displayed as box plots. The level of significance was determined using Kruskal-Wallis test with Dunn's post-test ($n \geq 4$; * $p < 0.05$; ** $p < 0.01$; *** $p < 0.001$). Western blot analyses of D39 Δ *cps*-infected (e) and H₂O₂-stimulated (f) 16HBE cells. e 16HBE cells were infected with different D39 mutant strains or (f) stimulated with H₂O₂ for indicated time points, cells were lysed, and 20 μ g of total protein was separated via SDS-PAGE. Representative images of GSDMD and β -actin as a loading control from 5 independent experiments are displayed ($n = 5$). g Western blot analyses of *Streptococcus pyogenes* 5448 or *Staphylococcus aureus* LUG2012-infected 16HBE cells. Original uncropped versions of the blots are shown in online suppl. Fig. 7. GSDMD, gasdermin-D.

flammasome, resulting in caspase-1 activation and IL-1 β release. Nevertheless, the final IL-1 β release is mainly a result of an apoptotic cell death.

Pneumococci are frequent asymptomatic colonizers of the nasopharyngeal cavity and in certain stress condition; they can disseminate to the lower respiratory tract and cause invasive diseases, including pneumonia [40]. Two major secreted cytotoxins, Ply and H₂O₂, are mainly responsible for the lytic injury of a wide range of human cells [41, 42]. As a pore-forming toxin, Ply is implicated in many cell-damaging processes [43–45]. Previous studies have shown that Ply activates the NLRP3 inflammasome [46]. However, it is noteworthy to mention that Ply is not actively secreted by *S. pneumoniae* due to a lack of an N-terminal signal peptide needed for secretion [47]. Instead, Ply is released via autolysis at the late stage of growth [48]. It has also been shown that Ply-deficient bacteria are as cytotoxic as their respective wild-type strains in the early phase of infection [4]. Therefore, it is plausible to expect that Ply-specific inflammasome activation and cell death occur at the later stages of infection. In contrast to Ply, only 1 study analyzed H₂O₂-mediated cell-damaging events in pneumococcal infections. A previous study showed that pneumococci-derived H₂O₂ suppresses ATP-mediated inflammasome activation in mouse bone marrow-derived macrophages. The authors proposed that pneumococci utilize H₂O₂ to suppress the immune system and through this mechanism, the bacteria might colonize and coexist with the host [28]. In the present study, the cytotoxic impact of pneumococcal H₂O₂ on bronchial epithelial cells was analyzed. In contrast to the study mentioned above, infections with H₂O₂-producing pneumococci were highly cytotoxic to the epithelial cells. This result is in line with other studies showing that H₂O₂ is of cytotoxic nature [49, 50]. Current literature implicates pneumococcal H₂O₂ as a major cause of lung tissue damage through the apoptotic pathways [51, 52]. However, little is known about its inflammasome-activating properties and pyroptosis. Notably, we find that caspase-1 and caspase-3/7 are activated by H₂O₂, indicating that inflammasome activation occurs and potentially both apoptotic and pyroptotic cell death pathways are simultaneously initiated in the presence of H₂O₂. Various inflammasome pathways have been studied so far, of which the NLRP3 inflammasome is the most well characterized. It can be activated by a wide range of stimuli, making it very diverse in nature [53]. In contrast to monocytes, the NLRP3 and pro-IL-1 β concentrations in resting epithelial cells are inadequate to initiate activation of the inflammasome, making the priming step manda-

tory [54]. Here, we used LPS and TNF because they are commonly accepted priming agents in inflammasome-related studies [23, 28, 54]. During a pneumococcal infection in the lung, the role of priming can be also provided by IL-1 β itself [54, 55]. Furthermore, pneumococcal lipoproteins can mediate a TLR2 response [56] and could also play a role in priming. However, our results demonstrate that the priming is dispensable for H₂O₂-mediated IL-1 β production in pneumococcal infections. This fact is further supported by previous studies which have shown that H₂O₂ can directly activate NF- κ B through the NF- κ B-inducing kinase [57–59].

Furthermore, our data show that caspase-1 or NLRP3 inhibition significantly reduced the H₂O₂-mediated cytolytic injury as well as IL-1 β release, indicating that H₂O₂ is a potent activator of the NLRP3 inflammasome. However, inhibition of the apoptotic pathway followed exactly the same pattern. In support of this, 2 studies demonstrated that H₂O₂ induces mitochondrial damage which in turn triggers both apoptotic signals and NLRP3-dependent IL-1 β secretion [51, 60]. In the next step, we aimed to analyze whether H₂O₂ mediates pyroptosis. The key molecule in this process is GSDMD. For many years, a linear model of pyroptosis was proposed. Activated caspase-1 cleaves both pro-IL-1 β and GSDMD to IL-1 β and GSDMD-N, respectively. The GSDMD-N perforates the lipid bilayer and IL-1 β is released through these pores [25]. Although our data demonstrate that H₂O₂ induces caspase-1 activation and IL-1 β production, IL-1 β release itself occurs in a GSDMD-independent fashion. Only an inactive form of GSDMD (43 kDa), a product of caspase-3 cleavage [61], was detected post H₂O₂ stimulations. In line with this, it was suggested that prolonged stimulation of the inflammasome can potentially result in GSDMD-independent cell death and IL-1 β release [62].

Nevertheless, cross-talks between the various cell death pathways in a complex cellular environment can still be expected. Recently, it was demonstrated that caspase-1 can also redundantly promote activation of apoptotic executioner caspase-3 and caspase-7 in macrophages [63]. Furthermore, caspase-3 can activate GSDME/DFNA5 to form membrane pores to induce secondary necrotic/pyroptotic cell death [64, 65]. Even more, cross-talks between pyroptosis and necroptosis have also been reported [66]. Zhao and colleagues have shown that H₂O₂ can induce necrosis through the RIP1/RIP3-PARP-AIF pathway [67]. Furthermore, mixed lineage kinase domain-like, a marker for necroptosis, is able to activate the NLRP3 inflammasome and simultaneously rupture the cell membrane, resulting in GSDMD-independent IL-1 β release [66].

In conclusion, this study strongly supports the concept that pneumococci-derived H₂O₂ has a detrimental influence on human bronchial epithelial cells. Although IL-1 β release is mainly dependent on the apoptotic pathway, H₂O₂ mediates caspase-1-dependent IL-1 β production. It is noteworthy to mention that in a complex cellular environment, it is plausible to expect cross-talks between the various cell death pathways. Therefore, to delineate the complex nature of cell death induced by H₂O₂, further experimental studies pertaining to other cellular pathways such as necroptosis are warranted.

Acknowledgement

We would like to acknowledge all partners of the collaborative project “KoInfekt.”

Statement of Ethics

The article is exempt from ethical committee approval as all work was performed in vitro using a cell line and no primary human samples were used.

Conflict of Interest Statement

The authors declare no conflict of interest.

Funding Sources

This research was supported by the Federal Excellence Initiative of Mecklenburg Western Pomerania and European Social Fund Grant KoInfekt (ESF_14-BM-A55-0001_16 to S.H.) and the German Research Foundation (DFG; grant no.: 407176682 to N.S.).

Author Contributions

S.S., S.H., and N.S. designed the study. S.S., L.H.J., P.S., and G.B. performed the experiments. S.S., L.H.J., and N.S. analyzed the data. S.S. and N.S. wrote the manuscript. S.S., L.J., P.S., G.B., S.H., and N.S. read, edited, and reviewed the manuscript.

References

- Musher DM, Thorner AR. Community-acquired pneumonia. *N Engl J Med*. 2014 Oct 23;371(17):1619–28.
- Kadioglu A, Weiser JN, Paton JC, Andrew PW. The role of *Streptococcus pneumoniae* virulence factors in host respiratory colonization and disease. *Nat Rev Microbiol*. 2008 Apr;6(4):288–301.
- Siemens N, Oehmcke-Hecht S, Mettenleiter TC, Kreikemeyer B, Valentin-Weigand P, Hammerschmidt S. Port d'Entrée for respiratory infections: does the Influenza A virus pave the way for bacteria? *Front Microbiol*. 2017;8:2602.
- Cuyppers F, Klabunde B, Gesell Salazar M, Surabhi S, Skorka SB, Burchardt G, et al. Adenosine triphosphate neutralizes pneumolysin-induced neutrophil activation. *J Infect Dis*. 2020 Oct 13;222(10):1702–12.
- Spellerberg B, Cundell DR, Sandros J, Pearce BJ, Idänpään-Heikkilä I, Rosenow C, et al. Pyruvate oxidase, as a determinant of virulence in *Streptococcus pneumoniae*. *Mol Microbiol*. 1996 Feb;19(4):803–13.
- Bienert GP, Schjoerring JK, Jahn TP. Membrane transport of hydrogen peroxide. *Biochimica Biophysica Acta*. 2006 Aug 1;1758(8):994–1003.
- Pfister HW, Koedel U, Lorenzl S, Tomasz A. Antioxidants attenuate microvascular changes in the early phase of experimental pneumococcal meningitis in rats. *Stroke*. 1992 Dec; 23(12):1798–804.
- Hoffmann OM, Becker D, Weber JR. Bacterial hydrogen peroxide contributes to cerebral hyperemia during early stages of experimental pneumococcal meningitis. *J Cereb Blood Flow Metab*. 2007 Nov;27(11):1792–7.
- Hirst RA, Sikand KS, Rutman A, Mitchell TJ, Andrew PW, O'Callaghan C. Relative roles of pneumolysin and hydrogen peroxide from *Streptococcus pneumoniae* in inhibition of ependymal ciliary beat frequency. *Infect Immun*. 2000 Mar;68(3):1557–62.
- Feldman C, Anderson R, Cockeran R, Mitchell T, Cole P, Wilson R. The effects of pneumolysin and hydrogen peroxide, alone and in combination, on human ciliated epithelium in vitro. *Respir Med*. 2002 Aug;96(8):580–5.
- Duane PG, Rubins JB, Weisel HR, Janoff EN. Identification of hydrogen peroxide as a *Streptococcus pneumoniae* toxin for rat alveolar epithelial cells. *Infect Immun*. 1993 Oct; 61(10):4392–7.
- Crystal RG, Randell SH, Engelhardt JF, Voynow J, Sunday ME. Airway epithelial cells: current concepts and challenges. *Proc Am Thorac Soc*. 2008;5(7):772–7.
- Whitsett JA, Alenghat T. Respiratory epithelial cells orchestrate pulmonary innate immunity. *Nat Immunol*. 2015 Jan;16(1):27–35.
- LeMessurier KS, Tiwary M, Morin NP, Samarasinghe AE. Respiratory Barrier as a safeguard and regulator of defense against influenza A virus and *Streptococcus pneumoniae*. *Front Immunol*. 2020;11:3.
- Leiva-Juárez MM, Kolls JK, Evans SE. Lung epithelial cells: therapeutically inducible effectors of antimicrobial defense. *Mucosal Immunol*. 2018;11(1):21–34.
- Fink SL, Cookson BT. Apoptosis, pyroptosis, and necrosis: mechanistic description of dead and dying eukaryotic cells. *Infect Immun*. 2005 Apr;73(4):1907–16.
- Porter AG, Janicke RU. Emerging roles of caspase-3 in apoptosis. *Cell Death Differ*. 1999 Feb;6(2):99–104.
- Surabhi S, Cuyppers F, Hammerschmidt S, Siemens N. The role of NLRP3 inflammasome in pneumococcal infections. *Front Immunol*. 2020 December 14;11(3277):614801.
- Lamkanfi M, Dixit VM. Modulation of inflammasome pathways by bacterial and viral pathogens. *J Immunol*. 2011 Jul 15;187(2):597–602.

- 20 Amores-Iniesta J, Barberà-Cremades M, Martínez CM, Pons JA, Revilla-Nuin B, Martínez-Alarcón L, et al. Extracellular ATP activates the NLRP3 inflammasome and is an early danger signal of skin allograft rejection. *Cell Rep*. 2017 Dec 19;21(12):3414–26.
- 21 Eigenbrod T, Dalpke AH. Bacterial RNA: an underestimated stimulus for innate immune responses. *J Immunol*. 2015 Jul 15;195(2):411–8.
- 22 Greaney AJ, Leppla SH, Moayeri M. Bacterial exotoxins and the inflammasome. *Front Immunol*. 2015 November 10;6(570):570.
- 23 Netea MG, Nold-Petry CA, Nold MF, Joosten LA, Opitz B, van der Meer JH, et al. Differential requirement for the activation of the inflammasome for processing and release of IL-1beta in monocytes and macrophages. *Blood*. 2009 Mar 5;113(10):2324–35.
- 24 Gritsenko A, Yu S, Martin-Sanchez F, del Olmo ID, Nichols EM, Davis DM, et al. Priming is dispensable for NLRP3 inflammasome activation in human monocytes. *Front Immunol*. 2020 Sep 30;11:565924.
- 25 He WT, Wan H, Hu L, Chen P, Wang X, Huang Z, et al. Gasdermin D is an executor of pyroptosis and required for interleukin-1β secretion. *Cell Res*. 2015 Dec;25(12):1285–98.
- 26 Shi J, Zhao Y, Wang K, Shi X, Wang Y, Huang H, et al. Cleavage of GSDMD by inflammatory caspases determines pyroptotic cell death. *Nature*. 2015 Oct 29;526(7575):660–5.
- 27 Liu X, Zhang Z, Ruan J, Pan Y, Magupalli VG, Wu H, et al. Inflammasome-activated gasdermin D causes pyroptosis by forming membrane pores. *Nature*. 2016 Jul 7;535(7610):153–8.
- 28 Erttmann SF, Gekara NO. Hydrogen peroxide release by bacteria suppresses inflammasome-dependent innate immunity. *Nat Commun*. 2019 Aug 2;10(1):3493.
- 29 Dostert C, Pétrilli V, Van Bruggen R, Steele C, Mossman BT, Tschopp J. Innate immune activation through Nalp3 inflammasome sensing of asbestos and silica. *Science*. 2008 May 2;320(5876):674–7.
- 30 Zhou R, Tardivel A, Thorens B, Choi I, Tschopp J. Thioredoxin-interacting protein links oxidative stress to inflammasome activation. *Nat Immunol*. 2010 Feb;11(2):136–40.
- 31 Siemens N, Chakraborti B, Shambat SM, Morgan M, Bergsten H, Hyldegaard O, et al. Biofilm in group A streptococcal necrotizing soft tissue infections. *JCI Insight*. 2016 Jul 7;1(10):e87882.
- 32 Mairpady Shambat S, Chen P, Nguyen Hoang AT, Bergsten H, Vandenesch F, Siemens N, et al. Modelling staphylococcal pneumonia in a human 3D lung tissue model system delineates toxin-mediated pathology. *Dis Model Mech*. 2015 Nov;8(11):1413–25.
- 33 Hammerschmidt S, Talay SR, Brandtzaeg P, Chhatwal GS. SpsA, a novel pneumococcal surface protein with specific binding to secretory immunoglobulin A and secretory component. *Mol Microbiol*. 1997 Sep;25(6):1113–24.
- 34 Gómez-Mejía A, Gámez G, Hirschmann S, Kluger V, Rath H, Böhm S, et al. Pneumococcal metabolic adaptation and colonization are regulated by the two-component regulatory system 08. *mSphere*. 2018 May/June;3(3):e00165-18.
- 35 Battig P, Muhlemann K. Influence of the spxB gene on competence in *Streptococcus pneumoniae*. *J Bacteriol*. 2008 Feb;190(4):1184–9.
- 36 Schmidt F, Kakar N, Meyer TC, Depke M, Masouris I, Burchhardt G, et al. In vivo proteomics identifies the competence regulon and AlIB oligopeptide transporter as pathogenic factors in pneumococcal meningitis. *PLoS Pathog*. 2019 Jul;15(7):e1007987.
- 37 Schulz C, Gierok P, Petruschka L, Lalk M, Mäder U, Hammerschmidt S. Regulation of the arginine deiminase system by ArgR2 interferes with arginine metabolism and fitness of *Streptococcus pneumoniae*. *mBio*. 2014 Dec 23;5(6):e01858-14.
- 38 Zheng D, Liwinski T, Elinav E. Inflammasome activation and regulation: toward a better understanding of complex mechanisms. *Cell Discov*. 2020;6(1):36.
- 39 Bals R. Epithelial antimicrobial peptides in host defense against infection. *Respir Res*. 2000;1(3):141–50.
- 40 Song JY, Nahm MH, Moseley MA. Clinical implications of pneumococcal serotypes: invasive disease potential, clinical presentations, and antibiotic resistance. *J Korean Med Sci*. 2013 Jan;28(1):4–15.
- 41 Kim JY, Paton JC, Briles DE, Rhee DK, Pyo S. *Streptococcus pneumoniae* induces pyroptosis through the regulation of autophagy in murine microglia. *Oncotarget*. 2015 Dec 29;6(42):44161–78.
- 42 Brooks LRK, Mias GI. *Streptococcus pneumoniae*'s virulence and host immunity: aging, diagnostics, and prevention. *Front Immunol*. 2018;9:1366.
- 43 Witznath M, Pache F, Lorenz D, Koppe U, Gutbier B, Tabeling C, et al. The NLRP3 inflammasome is differentially activated by pneumolysin variants and contributes to host defense in pneumococcal pneumonia. *J Immunol*. 2011 Jul 1;187(1):434–40.
- 44 Fatykhova D, Rabes A, Machnik C, Gurusankar K, Pache F, Berg J, et al. Serotype 1 and 8 *Pneumococci* evade sensing by inflammasomes in human lung tissue. *PLoS One*. 2015;10(8):e0137108.
- 45 Jahn K, Handtke S, Palankar R, Weifsmüller S, Nouailles G, Kohler TP, et al. Pneumolysin induces platelet destruction, not platelet activation, which can be prevented by immunoglobulin preparations in vitro. *Blood Adv*. 2020 Dec 22;4(24):6315–26.
- 46 McNeela EA, Burke A, Neill DR, Baxter C, Fernandes VE, Ferreira D, et al. Pneumolysin activates the NLRP3 inflammasome and promotes proinflammatory cytokines independently of TLR4. *PLoS Pathog*. 2010 Nov 11;6(11):e1001191.
- 47 Walker JA, Allen RL, Falmagne P, Johnson MK, Boulnois GJ. Molecular cloning, characterization, and complete nucleotide sequence of the gene for pneumolysin, the sulfhydryl-activated toxin of *Streptococcus pneumoniae*. *Infect Immun*. 1987;55(5):1184–9.
- 48 Benton KA, Paton JC, Briles DE. Differences in virulence for mice among *Streptococcus pneumoniae* strains of capsular types 2, 3, 4, 5, and 6 are not attributable to differences in pneumolysin production. *Infect Immun*. 1997;65(4):1237–44.
- 49 Brissac T, Shenoy AT, Patterson LA, Orihuela CJ. Cell invasion and pyruvate oxidase-derived H₂O₂ are critical for *Streptococcus pneumoniae*-mediated cardiomyocyte killing. *Infect Immun*. 2018 Jan;86(1):e00569-17.
- 50 Gao Y, Xu W, Dou X, Wang H, Zhang X, Yang S, et al. Mitochondrial DNA leakage caused by *Streptococcus pneumoniae* hydrogen peroxide promotes type I IFN expression in lung cells. *Front Microbiol*. 2019;10:630.
- 51 Braun JS, Sublett JE, Freyer D, Mitchell TJ, Cleveland JL, Tuomanen EI, et al. Pneumococcal pneumolysin and H₂O₂ mediate brain cell apoptosis during meningitis. *J Clin Invest*. 2002 Jan;109(1):19–27.
- 52 Rai P, Parrish M, Tay IJJ, Li N, Ackerman S, He F, et al. *Streptococcus pneumoniae* secretes hydrogen peroxide leading to DNA damage and apoptosis in lung cells. *Proc Natl Acad Sci U S A*. 2015;112(26):E3421–30.
- 53 Man SM, Karki R, Kanneganti TD. Molecular mechanisms and functions of pyroptosis, inflammatory caspases and inflammasomes in infectious diseases. *Immunol Rev*. 2017 May;277(1):61–75.
- 54 Kelley N, Jeltema D, Duan Y, He Y. The NLRP3 inflammasome: an overview of mechanisms of activation and regulation. *Int J Mol Sci*. 2019 Jul 6;20(13):3328.
- 55 Swanson KV, Deng M, Ting JP-Y. The NLRP3 inflammasome: molecular activation and regulation to therapeutics. *Nat Rev Immunol*. 2019;19(8):477–89.
- 56 Tomlinson G, Chimalapati S, Pollard T, Lapp T, Cohen J, Camberlein E, et al. TLR-mediated inflammatory responses to *Streptococcus pneumoniae* are highly dependent on surface expression of bacterial lipoproteins. *J Immunol*. 2014 Oct 1;193(7):3736–45.
- 57 Schreck R, Rieber P, Baeuerle PA. Reactive oxygen intermediates as apparently widely used messengers in the activation of the NF-kappa B transcription factor and HIV-1. *EMBO J*. 1991 Aug;10(8):2247–58.
- 58 Li Q, Sanlioglu S, Li S, Ritchie T, Oberley L, Engelhardt JF. GPx-1 gene delivery modulates NFκB activation following diverse environmental injuries through a specific subunit of the IKK complex. *Antioxid Redox Signal*. 2001 Jun;3(3):415–32.
- 59 Zhang J, Johnston G, Stebler B, Keller ET. Hydrogen peroxide activates NFκB and the interleukin-6 promoter through NFκB-inducing kinase. *Antioxid Redox Signal*. 2001 Jun;3(3):493–504.

- 60 Shimada K, Crother TR, Karlin J, Dagvadorj J, Chiba N, Chen S, et al. Oxidized mitochondrial DNA activates the NLRP3 inflammasome during apoptosis. *Immunity*. 2012 Mar 23;36(3):401–14.
- 61 Taabazuing CY, Okondo MC, Bachovchin DA. Pyroptosis and apoptosis pathways engage in bidirectional crosstalk in monocytes and macrophages. *Cell Chem Biol*. 2017 Apr 20;24(4):507–e4.
- 62 Monteleone M, Stanley AC, Chen KW, Brown DL, Bezbradica JS, von Pein JB, et al. Interleukin-1 β maturation triggers its relocation to the plasma membrane for gasdermin-D-dependent and -independent secretion. *Cell Rep*. 2018 Aug 7;24(6):1425–33.
- 63 de Vasconcelos NM, Van Opdenbosch N, Van Gorp H, Martín-Pérez R, Zecchin A, Vandenaabeele P, et al. An apoptotic caspase network safeguards cell death induction in pyroptotic macrophages. *Cell Rep*. 2020 Jul 28;32(4):107959.
- 64 Rogers C, Fernandes-Alnemri T, Mayes I, Alnemri D, Cingolani G, Alnemri ES. Cleavage of DFNA5 by caspase-3 during apoptosis mediates progression to secondary necrotic/pyroptotic cell death. *Nat Commun*. 2017 Jan 3;8:14128.
- 65 de Vasconcelos NM, Lamkanfi M. Recent insights on inflammasomes, gasdermin pores, and pyroptosis. *Cold Spring Harb Perspect Biol*. 2020 May 1;12(5):a036392.
- 66 Gutierrez KD, Davis MA, Daniels BP, Olsen TM, Ralli-Jain P, Tait SWG, et al. MLKL activation triggers NLRP3-mediated processing and release of IL-1 β independently of gasdermin-D. *J Immunol*. 2017 Mar 1;198(5):2156–64.
- 67 Zhao L, Lin H, Chen S, Chen S, Cui M, Shi D, et al. Hydrogen peroxide induces programmed necrosis in rat nucleus pulposus cells through the RIP1/RIP3-PARP-AIF pathway. *J Orthop Res*. 2018 Apr;36(4):1269–82.

Supplementary material

Hydrogen peroxide is crucial for NLRP3 inflammasome mediated IL-1 β production and cell death in pneumococcal infections of bronchial epithelial cells

Surabhi Surabhi^a, Lana H. Jachmann^a, Patience Shumba^a, Gerhard Burchhardt^a, Sven Hammerschmidt^a, Nikolai Siemens^a

^a Department of Molecular Genetics and Infection Biology, Interfaculty Institute for Genetics and Functional Genomics, Center for Functional Genomics of Microbes, University of Greifswald, Greifswald, Germany

Short Title: H₂O₂ activates NLRP3 inflammasome

Corresponding Author:

Dr. Nikolai Siemens

Department of Molecular Genetics and Infection Biology

University of Greifswald

Felix-Hausdorff-Str. 8

17487 Greifswald

Germany

phone: +49 (0) 3834 420 57 11

E-mail: nikolai.siemens@uni-greifswald.de

Supplementary Figures

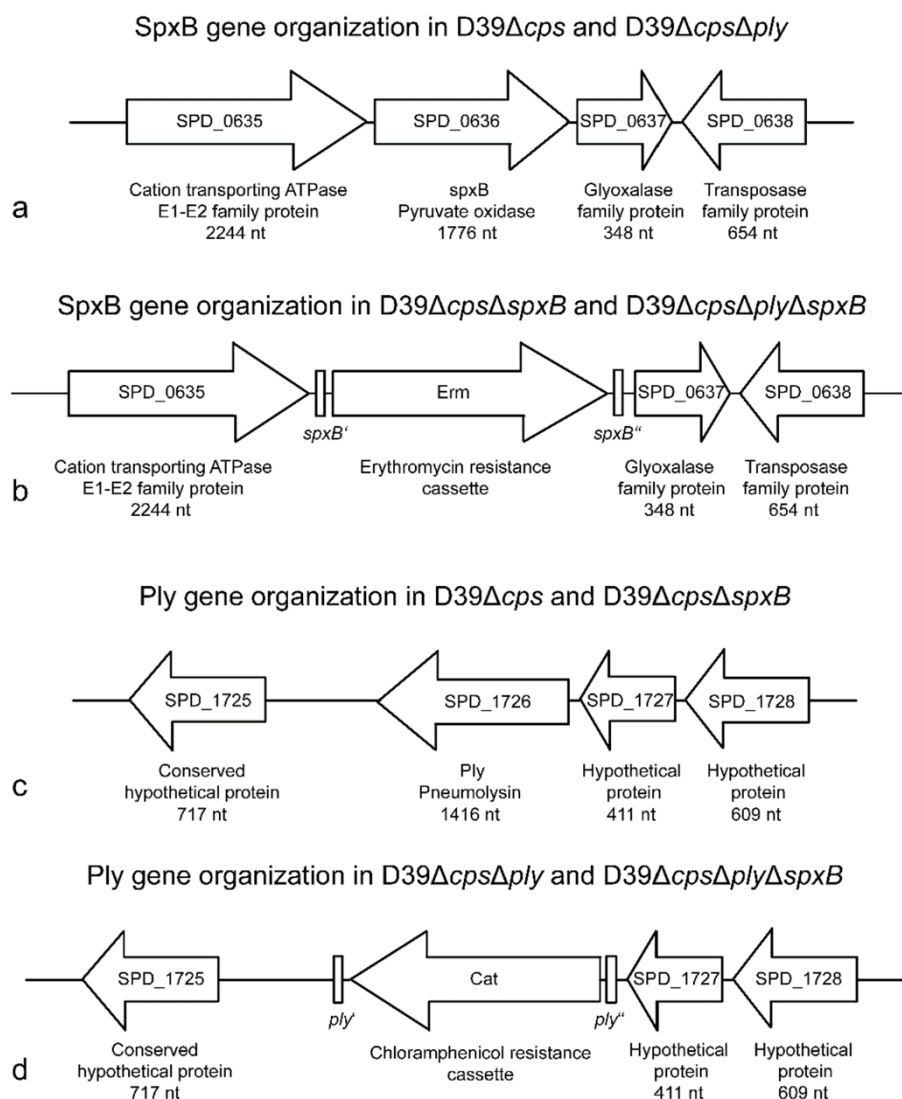


Fig. S1. Gene organization in *S. pneumoniae* *D39Δcps* mutants. Gene organization of *spxB* (*SPD_0636*) in (a) *D39Δcps*, *D39ΔcpsΔply*, (b) *D39ΔcpsΔspxB* and *D39ΔcpsΔplyΔspxB*. Gene organization of *ply* (*SPD_1726*) in (c) *D39Δcps*, *D39ΔcpsΔspxB*, (d) *D39ΔcpsΔply* and *D39ΔcpsΔplyΔspxB*. The gene organization maps were created using KEGG database.

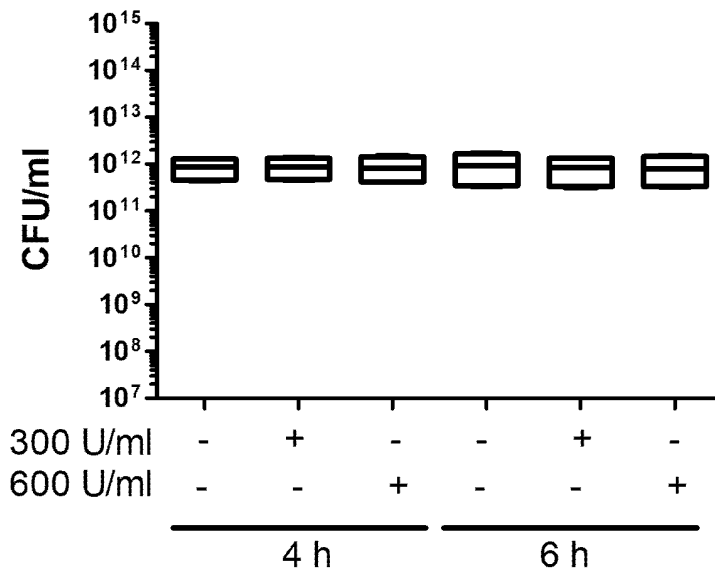


Fig. S2. Catalase has no bactericidal activity. *S. pneumoniae* D39 Δ *cps* was incubated with 300 and 600 U/ml catalase at 37°C. After 4 and 6 h (equivalent to the infection time in Fig. 1) of incubation, bacterial counts were determined by serial dilution. The data are displayed as box plots.

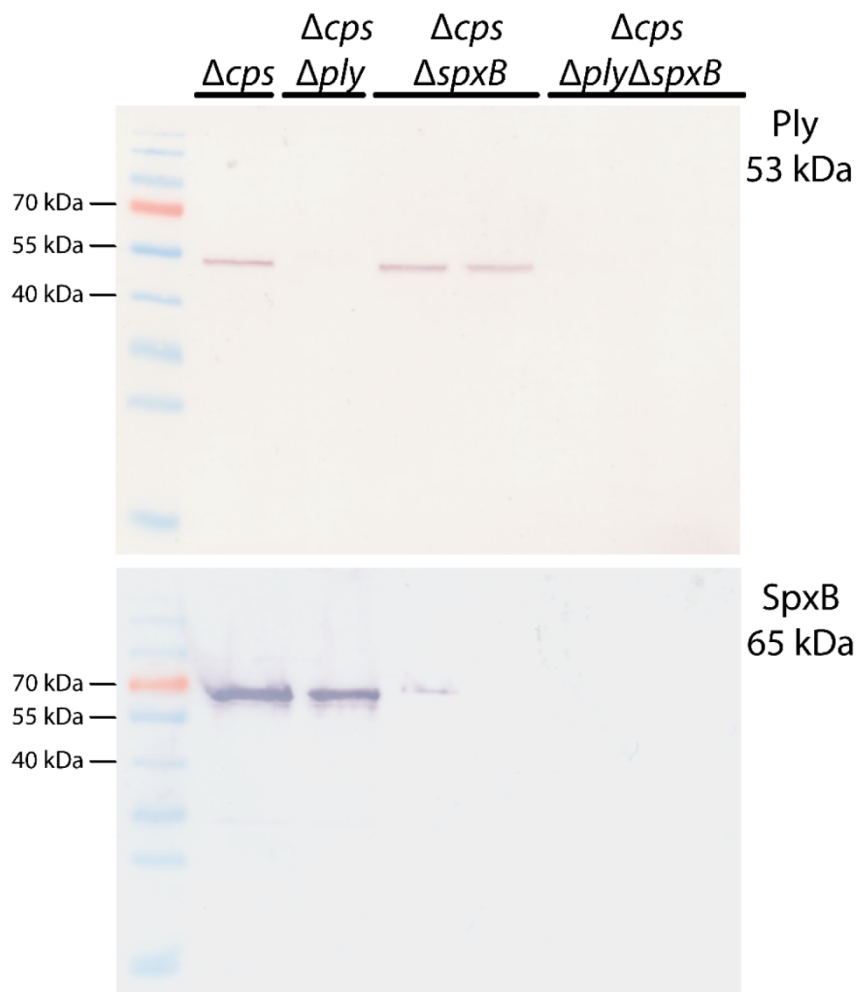


Fig. S3. Ply and SpxB Immunoblots. Bacterial lysates of D39 Δcps and the isogenic mutants were analysed for the production of Ply and SpxB protein by performing immunoblot. Bacterial lysates were separated using a 12% SDS gel and blotted onto a PVDF membrane. The membrane was blocked with 5% (v/v) skim milk prior to primary antibody incubations. 1:1000 dilution of mice anti-sera against Ply and SpxB were used. Anti-mice IgG Alkaline phosphatase-linked Antibody was used as a secondary antibody.

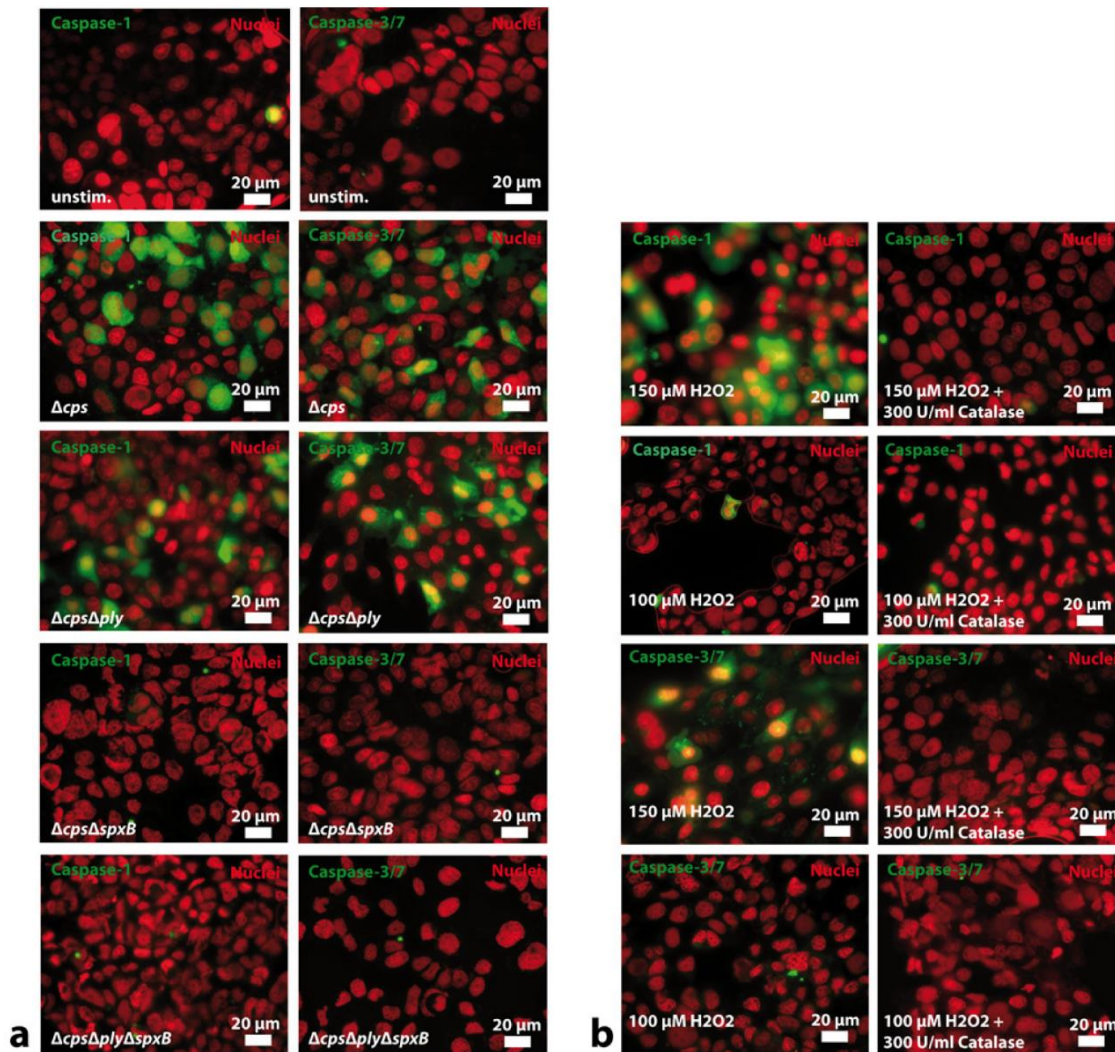


Fig. S4. H_2O_2 and *S. pneumoniae* strains with functional SpxB activate caspase-1 and caspase-3/7 in 16HBE cells. LPS-primed 16HBE cells were infected with D39 Δcps and the isogenic mutants at MOI 50 (a), or stimulated with 150 μM and 100 μM H_2O_2 in the presence or absence catalase (b) for 4 h and caspase-1 and caspase 3/7 activation was assessed. The cells were stained using fluorescent inhibitor probe FAM-YVAD-FMK and FAM-DEVD-FMK to microscopically visualize active caspase-1 and caspase-3/7, respectively. Nuclear-ID stain was used to visualize cell nuclei. Representative images of four independent experiments are shown.

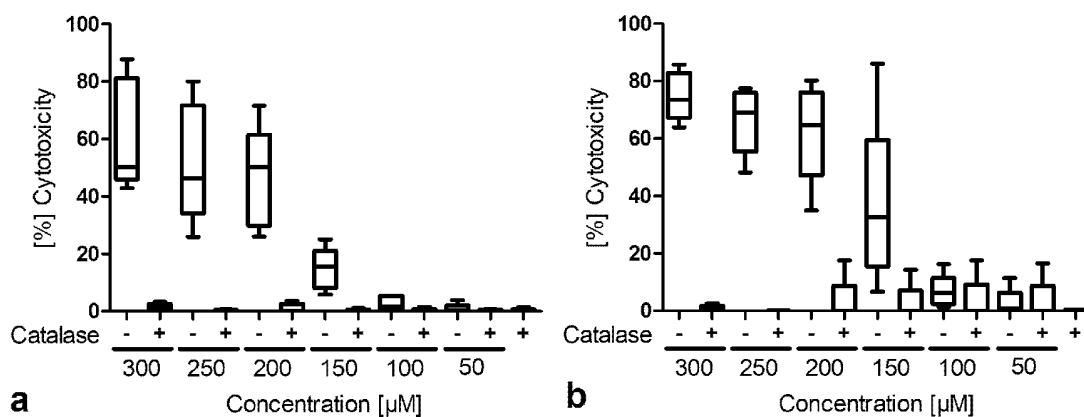


Fig. S5. Hydrogen peroxide kills 16HBE cells. Unprimed human bronchial epithelial cells were stimulated with various concentrations of H₂O₂ in the presence or absence of catalase for 4 h (a) and 6 h (b). Cytotoxicity was evaluated at the indicated time points. The data are displayed as box plots (n=5).

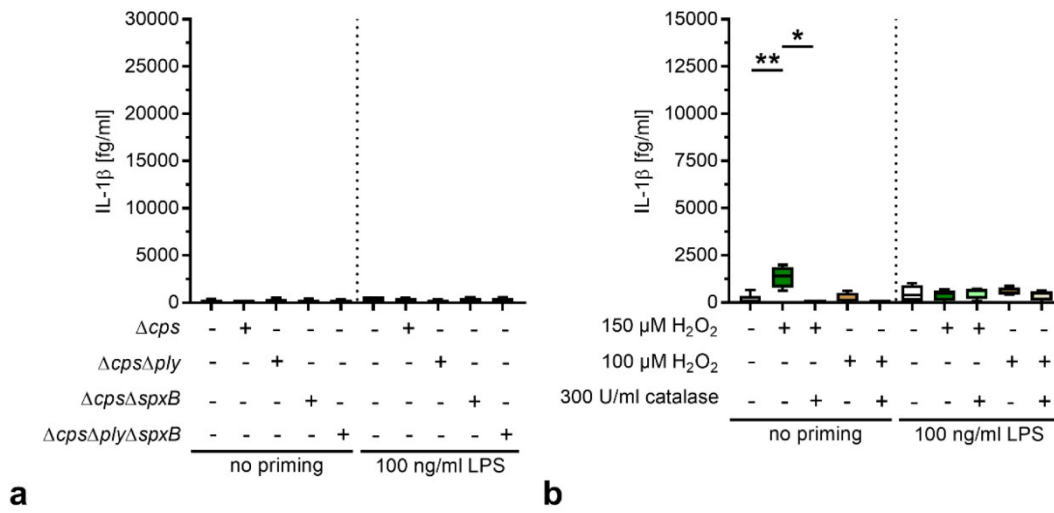


Fig. S6. IL-1 β release after 4 h of bacterial infection or H₂O₂ stimulation. Unprimed or LPS-primed human bronchial epithelial cells were infected with D39 Δcps and the isogenic mutants at MOI 50 (a), or stimulated with 150 μM and 100 μM H₂O₂ in the presence or absence of catalase (b). IL-1 β release was evaluated at 4 h post infection or stimulation. The data are displayed as box plots. The level of significance was determined using Kruskal Wallis test with Dunn's post-test ($n \geq 4$; *, $p < 0.05$; **, $p < 0.01$; ***, $p < 0.001$).

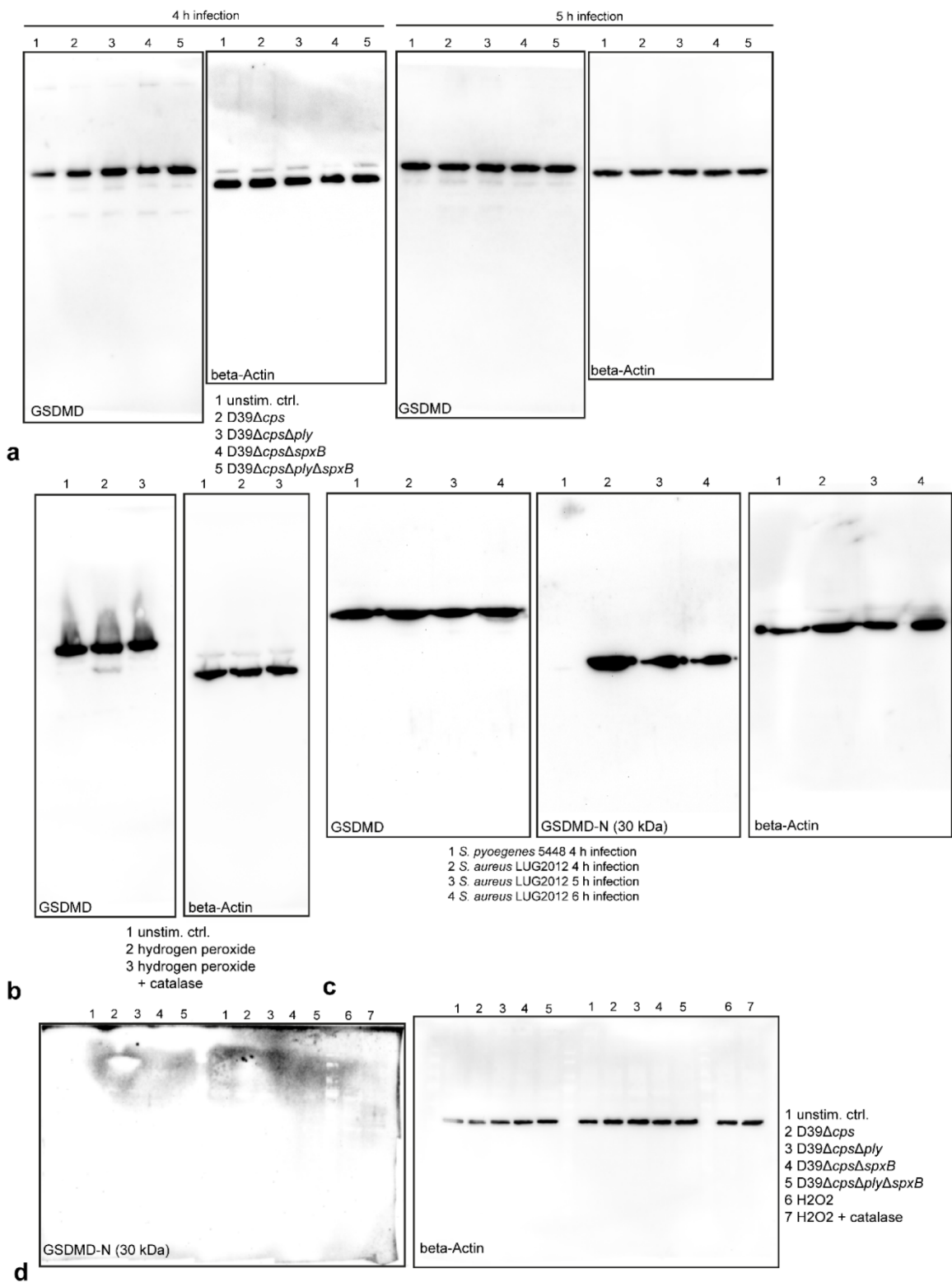


Fig. S7. Original Western blots of blots displayed in Figure 6. (a) Analyses of bacterial (D39Δcps and mutants) infections. (b) Analysis of hydrogen peroxide stimulations. (c) Analyses of bacterial (*S. pyogenes* and *Staphylococcus aureus*) infections. (d) Specific GSDMD-N analysis in pneumococcal infections (lanes 1-5 left: 4 h infections; lanes 1-5 right: 5 h infections; lanes 6-7: 4 h H₂O₂ stimulations).

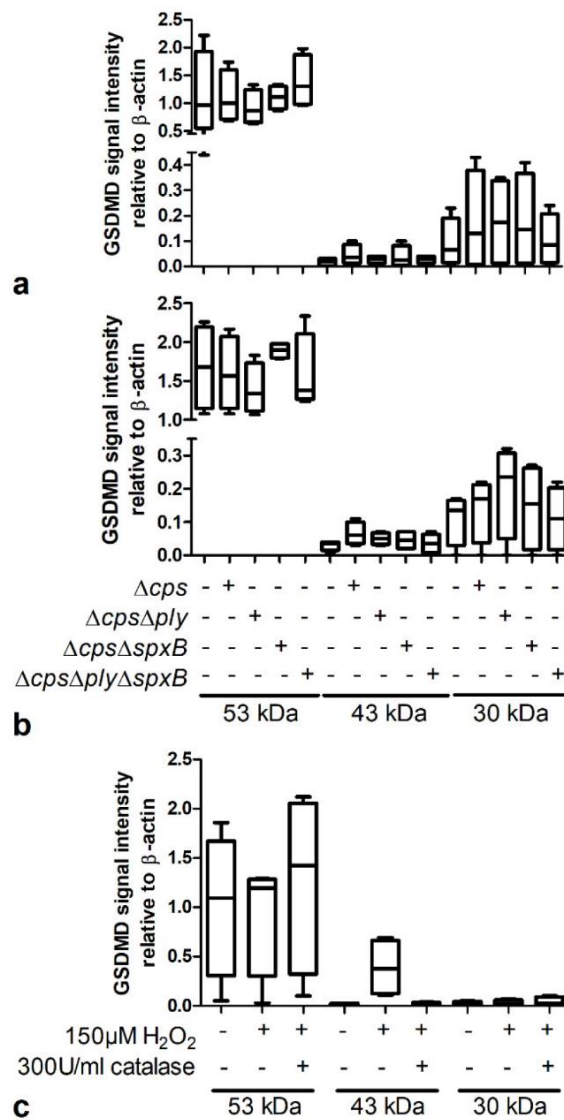


Fig. S8. Quantification of Gasdermin D Western blots as displayed in Figure 6e-f and Figure S7. Quantification of Gasdermin D blots after (a) 4 h and (b) 5 h of bacterial (D39 Δcps and mutants) infections. (c) Quantification of Gasdermin D blots post hydrogen peroxide stimulations.

PAPER 3**Bronchial Epithelial Cells Accumulate Citrate Intracellularly in Response to Pneumococcal Hydrogen Peroxide**

Surabhi Surabhi, Lana H. Jachmanna, Sven Hammerschmidt, Michael Lalk,
Karen Methling, Nikolai Siemens

Submitted in ACS Infectious Diseases, on 2021, July 12

Author contributions:

As first author in this publication, **SS** significantly contributed with the conception, execution and analysis of all the experiments performed in this study. Additionally, **SS** prepared the manuscript draft, participated in the construction of the figures and was involved in the scientific revision and editing of the final version of this manuscript.

Conception and design: **SS**, **KM** and **NS**

Experimental work: **SS**, **LJ**, and **KM**

Collection and analysis of the data: **SS**, **LJ**, **KM** and **NS**

Manuscript draft preparation: **SS**, **KM** and **NS**

Critical revision and editing of the manuscript: **SS**, **LJ**, **SH**, **ML**, **KM**, and **NS**

Surabhi Surabhi

Prof. Dr. Nikolai Siemens



From : ACS Infectious Diseases <onbehalf@manuscriptcentral.com>
Subject : Siemens, Nikolai id-2021-00372e - Manuscript Submission to ACS Infectious Diseases 12-Jul-2021
Date : 12-07-2021 14:16
To : <nikolai.siemens@uni-greifswald.de>;
CC : <surabhi.surabhi@uni-greifswald.de>; <ana.jachmann@gmx.de>; <lalk@uni-greifswald.de>;
<sven.hammerschmidt@uni-greifswald.de>; <methling@uni-greifswald.de>; <nikolai.siemens@uni-greifswald.de>;

Click [here](#) if you think this message is spam.

12-Jul-2021

Journal: ACS Infectious Diseases
Manuscript ID: id-2021-00372e
Title: "Bronchial epithelial cells accumulate citrate intracellularly in response to pneumococcal hydrogen peroxide"
Authors: Surabhi, Surabhi; Jachmann, Lana; Lalk, Michael; Hammerschmidt, Sven; Methling, Karen; Siemens, Nikolai
Manuscript Status: Submitted

Dear Dr. Siemens:

Your manuscript has been successfully submitted to ACS Infectious Diseases.

Please reference the above manuscript ID in all future correspondence. If there are any changes in your contact information, please log in to ACS Paragon Plus with your ACS ID at <http://paragonplus.acs.org/login> and select "Edit Your Profile" to update that information.

You can view the status of your manuscript by checking your "Authoring Activity" tab on ACS Paragon Plus after logging in to <http://paragonplus.acs.org/login>.

Journal Publishing Agreement and Copyright

Upon acceptance, ACS Publications will require the corresponding author to sign and submit a Journal Publishing Agreement. This agreement gives authors a number of rights regarding the use of their manuscripts. At acceptance, the corresponding author will receive an email linking through to the Journal Publishing Agreement Wizard, which helps you select the most appropriate license for your manuscript.

For more information please see: https://pubs.acs.org/page/copyright/journals/jpa_faqs.html

ACS Authoring Services

Did you know that ACS provides authoring services to help scientists prepare their manuscripts and communicate their research more effectively? Trained chemists with field-specific expertise are available to edit your manuscript for grammar, spelling, and other language errors, and our figure services can help you increase the visual impact of your research.

Visit <https://authoringservices.acs.org> to see how we can help you! Please note that the use of these services does not guarantee that your manuscript will be accepted for publication.

Thank you for submitting your manuscript to ACS Infectious Diseases.

Sincerely,

ACS Infectious Diseases

PLEASE NOTE: This email message, including any attachments, contains confidential information related to peer review and is intended solely for the personal use of the recipient(s) named above. No part of this communication or any related attachments may be shared with or disclosed to any third party or organization without the explicit prior written consent of the journal Editor and ACS. If the reader of this message is not the intended recipient or is not responsible for delivering it to the intended recipient, you have received this communication in error. Please notify the sender immediately by e-mail, and delete the original message.

As an author or reviewer for ACS Publications, we may send you communications about related journals, topics or products and services from the American Chemical Society. Please email us at Pubupdates@acs.org if you do not want to receive these. Note, you will still receive updates about your manuscripts, reviews, or future invitations to review.

Thank you.

Letter

Bronchial epithelial cells accumulate citrate intracellularly in response to pneumococcal hydrogen peroxide

Surabhi Surabhi, Lana H. Jachmann, Michael Lalk, Sven Hammerschmidt, Karen Methling,
Nikolai Siemens

ABSTRACT: Community-acquired pneumonia is an infection of the lower respiratory tract caused by various viral and bacterial pathogens, including influenza A virus (IAV), *Streptococcus pneumoniae*, and *Staphylococcus aureus*. To understand the disease pathology, it is important to delineate host metabolic responses to an infection. In this study, metabolome profiling of mono- and co-infected human bronchial epithelial cells was performed. We show that IAV and *S. aureus* silently survive within the cells with almost negligible effects on the host metabolome. In contrast, *S. pneumoniae* significantly altered various host pathways such as glycolysis, tricarboxylic acid cycle, and amino acid metabolism. Intracellular citrate accumulation was the most prominent signature of pneumococcal infections and was directly attributed to the action of pneumococci-derived hydrogen peroxide. No co-infection specific metabolome signatures were observed.

Keywords: metabolism, citrate, infection, *Streptococcus pneumoniae*, *Staphylococcus aureus*, influenza A virus

Community-acquired pneumonia (CAP) is a common disease of the lungs in individuals without recent hospitalization. The annual incidence rate ranges from five to eleven cases per 1,000 populations in Europe and North America.¹ *Streptococcus pneumoniae* (pneumococcus) and *Staphylococcus aureus* remain the most commonly identified Gram-positive bacterial causes of CAP.² During seasonal influenza outbreaks, the circulating influenza viruses, including influenza A virus (IAV), become prevalent in CAP. The acquisition of IAV often results in secondary bacterial infections contributing to severe additional complications.²

Several omics technologies contributed fundamentally to the understanding of host responses in respiratory infections. Many studies analyzed host transcriptome or proteome profiles.³⁻⁴ To unravel the dynamic nature of host pathogen interactions, it is crucial to understand host cellular metabolome because it directly influences its phenotype.⁵ Metabolic pathways provide energy sources, which are utilized by e.g., lung epithelial cells for specialized functions such as surfactant production and ciliary beating. Therefore, the active cellular metabolome does not only plays a role in maintaining cellular health but is also indirectly implied in mucociliary pathogen clearance.⁶ Lung epithelial cells are amongst the first cells to encounter a pathogen and recent studies have linked their metabolic dysfunction to the pathobiology of respiratory diseases.⁷

Energy metabolism in a cell is a prerequisite for self-preservation. Carbon sources (e.g., glucose) are catabolized in three successive processes, glycolysis, tricarboxylic acid cycle (TCA cycle), and oxidative phosphorylation to produce ATP. The TCA cycle acts as an epicenter for both anabolic and catabolic pathways. For instance, metabolites of the TCA cycle such as citrate are involved in *de novo* nucleotide and lipid synthesis. Meanwhile, amino and fatty acids are catabolized and feed into the TCA cycle.⁸ To understand the influence of respiratory bacterial mono and bacterial-viral co-infections on glycolysis, TCA cycle, and

amino acid production, a cell culture based system of human bronchial epithelial (16HBE) cells was used.

All mono and co-infections were conducted as depicted in Figure 1A. First, H1N1 replication in 16HBE cells was confirmed. Irrespective of the infectious dose, equal levels of nucleoprotein (NP) mRNA expression were detected 24 h after infection (Figure 1B). Based on these results, a multiplicity of infection (MOI) of 0.1 was used for all subsequent experiments.

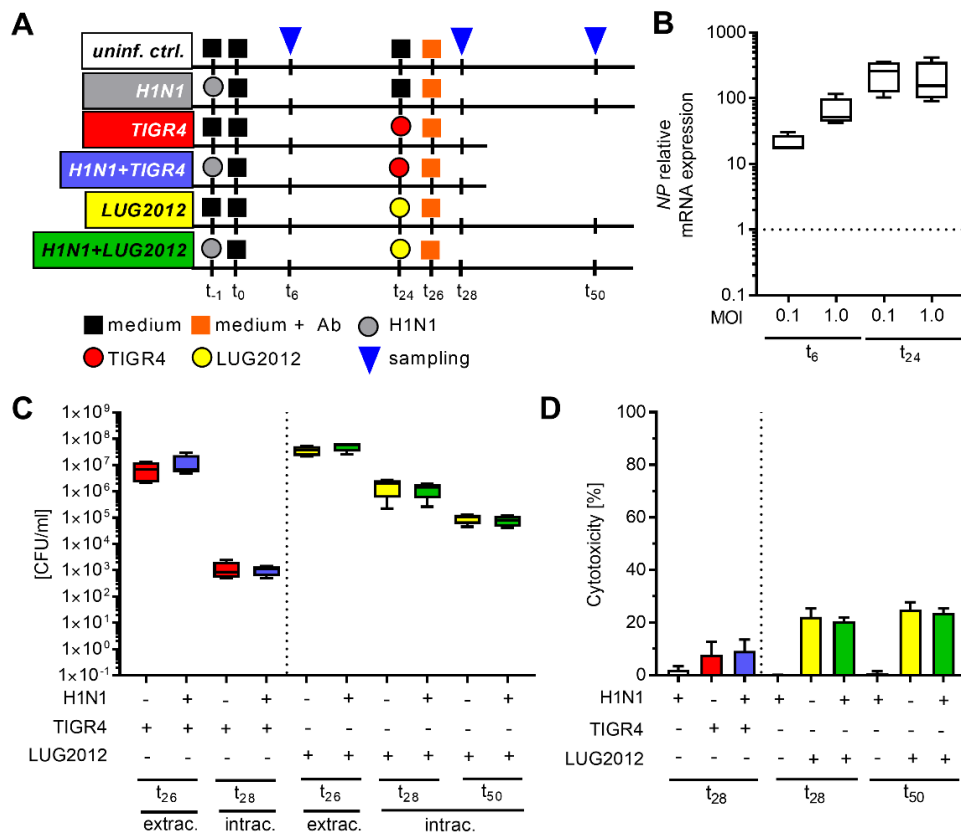


Figure 1. Pneumococcal, staphylococcal, and IAV single and co-infections of 16HBE cells. (A) Schematic illustration of single pneumococcal (TIGR4), staphylococcal (LUG2012), IAV (H1N1) as well as co-infections. (B) Validation of viral replication in 16HBE cells at indicated time points post infection. (C) Counts of adherent (extrac.) and intracellular (intrac.) bacteria at indicated time points post infection. The data are displayed as box-and-whiskers plots of four independent experiments (n=4). (D) Cytotoxicity towards 16HBE cells after indicated time points of infection. Bars represent the mean values ±SD from four independent experiments (n=4). Abbreviations: antibiotics (Ab); multiplicity of infection (MOI); colony forming units (CFU).

Next, pneumococcal (TIGR4) and staphylococcal (LUG2012) infections of uninfected or H1N1-infected 16HBE cells were performed and infectivity, as well as cytotoxicity were

assessed. Irrespective of the prior H1N1 infection, approximately equal numbers of adherent bacteria were recovered from 16HBE-cells (Figure 1C). Contrary to pneumococci, which are considered an extracellular pathogen, staphylococci can reside within the cells for a longer period without killing them. Assessment of intracellular bacteria revealed that almost negligible numbers of TIGR4 were located intracellularly (Figure 1C). In contrast, high numbers of LUG2012 were recovered from the intracellular compartment, even over a longer period of time (t_{28} - t_{50} ; Figure 1C). Again, no differences in bacterial counts between single bacterial and co-infected cells were measured. Analyses of the cell viability showed that H1N1, when used with a MOI 0,1, alone did not harm the cells. In contrast, bacterial infections resulted in a moderate cytotoxicity (Figure 1D).

Next, intracellular metabolites of glycolysis, TCA cycle, and amino acids of single and co-infected cells were determined. In general, no specific co-infection signatures were observed. The majority of changes in metabolite concentrations were exclusively mediated by single or subsequent pneumococcal infections and independent of a previous H1N1 infection (Figures 2-3 and S1-S3). H1N1 and LUG2012 infections had no or minor impact on intracellular metabolite composition, respectively (Figures 2-3 and S1-S3). In congruence with elevated *SLC2A* (glucose transport family) mRNA expression at t_{28} , glucose consumption increased in all infections (Figures 2A-B, Figures S1A-B). At t_{28} , levels of intracellular glucose-6-phosphate, fructose-6-phosphate, dihydroxyacetone phosphate, and fructose were significantly higher in cells infected with TIGR4 (Figure 2, Figure S1). In contrast, levels of other glycolysis metabolites such as 3-phosphoglycerate, 2-phosphoglycerate, and phosphoenolpyruvate as well as relative mRNA expression of genes encoding for glycolytic enzymes remained unaffected (Figure 2, Figure S1, Table S1).

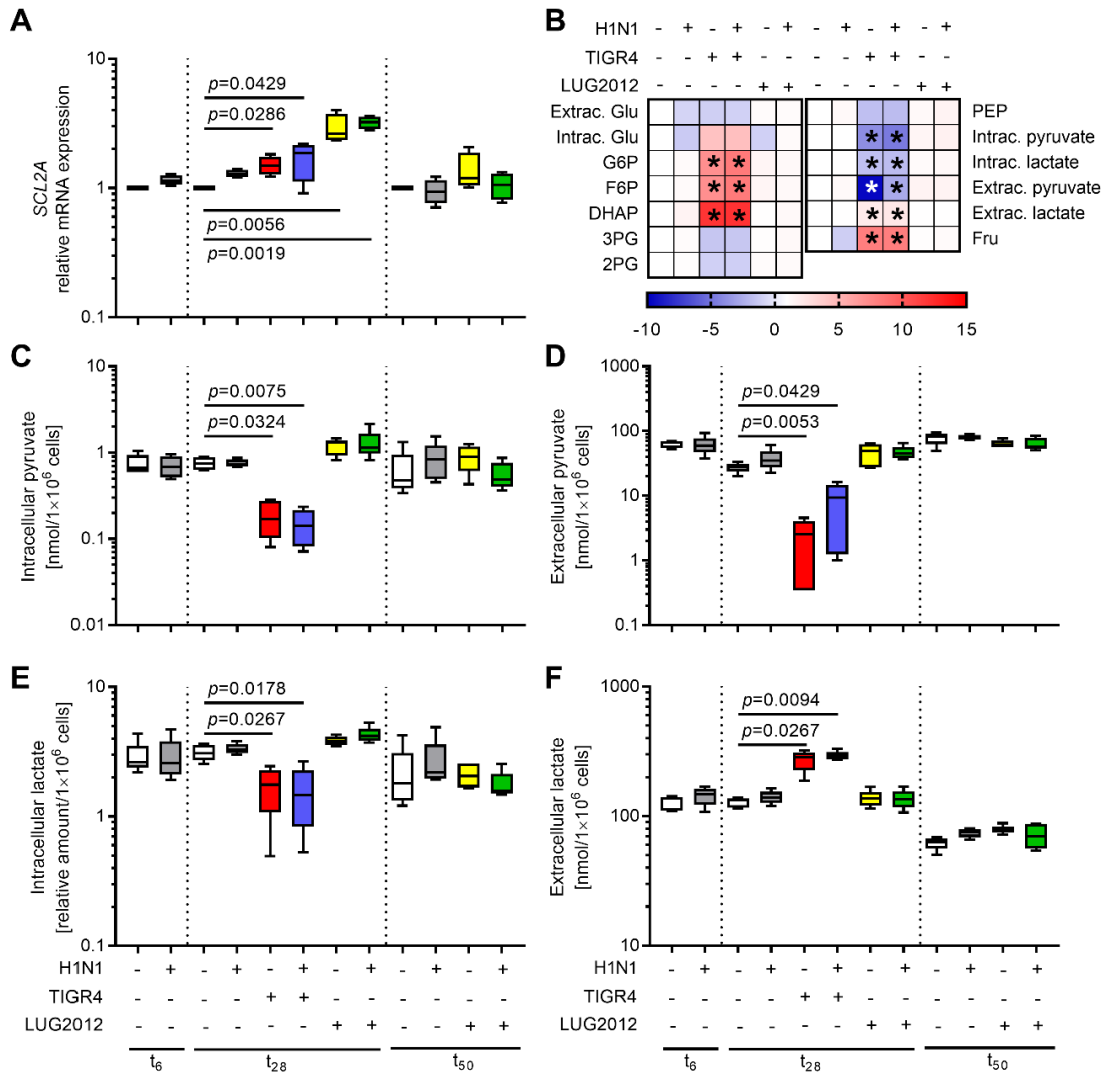


Figure 2. Profile of intermediate glycolysis metabolites in response to different infections. (A) Relative *SCL2A* (glucose transporter) mRNA expression at indicated time points post infection. (B) Heat map depicting fold changes of glycolysis metabolites in response to infections as compared to the uninfected control (t_{28}). Asterisks indicate significant changes between the infected cells and the corresponding uninfected control ($p < 0.05$). Intracellular and extracellular concentrations of (C-D) pyruvate and (E-F) lactate. The data are displayed as box-and-whiskers of five independent experiments ($n=5$). The level of significance between the groups was determined using Kruskal Wallis test with Dunn's post-test.

Next, the end products of host cell glycolysis were determined. Pyruvate can be either converted to lactate or fueled into the TCA cycle via acetyl-CoA, among others. In most infections, intra- as well as extracellular pyruvate and lactate concentration remained at a level similar to the uninfected control of the respective time point (Figure 2C-F). However, a significant decrease in both intra- and extracellular pyruvate was detected in pneumococci

single and co-infected 16HBE-cells (Fig 2C-D). In contrast, intracellular lactate levels dropped while extracellular amounts increased (Figure 2F). In summary, *S. aureus* and H1N1 infections had no significant impact on glycolysis, whereas pneumococci substantially altered several steps of the pathway (Figure 2B). It is important to note that pneumococci are lactate producing bacteria and thus, extracellular lactate is probably not only produced by 16HBE cells.

To investigate whether pyruvate potentially entered the TCA cycle, intermediates of this cycle were analyzed. Irrespective of the infection time, intracellular concentrations of TCA cycle intermediates did not change for viral and *S. aureus* infections (Figure 3). In contrast, cells infected with pneumococci showed a significant increase in intracellular concentrations of citrate and a moderate increase of aconitate in H1N1-pneumococcal co-infection (Figure 3A-B). However, levels of other TCA cycle metabolites decreased in response to all pneumococcal infections (Figure 3C-G). Again, no major changes in transcription of genes encoding for TCA cycle enzymes were determined (Table S1).

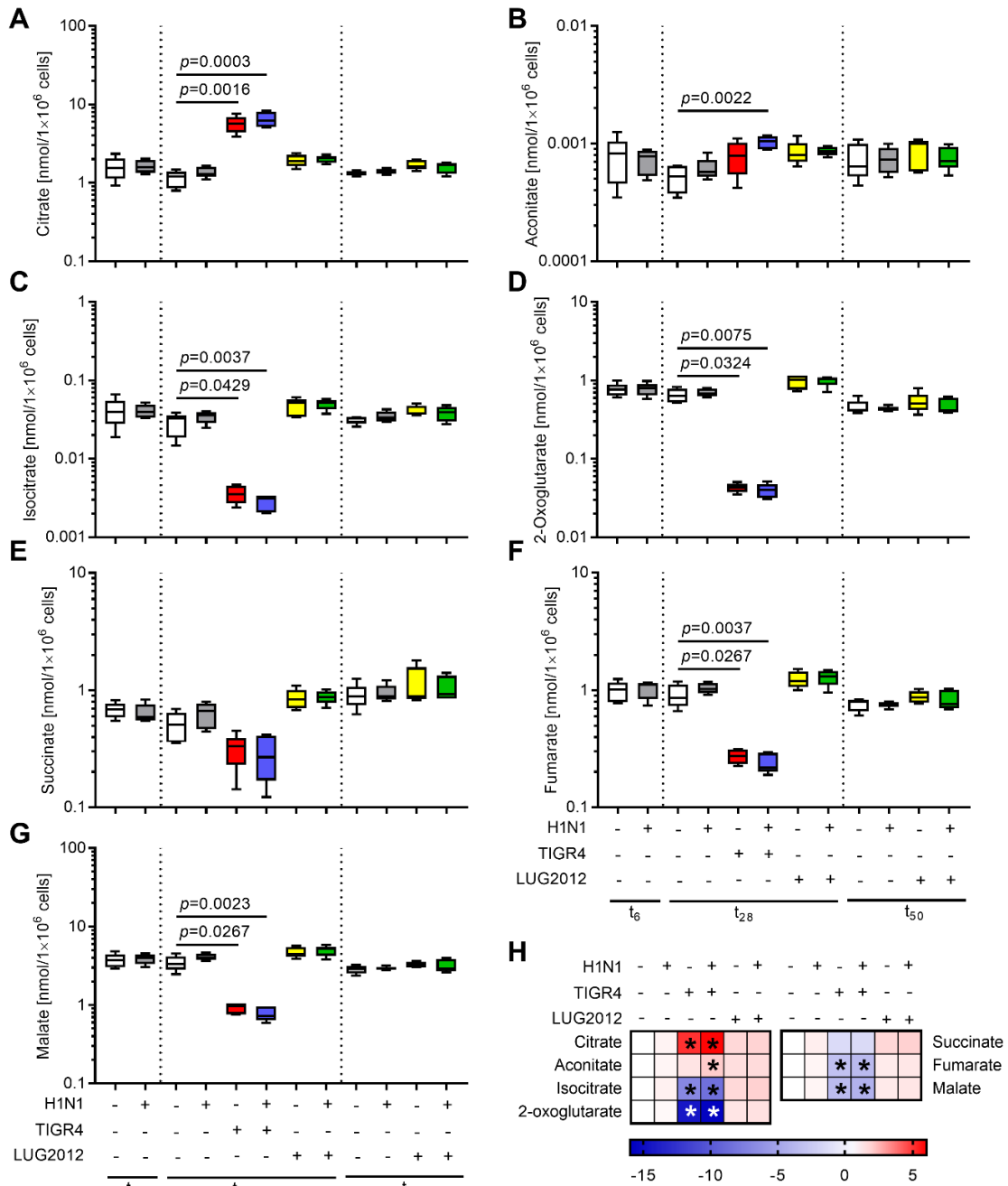


Figure 3. Intracellular profile of TCA-cycle intermediates in response to different infections. Intracellular concentration of (A) citrate, (B) aconitate, (C) isocitrate, (D) 2-oxoglutarate, (E) succinate, (F) fumarate, and (G) malate are shown. The data are displayed as box-and-whiskers of five independent experiments (n=5). The level of significance between the groups was determined using Kruskal Wallis test with Dunn's post-test. (H) Heat map summarizing fold changes of TCA cycle metabolites in response to infections as compared to the uninfected control (t₂₈). Asterisks indicate significant changes between the infected cells and the corresponding uninfected control ($p < 0.05$).

As a part of protein catabolism, amino acids are deaminated and fed into the TCA cycle. Therefore, changes in the intracellular profile of amino acids and their corresponding keto acids were monitored (Figures S2-S3). All infections involving pneumococci induced a significant decrease in the intracellular levels of glucogenic amino acids such as glycine, proline, threonine and asparagine (Figure S2). In contrast, ketogenic amino acid lysine and non-proteinogenic amino acid ornithine showed higher intracellular abundance in all pneumococcal infection (Figure S2). Cells also use glutamine as an energy source via glutaminolysis, wherein glutamine is converted to glutamate through a deamination reaction catalyzed by glutaminase. Glutamate is converted to the TCA cycle intermediate α -ketoglutarate by glutamate dehydrogenase.⁹ At t_{28} , higher intracellular concentrations of glutamine and lower intracellular levels of glutamate were characteristic for all *S. aureus* infections. Both values normalized to that of the uninfected control at t_{50} (Figure S2).

All analyses show that IAV and *S. aureus* infections are more of silent nature with a very limited impact on host metabolome. In viral infections, virus multiplication and viral protein production are accompanied by a phenomenon that is termed "host shutoff".¹⁰ This shutoff is regulated at both, transcriptional¹¹ and translational levels.¹² In contrast to bacteria, viruses solely rely on host resources for multiplication. Transcriptome studies showed that host pathways that are pivotal for IAV survival such as oxidative phosphorylation are less affected during IAV infections.¹³ However, it has also been shown that cells infected with IAV increase glucose uptake and upregulate glycolysis.¹⁴ The incongruence with these studies might be explained by the mild infectivity of the used H1N1.

Pneumococci are mainly extracellular pathogens, whereas staphylococci can internalize and persist within the cells for a prolonged period of time.¹⁵ To adapt to the intracellular environment, *S. aureus* adjusts its regulatory network accordingly.¹⁶ Metabolic analyses of A549 cells infected with high inoculum of *S. aureus* have shown significant changes in nutrient uptake, energy metabolism, nucleotide and amino acid metabolic pathways, especially

beyond 6 h of infection. In contrast, we observed only minor changes in the host metabolome most likely due to the cell specific responses to low inoculum infections.

A hallmark of pneumococcal infections was intracellular citrate accumulation. Citrate is a key substrate in cellular energy metabolism and is produced within mitochondria. It gets exported to the cytoplasm via mitochondrial citrate carrier, CIC, encoded by the *SLC25A1* gene.¹⁷ In the cytosol, citrate is converted to acetyl-CoA and oxaloacetate, which are incorporated into fatty acid and nucleotide synthesis, respectively. Therefore, *SLC25A* expression was analyzed (Table S1). No major changes were detected in *SLC25A* transcription compared to the uninfected control and in general, genes encoding for TCA cycle enzymes were mostly not affected (Table S1). Although it is speculative, most likely pneumococcal factors inhibit either aconitase or CIC at the protein level, which results in accumulation of citrate. Consequently, stored citrate potentially blocks the entire TCA cycle. It was demonstrated that *Bacillus subtilis* protein CcpC represses aconitase and citrate synthase transcription and such orthologs were also found in pneumococci.¹⁸⁻¹⁹ Whether these orthologs are able to repress host pathways is not yet clear. However, pneumococci produce hydrogen peroxide (H_2O_2) via carbohydrate-metabolizing enzyme pyruvate oxidase SpxB.²⁰ Iron-sulfur cluster containing enzymes such as aconitase are highly susceptible to inactivation by reactive oxygen species.²¹⁻²³ Aconitase is irreversibly inactivated by H_2O_2 , which results in citrate accumulation.²³ To determine the impact of pneumococcal H_2O_2 on intracellular citrate accumulation, TIGR4 Δ *spxB* mutant was generated. The mutant was verified via immunoblots targeting SpxB protein (Figure 4A). (Surabhi et al., 2021) *SpxB*-deficient mutant produced significantly lower amounts of H_2O_2 as compared to the wild-type strain (Figure 4B). To quantify intracellular citrate accumulation, 16HBE cells were infected with TIGR4 or its isogenic mutant lacking *spxB* following the protocol as depicted in Figure 1A. Furthermore, wild-type infections were carried out in the presence of catalase and direct stimulations with H_2O_2 , in the presence or absence of catalase were performed. Cytotoxicity towards cells (Figure 4C) as well as intracellular citrate concentrations (Figure 4D) were assessed. While 4 h of infection/stimulations remained

almost non-toxic to the cells, a significant increase in intracellular citrate was observed for TIGR4 wild-type infections and H₂O₂ stimulations. The intracellular citrate concentrations significantly diminished in infections/stimulations supplemented with catalase and remained unchanged for infections with TIGR4 Δ *spxB*.

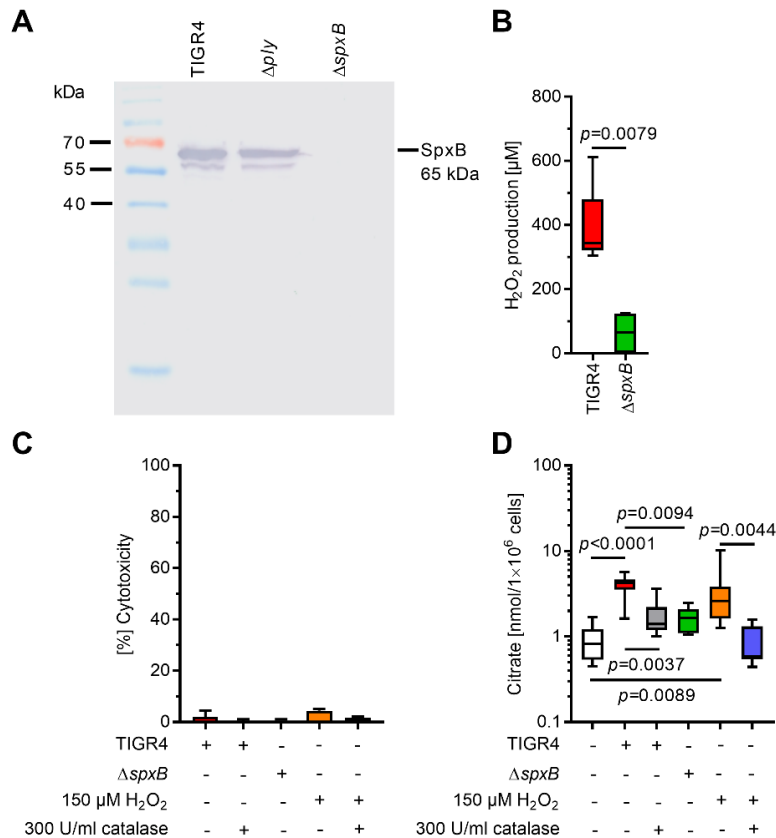


Figure 4. Hydrogen peroxide produced by pneumococci is responsible for intracellular citrate accumulation in infected cells. (A) TIGR4 Δ *spxB* mutant was verified via immunoblots targeting SpxB protein, (B) H₂O₂ production by pneumococci was quantified by colorimetric analysis of bacterial culture supernatants (n=4). 16HBE cells were infected with pneumococcal strains or stimulated with H₂O₂ in the presence or absence of catalase. Cytotoxicity towards the cells (C) and intracellular citrate concentrations (D) were assessed (n \geq 5). The data in (D) are displayed as box plots. Bars in (C) denote mean values \pm SD. The level of significance was determined using Kruskal Wallis test with Dunn's post-test.

These results clearly indicate that the intracellular citrate accumulation can be attributed to the action of pneumococcal H₂O₂. Endogenously generated H₂O₂ has been linked to oxidative damage.²⁰ Furthermore, it was shown that *Salmonella typhimurium* infections activate the NLRP3 inflammasome via excessive citrate accumulation through promoting the formation of

mitochondrial ROS.²⁴ In line with this, we recently demonstrated that pneumococci-derived H₂O₂ activates NLRP3 inflammasome and induces apoptosis in 16HBE cells (Surabhi et al., 2021). Host citrate can also be diverted towards itaconate production, an antibacterial compound, which is derived from decarboxylation of cis-aconitate. Itaconate inhibits isocitrate lyase, an enzyme in the glyoxylate shunt that is beneficial for bacterial survival during an infection.²⁵ Itaconate is produced in response to bacterial pathogens such as *Mycobacterium tuberculosis*.²⁶ However, itaconate was not detected in any of experimental conditions of this study.

In conclusion, we show that each respiratory pathogen has its own specific way of interaction with host metabolome. IAV and *S. aureus* rather use the host resources for survival and multiplication. Pneumococci significantly altered various host metabolome pathways. TCA cycle inhibition and citrate accumulation in response to H₂O₂ were the most prominent signatures of pneumococcal infections. However, host metabolic programming may differ in respect to different strains within one species and *in vitro* versus *in vivo* infections. Therefore, further studies are warranted to determine the role of citrate in pneumococcal infections .

METHODS

Bacterial and Viral Strains and Cell Culture Conditions. Influenza A virus A/Bayern/74/2009 (H1N1) was a gift from the Federal Research Institute for Animal Health (FLI, Riems, Germany).

S. pneumoniae strain TIGR4 and the isogenic mutant TIGR4 Δ *spxB* were grown on blood agar plates (Oxoid) and cultured to exponential growth phase (OD₆₀₀ 0.35-0.4) in Todd-Hewitt broth supplemented with 0.5% (w/v) yeast extract (Roth). TIGR4 Δ *spxB* mutant was generated following the protocol as previously described (Surabhi et al., 2021). Detailed protocols can be found within the Supporting Information. *S. aureus* strain LUG2012 was cultured overnight at 37°C in casein hydrolysate and yeast extract medium.²⁷

Bronchial epithelial 16HBE14o-cells (16HBE) were cultured in minimum essential medium (MEM; Gibco) supplemented with 10% (v/v) fetal bovine serum (Life Technologies), 2 mM L-glutamine (Invitrogen), 10 mM HEPES, and 1% (v/v) Minimal Essential Amino Acids (both GE Healthcare) in fibronectin coated flasks (Corning) at 37°C and 5% CO₂ atmosphere.

16HBE Cell Infections and stimulations. 16HBE single and co-infections were conducted as depicted in Figure 1A. Briefly, all infections were performed in MEM. Co-infections: 80% confluent T75 flasks were infected with H1N1 in 4 ml MEM media supplemented with 0.3% [w/v] BSA and 1 µg/ml TPCK at a MOI of 0.1 for 1 h (t₁). At t₀, the infectious media was removed, cells were washed with PBS and fresh MEM was added for 24 h (t₂₄). To ensure comparable bacterial infection rates, H1N1-infected cells were washed with PBS and infected with TIGR4 at MOI of 50 or with LUG2012 at MOI of 10 for 2 h (t₂₆). Next, the media was removed, cells were washed, and extracellular bacteria were killed by addition of MEM containing antibiotics (TIGR4: 200 µg/ml Gentamycin, 100 U/ml Penicillin G; LUG2012: 550 µg/ml Gentamicin, 280 U/ml Penicillin G, 5 U/ml Lysostaphin (all Sigma Aldrich)). The cells were treated with antibiotics for 2 h (TIGR4, LUG2012) or 24 h (LUG2012). In case of

single H1N1 or single bacterial infections and uninfected controls, the respective infectious media were replaced by MEM (t_{-1} , t_0 , t_{24}) or MEM containing antibiotics (t_{26}).

Sampling of 16HBE Cells and Extraction of Metabolites for GC-MS Analysis. At t_6 , t_{28} , and t_{50} , cells were harvested according to a protocol described previously with a minor modification.²⁸ Briefly, the supernatants were collected and stored at -80°C . Cell culture flask was washed four times with ice-cold NaCl solution (135 mmol/l). 10 ml ice cold methanol were added to the flask and cells were collected. Flask was washed with 10 ml ice cold double distilled water and transferred into the same tube. Samples were shock frozen in liquid nitrogen and stored until extraction at -80°C .

Samples were processed as described previously with minor modifications.²⁸ In brief, 2 ml ice cold chloroform and internal standards were added to the thawed samples. The samples were mixed and centrifuged (10 min, 8000 rpm, 4°C). The separated aqueous phase was transferred to a new tube, frozen (-80°C) and lyophilized.

Lyophilized samples were derivatized as described previously.²⁹ An Agilent 7890B GC system with an autosampler, an injector (G4513A), and a coupled mass selective detector (5977B MSD) (Agilent) was used. High abundant metabolites were analyzed by scan acquisition. GC-MS parameters were used as follows: the injection volume of $0.5\ \mu\text{l}$ was split 1:25. The oven program started with an initial temperature hold at 70°C for 2 min and continued with a heating rate of $10^{\circ}\text{C}/\text{min}$ up to 150°C and $20^{\circ}\text{C}/\text{min}$ up to 325°C , with a hold for 7 min. After a solvent delay of 5.8 min, mass spectra were acquired within a mass range of 50 to 500 atomic mass units. All other parameters of GC and MSD were set as described before.²⁹

Low abundant metabolites were analyzed using a SIM acquisition method. Injection volume was $2\ \mu\text{l}$ and split ratio 1:10. The oven program started at 70°C with a hold for 1 min followed by a heating rate of $1.5^{\circ}\text{C}/\text{min}$ up to 76°C , $5^{\circ}\text{C}/\text{min}$ up to 220°C , and $20^{\circ}\text{C}/\text{min}$ up to 325°C , with a hold for 8 min. All other parameters of GC and MSD were set as described above.

The quantification of metabolites was performed using MassHunter Quantitative Analysis B.08.00 (Agilent). The areas of peaks were normalized to the area of peaks of internal standard compounds (Table S2). Absolute concentrations of metabolites were determined using a calibration from 0.05 to 100 nmol/sample for SIM mode and from 1 to 500 nmol/sample for scan mode. Relative quantification of metabolites (relative amount=area metabolite/area internal standard) was done with concentrations below and above the calibration range. All metabolite concentrations were related to the respective cell number.

Statistical Analysis. Statistical significance of differences was determined using Kruskal Wallis test with Dunn's post-test. Statistics were performed using GraphPad Prism version 7 (GraphPad software). A *p* value less than 0.05 was considered significant.

ASSOCIATED CONTENT

Supporting Information

Methods

Table S1. Relative mRNA expression of various enzymes involved in energy metabolism

Table S2. Primers used in this study

Table S3. Internal standards for GC-MS analysis

Table S4. Parameters for SIM method (GC-MS)

Figure S1. Profile of intermediate glycolysis metabolites

Figures S2-S3. Intracellular profile of amino acids in response to infections (part 1 and part 2)

AUTHORS INFORMATION

Corresponding Authors

Nikolai Siemens – Department of Molecular Genetics and Infection Biology, University of Greifswald, D-17489, Greifswald, Germany; Phone: +4938344205711; Email: nikolai.siemens@uni-greifswald.de

Karen Methling – Institute of Biochemistry, University of Greifswald, D-17489 Greifswald, Germany; Phone: +4938344204167; Email: methling@uni-greifswald.de

Authors

Surabhi Surabhi – Department of Molecular Genetics and Infection Biology, University of Greifswald, D-17489 Greifswald, Germany

Lana H. Jachmann – Department of Molecular Genetics and Infection Biology, University of Greifswald, D-17489 Greifswald, Germany

Michael Lalk – Institute of Biochemistry, University of Greifswald, D-17489 Greifswald, Germany

Sven Hammerschmidt – Department of Molecular Genetics and Infection Biology, University of Greifswald, D-17489 Greifswald, Germany

Author Contributions

S.S., K.M., and N.S. designed the study. S.S., L.H.J., and K.M. performed the experiments. S.S., L.H.J., K.M., and N.S. analyzed the data. S.S., K.M., and N.S. wrote the manuscript. S.S., L.H.J., S.H., M.L., K.M., and N.S. read, edited, and reviewed the manuscript.

Notes

All authors: No reported conflicts of interest.

ACKNOWLEDGEMENTS

This research was supported by the Federal Excellence Initiative of Mecklenburg Western Pomerania and European Social Fund (ESF) Grant Kolnfekt (ESF_14-BM-A55-0001_16 to SH and ESF_14-BM-A55-0005_16 to ML) and the German Research Foundation (DFG; 407176682 to N.S.).

REFERENCES

1. Lim, W. S.; Baudouin, S. V.; George, R. C.; Hill, A. T.; Jamieson, C.; Le Jeune, I.; Macfarlane, J. T.; Read, R. C.; Roberts, H. J.; Levy, M. L.; Wani, M.; Woodhead, M. A.; Pneumonia Guidelines Committee of the, B. T. S. S. o. C. C., BTS guidelines for the management of community acquired pneumonia in adults: update 2009. *Thorax* **2009**, *64 Suppl 3*, iii1-55. DOI: 10.1136/thx.2009.121434.
2. Siemens, N.; Oehmcke-Hecht, S.; Mettenleiter, T. C.; Kreikemeyer, B.; Valentin-Weigand, P.; Hammerschmidt, S., Port d'Entree for Respiratory Infections - Does the Influenza A Virus Pave the Way for Bacteria? *Front Microbiol* **2017**, *8*, 2602. DOI: 10.3389/fmicb.2017.02602.
3. Bogdanow, B.; Wang, X.; Eichelbaum, K.; Sadewasser, A.; Husic, I.; Paki, K.; Budt, M.; Hergeselle, M.; Vetter, B.; Hou, J.; Chen, W.; Wiebusch, L.; Meyer, I. M.; Wolff, T.; Selbach, M., The dynamic proteome of influenza A virus infection identifies M segment splicing as a host range determinant. *Nature Communications* **2019**, *10* (1), 5518. DOI: 10.1038/s41467-019-13520-8.
4. Nicolas de Lamballerie, C.; Pizzorno, A.; Dubois, J.; Julien, T.; Padey, B.; Bouveret, M.; Traversier, A.; Legras-Lachuer, C.; Lina, B.; Boivin, G.; Terrier, O.; Rosa-Calatrava, M., Characterization of cellular transcriptomic signatures induced by different respiratory viruses in human reconstituted airway epithelia. *Scientific Reports* **2019**, *9* (1), 11493. DOI: 10.1038/s41598-019-48013-7.
5. Tan, K. C.; Ipcho, S. V.; Trengove, R. D.; Oliver, R. P.; Solomon, P. S., Assessing the impact of transcriptomics, proteomics and metabolomics on fungal phytopathology. *Molecular plant pathology* **2009**, *10* (5), 703-15. DOI: 10.1111/j.1364-3703.2009.00565.x.
6. Liu, G.; Summer, R., Cellular Metabolism in Lung Health and Disease. *Annual review of physiology* **2019**, *81*, 403-428. DOI: 10.1146/annurev-physiol-020518-114640.
7. Hiemstra, P. S.; van der Does, A. M., Reprogramming of cellular metabolism: driver for airway remodelling in COPD? *European Respiratory Journal* **2017**, *50* (5), 1702197. DOI: 10.1183/13993003.02197-2017.
8. Martínez-Reyes, I.; Chandel, N. S., Mitochondrial TCA cycle metabolites control physiology and disease. *Nature Communications* **2020**, *11* (1), 102. DOI: 10.1038/s41467-019-13668-3.
9. DeBerardinis, R. J.; Mancuso, A.; Daikhin, E.; Nissim, I.; Yudkoff, M.; Wehrli, S.; Thompson, C. B., Beyond aerobic glycolysis: transformed cells can engage in glutamine metabolism that exceeds the requirement for protein and nucleotide synthesis. *Proceedings of the National Academy of Sciences of the United States of America* **2007**, *104* (49), 19345-50. DOI: 10.1073/pnas.0709747104.
10. Rivas, H. G.; Schmaling, S. K.; Gaglia, M. M., Shutoff of Host Gene Expression in Influenza A Virus and Herpesviruses: Similar Mechanisms and Common Themes. *Viruses* **2016**, *8* (4), 102. DOI: 10.3390/v8040102.
11. Rodriguez, A.; Pérez-González, A.; Nieto, A., Influenza virus infection causes specific degradation of the largest subunit of cellular RNA polymerase II. *Journal of virology* **2007**, *81* (10), 5315-24. DOI: 10.1128/jvi.02129-06.
12. Park, Y. W.; Katze, M. G., Translational control by influenza virus. Identification of cis-acting sequences and trans-acting factors which may regulate selective viral mRNA translation. *The Journal of biological chemistry* **1995**, *270* (47), 28433-9. DOI: 10.1074/jbc.270.47.28433.
13. Bercovich-Kinori, A.; Tai, J.; Gelbart, I. A.; Shitrit, A.; Ben-Moshe, S.; Drori, Y.; Itzkovitz, S.; Mandelboim, M.; Stern-Ginossar, N., A systematic view on influenza induced host shutoff. *eLife* **2016**, *5*. DOI: 10.7554/eLife.18311.
14. Ritter, J. B.; Wahl, A. S.; Freund, S.; Genzel, Y.; Reichl, U., Metabolic effects of influenza virus infection in cultured animal cells: Intra- and extracellular metabolite profiling. *BMC systems biology* **2010**, *4*, 61. DOI: 10.1186/1752-0509-4-61.
15. Fraunholz, M.; Sinha, B., Intracellular Staphylococcus aureus: live-in and let die. *Frontiers in cellular and infection microbiology* **2012**, *2*, 43. DOI: 10.3389/fcimb.2012.00043.
16. Surmann, K.; Michalik, S.; Hildebrandt, P.; Gierok, P.; Depke, M.; Brinkmann, L.; Bernhardt, J.; Salazar, M. G.; Sun, Z.; Shteynberg, D.; Kusebauch, U.; Moritz, R. L.; Wollscheid, B.; Lalk, M.; Völker,

- U.; Schmidt, F., Comparative proteome analysis reveals conserved and specific adaptation patterns of *Staphylococcus aureus* after internalization by different types of human non-professional phagocytic host cells. *Front Microbiol* **2014**, *5*, 392. DOI: 10.3389/fmicb.2014.00392.
17. Palmieri, F., The mitochondrial transporter family SLC25: Identification, properties and physiopathology. *Molecular Aspects of Medicine* **2013**, *34* (2), 465-484. DOI: <https://doi.org/10.1016/j.mam.2012.05.005>.
18. Iyer, R.; Baliga, N. S.; Camilli, A., Catabolite Control Protein A (CcpA) Contributes to Virulence and Regulation of Sugar Metabolism in *Streptococcus pneumoniae*. *Journal of Bacteriology* **2005**, *187* (24), 8340-8349. DOI: 10.1128/jb.187.24.8340-8349.2005.
19. Jourlin-Castelli, C.; Mani, N.; Nakano, M. M.; Sonenshein, A. L., CcpC, a novel regulator of the LysR family required for glucose repression of the *citB* gene in *Bacillus subtilis*. *Journal of molecular biology* **2000**, *295* (4), 865-78. DOI: 10.1006/jmbi.1999.3420.
20. Spellerberg, B.; Cundell, D. R.; Sandros, J.; Pearce, B. J.; Idanpaan-Heikkila, I.; Rosenow, C.; Masure, H. R., Pyruvate oxidase, as a determinant of virulence in *Streptococcus pneumoniae*. *Molecular microbiology* **1996**, *19* (4), 803-13. DOI: 10.1046/j.1365-2958.1996.425954.x.
21. Cantu, D.; Schaack, J.; Patel, M., Oxidative inactivation of mitochondrial aconitase results in iron and H₂O₂-mediated neurotoxicity in rat primary mesencephalic cultures. *PLoS One* **2009**, *4* (9), e7095-e7095. DOI: 10.1371/journal.pone.0007095.
22. Flint, D. H.; Tuminello, J. F.; Emptage, M. H., The inactivation of Fe-S cluster containing hydro-lyases by superoxide. *The Journal of biological chemistry* **1993**, *268* (30), 22369-76.
23. Nulton-Persson, A. C.; Szveda, L. I., Modulation of Mitochondrial Function by Hydrogen Peroxide *. *Journal of Biological Chemistry* **2001**, *276* (26), 23357-23361. DOI: 10.1074/jbc.M100320200.
24. Wynosky-Dolfi, M. A.; Snyder, A. G.; Philip, N. H.; Doonan, P. J.; Poffenberger, M. C.; Avizonis, D.; Zwack, E. E.; Riblett, A. M.; Hu, B.; Strowig, T.; Flavell, R. A.; Jones, R. G.; Freedman, B. D.; Brodsky, I. E., Oxidative metabolism enables *Salmonella* evasion of the NLRP3 inflammasome. *The Journal of experimental medicine* **2014**, *211* (4), 653-68. DOI: 10.1084/jem.20130627.
25. Krátký, M.; Vinšová, J., Advances in mycobacterial isocitrate lyase targeting and inhibitors. *Current medicinal chemistry* **2012**, *19* (36), 6126-37. DOI: 10.2174/092986712804485782.
26. Shin, J. H.; Yang, J. Y.; Jeon, B. Y.; Yoon, Y. J.; Cho, S. N.; Kang, Y. H.; Ryu, D. H.; Hwang, G. S., (1)H NMR-based metabolomic profiling in mice infected with *Mycobacterium tuberculosis*. *Journal of proteome research* **2011**, *10* (5), 2238-47. DOI: 10.1021/pr101054m.
27. Mairpady Shambat, S.; Chen, P.; Nguyen Hoang, A. T.; Bergsten, H.; Vandenesch, F.; Siemens, N.; Lina, G.; Monk, I. R.; Foster, T. J.; Arakere, G.; Svensson, M.; Norrby-Teglund, A., Modelling staphylococcal pneumonia in a human 3D lung tissue model system delineates toxin-mediated pathology. *Dis Model Mech* **2015**, *8* (11), 1413-25. DOI: 10.1242/dmm.021923.
28. Gierok, P.; Harms, M.; Richter, E.; Hildebrandt, J. P.; Lalk, M.; Mostertz, J.; Hochgräfe, F., *Staphylococcus aureus* alpha-toxin mediates general and cell type-specific changes in metabolite concentrations of immortalized human airway epithelial cells. *PLoS One* **2014**, *9* (4), e94818. DOI: 10.1371/journal.pone.0094818.
29. Dorries, K.; Schlueter, R.; Lalk, M., Impact of Antibiotics with Various Target Sites on the Metabolome of *Staphylococcus aureus*. *Antimicrob Agents Ch* **2014**, *58* (12), 7151-7163. DOI: 10.1128/Aac.03104-14.

Supporting information

Bronchial epithelial cells accumulate citrate intracellularly in response to pneumococcal hydrogen peroxide

Surabhi Surabhi, Lana H. Jachmann, Michael Lalk, Sven Hammerschmidt, Karen Methling, Nikolai Siemens

AUTHORS INFORMATION

Corresponding Authors

Nikolai Siemens – Department of Molecular Genetics and Infection Biology, University of Greifswald, D-17489, Greifswald, Germany; Phone: +4938344205711; Email: nikolai.siemens@uni-greifswald.de

Karen Methling – Institute of Biochemistry, University of Greifswald, D-17489 Greifswald, Germany; Phone: +4938344204167; Email: methling@uni-greifswald.de

Authors

Surabhi Surabhi – Department of Molecular Genetics and Infection Biology, University of Greifswald, D-17489 Greifswald, Germany

Lana H. Jachmann – Department of Molecular Genetics and Infection Biology, University of Greifswald, D-17489 Greifswald, Germany

Michael Lalk – Institute of Biochemistry, University of Greifswald, D-17489 Greifswald, Germany

Sven Hammerschmidt – Department of Molecular Genetics and Infection Biology, University of Greifswald, D-17489 Greifswald, Germany

METHODS

Pneumococcal mutant generation and characterization. For the generation of TIGR4 Δ *spxB*, the mutated *spxB* gene region containing the erythromycin (*erm*) resistance cassette was amplified from the genomic DNA of the D39 Δ *spxB* mutant, which was kindly provided by K. Mühlemann (University of Bern, Bern, Switzerland). The following primers: 5'-GGAGAACGTTTCCAATTCTATG-3' and 5'-GACCGGATTGCTCCGATCTT-3' were used for the amplification. The resulting 3.1 kb fragment was digested with *XcmI*, ligated into the pGXT plasmid, and transformed into *E. coli* DH5 α . The purified pGXT-*spxB:erm* plasmid was used for transformation of TIGR4 Δ *spxB*. Bacteria were allowed to grow for 2 h at 37°C and selected on blood agar plates containing 5 μ g/ml erythromycin. The resulting TIGR4 Δ *spxB* mutants were screened by colony PCR using the following primers: 5'-GCGCGCTAGCACTCAAGGGAAAATTACTGC-3 and 5'-GCGCGAGCTCTTATTTAATTGCGCGTGATTG-3'.

Absence of SpxB was confirmed via Western blot analyses. TIGR4 wild type and Δ *spxB* mutant were cultivated in THY medium until the late exponential growth phase. Bacteria were lysed, protein extracts were separated using a 12% SDS gel and blotted onto a nitrocellulose membrane. The membrane was blocked with 5% (v/v) skim milk prior to primary antibody incubations. Mouse polyclonal antibody (1:1000 dilution; in-house production by the laboratory of S.H.) was used for detection of SpxB. Anti-mice IgG Alkaline phosphatase-linked antibody was used as a secondary antibody. Hydrogen peroxide production by pneumococci was calorimetrically quantified as described by [Surabhi et al, 2021](#).

Microbiological and Cell Viability Analyses. The experimental setup was scaled down to 6-well plates. 1.0×10^6 cells were seeded in fibronectin-coated plates and the infections were performed as described above. Viable counts of bacteria released from lysed cells were determined by plating serial dilutions on blood agar. Cell stimulations were performed with 150

$\mu\text{M H}_2\text{O}_2$ for 4 h in the presence or absence of 300 U/ml catalase. Cell viability was assessed via CytoTox 96 Non-Radio Kit (Promega) according to manufacturer's guidelines.

Quantitative Reverse Transcription PCR Analysis (qRT-PCR). Total RNA was isolated at t_6 , t_{28} , and t_{50} using RiboPure RNA purification Kit (Ambion) according to manufacturer's guidelines. cDNA synthesis was performed using the Superscript first-strand synthesis system for RT-PCR (Invitrogen). Primer sets used for the analyses are summarized in Table S2. The real-time PCR amplification was performed with iTaq Universal SYBR Green Supermix kit (Biorad) using a StepOnePlus sequence detection system (Applied Biosystems). The levels of β -actin transcription were used for normalization.

Colorimetric Metabolite Measurement. Intracellular citrate and extracellular glucose, pyruvate, and lactate concentrations in cell lysates and infection supernatants were measured using the colorimetric assay kits (all Sigma-Aldrich). The assays were performed according to manufacturer's guidelines.

Table S1. Relative mRNA expression of various enzymes involved in energy metabolism.

Gene	Time point			6 h						28 h						50 h												
	Sample	uninfected		H1N1	uninfected		H1N1	Sp	H1N1+Sp	Sa	uninfected		H1N1+Sa	H1N1	Sa	uninfected		H1N1	Sa	uninfected		H1N1+Sa	H1N1	Sa	H1N1+Sa			
		Mean	±S.D.		Mean	±S.D.					Mean	±S.D.				Mean	±S.D.			Mean	±S.D.					Mean	±S.D.	Mean
<i>SLC2A</i>	Mean	1,00	1,15	1,29	1,51	1,72	2,91	3,22	1,00	0,95	1,37	1,06	1,00	0,95	1,37	1,06	1,00	0,95	1,37	1,06	1,00	0,95	1,37	1,06	1,00	0,95	1,37	1,06
	±S.D.	0,00	0,10	0,09	0,25	0,57	0,79	0,37	0,00	0,21	0,48	0,25	0,00	0,21	0,48	0,25	0,00	0,21	0,48	0,25	0,00	0,21	0,48	0,25	0,00	0,21	0,48	0,25
<i>HK1</i>	Mean	1,00	0,90	1,28	1,12	1,04	1,11	1,24	1,00	1,19	0,93	0,92	1,00	1,19	0,93	0,92	1,00	1,19	0,93	0,92	1,00	1,19	0,93	0,92	1,00	1,19	0,93	0,92
	±S.D.	0,00	0,28	0,29	0,33	0,30	0,24	0,52	0,00	0,27	0,08	0,37	0,00	0,27	0,08	0,37	0,00	0,27	0,08	0,37	0,00	0,27	0,08	0,37	0,00	0,27	0,08	0,37
<i>GPI</i>	Mean	1,00	1,09	1,15	1,02	0,94	0,96	1,04	1,00	1,29	1,52	1,47	1,00	1,29	1,52	1,47	1,00	1,29	1,52	1,47	1,00	1,29	1,52	1,47	1,00	1,29	1,52	1,47
	±S.D.	0,00	0,25	0,44	0,49	0,42	0,34	0,43	0,00	0,55	0,75	0,75	0,00	0,55	0,75	0,75	0,00	0,55	0,75	0,75	0,00	0,55	0,75	0,75	0,00	0,55	0,75	0,75
<i>PFKP</i>	Mean	1,00	1,13	0,95	0,86	0,91	1,12	1,17	1,00	1,25	1,17	1,12	1,00	1,25	1,17	1,12	1,00	1,25	1,17	1,12	1,00	1,25	1,17	1,12	1,00	1,25	1,17	1,12
	±S.D.	0,00	0,22	0,17	0,14	0,23	0,19	0,26	0,00	0,33	0,15	0,15	0,00	0,33	0,15	0,15	0,00	0,33	0,15	0,15	0,00	0,33	0,15	0,15	0,00	0,33	0,15	0,15
<i>PFKM</i>	Mean	1,00	1,33	0,59	0,47	0,59	0,64	0,51	1,00	2,49	5,33	3,51	1,00	2,49	5,33	3,51	1,00	2,49	5,33	3,51	1,00	2,49	5,33	3,51	1,00	2,49	5,33	3,51
	±S.D.	0,00	0,08	0,09	0,26	0,30	0,30	0,37	0,00	2,78	9,23	5,57	0,00	2,78	9,23	5,57	0,00	2,78	9,23	5,57	0,00	2,78	9,23	5,57	0,00	2,78	9,23	5,57
<i>PFKFB2</i>	Mean	1,00	1,07	1,41	0,81	1,09	1,53	1,88	1,00	0,95	0,90	0,79	1,00	0,95	0,90	0,79	1,00	0,95	0,90	0,79	1,00	0,95	0,90	0,79	1,00	0,95	0,90	0,79
	±S.D.	0,00	0,24	0,24	0,13	0,73	1,02	1,34	0,00	0,10	0,14	0,44	0,00	0,10	0,14	0,44	0,00	0,10	0,14	0,44	0,00	0,10	0,14	0,44	0,00	0,10	0,14	0,44
<i>PFKFB3</i>	Mean	1,00	1,03	1,18	1,13	0,95	1,31	1,29	1,00	1,12	0,85	0,77	1,00	1,12	0,85	0,77	1,00	1,12	0,85	0,77	1,00	1,12	0,85	0,77	1,00	1,12	0,85	0,77
	±S.D.	0,00	0,30	0,10	0,35	0,17	0,29	0,30	0,00	0,07	0,10	0,24	0,00	0,07	0,10	0,24	0,00	0,07	0,10	0,24	0,00	0,07	0,10	0,24	0,00	0,07	0,10	0,24
<i>PFKFB4</i>	Mean	1,00	1,02	0,96	1,55	1,51	1,67	1,64	1,00	1,46	1,94	1,59	1,00	1,46	1,94	1,59	1,00	1,46	1,94	1,59	1,00	1,46	1,94	1,59	1,00	1,46	1,94	1,59
	±S.D.	0,00	0,38	0,25	0,60	0,90	0,66	0,72	0,00	0,77	0,77	0,56	0,00	0,77	0,77	0,56	0,00	0,77	0,77	0,56	0,00	0,77	0,77	0,56	0,00	0,77	0,77	0,56
<i>ALDOA</i>	Mean	1,00	1,02	0,97	0,82	0,91	1,00	0,87	1,00	1,10	0,99	1,35	1,00	1,10	0,99	1,35	1,00	1,10	0,99	1,35	1,00	1,10	0,99	1,35	1,00	1,10	0,99	1,35
	±S.D.	0,00	0,37	0,04	0,10	0,18	0,26	0,17	0,00	0,15	0,28	0,21	0,00	0,15	0,28	0,21	0,00	0,15	0,28	0,21	0,00	0,15	0,28	0,21	0,00	0,15	0,28	0,21
<i>TPI</i>	Mean	1,00	0,92	0,81	0,77	1,30	0,90	1,00	1,00	1,84	2,56	2,16	1,00	1,84	2,56	2,16	1,00	1,84	2,56	2,16	1,00	1,84	2,56	2,16	1,00	1,84	2,56	2,16
	±S.D.	0,00	0,11	0,24	0,21	0,41	0,23	0,45	0,00	0,81	1,30	1,16	0,00	0,81	1,30	1,16	0,00	0,81	1,30	1,16	0,00	0,81	1,30	1,16	0,00	0,81	1,30	1,16
<i>GAPDH</i>	Mean	1,00	0,99	0,93	1,22	1,24	0,70	0,66	1,00	1,00	1,88	1,86	1,00	1,00	1,88	1,86	1,00	1,00	1,88	1,86	1,00	1,00	1,88	1,86	1,00	1,00	1,88	1,86
	±S.D.	0,00	0,16	0,30	0,41	0,95	0,44	0,31	0,00	0,43	0,74	1,31	0,00	0,43	0,74	1,31	0,00	0,43	0,74	1,31	0,00	0,43	0,74	1,31	0,00	0,43	0,74	1,31
<i>PGK1</i>	Mean	1,00	1,04	0,96	0,93	0,86	0,75	0,68	1,00	1,00	1,56	1,42	1,00	1,00	1,56	1,42	1,00	1,00	1,56	1,42	1,00	1,00	1,56	1,42	1,00	1,00	1,56	1,42
	±S.D.	0,00	0,32	0,24	0,06	0,41	0,32	0,27	0,00	0,21	0,45	0,60	0,00	0,21	0,45	0,60	0,00	0,21	0,45	0,60	0,00	0,21	0,45	0,60	0,00	0,21	0,45	0,60
<i>PGAM1</i>	Mean	1,00	1,14	0,90	0,95	1,28	0,91	0,89	1,00	1,19	1,86	1,26	1,00	1,19	1,86	1,26	1,00	1,19	1,86	1,26	1,00	1,19	1,86	1,26	1,00	1,19	1,86	1,26
	±S.D.	0,00	0,13	0,24	0,15	0,27	0,27	0,32	0,00	0,20	0,51	1,05	0,00	0,20	0,51	1,05	0,00	0,20	0,51	1,05	0,00	0,20	0,51	1,05	0,00	0,20	0,51	1,05

<i>ENO1</i>	Mean ±S.D.	1,00 0,00	1,01 0,23	1,00 0,00	0,90 0,20	0,73 0,17	0,42 0,25	0,51 0,30	0,54 0,37	1,00 0,00	0,75 0,15	1,49 0,32	1,22 0,44
<i>ENO2</i>	Mean ±S.D.	1,00 0,00	0,64 0,59	1,00 0,00	0,67 0,49	0,92 0,44	2,70 3,05	1,11 1,49	2,30 2,75	1,00 0,00	1,08 0,68	1,68 2,24	0,90 0,41
<i>LDHB</i>	Mean ±S.D.	1,00 0,00	1,09 0,58	1,00 0,00	0,97 0,30	1,33 0,18	1,70 1,06	1,18 0,34	1,38 0,51	1,00 0,00	1,08 0,28	0,95 0,61	1,18 0,56
<i>CS</i>	Mean ±S.D.	1,00 0,00	1,05 0,17	1,00 0,00	0,96 0,12	0,88 0,13	0,54 0,27	0,67 0,37	0,65 0,34	1,00 0,00	0,71 0,20	1,08 0,22	0,87 0,18
<i>ACO1</i>	Mean ±S.D.	1,00 0,00	1,06 0,36	1,00 0,00	1,12 0,21	0,84 0,24	0,81 0,65	1,42 1,05	1,06 0,88	1,00 0,00	1,06 0,22	1,18 0,19	0,92 0,52
<i>ACO2</i>	Mean ±S.D.	1,00 0,00	1,07 0,27	1,00 0,00	1,13 0,25	0,68 0,18	0,88 0,34	1,62 0,91	1,26 0,53	1,00 0,00	0,94 0,11	1,06 0,51	0,71 0,50
<i>IDH3A</i>	Mean ±S.D.	1,00 0,00	1,25 0,33	1,00 0,00	1,31 0,63	1,05 0,64	0,88 0,64	1,18 0,82	1,12 1,09	1,00 0,00	1,46 0,57	1,70 0,48	2,12 2,68
<i>IDH3B</i>	Mean ±S.D.	1,00 0,00	1,29 0,60	1,00 0,00	1,27 0,44	0,80 0,18	0,99 0,63	1,23 0,77	1,02 0,75	1,00 0,00	1,23 0,11	1,25 0,39	0,68 0,37
<i>IDH3G</i>	Mean ±S.D.	1,00 0,00	0,95 0,09	1,00 0,00	0,94 0,38	0,92 0,21	0,76 0,28	1,28 1,33	0,82 0,48	1,00 0,00	1,37 0,14	1,16 0,37	1,52 1,02
<i>MDH1</i>	Mean ±S.D.	1,00 0,00	1,15 0,28	1,00 0,00	1,45 0,72	0,95 0,25	1,74 1,38	1,45 1,57	1,61 1,74	1,00 0,00	1,39 0,36	1,16 0,45	1,18 0,45
<i>OGDH</i>	Mean ±S.D.	1,00 0,00	1,36 0,83	1,00 0,00	1,04 0,43	0,61 0,15	0,78 0,13	1,45 0,66	0,92 0,23	1,00 0,00	1,17 0,13	1,18 0,25	1,14 0,50
<i>PDHB</i>	Mean ±S.D.	1,00 0,00	0,95 0,28	1,00 0,00	1,01 0,07	0,88 0,17	1,13 0,47	0,93 0,24	0,98 0,53	1,00 0,00	1,01 0,15	1,29 0,42	1,11 0,59
<i>SUCLA2</i>	Mean ±S.D.	1,00 0,00	1,21 0,32	1,00 0,00	0,98 0,06	0,91 0,24	1,21 0,25	1,08 0,24	1,06 0,31	1,00 0,00	1,23 0,24	1,21 0,24	1,36 0,54
<i>SLC25A</i>	Mean ±S.D.	1,00 0,00	0,97 0,17	1,00 0,00	1,08 0,42	0,95 0,42	1,45 0,56	1,28 0,65	1,32 0,44	1,00 0,00	0,97 0,38	1,06 0,38	1,00 0,22

Abbreviations: Sp- *S. pneumoniae* and Sa- *S. aureus*.

Table S2. Primers used in this study

Gene	Forward primer (5'-3')	Reverse primer (5'-3')
Viral nucleoprotein	TTCCACAAGAGGGGTCCAGA	TCCGTCCCTTCATTGTTCCCG
Human Beta actin	CTCTCCAGCCTTCCCTTCT	AGCACTGTGTTGGCGTACAG
Glucose transporter 3	CTGAGGACGTGGAGAAAAC	CCTTTATGATCTTCTCAGGAGCATT
Hexokinase-1	GTCTGGACCGGGGAATCTTG	CCACCACGTCCAGGTCAAAT
Glucose-6-Phosphate Isomerase	AAGGACCGCTTCAACCACTT	CTCGACCCTCGGTGTAGTTG
Phosphofructokinase, platelet	TGCGGAAGTTCCTGGAGCAC	TGGTAGCCCTCGTAGATGAAAGT
Phosphofructokinase, Muscle	AGCACCGGAAGAGTCGCTA	AGAAAGCTTCCCAGCTGTTCT
6-phosphofructo-2-kinase 2	CCAAGGCAGGGAGGGATCTT	TGTAGGAGGCCCCATGAACATTT
6-Phosphofructo-2-Kinase 3	AATTGCGGTTTTTCGATGCCA	TTCTGCCGAGTTGCAGTCTT
6-phosphofructo-2-kinase 4	GATGCCATACAGCAATGGGC	GGCCAACATTGAACTCCCGA
Aldolase A	CCTTTTCCTTTCCCCAGTTG	ATCCAACCCCTTGGGTGGTAGT
Triosephosphate isomerase	GGAAGATGAACGGGGCGGAA	CAATCAGTCATCTGACTCCCC
glyceraldehyde-3-phosphate dehydrogenase	CCTCCGGGTGATGCTTTTCC	GGAACATGTAACCCATGAGTTGAG
Phosphoglycerate Kinase 1	GACCGAATCACCGACCTCTC	AGCAGCCTTAATCCTCTGGTT
Phosphoglycerate Mutase 1	GGCTGCTACTCCGGAACTCG	TCAGCACCAAGTTGTAGGCG
Enolase 1	ACCCAGTGGCTAGAAGTTTAC	CCATGGGCTGTGGGTTCTAA
Enolase 2	CCACCAATGTGGGGATGAA	TGGAGACCCACAGGATAGTCCC
Lactate Dehydrogenase B	CCTTGCTTCTCCGCACGAC	ATCAGCCAGAGACTTCCCAG
Pyruvate Dehydrogenase	GAGGCGCTTTCACCTGGACC	CGACTAACCTTGTATGCCCCAT
Citrate Synthase	GTGCTTCCCTCCACGAAATTTGA	CCTTCATGCCCTCTCATGCCA
Aconitase 1	ATCCTGGAGTGTGGAACACG	CGAGCAGGCTTAAATGGGCAC
Aconitase 2	TGGTGACTCGGCTGCAGAAAG	CGACTTGCCTCGCTCAAATTC
Isocitrate dehydrogenases	TGGTGGTGTTCAGACAGTAACTT	TGAATGGCAGTGACGTTCCG
Isocitrate dehydrogenases	GCCGTCAAAGGAGGTGTTCAA	CTTACGCCCTCAGCCGCATA
Isocitrate dehydrogenases	GGAGGCTCTCACTTTCCGTC	AGCGGACGGGAGGAATGTTT
Malate dehydrogenase	TGTTGAAATTTGCCCCGACG	CAGCACAAAGAAATATAGGCTGATCT

Oxoglutarate Dehydrogenase	OGDH	GGCATATCAGATACGAGGGCA	GATCTCCCGCAGAGGAAGTG
Succinyl-CoA ligase	SUCLA2	TGGTACGGTTACAAGGTACACG	TGCTTGCTTCGCTAAGGTCA
Mitochondrial citrate carrier	SLC25A1	CCCCATGGAGACCATCAAG	CCTGGTACGTCCCCTTCAG

Table S3. Internal standards for GC-MS analysis.

Metabolite	labeled internal standard compound	[nmol/sample]	internal standard compounds purchased from
L-alanine, urea	L-alanine- ¹³ C ₃ ¹⁵ ND ₄	41	Cambridge Isotope Laboratories, Inc.
citrate, isocitrate	citrate- ¹³ C ₆	20	SIGMA-ALDRICH
fumarate	fumarate- ¹³ C ₄	20	SIGMA-ALDRICH
fructose, glucose, <i>myo</i> -inositol	glucose- ¹³ C ₆	20	SIGMA-ALDRICH
L-arginine	L-arginine- ¹³ C ₆ ¹⁵ N ₄ D ₇	16	Cambridge Isotope Laboratories, Inc.
L-asparagine	L-asparagine- ¹³ C ₄ ¹⁵ N ₂ D ₃	23	Cambridge Isotope Laboratories, Inc.
L-aspartate, 5-oxoproline, 4-hydroxyproline	L-aspartate- ¹³ C ₄ ¹⁵ ND ₃	19,5	Cambridge Isotope Laboratories, Inc.
L-cysteine	L-cysteine- ¹³ C ₃ ¹⁵ ND ₃	1,5	Cambridge Isotope Laboratories, Inc.
L-glutamate	L-glutamate- ¹³ C ₅ ¹⁵ ND ₅	33	Cambridge Isotope Laboratories, Inc.
L-glutamine	L-glutamine- ¹³ C ₅ ¹⁵ N ₂ D ₅	23	Cambridge Isotope Laboratories, Inc.
glycine	glycine- ¹³ C ₂ ¹⁵ ND ₂	22	Cambridge Isotope Laboratories, Inc.
L-isoleucine	L-isoleucine- ¹³ C ₆ ¹⁵ ND ₁₀	23	Cambridge Isotope Laboratories, Inc.
L-leucine	L-leucine- ¹³ C ₆ ¹⁵ ND ₁₀	38	Cambridge Isotope Laboratories, Inc.
L-lysine	L-lysine- ¹³ C ₆ ¹⁵ N ₂ D ₉	34	Cambridge Isotope Laboratories, Inc.
L-malate	L-malate- ¹³ C ₄	20	Cambridge Isotope Laboratories, Inc.
L-methionine	L-methionine- ¹³ C ₅ ¹⁵ ND ₈	19,5	Cambridge Isotope Laboratories, Inc.
L-phenylalanine	L-phenylalanine- ¹³ C ₉ ¹⁵ ND ₈	16	Cambridge Isotope Laboratories, Inc.
L-proline	L-proline- ¹³ C ₅ ¹⁵ ND ₇	23,5	Cambridge Isotope Laboratories, Inc.
L-serine	L-serine- ¹³ C ₃ ¹⁵ ND ₃	18,5	Cambridge Isotope Laboratories, Inc.
L-threonine, beta-alanine	L-threonine- ¹³ C ₄ ¹⁵ ND ₅	20,5	Cambridge Isotope Laboratories, Inc.
L-tryptophan	L-tryptophan- ¹³ C ₁₁ ¹⁵ N ₂ D ₈	24	Cambridge Isotope Laboratories, Inc.
L-tyrosine	L-tyrosine- ¹³ C ₉ ¹⁵ ND ₇	22	Cambridge Isotope Laboratories, Inc.
L-valine	L-valine- ¹³ C ₅ ¹⁵ ND ₈	26,5	Cambridge Isotope Laboratories, Inc.

2-oxoglutarate, phosphoenolpyruvate	<i>N,N</i> -dimethylphenylalanine	20	SIGMA-ALDRICH
L-ornithine	L-ornithine- ¹³ C ₅	20	SIGMA-ALDRICH
2-phosphoglycerate, 3- phosphoglycerate, fructose 6-phosphate, glucose 6- phosphate, dihydroxyacetonphosphate	<i>p</i> -chlorophenylalanine	20	Bachem
pyruvate, lactate	pyruvate- ¹³ C ₃	20	SIGMA-ALDRICH
aconitate	ribitol	20	Merck
succinate	succinate- ¹³ C ₄	20	SIGMA-ALDRICH

Table S4. Parameters for SIM method (GC-MS).

Metabolite	RT [min]	quantifier m/z	qualifier m/z
succinate	16,30	247,1	172,1
fumarate	17,32	245,1	115,1
malate	20,88	233,1	245,1
cysteine	22,44	220,1	218,1
phosphoenolpyruvate	23,48	369,1	217,1
dihydroxyacetonphosphate	26,75	315,1	400,1
aconitate	26,92	229,1	375,1
2-phosphoglycerate	27,51	387,1	315,1
3-phosphoglycerate	28,09	357,1	387,1
citrate	28,36	273,1	363,2
isocitrate	28,42	245,1	319,1
fructose-6-phosphate	36,18	299,1	315,1
glucose-6-phosphate	36,27	387,2	299,1

Supplementary Figures

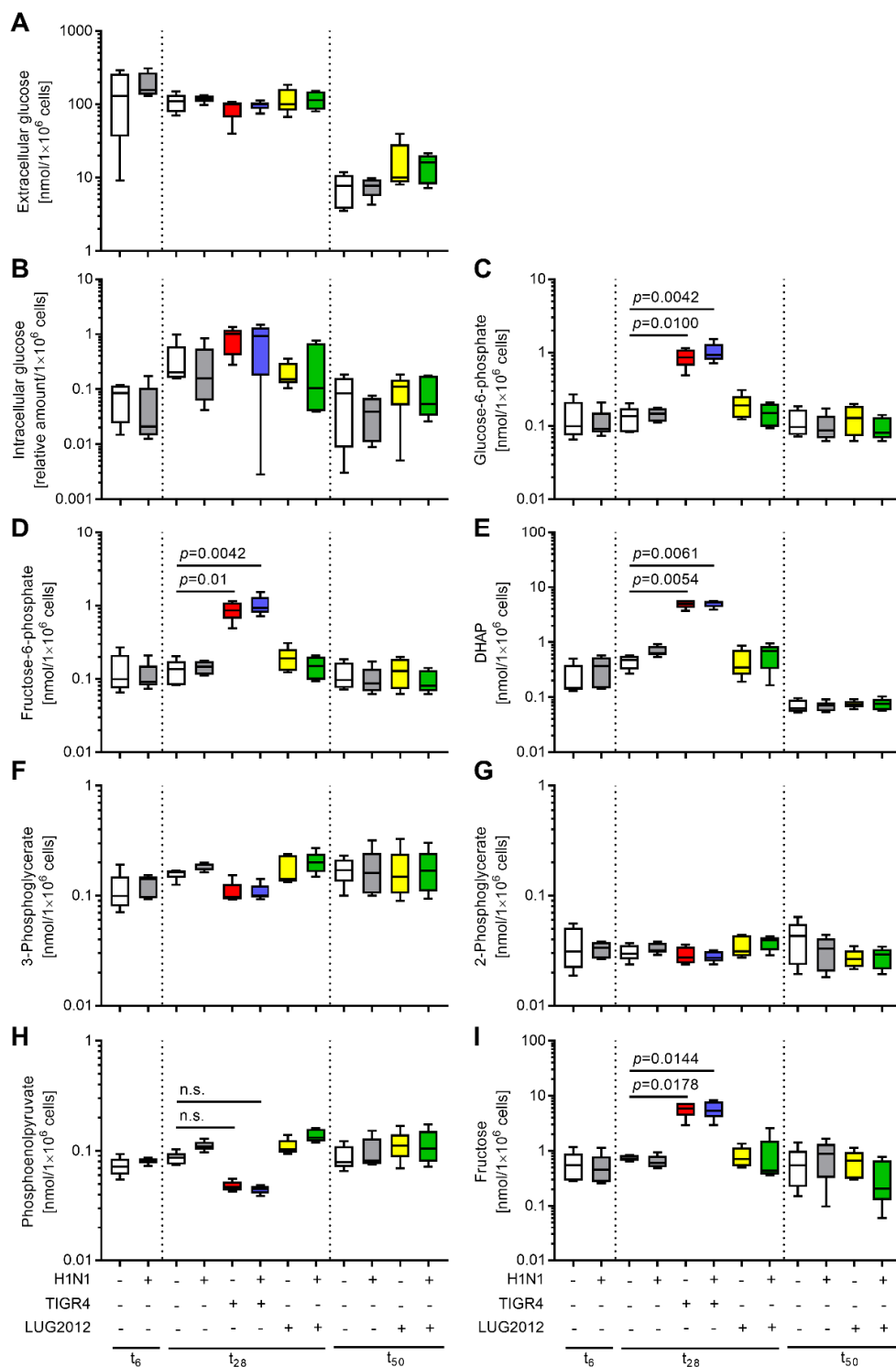


Figure S1. Profile of intermediate glycolysis metabolites in response to different infections. (A) Extracellular and intracellular concentrations of (B) glucose, (C) glucose-6-phosphate, (D) fructose-6-phosphate, (E) DHAP, (F) 3-phosphoglycerate, (G) 2-phosphoglycerate, (H) phosphoenolpyruvate, and (I) fructose are depicted. The data are displayed as box-and-whiskers of five independent experiments (n=5). The level of significance between the groups was determined using Kruskal Wallis test with Dunn's post-test.

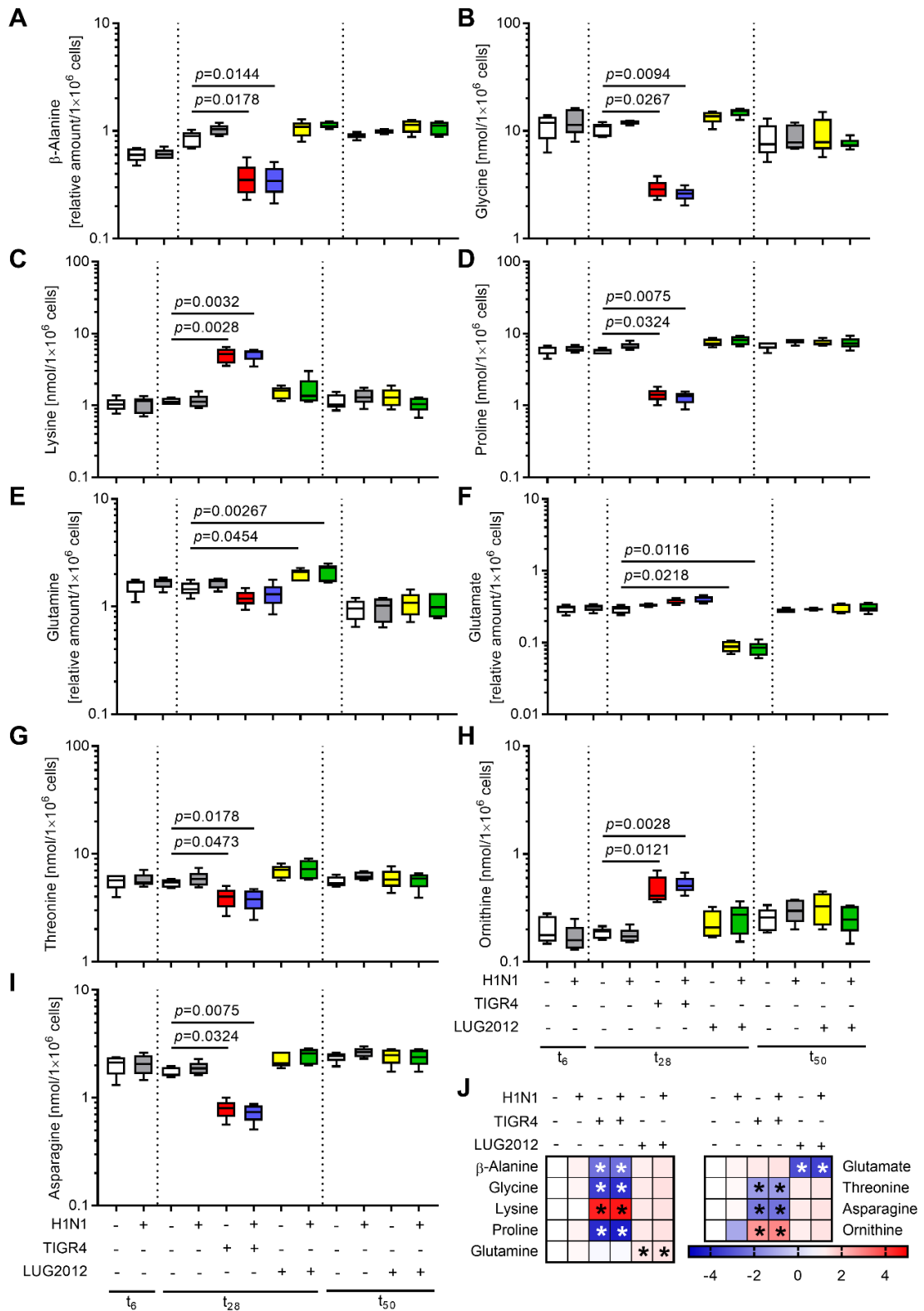


Figure S2. Intracellular profile of amino acids in response to infections (Part 1). Intracellular concentrations of (A) β -alanine, (B) glycine, (C) lysine, (D) proline, (E) glutamine, (F) glutamate, (G) threonine, (H) ornithine, and (I) asparagine are displayed. The data are displayed as box-and-whiskers of five independent experiments ($n=5$). The level of significance between the groups was determined using Kruskal Wallis test with Dunn's post-test. (J) Heat map summarizing fold changes of amino acids in response to infections as compared to the uninfected control (t_{28}). Asterisks indicate significant changes between the infected cells and the corresponding uninfected control ($p<0.05$).

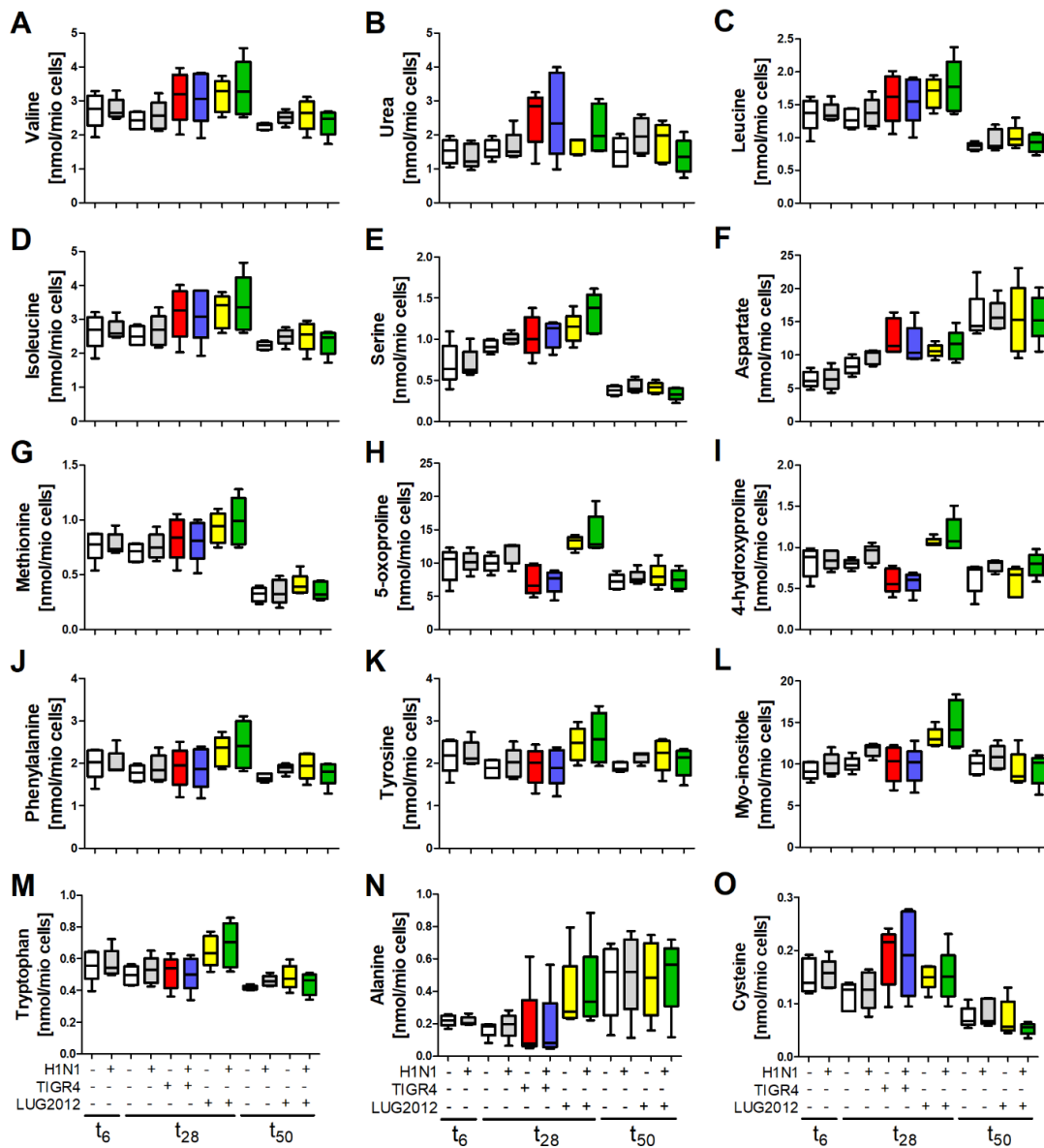


Figure S3. Intracellular profile of amino acids in response to infections (part 2). Intracellular concentrations of (A) valine, (B) urea, (C) leucine, (D) isoleucine, (E) serine, (F) aspartate, (G) methionine, (H) 5-oxoproline, (I) 4-hydroxyproline, (J) phenylalanine, (K) tyrosine, (L) myo-inositol, (M) tryptophan, (N) alanine and (O) cysteine are displayed. The data are displayed as box-and-whiskers of five independent experiments (n=5).

PAPER 4**Adenosine Triphosphate Neutralizes Pneumolysin-Induced Neutrophil Activation**

Fabian Cuypers, Björn Klabunde, Manuela Gesell Salazar, **Surabhi Surabhi**, Sebastian B. Skorka, Gerhard Burchhardt, Stephan Michalik, Thomas Thiele, Manfred Rohde, Uwe Völker, Sven Hammerschmidt, and Nikolai Siemens; KoInfekt Study Group

Published in The Journal of Infectious Diseases, 2020 Oct 13,
DOI: 10.1093/infdis/jiaa277

Author contributions:

As a co-author in this publication, **SS** participated in performing some of the experiments. Additionally, **SS** also contributed in the scientific revision and editing of the final version of this manuscript.

Conception and design: FC, BK, and NS

Experimental work: FC, BK, MGS, **SS**, SBS, GB, TT, MR, and NS

Collection and analysis of the data: FC, BK, MGS, SM, MR, and NS

Manuscript draft preparation: FC and NS

Critical revision and editing of the manuscript: FC, BK, MGS, **SS**, SBS, GB, SM, TT, MR, SH, UV, and NS

Surabhi Surabhi

Prof. Dr. Nikolai Siemens

Adenosine Triphosphate Neutralizes Pneumolysin-Induced Neutrophil Activation

Fabian Cuypers,¹ Björn Klabunde,^{1,9} Manuela Gesell Salazar,² Surabhi Surabhi,¹ Sebastian B. Skorka,¹ Gerhard Burchhardt,¹ Stephan Michalik,² Thomas Thiele,³ Manfred Rohde,⁴ Uwe Völker,² Sven Hammerschmidt,¹ and Nikolai Siemens¹; Kolnfekt Study Group

¹Department of Molecular Genetics and Infection Biology, Interfaculty Institute for Genetics and Functional Genomics, Center for Functional Genomics of Microbes, University of Greifswald, Greifswald, Germany, ²Department of Functional Genomics, Interfaculty Institute for Genetics and Functional Genomics, Center for Functional Genomics of Microbes, University Medicine Greifswald, Greifswald, Germany, ³Institute for Immunology and Transfusion Medicine, University Medicine Greifswald, Greifswald, Germany, and ⁴Central Facility for Microscopy, Helmholtz Centre for Infection Research, Braunschweig, Germany

Background. In tissue infections, adenosine triphosphate (ATP) is released into extracellular space and contributes to purinergic chemotaxis. Neutrophils are important players in bacterial clearance and are recruited to the site of tissue infections. Pneumococcal infections can lead to uncontrolled hyperinflammation of the tissue along with substantial tissue damage through excessive neutrophil activation and uncontrolled granule release. We aimed to investigate the role of ATP in neutrophil response to pneumococcal infections.

Methods. Primary human neutrophils were exposed to the pneumococcal strain TIGR4 and its pneumolysin-deficient mutant or directly to different concentrations of recombinant pneumolysin. Neutrophil activation was assessed by measurement of secreted azurophilic granule protein resistin and profiling of the secretome, using mass spectrometry.

Results. Pneumococci are potent inducers of neutrophil degranulation. Pneumolysin was identified as a major trigger of neutrophil activation. This process is partially lysis independent and inhibited by ATP. Pneumolysin and ATP interact with each other in the extracellular space leading to reduced neutrophil activation. Proteome analyses of the neutrophil secretome confirmed that ATP inhibits pneumolysin-dependent neutrophil activation.

Conclusions. Our findings suggest that despite its cytolytic activity, pneumolysin serves as a potent neutrophil activating factor. Extracellular ATP mitigates pneumolysin-induced neutrophil activation.

Keywords. neutrophils; pneumolysin; ATP; *Streptococcus pneumoniae*; degranulation.

Neutrophil migration to the site of infection is a crucial step in host defense. During an infection and subsequent hyperinflammation, multiple cell types release nucleotides, including adenosine triphosphate (ATP) [1]. ATP belongs to the diverse group of danger-associated molecular patterns and its release from intracellular into extracellular space is associated with devastating conditions such as sepsis and shock [2]. In the course of tissue infections, extracellular ATP levels can rise up to mM ranges [3, 4]. Neutrophils transmigrate towards a chemotactic gradient of inflammatory mediators. The presence of extracellular ATP stimulates purinergic signaling through P2 receptors and enhances neutrophil migration, referred to as purinergic chemotaxis [5]. It has been reported

that P2 receptor-deficient mice show increased susceptibility to *Pseudomonas aeruginosa* lung infections [6], which suggests that extracellular ATP and P2 receptors potentially exert a protective role against infection of the lungs.

Once neutrophils have reached the infection site, 3 distinct mechanisms to fight an infection occur: phagocytosis, degranulation, and formation of neutrophil extracellular traps (NETs) [7–9]. Critical components of all these processes are granule effector molecules, including proteolytic enzymes and antimicrobial peptides and proteins [10]. The release of granule components, a process called degranulation, is tightly controlled. At the site of infection, receptor recognition induces cytoskeletal remodeling, which leads to mobilization of the granules to the outer membrane. Once the neutrophil membrane is reached, granules fuse with the neutrophil membrane, which in turn results in exocytosis of granular components [11]. Although neutrophils and neutrophil-derived components are crucial for clearance of the pathogens, they also cause substantial tissue damage [8, 12, 13]. In mouse models of pneumococcal lung infections, early neutrophil recruitment was associated with a decrease of bacterial burden in the lungs [14]. However, persistent neutrophil influx was linked to disease severity at later stages of infection [14].

Received 13 March 2020; editorial decision 13 May 2020; accepted 18 May 2020; published online May 23, 2020.

⁹Present affiliation: Institute for Lung Research, Philipps-University Marburg, Marburg, Germany.

Correspondence: Nikolai Siemens, PhD, Department of Molecular Genetics and Infection Biology, Center for Functional Genomics of Microbes, University of Greifswald, Felix-Hausdorff-Straße 8, D-17489 Greifswald, Germany (nikolai.siemens@uni-greifswald.de).

The Journal of Infectious Diseases® 2020;222:1702–12

© The Author(s) 2020. Published by Oxford University Press for the Infectious Diseases Society of America. All rights reserved. For permissions, e-mail: journals.permissions@oup.com. DOI: 10.1093/infdis/jiaa277

Streptococcus pneumoniae (pneumococcus) is a gram-positive bacterium that frequently colonizes asymptotically the upper respiratory tract of healthy individuals [15]. However, imbalances in the immune system can lead to migration of pneumococci, resulting in severe life-threatening diseases such as pneumonia, meningitis, and sepsis [16]. It is widely accepted that pneumococci are the leading cause of community-acquired pneumonia [17]. Pneumococci are equipped with an arsenal of virulence factors responsible for disease manifestation and progression [18, 19]. Among them, pneumolysin (Ply) is one of the major pneumococcal virulence factors [20]. Ply is a cytotoxin, which is expressed by virtually all pneumococci [19]. It oligomerizes as rings on cholesterol-rich lipid membranes and triggers formation of membrane pores [21]. Recently, it was discovered that Ply interacts with mannose receptor C type 1 (MRC-1/CD206) on human dendritic cells and mouse alveolar macrophages [22]. This interaction allows pneumococci to dampen proinflammatory responses and to establish residency in the airways [22]. In contrast to other immune cells, neutrophil activation and degranulation in response to Ply is relatively unexplored. It was shown that Ply induces neutrophil activation, leading to a release of neutrophil elastase [23]. Subsequently, neutrophil elastase induces detachment of alveolar epithelial cells [23]. The authors suggested that P2X₇ receptor (P2X₇R), which is an ionotropic ATP receptor, is involved in Ply-mediated neutrophil activation [23]. Furthermore, it was shown that Ply promotes formation of prothrombotic neutrophil-platelet aggregates [24]. Ullah and colleagues have demonstrated that although pneumococcus is a potent stimulator of NET formation, Ply itself is not required for this process [25].

Here, we investigated the degree and specificity of Ply-mediated activation of human primary neutrophils and the role of the ATP-P2X₇R-axis in this process. We show that even at sublytic concentrations Ply is a potent inducer of neutrophil degranulation. Furthermore, we demonstrate that the activating properties of Ply are neutralized by extracellular ATP.

METHODS

Ethics Statement

Blood samples from healthy volunteers were used in this study. Donors were individuals well acquainted with the research conducted and written informed consent was obtained. The ethical research committee at the University Medicine Greifswald approved the study (BB 006/18). All experiments were carried out in accordance with the approved guidelines.

Bacterial Strains and Culture Conditions

S. pneumoniae TIGR4 and its isogenic mutant Δ ply were cultured to exponential growth phase (optical density [OD]₆₀₀,

0.35–0.4) in Todd-Hewitt broth supplemented with 0.5% (w/v) yeast extract (THY; Roth).

For construction of pASK-IBA5_Ply expression vector, genomic DNA from *S. pneumoniae* TIGR4 wild-type strain was purified. Ply was amplified with Phusion polymerase (NEB) by using the following primer sets: forward, 5'-CGGGATCCGCAAATAAAGCAGTAAATGAC-3' and reverse, 5'-GCGGTACCTAGTCATTTTCTACCTGAG-3'. The amplified fragments were digested with *Bam*HI and *Kpn*I and ligated into the vector pASK-IBA2 (IBA). For expression, *Escherichia coli* DH5 α containing the pASK-IBA5_Ply expression vector was cultured in Luria-Bertani (LB) medium at 37°C with shaking. At OD₅₅₀ 0.6–0.8, expression was induced with 200 ng/mL anhydrotetracycline, the cells were incubated for 3 hours at room temperature with shaking, and processed as detailed previously [13]. The recombinant Ply appeared as a single band of the correct molecular weight as determined by sodium dodecyl sulfate polyacrylamide gel electrophoresis (SDS-PAGE) and silver staining (Supplementary Figure 2A).

Pneumococcal Survival in Complex Media

The survival assay was performed as previously described [26]. Briefly, a 20- μ L aliquot of the suspension containing 5 \times 10⁴ wild-type and Δ ply pneumococci was inoculated into 480 μ L of heparinized human blood, plasma, or THY medium. After 2 hours of incubation at 37°C with rotation, the colony forming units were determined by plating serial dilutions on blood agar plates and compared to the initial inoculum.

Isolation and Stimulation of Primary Human Neutrophils

Human neutrophils were isolated from healthy donors using a density gradient centrifugation on Polymorphprep (Axis Shield) [12]. After isolation, neutrophils were either suspended in Hank's balanced salt solution (Life Technologies) supplemented with autologous plasma (5% v/v) or RPMI1640 medium supplemented with 10 mM L-glutamine, 25 mmol/L HEPES (all HyClone), and 5% fetal calf serum. Neutrophils (5 \times 10⁵) were infected with bacteria (multiplicity of infection 10) in RPMI medium or stimulated with different concentrations of recombinant Ply, ATP (Invivogen), or dilutions of bacterial lysates for 2 hours. To inhibit P2X₇R, neutrophils were treated with AZ10606120 (R&D Systems) for 30 minutes prior to stimulations. Neutrophil supernatants were collected and stored for further analyses at –80°C.

Cytotoxicity was determined by measurement of the lactate dehydrogenase activity via CytoTox 96 Non-Radio Kit (Promega) according to manufacturer's guidelines.

For immune analysis, neutrophils were fixed in 2% (v/v) formaldehyde and immunostained as previously described [12, 27]. The following reagents were used: rabbit anti-Ply antibody (in-house production by the laboratory of S. H.), and Nuclear-ID Red DNA stain (Enzo Life Science). Specific Ply-staining was detected by Alexa 488-conjugated goat anti-rabbit

IgG (Molecular Probes). The staining was visualized using an Axio Observer Z1 microscope (Zeiss) or FACS Aria III (BD).

Human Resistin Enzyme-Linked Immunosorbent Assay

Resistin concentrations in supernatants of neutrophils were measured by an enzyme-linked immunosorbent assay (ELISA; BioVendor) according to the manufacturer's instructions.

Microscale Thermophoresis

Microscale thermophoresis (MST) analyses were performed as previously described [28]. Briefly, recombinant Ply was NT-647-labeled according to manufacturer's guidelines (NanoTemper Technologies). The concentration of NT-647-labeled Ply was kept constant (2.6 μ M), while the concentrations of nonlabeled ATP, dATP, and ADP varied (up to 100 mM). The assay was performed in MST buffer (50 mM Tris-HCl pH 7.8, 150 mM NaCl, 10 mM MgCl₂) containing 0.05% Tween. The samples were loaded into Monolith NT.115 capillaries and the MST was performed using a Monolith NT.115 machine and MO Control software (NanoTemper Technologies). The resulting plot was analyzed via MO Affinity Analysis software (NanoTemper Technologies) by fitting a 1:1 binding model (K_d model).

Field Emission Scanning Electron Microscopy

Field emission scanning electron microscopy (FESEM) analysis was performed as previously described [29]. The detailed protocol is summarized in the [Supplementary Material](#).

Statistical Analysis

If not otherwise indicated, statistical significance of difference was determined using Kruskal Wallis test with Dunn posttest. Statistics were performed using GraphPad Prism version 7 (GraphPad Software). A *P* value less than .05 was considered significant.

Protein Extraction, Digestion for Mass Spectrometry, Identification, Quantification, and Data Analysis

For proteomic analyses 500 μ L neutrophil supernatant was reduced with dithiothreitol (2.5 mM, 60 minutes, 60°C) and alkylated with iodoacetamide (10 mM, 30 minutes, 37°C, dark). Proteins were enriched using 2 μ L of SP3 beads (hydrophobic: Sera-Mag Speedbeads carboxylate-modified particles [Thermo Fisher Scientific]; hydrophilic: Speedbead magnetic carboxylate-modified particles [GE Healthcare]). Beads were added to each sample and solutions were adjusted to 70% (v/v) with acetonitrile:water. For the on-bead protein digestion with trypsin and for peptide purification an adapted SP3 protocol was used as described previously [30]. Peptides were suspended in 2% (v/v) dimethyl sulfoxide and mixed with equal amounts of 4% (v/v) acetonitrile. Tryptic peptide solutions were analyzed by liquid chromatography-mass spectrometry/mass spectrometry (LC-MS/MS) on a reverse-phase high-performance liquid

chromatography (HPLC) system (UltiMate 3000 nano-LC system; Thermo Fisher Scientific) coupled to an Q Exactive HF mass spectrometer in a data-independent acquisition (DIA) mode. To generate a specific ion library, pools of the supernatants of different donors of each group were analyzed in data-dependent acquisition mode. Instrument setup and methods for data-dependent and independent acquisition mode are displayed in [Supplementary Tables 1–3](#).

The ion library was constructed with Spectronaut version 13 (Biognosys AG) based on a database search against a Uniprot/Swissprot database limited to human entries (version 04/2019), using trypsin/P digest rule with a maximum number of 2 missed cleavages, carbamidomethylation as static, methionine oxidation, and acetylation (protein terminus) as variable modifications. The analyses of DIA data were performed using Spectronaut version 13 (Biognosys AG). Settings are specified in [Supplementary Table 4](#).

Further DIA-MS data analysis was performed using R (R version 3.6.1) using the tidyverse package (version 1.2.1) according to the following steps: (1) median normalization of the Spectronaut raw data over MS2 total peak area intensities (EG. TotalQuantity) for all ions (*q* value < 0.01), (2) replacement of zero intensity values by half-minimal intensity value from the whole dataset, (3) calculation of the sum over ions per sample and peptide to generate peptide intensity data, and (4) generation of Hi3 protein-intensity data. For proteins identified with at least 2 peptides the ROPECA statistical analysis [31] on peptide level was performed using the median for the aggregation of the signal ratios to the signal log₂ ratio on protein level [32]. The principle component analysis of the scaled data was carried out using the FactoMineR package (version 1.41). Plots were generated using the FactoMineR package (version 1.41), factoextra package (version 1.0.5), and tidyverse package (version 1.2.1). Functional enrichment analyses were carried with the g:Profiler tool, version e99_eg46_p14_f929183, using the g:SCS (Set Counts and Sizes) correction method [33].

RESULTS

S. pneumoniae Activates Neutrophils

First, we assessed the role of Ply in bacterial survival in complex medium and ex vivo in human plasma and blood. TIGR4 wild type and Δ ply pneumococci were incubated in THY, freshly collected human blood, or plasma for 2 hours. Viable bacteria were determined by plating serial dilutions. Both strains survived in THY and human plasma ([Figure 1A](#) and [1B](#)). However, the bacteria were efficiently killed in blood ([Figure 1C](#)) indicating that cellular blood components are responsible for killing of the pathogen. Because neutrophils are the major leukocyte component of the blood and the first responders, we assessed neutrophil activation. The analyses of resistin as an activation marker revealed that both strains efficiently activate neutrophils

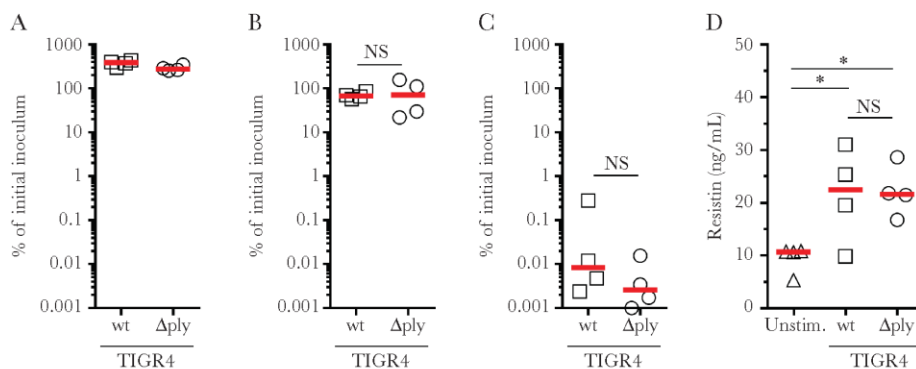


Figure 1. *Streptococcus pneumoniae* is efficiently killed by cellular blood components. TIGR4 wt or Δply mutant were incubated in THY (A), human plasma (B), or human blood (C) for 2 hours and bacterial numbers were determined. Percentage of initial inoculum is shown. D, Resistin release by the whole human blood in response to bacterial infection. The data show results from 4 independent experiments using 4 donors (n = 4). Horizontal lines depict median values. The level of significance was determined using 2-tailed Mann-Whitney U test. **P* < .05. Abbreviations: NS, not significant; ply, pneumolysin; THY, Todd-Hewitt broth with yeast extract; unstim., unstimulated; wt; wild type.

(Figure 1D). No differences in bacterial survival and neutrophil activation between TIGR4 wild type and the isogenic Δply mutant were observed.

Pneumolysin Is a Potent Trigger of Neutrophil Activation

To exclude potential additive effects of activation due to other cellular and acellular compartments of the whole blood, purified human neutrophils were incubated with the bacteria or bacterial lysates and cytotoxicity towards the cells and degranulation were assessed. When challenged with bacteria, only minor cytotoxic effects towards neutrophils were noted (Figures 2A). Both, TIGR4 wild type and Δply mutant induced degranulation of neutrophils to an equal extent (Figure 2B). Next, neutrophils were stimulated with the cytoplasmic fraction of bacterial lysates. Although TIGR4 wild type lysates were highly hemolytic (Supplementary Figure 1), only minor cytolytic effects towards

neutrophils were noted (Figure 2C). However, neutrophils responded by releasing high amounts of resistin (Figure 2D). Lysates of the Δply mutant strain did not induce cytotoxicity or neutrophil activation (Figure 2C and 2D). This result suggested that Ply is one of the major pneumococcal cytoplasmic components responsible for activation of neutrophils and this effect is not fully lysis dependent.

Exogenous ATP Neutralizes Ply-Induced Neutrophil Lysis and Activation

It has been suggested that P2X₇R, which serves as an ATP receptor, is involved in Ply-induced neutrophil activation [23]. Therefore, we assessed direct effects of active purified Ply (Supplementary Figure 2A–C) and exogenous ATP in neutrophil activation. First, neutrophils were stimulated with different concentrations of Ply with and without supplementation of autologous plasma. Concentration-dependent lysis of neutrophils

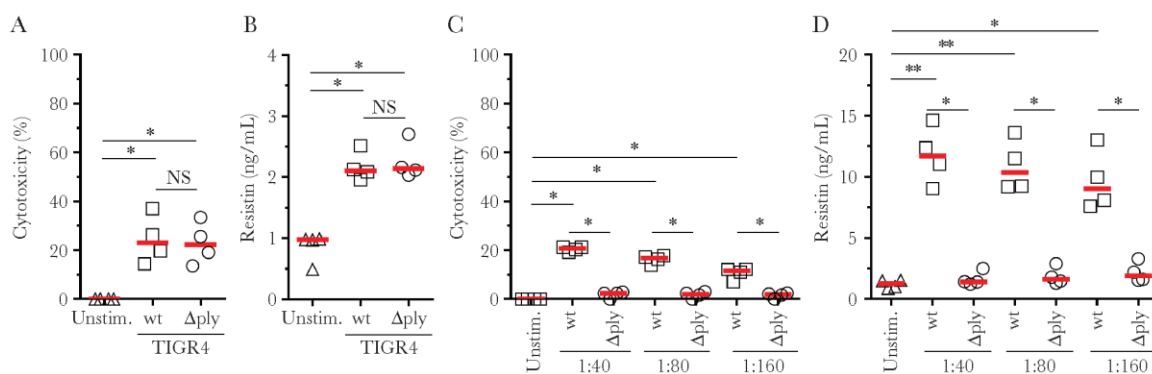


Figure 2. Pneumolysin is a cytoplasmic pneumococcal trigger of neutrophil degranulation. Purified neutrophils were stimulated with bacteria (A and B) or with cytoplasmic fraction of pneumococcal lysates at indicated dilutions (C and D) for 2 hours and cytotoxicity (A and C) and neutrophil degranulation (B and D) were assessed. Each symbol represents purified neutrophils from 1 donor (n = 4). Horizontal lines depict median values. The level of significance between the groups was determined using Kruskal Wallis test with Dunn posttest. * *P* < .05; ** *P* < .01. Abbreviations: NS, not significant; ply, pneumolysin; unstim., unstimulated; wt; wild type.

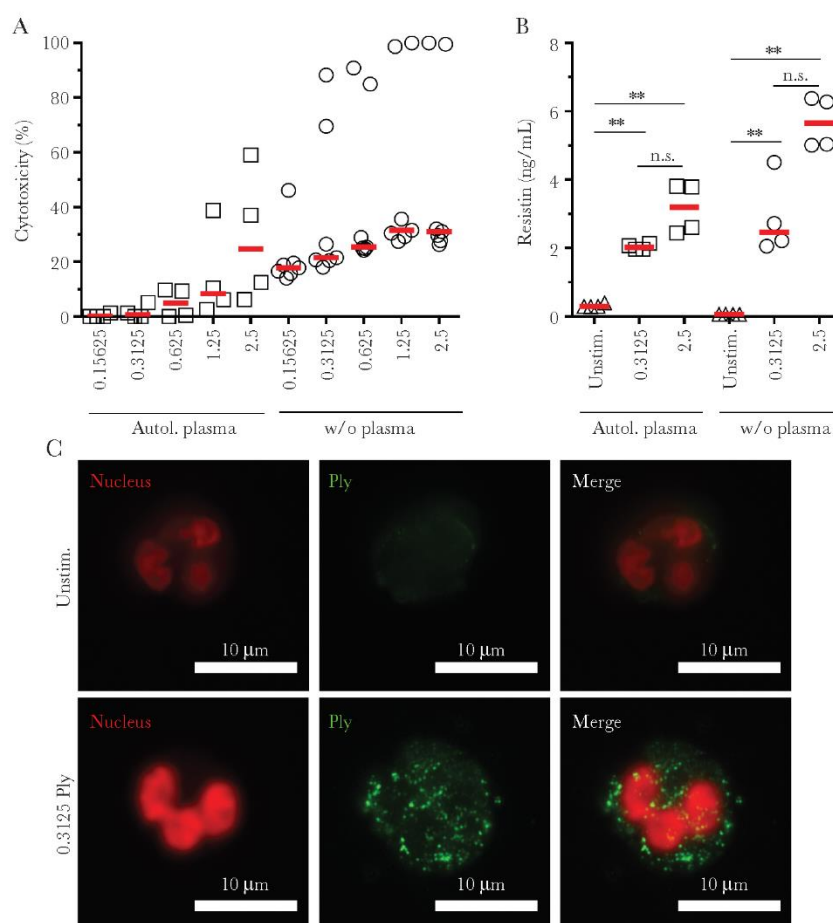


Figure 3. Pneumolysin activates human neutrophils. Purified primary neutrophils from healthy volunteers were stimulated with indicated concentrations ($\mu\text{g mL}^{-1}$) of pneumolysin for 2 hours and cytotoxicity (A) and neutrophil degranulation (B) were assessed. Each symbol represents purified neutrophils from 1 donor ($n \geq 4$). Horizontal lines depict median values. The level of significance between the groups was determined using Kruskal Wallis test with Dunn posttest. $^{**} P < .01$. C, Representative immunofluorescence micrographs of Ply on primary neutrophils after 2 hours of stimulation. Abbreviations: autol., autologous; NS, not significant; Ply, pneumolysin; w/o, without.

was observed (Figure 3A). Based on cytotoxicity tests with plasma supplementation, 0.3125 μg Ply was defined as a sublytic amount of the toxin. In contrast to the results of neutrophil viability post Ply stimulations, even sublytic concentrations of Ply induced neutrophil degranulation (Figure 3B). No significant differences between sublytic and lytic amounts of Ply in neutrophil activation were observed (Figure 3B). The presence of Ply on neutrophils was further confirmed via immunofluorescence microscopy. Ply was readily detectable on neutrophils incubated with 0.3125 μg Ply (Figure 3C). However, autologous plasma supplementation reduced neutrophil activation due to the presence of anti-Ply antibodies (Supplementary Figure 2D). To avoid antibody-mediated inhibitory effects, all following experiments were performed without plasma supplementation.

Next, neutrophils were stimulated with sublytic (0.3125 $\mu\text{g mL}^{-1}$) and lytic (2.5 $\mu\text{g mL}^{-1}$) Ply concentrations in the presence or absence

of P2X₇R agonist ATP and/or specific pharmacological P2X₇R-inhibitor AZ10606120 (Figure 4 and Supplementary Figure 3). Increasing concentrations of ATP reduced Ply-mediated neutrophil lysis (Supplementary Figure 3) and degranulation (Figure 4A), while AZ10606120 had no significant effect in any of the experiments. ATP (3 mM) almost completely abolished or significantly reduced excessive neutrophil degranulation when sublytic or lytic concentrations of Ply were used, respectively (Figure 4A).

Secretome Analyses of Neutrophils

To verify the observed results on the global level, secretome composition of neutrophils was quantitatively profiled by mass spectrometry. The presence of 3 mM ATP substantially reduced Ply-mediated degranulation (Figure 4B). Significantly fewer peptides/proteins were detected in samples that were subjected to both Ply and ATP as compared to single Ply stimulations

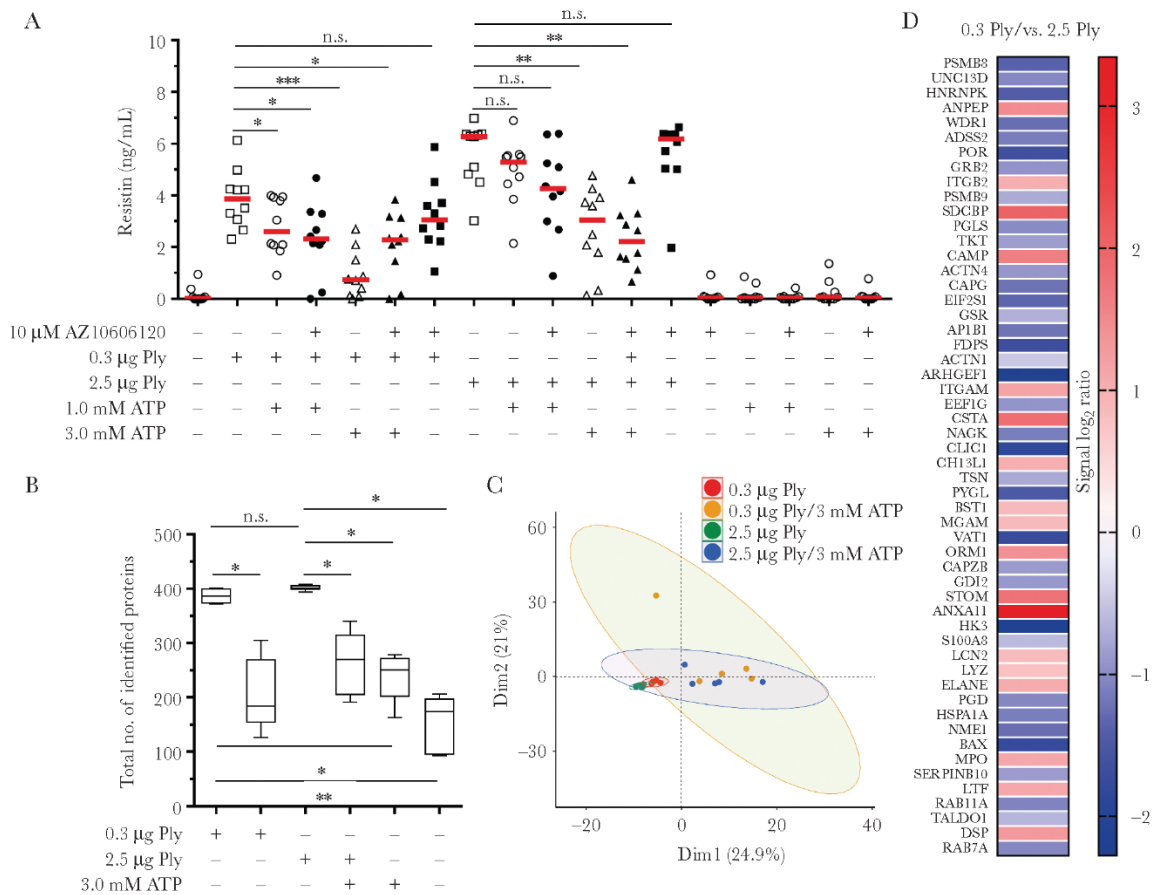


Figure 4. Extracellular ATP neutralizes pneumolysin-dependent neutrophil activation. *A*, Purified primary neutrophils from healthy volunteers were stimulated with indicated concentrations of single agents or in combination for 2 hours and neutrophil degranulation was assessed. Each symbol represents purified neutrophils from 1 donor ($n = 10$). Horizontal lines depict median values. *B*, Total numbers of secreted proteins identified in neutrophil supernatants post indicated stimulations ($n = 5$). The level of significance between the groups was determined using Kruskal Wallis test with Dunn posttest. *C*, Principal component analysis of secreted proteins. Each dot represents 1 donor ($n = 5$). The ellipses indicate the calculated 95% probability region for a bivariate normal distribution with an average center of groups. *D*, Heat map of significantly different protein abundancies in neutrophil secretome post 0.3125 μ g vs 2.5 μ g Ply stimulations. The data are displayed as signal log₂ ratios from 5 donors ($n = 5$). * $P < .05$; ** $P < .01$; *** $P < .001$. Abbreviations: Dim, dimension; NS, not significant; Ply, pneumolysin.

(Figure 4B and Supplementary Table 1). Furthermore, principal component analysis showed that both groups of Ply stimulations, sublytic and lytic concentrations, cluster together, suggesting that a sublytic amount of Ply is sufficient to activate neutrophils (Figure 4C). The analyses further confirmed that neutrophil stimulation with sublytic concentrations of Ply led to a release of granule content that was almost equivalent to the content found in lysis (Figure 4B and Supplementary Tables 5 and 6). Only 54 proteins/peptides showed altered abundance in neutrophil supernatants after different Ply stimulations (Figure 4D and Supplementary Tables 5 and 6). In addition, comparison of only Ply and respective additive ATP stimulations of neutrophils revealed substantial reduction of protein amounts in supernatants if ATP was used (Figure 5A and 5B, and Supplementary Table

6). Only 7 proteins, which belong to the cytosolic fraction, were found in higher abundance in neutrophil supernatants post Ply/ATP stimulations (Figure 5A). Pathway analyses by g:Profiler confirmed that the use of ATP inhibits major neutrophil defense mechanisms, including activation, degranulation, and immune responses (Figure 5C).

ATP Binds to Ply and Subsequently Reduces its Binding to Neutrophils

Because our experiments suggest that P2X₇R does not seem to be involved in Ply-mediated neutrophil activation, we further hypothesized that ATP potentially neutralizes Ply already in the extracellular space. MST analyses revealed that ATP and Ply interact with each other, albeit weakly (Figure 6). ATP and even ADP bind

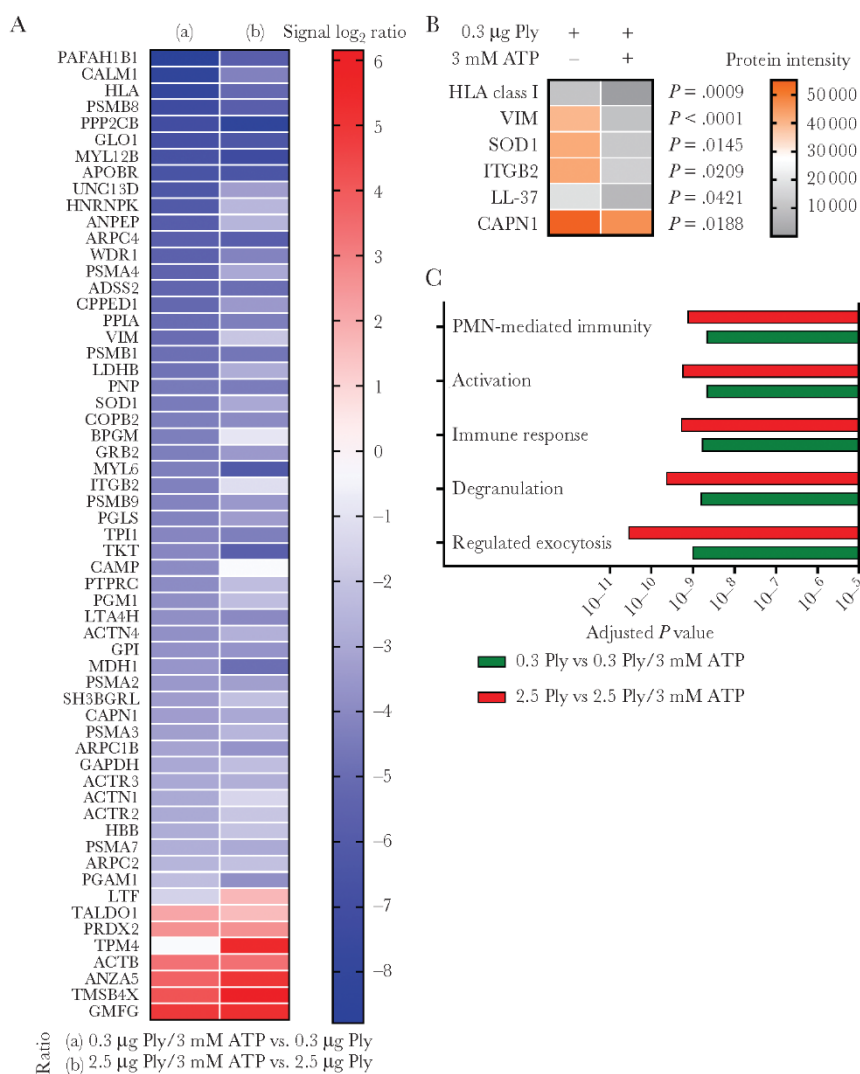


Figure 5. Comparison of neutrophil secretome profiles in response to pneumolysin (Ply) and Ply-ATP stimulations. **A**, Heat map of significantly different protein abundances ($q < 0.05$; $FC > 2$) in neutrophil secretome post 0.3125 µg/3 mM ATP vs 0.3125 µg and 2.5 µg Ply/3 mM ATP vs 2.5 µg Ply stimulations. The data are displayed as signal log₂ ratios from 5 donors ($n = 5$). **B**, Heat map highlighting significant differences of protein/peptide abundancies in neutrophils secretomes from (A). The data are displayed as mean protein intensities of the indicated stimulations from 5 donors ($n = 5$). **C**, Top 5 downregulated pathways by addition of ATP to pneumolysin stimulations. Displayed are adjusted P values as determined by functional profiling in the g:Profiler database (version e98_eg45_p14_ce5b097).

to Ply in a mM range (Figure 6A and 6C). In contrast, dATP did not show interactions with Ply (Figure 6B). These results are further supported by flow cytometry and FESEM analyses. Ply was readily detectable on about 50% of the total neutrophil population post Ply stimulations (Figure 6D and Supplementary Figure 4). Addition of 3 mM ATP to Ply stimulations almost completely abolished Ply binding to neutrophils (Figure 6D). FESEM analyses of neutrophil morphology confirmed their activation post sublytic Ply stimulations (Supplementary

Figure 5A), which were abolished by addition of ATP. However, interindividual variations were also detected (Supplementary Figure 5B). In contrast to donor 1, addition of ATP did not inhibit Ply-mediated neutrophil activation of donor 2 (Supplementary Figure 5).

DISCUSSION

Neutrophils are the most abundant leukocytes in humans and the first recruited responders at the site of infection. In this study,

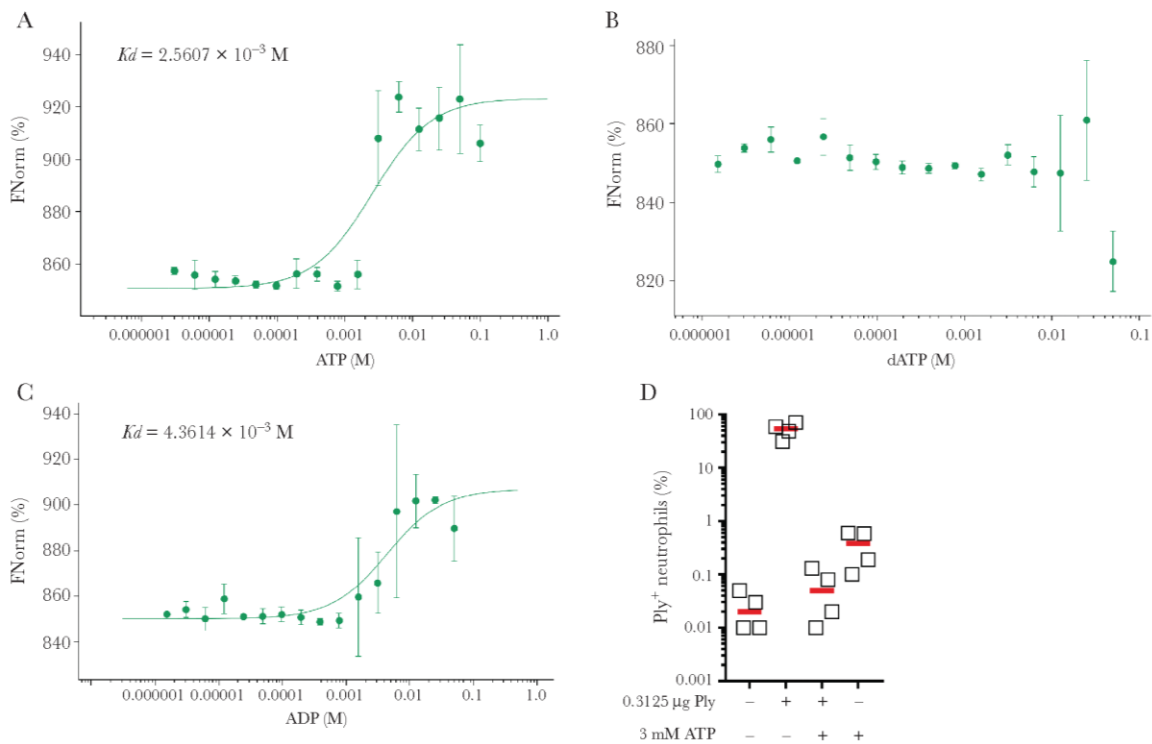


Figure 6. ATP and Ply interact with each other. Purified recombinant Ply was NT-647 labeled and binding affinities with ATP (A), dATP (B), and ADP (C) were determined using microscale thermophoresis. Each symbol represents mean values \pm SD from 3 independent experiments ($n = 3$). The K_d values are indicated in the corresponding figures. D, Summary of the FACS data of Ply-positive neutrophils post indicated stimulations. Each symbol represents purified neutrophils from 1 donor ($n = 4$). Horizontal lines depict median values. Abbreviations: FACS, fluorescence-activated cell sorting; Ply, pneumolysin.

we show that Ply is one of the major pneumococcal neutrophil activators. At sublytic concentrations, Ply induced degranulation, resulting in a release of resistin and other granule components. Notably, these actions were neutralized by extracellular ATP. Analyses of resistin and the whole proteome secreted by neutrophils revealed that addition of ATP significantly diminished Ply-mediated neutrophil degranulation. This reduction in neutrophil activation can be attributed to the interaction of Ply with ATP. The Ply-ATP interaction in the extracellular space abolished accumulation of Ply on neutrophil surfaces and subsequently reduced their activation.

Hyperinflammatory conditions, such as bacterial infections, are associated with the release of nucleotides and in particular ATP. During apoptosis or necrosis, ATP is actively or passively released from dying cells and in certain conditions ATP is detected in mM ranges [1]. In the extracellular compartment, ATP functions as a signaling molecule through the activation of purinergic P2 receptors [34]. Beneficial roles for extracellular ATP, including a function as a chemoattractant, are reported [35]. However, high ATP levels are also associated with devastating conditions such as sepsis [36]. Two subclasses

of P2 receptors exist, metabotropic P2Y and ionotropic P2X receptors [34]. P2X receptors, including P2X₁R, P2X₃R, and P2X₇R, have low affinity for ATP and are activated by ATP in mM range [37]. P2X₇R, which is expressed on neutrophils and monocyte-derived cells, activates inflammasome in a procaspase 1 dependent manner [38]. Furthermore, it was shown that loss-of-function mutations in the P2X₇R gene are associated with increased susceptibility of the human host to tuberculosis [39]. The role of P2 receptors in pneumococcal infections is not clear yet. However, it was shown that vital pneumococci can suppress ATP-mediated responses of alveolar epithelial cells [40]. Furthermore, Domon and colleagues have demonstrated that Ply colocalizes with P2X₇R [23]. In contrast to the study by Domon et al [23], our data do not indicate such interactions. Our experiments revealed that despite its cytolytic properties, Ply also serves as a potent trigger of neutrophil activation. The global secretome analyses and resistin determination of sublytic Ply stimulations show that almost equal numbers and quantities of proteins are released by neutrophils as compared to lytic stimulations. Furthermore, pharmacological inhibition of P2X₇R did not

reduce Ply-mediated activation, indicating that other neutrophil surface molecules might serve as potential Ply receptors. However, supplementation of Ply stimulations with P2X₇R agonist ATP almost completely abolished neutrophil degranulation. Further analyses revealed that ATP interacts with Ply at the mM range and subsequently reduces Ply binding to neutrophils and their activation. Therefore, our data indicate that Ply actions are neutralized through ATP in the extracellular space. However, interindividual differences in Ply-mediated neutrophil activation post addition of ATP were detected. It should be noted that viable wild-type and Δ ply pneumococci induced cytolysis and degranulation of neutrophils to the same extent. Neutrophil activation is a multifactorial process that involves several bacterial surface-associated and secreted factors [12]. One potential pneumococcal secreted factor contributing to the initial neutrophil activation is H₂O₂. In contrast to H₂O₂, Ply is released through autolysis of pneumococci and worsens the already established infection through its activating and cytolytic activities. Assuming that ATP is already released in response to H₂O₂-mediated cytolytic injury, it might dampen further Ply-mediated tissue pathology. In addition to ATP, even ADP binds to Ply. Whether ADP might also act as a potential Ply-neutralizing factor is not clear yet. However, ADP is a potent stimulator of P2Y receptors and the whole P2 receptor signaling is usually terminated by the conversion of ATP and ADP to AMP and adenosine by ectonucleotidases like CD39 or CD73 [41]. The balance between ATP/ADP and adenosine levels is crucial. Despite its beneficial actions, excessive release of ATP can contribute to the inflammatory tissue damage, while high levels of adenosine are mostly associated with immune suppression [36]. In line with this, Bou Ghanem and colleagues have shown that ATP-mediated neutrophil entry into the lungs correlates with initial control of pneumococcal burden [14]. However, as the infection progressed, further neutrophil influx was detrimental for bacterial clearance [14]. The authors linked the observed phenotype to the loss of CD73 expression [42]. Adenine production by CD73 was crucial to sustain antimicrobial efficacy of neutrophils [42]. However, the role of purinergic receptors and Ply was not explored in these studies.

Taken together, the data presented in this study support a concept that extracellular ATP has potentially a beneficial role in infections. It neutralizes excessive Ply-mediated neutrophil activation. Considering the great stimulatory capacity of pneumococci, it seems plausible that Ply-mediated neutrophil degranulation and activation may play a central role in tissue pathology in pneumococcal infection. On this note, whether such ATP actions apply only to Ply or also to other cholesterol-dependent cytolysins, including streptolysin O, listeriolysin O, or sulfolysin, and how such binding occurs biochemically warrant further studies.

Supplementary Data

Supplementary materials are available at *The Journal of Infectious Diseases* online. Consisting of data provided by the authors to benefit the reader, the posted materials are not copyedited and are the sole responsibility of the authors, so questions or comments should be addressed to the corresponding author.

Notes

Acknowledgments. We thank all volunteers for blood donation. Ulrike Lissner and Ina Schleicher are acknowledged for technical assistance.

Author contributions. F. C., B. K., and N. S. designed the study. F. C., B. K., M. G. S., S. S., S. B. S., G. B., T. T., M. R., and N. S. performed the experiments. F. C., B. K., M. G. S., S. M., M. R., and N. S. analyzed the data. F. C. and N. S. wrote the manuscript. F. C., B. K., M. G. S., S. S., S. B. S., G. B., S. M., T. T., M. R., S. H., U. V., and N. S. read, edited, and reviewed the manuscript.

Financial support. This work was supported by the Federal Excellence Initiative of Mecklenburg Western Pomerania and European Social Fund (grant numbers ESF_14-BM-A55-0001_16 and ESF_14-BM-A55-0003_16 to KoInfekt); Deutsche Forschungsgemeinschaft (grant number 407176682); and the Swedish Society of Medicine (grant number SLS-586271).

Potential conflicts of interest. All authors: No reported conflicts of interest. All authors have submitted the ICMJE Form for Disclosure of Potential Conflicts of Interest. Conflicts that the editors consider relevant to the content of the manuscript have been disclosed.

References

1. Idzko M, Ferrari D, Riegel AK, Eltzschig HK. Extracellular nucleotide and nucleoside signaling in vascular and blood disease. *Blood* **2014**; 124:1029–37.
2. la Sala A, Ferrari D, Di Virgilio F, Idzko M, Norgauer J, Girolomoni G. Alerting and tuning the immune response by extracellular nucleotides. *J Leukoc Biol* **2003**; 73:339–43.
3. Falzoni S, Donvito G, Di Virgilio F. Detecting adenosine triphosphate in the pericellular space. *Interface Focus* **2013**; 3:20120101.
4. Trautmann A. Extracellular ATP in the immune system: more than just a “danger signal”. *Sci Signal* **2009**; 2:pe6.
5. Chen Y, Corriden R, Inoue Y, et al. ATP release guides neutrophil chemotaxis via P2Y₂ and A₃ receptors. *Science* **2006**; 314:1792–5.
6. Geary C, Akinbi H, Korfhagen T, Fabre JE, Boucher R, Rice W. Increased susceptibility of purinergic receptor-deficient mice to lung infection with *Pseudomonas aeruginosa*. *Am J Physiol Lung Cell Mol Physiol* **2005**; 289:L890–5.

7. Brinkmann V, Reichard U, Goosmann C, et al. Neutrophil extracellular traps kill bacteria. *Science* **2004**; 303:1532–5.
8. Kolaczowska E, Kubes P. Neutrophil recruitment and function in health and inflammation. *Nat Rev Immunol* **2013**; 13:159–75.
9. Lee WL, Harrison RE, Grinstein S. Phagocytosis by neutrophils. *Microbes Infect* **2003**; 5:1299–306.
10. Borregaard N, Sørensen OE, Theilgaard-Mönch K. Neutrophil granules: a library of innate immunity proteins. *Trends Immunol* **2007**; 28:340–5.
11. Lacy P. Mechanisms of degranulation in neutrophils. *Allergy Asthma Clin Immunol* **2006**; 2:98–108.
12. Snäll J, Linnér A, Uhlmann J, et al. Differential neutrophil responses to bacterial stimuli: streptococcal strains are potent inducers of heparin-binding protein and resistin-release. *Sci Rep* **2016**; 6:21288.
13. Uhlmann J, Siemens N, Kai-Larsen Y, et al. Phosphoglycerate kinase-a novel streptococcal factor involved in neutrophil activation and degranulation. *J Infect Dis* **2016**; 214:1876–83.
14. Bou Ghanem EN, Clark S, Roggensack SE, et al. Extracellular adenosine protects against *Streptococcus pneumoniae* lung infection by regulating pulmonary neutrophil recruitment. *PLoS Pathog* **2015**; 11:e1005126.
15. Siemens N, Oehmcke-Hecht S, Mettenleiter TC, Kreikemeyer B, Valentin-Weigand P, Hammerschmidt S. Port d'entrée for respiratory infections—does the influenza a virus pave the way for bacteria? *Front Microbiol* **2017**; 8:2602.
16. McCullers JA. Insights into the interaction between influenza virus and pneumococcus. *Clin Microbiol Rev* **2006**; 19:571–82.
17. Vallés J, Diaz E, Martín-Loeches I, et al. Evolution over a 15-year period of the clinical characteristics and outcomes of critically ill patients with severe community-acquired pneumonia. *Med Intensiva* **2016**; 40:238–45.
18. Hammerschmidt S, Rohde M, Preissner KT. Extracellular matrix interactions with gram-positive pathogens. *Microbiol Spectr* **2019**; 7:10.1128/microbiolspec.GPP3-0041-2018.
19. Mitchell TJ, Dalziel CE. The biology of pneumolysin. *Subcell Biochem* **2014**; 80:145–60.
20. Kadioglu A, Taylor S, Iannelli F, Pozzi G, Mitchell TJ, Andrew PW. Upper and lower respiratory tract infection by *Streptococcus pneumoniae* is affected by pneumolysin deficiency and differences in capsule type. *Infect Immun* **2002**; 70:2886–90.
21. Vögele M, Bhaskara RM, Mulvihill E, et al. Membrane perforation by the pore-forming toxin pneumolysin. *Proc Natl Acad Sci U S A* **2019**; 116:13352–7.
22. Subramanian K, Neill DR, Malak HA, et al. Pneumolysin binds to the mannose receptor C type 1 (MRC-1) leading to anti-inflammatory responses and enhanced pneumococcal survival. *Nat Microbiol* **2019**; 4:62–70.
23. Domon H, Oda M, Maekawa T, Nagai K, Takeda W, Terao Y. *Streptococcus pneumoniae* disrupts pulmonary immune defence via elastase release following pneumolysin-dependent neutrophil lysis. *Sci Rep* **2016**; 6:38013.
24. Nel JG, Durandt C, Theron AJ, et al. Pneumolysin mediates heterotypic aggregation of neutrophils and platelets in vitro. *J Infect* **2017**; 74:599–608.
25. Ullah I, Ritchie ND, Evans TJ. The interrelationship between phagocytosis, autophagy and formation of neutrophil extracellular traps following infection of human neutrophils by *Streptococcus pneumoniae*. *Innate Immun* **2017**; 23:413–23.
26. Siemens N, Fiedler T, Normann J, et al. Effects of the ERES pathogenicity region regulator Ralp3 on *Streptococcus pyogenes* serotype M49 virulence factor expression. *J Bacteriol* **2012**; 194:3618–26.
27. Siemens N, Chakrakodi B, Shambat SM, et al; INFECT Study Group. Biofilm in group A streptococcal necrotizing soft tissue infections. *JCI Insight* **2016**; 1:e87882.
28. Wienken CJ, Baaske P, Rothbauer U, Braun D, Duhr S. Protein-binding assays in biological liquids using microscale thermophoresis. *Nat Commun* **2010**; 1:100.
29. Uhlmann J, Rohde M, Siemens N, et al. LL-37 triggers formation of *Streptococcus pyogenes* extracellular vesicle-like structures with immune stimulatory properties. *J Innate Immun* **2016**; 8:243–57.
30. Blankenburg S, Hentschker C, Nagel A, et al. Improving proteome coverage for small sample amounts: an advanced method for proteomics approaches with low bacterial cell numbers. *Proteomics* **2019**; 19:e1900192.
31. Suomi T, Elo LL. Enhanced differential expression statistics for data-independent acquisition proteomics. *Sci Rep* **2017**; 7:5869.
32. Suomi T, Seyednasrollah F, Jaakkola MK, Faux T, Elo LL. ROTS: an R package for reproducibility-optimized statistical testing. *PLoS Comput Biol* **2017**; 13:e1005562.
33. Raudvere U, Kolberg L, Kuzmin I, et al. g:Profiler: a web server for functional enrichment analysis and conversions of gene lists (2019 update). *Nucleic Acids Res* **2019**; 47:W191–8.
34. Khakh BS, Burnstock G. The double life of ATP. *Sci Am* **2009**; 301:84–90, 92.
35. Mihm S. Danger-associated molecular patterns (DAMPs): molecular triggers for sterile inflammation in the liver. *Int J Mol Sci* **2018**; 19:3104.
36. Ledderose C, Bao Y, Kondo Y, et al. Purinergic signaling and the immune response in sepsis: a review. *Clin Ther* **2016**; 38:1054–65.

-
37. Karmakar M, Katsnelson MA, Dubyak GR, Pearlman E. Neutrophil P2X7 receptors mediate NLRP3 inflammasome-dependent IL-1 β secretion in response to ATP. *Nat Commun* **2016**; 7:10555.
 38. Surprenant A, North RA. Signaling at purinergic P2X receptors. *Annu Rev Physiol* **2009**; 71:333–59.
 39. Coutinho-Silva R, Ojcius DM. Role of extracellular nucleotides in the immune response against intracellular bacteria and protozoan parasites. *Microbes Infect* **2012**; 14:1271–7.
 40. Olotu C, Lehmsiek F, Koch B, et al. *Streptococcus pneumoniae* inhibits purinergic signaling and promotes purinergic receptor P2Y2 internalization in alveolar epithelial cells. *J Biol Chem* **2019**; 294:12795–806.
 41. Yegutkin GG. Nucleotide- and nucleoside-converting ectoenzymes: important modulators of purinergic signalling cascade. *Biochim Biophys Acta* **2008**; 1783:673–94.
 42. Siwapornchai N, Lee JN, Tchalla EYI, et al. Extracellular adenosine enhances the ability of PMNs to kill *Streptococcus pneumoniae* by inhibiting IL-10 production [published online ahead of print 4 February 2020]. *J Leukoc Biol* doi: [10.1002/JLB.4MA0120-115RR](https://doi.org/10.1002/JLB.4MA0120-115RR).

Supplementary Data

**Adenosine Triphosphate Neutralizes Pneumolysin-induced
Neutrophil Activation**

Fabian Cuypers,¹ Björn Klabunde,^{1,#} Manuela Gesell Salazar,² Surabhi Surabhi,¹ KoInfekt Study Group, Sebastian B. Skorka,¹ Gerhard Burchhardt,¹ Stephan Michalik,² Thomas Thiele,³ Manfred Rohde,⁴ Uwe Völker,² Sven Hammerschmidt,¹ Nikolai Siemens¹

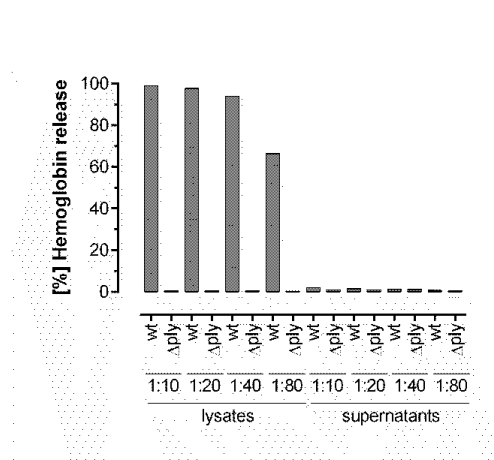
¹Department of Molecular Genetics and Infection Biology, Interfaculty Institute for Genetics and Functional Genomics, Center for Functional Genomics of Microbes, University of Greifswald, Greifswald, Germany, ²Department of Functional Genomics, Interfaculty Institute for Genetics and Functional Genomics, Center for Functional Genomics of Microbes, University Medicine Greifswald, Greifswald, Germany, ³Institute for Immunology and Transfusion Medicine, University Medicine Greifswald, Greifswald, Germany ⁴Central Facility for Microscopy, Helmholtz Centre for Infection Research, HZI, Braunschweig, Germany, #current address: Institute for Lung Research, Philipps-University Marburg, Marburg, Germany

Supplementary Data**Supplementary Methods****Field emission scanning electron microscopy**

For field emission scanning electron microscopy (FESEM) analysis, neutrophils were fixed with 1% formaldehyde in 0.1 M HEPES buffer (0.1 M HEPES, 0.01 M CaCl₂, 0.01 M MgCl₂ and 0.09 M sucrose; pH 6.9). Samples were washed with TE buffer (10 mM TRIS and 2 mM EDTA; pH 6.9), absorbed onto poly-L-lysine-coated coverslips, fixed with 1% glutaraldehyde at room temperature for 10 min, and dehydrated in a graded series of acetone (10, 30, 50, 70, 90 and 100%) with 15 min of incubation on ice for each step. Following critical-point drying with liquid CO₂ (CPD 300, Leica), samples were coated with a thin gold-palladium film (SCD 500, Bal-Tec) and examined in a field emission scanning electron microscope Zeiss Merlin (Zeiss) using the Everhart-Thornley SE-detector and Inlens SE-detector in a 75:25 ratio at an acceleration voltage of 5 kV and SmartSEM software v6.06

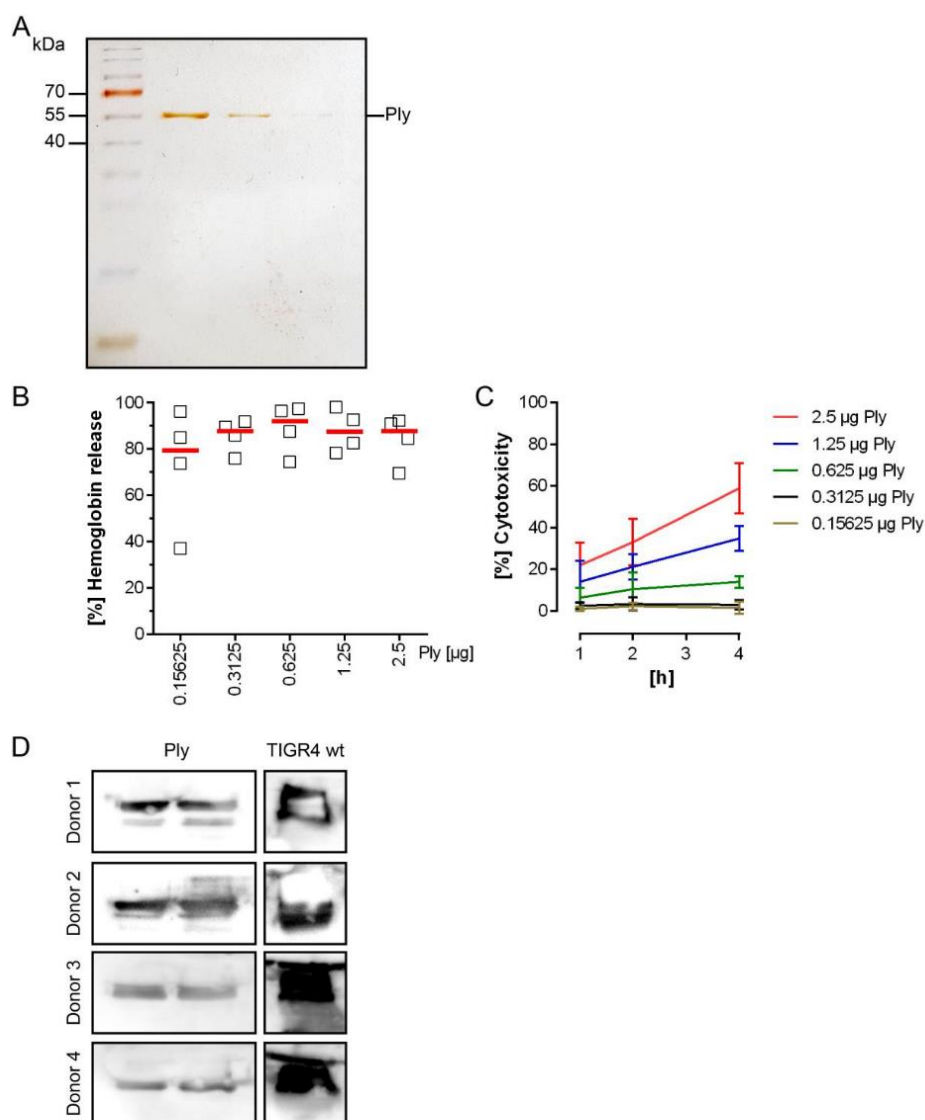
Supplementary Data

Supplementary Figures



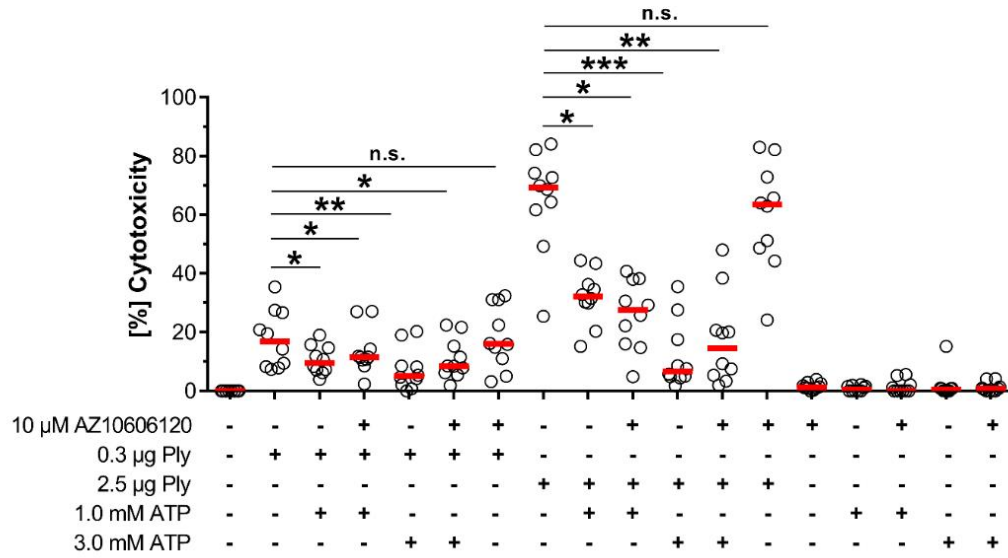
Supplementary Figure S1. Hemolytic activities of bacterial lysates and supernatants. Both, TIGR4 wt and Δply were grown until middle exponential phase ($OD_{600\text{ nm}}=0.6$), the bacteria was lysed via Lysing Matrix B and both, lysates and supernatants were sterile filtered (pore size $0.2\ \mu\text{m}$). Hemolytic assay was performed as detailed in the methods section.

Supplementary Data



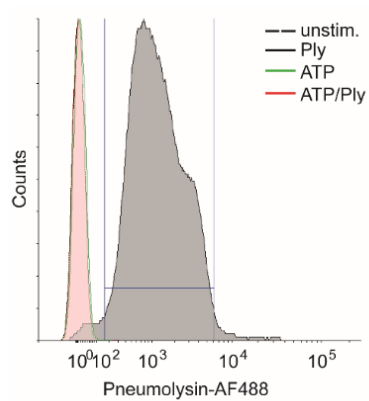
Supplementary Figure S2. (A) Silver staining of the purified recombinant Ply. (B) Hemolytic activity of the purified recombinant Ply. (C) Cytolytic activity of the purified recombinant Ply. A549 cells were seeded into 24-well plates and were subjected to Ply stimulations at indicated concentrations for indicated time points. PBS and Triton-X were used as negative and positive controls, respectively. (D) Presence of anti-pneumococcal antibodies in volunteer's plasma. Recombinant Ply or TIGR4 wt lysates were subjected to SDS-PAGE for 5 min within the separation gels. After blotting, the PVDF membrane was incubated with volunteer's plasma and potential antibodies were detected with secondary anti-human Ab.

Supplementary Data



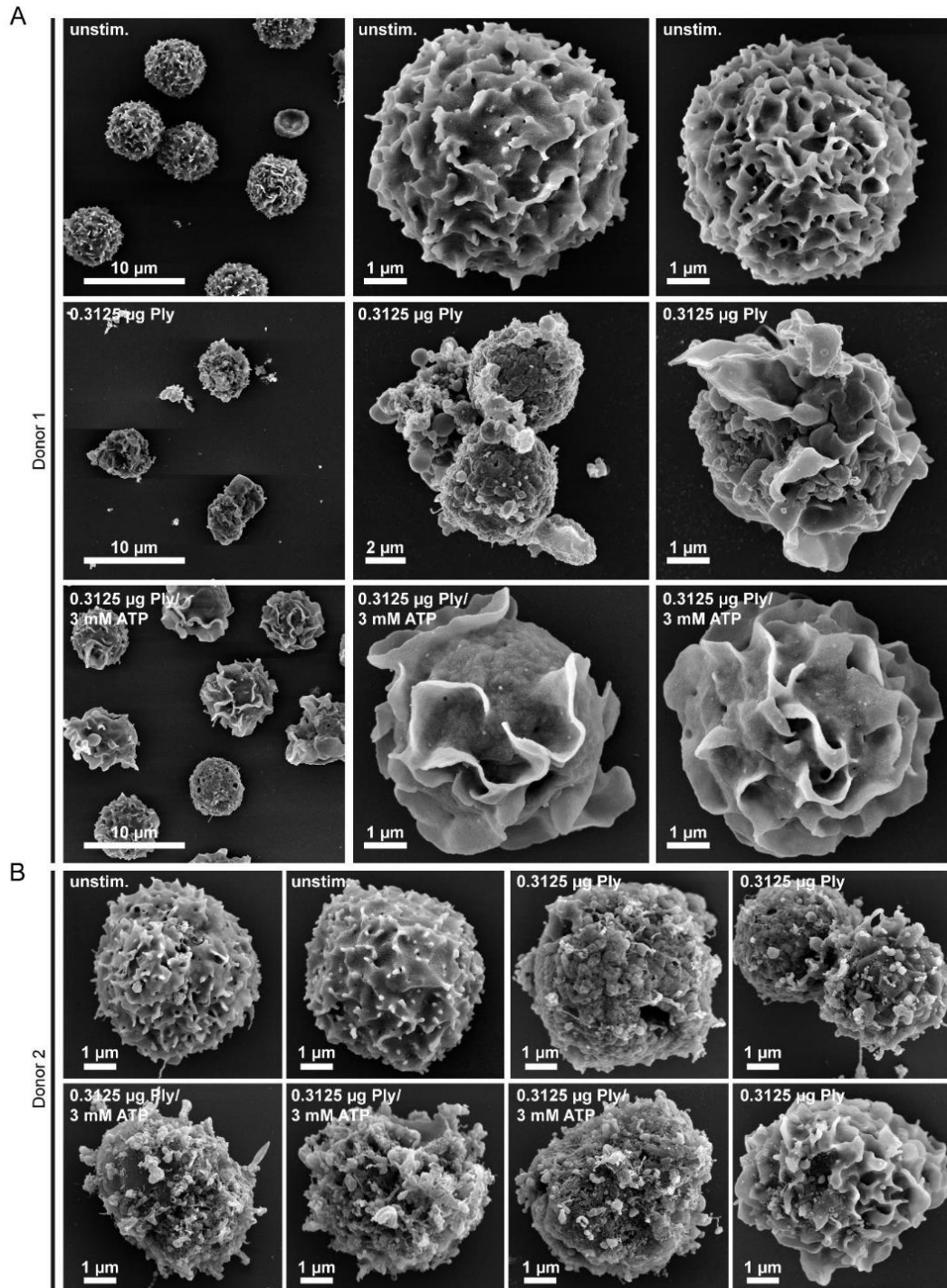
Supplementary Figure S3. Extracellular ATP neutralizes pneumolysin-dependent lysis. Purified primary neutrophils from healthy volunteers were stimulated with indicated concentrations of single agents or in combination for 2 h and cytotoxicity was assessed. Each symbol represents purified neutrophils from one donor ($n=10$). Horizontal lines depict median values. The level of significance between the groups was determined using Kruskal Wallis test with Dunnett's post-test (n.s., not significant; * $p<0.05$; ** $p<0.01$).

Supplementary Data



Supplementary Figure S4. Representative histogram of pneumolysin-positive neutrophils post 2 h stimulation.

Supplementary Data



Supplementary Figure S5. Neutrophil morphology after different stimulations. Representative FESEM images of neutrophils from donor 1 (A) and donor 2 (B) post indicated stimulations are shown.

Supplementary Data**Supplementary Tables****Supplementary Table S1.** Reversed phase liquid chromatography (RPLC).

<i>instrument</i>	Ultimate 3000 RSLC (Thermo Scientific)
<i>trap column</i>	75 μm inner diameter, packed with 3 μm C18 particles (Acclaim PepMap100, Thermo Scientific)
<i>analytical column</i>	Accucore 150-C18, (Thermo Fisher Scientific) 25 cm x 75 μm , 2,6 μm C18 particles, 150 \AA pore size
<i>buffer system</i>	binary buffer system consisting of 0.1% acetic acid in HPLC-grade water (buffer A) and 100% ACN in 0.1% acetic acid (buffer B)
<i>flow rate</i>	300 nl/min
<i>gradient</i>	linear gradient of buffer B from 2% up to 25%
<i>gradient duration</i>	120min
<i>column oven temperature</i>	40°C

Supplementary Data

Supplementary Figure S2. Parameter for mass spectrometric analyses in data dependent analyses (DDA).

<i>instrument</i>	Q Exactive HF*
<i>operation mode</i>	data-dependent
Full MS	
<i>MS scan resolution</i>	60,000
<i>AGC target</i>	3e6
<i>maximum ion injection time for the MS scan</i>	20 ms
<i>Scan range</i>	333 to 1650 m/z
<i>Spectra data type</i>	profile
dd-MS2	
<i>Resolution</i>	15,000
<i>MS/MS AGC target</i>	1e5
<i>maximum ion injection time for the MS/MS scans</i>	25 ms
<i>Spectra data type</i>	profile
<i>selection for MS/MS</i>	15 most abundant isotope patterns with charge ≥ 2 from the survey scan
<i>isolation window</i>	1,4 m/z
<i>Fixed first mass</i>	100 m/z
<i>dissociation mode</i>	HCD
<i>normalized collision energy</i>	27.5%
<i>dynamic exclusion</i>	30 s
<i>Charge exclusion</i>	unassigned, 1,>6

Supplementary Data

Supplementary Table S3. Parameter for mass spectrometric analyses in data independent analyses (DIA).

<i>instrument</i>	Q Exactive HF
<i>electrospray</i>	Nanospray Flex Ion Source
<i>operation mode</i>	data-independent
Full MS	
<i>MS scan resolution</i>	60000
<i>AGC target</i>	5e6
<i>maximum ion injection time for the MS scan</i>	200 ms
<i>Scan range</i>	333 to 1650 m/z
<i>Spectra data type</i>	profile
dd-MS2	
<i>Resolution</i>	30,000
<i>MS/MS AGC target</i>	3e6
<i>maximum ion injection time for the MS/MS scans</i>	auto
<i>Spectra data type</i>	profile
<i>selection for MS/MS</i>	1
<i>isolation window</i>	56 windows, 13 m/z
<i>Fixed first mass</i>	-
<i>dissociation mode</i>	higher energy collisional dissociation (HCD)
<i>normalized collision energy</i>	27.5%

Supplementary Data

Supplementary Figure S4. Spectronaut™ parameters used for data analyses (DIA).

<i>software</i>	Spectronaut version 13 (BiognoSYS, Schlieren, Switzerland)
<i>data extraction</i>	
<i>Intensity extraction MS1 and MS2</i>	maximum intensity
<i>MS1 and MS2 mass tolerance strategy</i>	dynamic
<i>XIC extraction</i>	
<i>XIC extraction window</i>	dynamic
<i>calibration</i>	
<i>Calibration mode</i>	automatic
<i>RT regression type</i>	Local (non-linear) regression
<i>identification</i>	
<i>Decoy method</i>	mutated
<i>Decoy limit strategy</i>	dynamic
<i>Machine learning</i>	per run
<i>Precursor Qvalue cutoff</i>	0.001
<i>Protein Qvalue cutoff</i>	0.01
<i>PValue Estimator</i>	Kernel Density Estimator
<i>quantification</i>	
<i>Interference correction</i>	True, MS1 Min. 2, MS2 Min. 3
<i>Quantity MS level</i>	MS2
<i>Quantity type</i>	area
<i>Data filtering</i>	Qvalue sparse
<i>Workflow</i>	
<i>Profiling strategy</i>	iRT profiling
<i>Profiling Row Selection</i>	Minimum Qvalue Row Selection, Qvalue Treshold 0.001
<i>Profiling Target Selection</i>	Profile only non-identified precursor, Identification Criterion Qvalue, Treshold 0.001
<i>Carry-over exact peak boundaries</i>	False
<i>Unify peptide peaks</i>	Select corresponding peak

Supplementary Data

Supplementary Table S5. Proteome analyses of neutrophil supernatants post indicated stimulations. Raw values of peptide intensities are displayed.

Supplementary Table S6. Statistical analyses of the abundance patterns of proteins in neutrophils supernatants post indicated stimulations.

Chapter 7

APPENDIX

7. Appendix

7.1 Eigenständigkeitserklärung

7.2 Curriculum vitae

7.3 Publications and conference contributions

7.3.1 Published peer-reviewed articles included in this thesis

- **Surabhi S**, Cuypers F, Hammerschmidt S, Siemens N. The Role of NLRP3 Inflammasome in Pneumococcal Infections. Published in *Frontiers in Immunology*, 2020. doi: 10.3389/fimmu.2020.614801
- **Surabhi S**, Jachmann L, Shumba P, Burchhardt G, Hammerschmidt S, Siemens N. Hydrogen peroxide is crucial for NLRP3 inflammasome mediated IL-1 β production in pneumococcal infections of bronchial epithelial cells. Accepted for publication in *Journal of Innate Immunity*, 2021. doi: 10.1159/000517855
- Cuypers F, Klabunde B, Gesell Salazar M, **Surabhi S**, Skorka S B, Burchhardt G, Michalik S, Thiele T, Rohde M, Völker U, Hammerschmidt S, Siemens N; KoInfekt Study Group. Adenosine Triphosphate Neutralizes Pneumolysin-Induced Neutrophil Activation. Published in *Journal of Infectious Diseases*, 2020. doi: 10.1093/infdis/jiaa277

7.3.2 Published peer-reviewed articles not included in this thesis

- Schultz D, **Surabhi S**, Stelling N, Rothe M, KoInfekt Study Group, Methling K, Hammerschmidt S, Siemens N, Lalk M. 16HBE Cell Lipid Mediator Responses to Mono and Co-Infections with Respiratory Pathogens. Published in *Metabolites*, 2020. doi: 10.3390/metabo10030113

7.3.3 Submitted manuscripts included in this thesis

- **Surabhi S**, Jachmann L, Hammerschmidt S, Lalk M, Methling K, Siemens N. Bronchial epithelial cells accumulate citrate intracellularly in response to pneumococcal hydrogen peroxide. Submitted in *ACS Infectious Diseases*, 2021

7.3.4 Submitted manuscripts not included in this thesis

- Sura T, **Surabhi S**, Maaß S, Hammerschmidt S, Siemens N, Becher D. Global Scale Investigation of the Proteome and Ubiquitinome of Bronchial Epithelial Cells in a Coinfection Model. Submitted in *Journal of Proteome Research*, 2021
- Cuypers F, Schäfer A, Skorka S, **Surabhi S**, Tölken L, Paulikat A, KoInfekt Study Group, Kohler T, Otto S, Mettenleiter T, Hammerschmidt S, Blohm U, Siemens N. Innate Immune Responses at the Early Onset of Pneumococcal and Influenza A Viral Co-infections. Submitted in *Scientific Reports*, 2021.

7.3.5 Participation in Conferences and other Scientific Events

- Sebastian B. Skorka, **Surabhi Surabhi**, Fabian Cuypers, Nicolas Stelling, Sven Hammerschmidt, and Nikolai Siemens. Pneumococcal and influenza A viral co-infections in *in vivo* and *in vitro* model systems. 14th European Meeting on the Molecular Biology of the Pneumococcus (Europneumo), Greifswald, Germany, June 11-14, 2019, (Poster presentation)
- **Surabhi Surabhi**, Sven Hammerschmidt, and Nikolai Siemens. Host pathogen interplay in *S. pneumoniae* and Influenza A virus mediated respiratory infection. Deutsche Gesellschaft für Hygiene und Mikrobiologie (DGHM), Göttingen, Germany, February 25-27, 2019 (Poster presentation).
- **Surabhi Surabhi**, Nicolas Stelling, Sven Hammerschmidt, and Nikolai Siemens. Infection patterns of colonizing and invasive *Streptococcus pneumoniae* strains with human cell compartments. 4th German Pneumococcal and Streptococcal symposium, Berlin, Germany, October 22-24, 2018 (Poster presentation).
- Sebastian Skorka, Fabian Cuypers, **Surabhi Surabhi**, Nicolas Stelling, Sven Hammerschmidt, and Nikolai Siemens. Bacterial and viral co-infections: a multi-disciplinary and multispecies approach to unravel signatures of respiratory infection. Poster presentation, 1st International Conference on Respiratory Pathogens (ICoRP), Rostock, Germany, November 01-03, 2017 (Poster presentation).
- Participated in Tissue-specific immunology workshop at Karolinska Institutet, Sweden, Stockholm. November 19-23, 2018.

7.4 Acknowledgments

I have received a great deal of support and assistance during my doctoral studies. First and foremost, I would like to express my deepest gratitude to Prof. Dr. Nikolai Siemens for providing me the opportunity to do my PhD on this interesting topic. Thank you for always being a highly motivating supervisor. Your meticulous and precise research attitude has certainly been infectious. I could not have imagined having a better advisor and mentor for my PhD study. Further, I would also like to thank my second supervisor, Prof. Dr. Sven Hammerschmidt. I would like to thank you for all the scientific insights, support, and guidance. Your passion for pneumococcal research has been truly inspirational.

A big thank you also goes to all the co-authors as well as all the cooperation partners from the Co-infect project partners who have contributed towards this thesis. Thank you very much for the scientific support, which has resulted in successful scientific publications.

I would also like to thank all the members of the Junior Research Group Dr. Siemens and the research group of Prof. Dr. Sven Hammerschmidt for the great working atmosphere. I thank Dr. Gerhard Burchhardt, Dr. Lothar Petruschka, Dr. Thomas Kohler, Dr. Mohammed Abdullah, and Dr. Franziska Voss, for their constant support and help with the many day to day difficulties I had during my time in the group. Our critical scientific discussions during departmental seminars have helped shape this thesis. I would like to thank Anke Tischer, Dr. Sylvia Kohler, Dr. Susann R ath and Nicole Born, who always helped me with administrative questions and problems. I would like to thank the technical staff, Birgit Rietow, Kristine Sievert-Giermann, Karsta Barnekow and Peggy StremLOW, for all the active support in everyday laboratory work and ordering consumables. I also thank them for motivating me to learn German.

I would also like to acknowledge my sincere thanks to friends and colleagues, Dr. Richael Mills, Dr. Jolien Seinen, Dr. Niamatullah Kakar, Dr. Fabian Cuypers, Murtadha Ali, Sebastian Skorcka, Nicolas Stelling, Stephanie Hirschmann, Patience Shumba, Kristin Jahn, Lisa Fr schke, Lana Jachmann, Antje Paulikat, Lea T lken, Max Brendal and Astrid Puppe. I thank you all for good times, kindness and friendship during these last four years. All the wonderful times in the lab, the lab-outings and movie nights will always be missed by me.

De-stressing during the PhD journey was also much needed. Firstly, I want to thank our Swim team. Thanks for the swimming lessons, I can now proudly say that, "Yes, I can swim". Thanks, Lisa, my swim coach for being so sweet and constantly motivating me to swim.

I also thank all the swim team members: Steffi, Antje, Lana, Jolien, Kristin, Richael and Patience, for such memorable and fun swim lessons. Secondly, I would like to thank ‘Team happy hour’. I always looked forward to Friday lunch with you guys. This time was not just fun, but the constructive scientific discussions also helped improve my thesis.

Thanks to all my friends: Sivapriya-Arvind, Indhu-Ganesh, Megha, Neha-Anurag, Archana-Anikesh, Nishant. Thank you guys for planning regular trips and making my vacations so much fun. A special thanks to my friend, Kritesh. Thank you for always being there for me.

Last but not least, I would like to thank my family. Thanks Aaanu, for teaching me the value of hard-work. Thank you Amma, for making me understand the importance of patience. I thank you both for being a great source of inspiration and strength. Thank you Shady, for always being by my side and constantly motivating me on an almost daily basis. I thank my in-laws, Maava and Maai, for their constant encouragement. Finally, Gautham, my amazing life-partner, thank you for the unconditional love, unfathomable patience and unlimited support. All your belief in me has kept me motivated to fulfil my pursuits.



EUROPÄISCHE UNION
Europäischer Sozialfonds

